ADA031776

AFML-TR-76-80

DEVELOPMENT OF TITANIUM ALLOY CASTING TECHNOLOGY

AIRESEARCH MANUFACTURING COMPANY OF ARIZONA
A DIVISION OF THE GARRETT CORPORATION
402 SOUTH 36th STREET
PHOENIX, ARIZONA 85010

AUGUST 1976

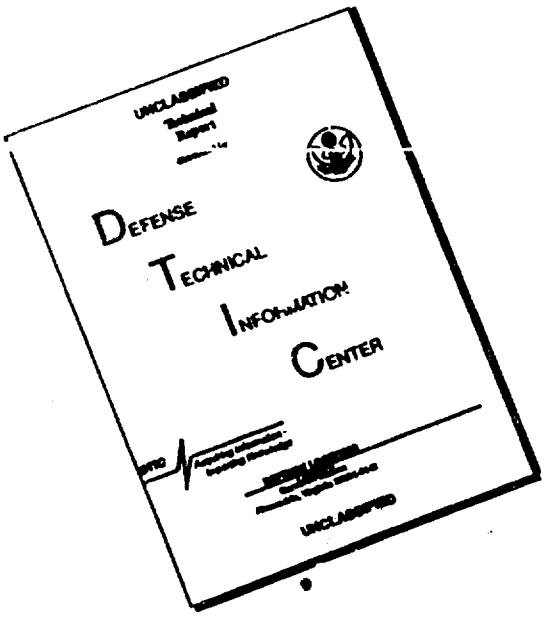
FINAL REPORT FOR PERIOD FEBRUARY 1974 - FEBRUARY 1976

Approved for public release; distribution unlimited

DDC
RECEIVED
NOV 9 1976
B

AIR FORCE MATERIALS LABORATORY
AIR FORCE SYSTEMS COMMAND
WRIGHT-PATTERSON AIR FORCE BASE, OHIO 45433

DISCLAIMER NOTICE



THIS DOCUMENT IS BEST QUALITY AVAILABLE. THE COPY FURNISHED TO DTIC CONTAINED A SIGNIFICANT NUMBER OF PAGES WHICH DO NOT REPRODUCE LEGIBLY.

NOTICE

When Government drawings, specifications, or other data are used for any purpose other than in connection with a definitely related government procurement operation, the United States Government thereby incurs no responsibility nor any obligation whatsoever; and the fact that the government may have formulated, furnished, or in any way supplied the said drawings, specifications, or other data, is not to be regarded by implication or otherwise as in any manner licensing the holder or any other person or corporation, or conveying any rights or permission to manufacture, use, or sell any patented invention that may in any way be related thereto.

This report has been reviewed by the Information Office (OI) and is releasable to the National Technical Information Service (NTIS). At NTIS, it will be available to the general public, including foreign nations.

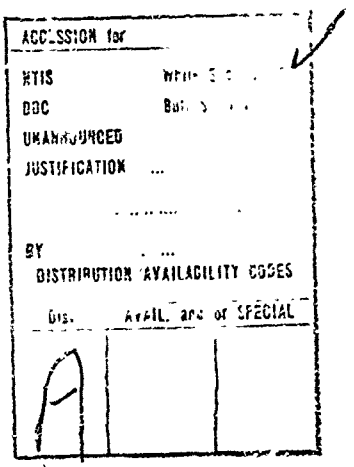
William R Kerr

WILLIAM R. KERR
Project Engineer

FOR THE COMMANDER

Nathan G. Tupper

NATHAN G. TUPPER
Acting Chief
Structural Metals Branch
Metals and Ceramics Division
Air Force Materials Laboratory



Copies of this report should not be returned unless return is required by security considerations, contractual obligations, or notice on a specific document.

UNCLASSIFIED

SECURITY CLASSIFICATION OF THIS PAGE (When Data Entered)

REPORT DOCUMENTATION PAGE

READ INSTRUCTIONS BEFORE COMPLETING FORM

1. REPORT NUMBER: AFML-TR-76-80	2. GOVT ACCESSION NO.
3. RECIPIENT'S CATALOG NUMBER	
4. TITLE (and Sub title): DEVELOPMENT OF TITANIUM ALLOY CASTING TECHNOLOGY,	5. TYPE OF REPORT & PERIOD COVERED: Final Technical Report, 15 Feb 1974-15 Feb 1976
6. PERFORMING ORG. REPORT NUMBER: 76-311721	
7. AUTHOR(s): Don R. Schuyler, John A. Petrusha, G. S. Hall (RMI Company), S. R. Seagle (RMI Company)	8. CONTRACT OR GRANT NUMBER(s): F33615-74-C-5055
9. PERFORMING ORGANIZATION NAME AND ADDRESS: THE GARRETT CORPORATION, AiResearch Mfg. Co. of Arizona, 402 S. 36th Street, Phoenix, Az 85034	10. PROGRAM ELEMENT, PROJECT, TASK AREA & WORK UNIT NUMBERS: Project/Task No. 73510818
11. CONTROLLING OFFICE NAME AND ADDRESS: Air Force Materials Laboratory (AFSC), Metals and Ceramics Division, Wright-Patterson AFB, Ohio 45433	12. REPORT DATE: August 1976 13. NUMBER OF PAGES: 292
14. MONITORING AGENCY NAME & ADDRESS (if different from Controlling Office): 311p.	15. SECURITY CLASS. (of this report): UNCLASSIFIED 15a. DECLASSIFICATION/DOWNGRADING SCHEDULE

16. DISTRIBUTION STATEMENT (of this Report)

Approved for public release; distribution unlimited

17. DISTRIBUTION STATEMENT (of the abstract entered in Block 20, if different from Report)

18. SUPPLEMENTARY NOTES

RMI Company, Niles, OH, was a major subcontractor and conducted alloy development activities.

19. KEY WORDS (Continue on reverse side if necessary and identify by block number)

Titanium Castings
Low-Melting Titanium Alloys
Induction Melting Crucibles
Ceramic Molds

20. ABSTRACT (Continue on reverse side if necessary and identify by block number)

DD FORM 1 JAN 73 1473 EDITION OF 1 NOV 65 IS OBSOLETE

UNCLASSIFIED

SECURITY CLASSIFICATION OF THIS PAGE (When Data Entered)

404 796

This program was conducted to develop the technologies necessary to establish a low-cost approach for producing titanium investment castings. This approach was based on using simpler and cheaper melting and casting techniques, common to steel and superalloy investment foundries, for producing high-quality, low-cost titanium castings. Program objectives included: (1) development of a low-melting titanium alloy displaying adequate tensile properties, (2) development of low reactivity ceramics for use in melting crucibles and investment mold facecoats, (3) establishing an induction melting and vacuum casting capability using the above technologies.

Alloy investigations conducted, by RMI Company, evaluated eight binary titanium alloy systems. Low melting alloys from the titanium-copper system displayed the greatest potential with the Ti-13Cu composition being selected as a base alloy for further work. Several Ti-13Cu base alloys exhibited an attractive combination of mechanical properties, heat treatment response and melting temperature.

Laboratory ceramic material investigations identifed yttria as the least reactive material, with thoria and a heavy-rare-earth-mixed-oxide (60% yttria) material also exhibiting low reactivity. Due to the poor thermal shock resistance of yttria, a titanium modified yttria material (Y_2O_3·15Ti) was developed for melting crucible applications. Initial mold investigations using the heavy-rare-earth-mixed-oxide (HREMO) were generally unsuccessful due to poor slurry stability and fine particle size.

Three low-melting alloys and the above ceramic materials were used in casting trials, at the AiResearch Casting Company to provide cast material for tensile property, chemical analysis, and metallographic evaluations. The alloys included Ti-13Cu-4.5Ni (melting temperature 2425°F), Ti-13Cu (2630°F) and Ti-13Cu-1.5Al (2605°F). The cast Ti-13Cu-1.5Al alloy demonstrated the ability to meet program tensile property goals, which were established as follows:

	UTS, ksi	YS, ksi	Elong.
Room Temperature	100	90	5%
600°F	60	50	5%

The Ti-13Cu-4.5Ni alloy, cast into an advanced experimental mold system (Y_2O_3 plus Y_2O_3/K_2SiO_3 binder), experienced minimal mold/metal reaction and the as cast surfaces exhibited low levels of contamination.

The concept of producing titanium castings using low-melting alloys, vacuum induction melting in a ceramic crucible, and low-reactivity investment molds, was successfully demonstrated, and offers the potential for further production of low-cost, high-quality, titanium castings.

PREFACE

This final technical report covers work submitted by the AiResearch Manufacturing Company of Arizona, POB 5217, Phoenix, Arizona (85010), performed under Contract F33615-74-C-5055, Project/Task Number 73510818, from 15 February 1974 to 15 January 1976. This report has been given the AiResearch internal designation of 76-311721 and was submitted by the authors for approval in May 1976.

This 24-month contract was under the technical direction of Mr. W. R. Kerr (AFML/LLS) of the Air Force Materials Laboratory, Metals and Ceramics Division, Wright-Patterson Air Force Base, Ohio, 45443.

Mr. John A. Petrusha (AiResearch) was the program manager, and Don R. Schuyler (AiResearch) the principal investigator. The assistance of Messrs. Keith W. Benn (AiResearch), Muneo Fujii (AiResearch), Dave W. Richerson (AiResearch), Richard F. Roe (Coors Porcelain) and Dave Mustoe (Coors Porcelain) is gratefully acknowledged. The contributions of AiResearch Casting Company personnel, under the direction of Hal Simmons and Emil Raulin are appreciated.

Alloy development activities for the program were subcontracted to RMI Company, Niles, Ohio and supervised by G. S. Hall, under the technical management of S. R. Seagle, Manager of Research. Special appreciation is extended to Dr. H. B. Bomberger, for his interest and helpful discussions during the course of this investigation. Appreciation is further extended to the RMI Company, Research and Development staff for providing able assistance in conducting the work under this contract.

SUMMARY

This program was conducted to develop the technologies necessary to establish a low cost aproach for producing titanium investment castings. The low cost approach was based on using simpler and cheaper melting and casting techniques common to steel and superalloy investment foundries for producing high-quality low cost titanium castings. The program was organized to develop the materials, and adapt applicable technologies common to these foundries, to titanium castings production as follows:

- o A titanium alloy having a melting point considerably below existing commercial alloys, to reduce its reactivity with crucible and mold materials, was required.
- o A melting crucible material was required that displayed minimum reactivity with molten titanium and could be used for repeated melting operations.
- o Developing a mold system that would contain the low-melting alloy with minimum cast surface contamination, was required.
- o Establish an induction melting and vacuum casting capability that involved these technologies.

The program was organized into two phases, with Phase I encompassing alloy and ceramic materials development activities and Phase II encompassing process development and production of titanium castings using Phase I technology. Objectives were to develop materials and procedures necessary for titanium investment castings production from low-melting titanium alloys (2200-2400°F), capable of meeting the following tensile property goals:

Temperature (°F)	UTS (ksi)	YS (ksi	Elongation (%)
75	100	90	5.0
600	60	50	5.0

During Phase I, RMI Company under subcontract activities evaluated a variety of low-melting titanium alloy systems. This included 32 alloys from 8 titanium binary systems which were evaluated metallurgically and by mechanical property testing. Alloys from the titanium-copper system displayed the greatest potential, and composition Ti-13Cu was selected as a base alloy for further work. Several Ti-13Cu base alloys exhibited an attractive combination of mechanical properties, heat treatment response, and melting point.

Phase I work also included evaluations of a variety of ceramic materials for reactivity with low-melting titanium alloys. Controlled laboratory melts of low-melting titanium alloys were made in small crucibles from candidate ceramic materials. After solidification, titanium alloy melts were evaluated for contamination by chemical analysis, metallographic examination and hardness testing. This work identified yttria as the least reactive material, with thoria and a heavy-rare-earth-mixed-oxide (60 percent yttria) material also exhibiting low reactivity. Due to poor thermal shock resistance of yttria, a titanium modified yttria material ($Y_2O_3 \cdot 15Ti$) was developed for melting crucible applications. Reactivity of this modified yttria composition was slightly greater than pure yttria, but comparable to thoria and heavy-rare-earth-mixed-oxide. A limited amount of laboratory development work was also conducted, with the more promising ceramic materials, to identify binder systems and processing techniques that would allow investment mold fabrication.

During Phase II, two vacuum investment casting trials were conducted, at AiResearch Casting Company, using Phase I developed

materials. The initial casting trial utilized Y_2O_3·15Ti melting crucibles and two low-melting titanium alloys (Ti-13Cu and Ti-13Cu-4.5Ni). A total of fifteen castings were made using only the standard zircon shell mold system, due to slurry stability and sintering problems encountered with the experimental mold system. This casting trial demonstrated viability of the Y_2O_3·15Ti melting crucible and satisfactory castings were produced despite surface quality problems resulting from mold/metal reactions with the zircon mold system. Testing demonstrated attractive tensile properties for both low melting alloys in the cast form, despite oxygen contamination levels near 0.4 percent and the presence of Y_2O_3 inclusions.

For the second casting trial, the Ti-13Cu alloy was modified by adding 1.5 percent aluminum to improve the tensile strength. The Y_2O_3·15Ti melting crucible was again used for this casting trial along with several experimental and current production mold systems. This casting activity was successfully completed and metallurgical and mechanical property evaluations conducted. Significant internal porosity was present in the cast test bars from the primary mold system (graphite investment), due to the low mold preheat temperature. This porosity was eliminated by hot isostatic pressing (HIP) and in the HIP plus heat treat condition, the cast Ti-13Cu-1.5Al alloy satisfied program tensile property goals except for room temperature tensile elongation (4.7 versus a goal of 5.0 percent). Castings again displayed yttrium and oxygen contamination levels as well as yttria inclusions equivalent to those observed in the first casting trial. Casting evaluation also showed the experimental mold system with a yttria plus yttria/potassium silicate facecoat experienced little mold/metal reaction.

The concept of producing low-melting titanium alloy castings using vacuum investment melting and casting techniques was demonstrated. Casting contamination levels (0.2-0.4 percent oxygen and 0.2-0.5 percent yttrium) correlated directly to alloy melting,

and resultant casting process temperatures. Promising alloys based on the titanium-copper binary system, a ceramic melting crucible, and an advanced ceramic mold facecoat system were identified. Development of these technologies provides a strong foundation for future establishment of a low-cost investment casting process for producing titanium castings.

TABLE OF CONTENTS

	Page
Preface	iii
Summary	iv
List of Illustrations	xi
List of Tables	xv
1.0 INTRODUCTION	1
2.0 PROGRAM APPROACH	4
3.0 RESULTS AND DISCUSSION	7
3.1 Phase I Alloy Development	7
3.1.1 Alloy Evaluation Procedures	10
3.1.2 General Results	13
3.1.2.1 Ingot Structure	13
3.1.2.2 Chemical Analyses	14
3.1.2.3 Alloy Melting Points	15
3.1.2.4 Salt Spray Corrosion	15
3.1.2.5 Density Measurements	17
3.1.3 Task I - Investigations	17
3.1.3.1 Alloy Selection	17
3.1.3.2 Results	23
3.1.4 Task II - Investigations	30
3.1.4.1 Alloy Selection	30
3.1.4.2 Initial Tensile Property Evaluations	32
3.1.4.3 Additional Tensile Property Evaluations	34
3.1.4.4 Microstructural Evaluation	35
3.1.5 Task III - Investigations	37
3.1.5.1 Alloy Selections	38
3.1.5.2 Tensile Property Evaluation	39
3.1.5.3 Influence of Thermal Exposure on Tensile Properties	42
3.1.5.4 Microstructural Evaluation	42
3.1.6 Discussion of Alloy Evaluation	45
3.1.7 Summary - Alloy Development	53
3.2 Phase I Crucible/Mold Material Investigations	54
3.2.1 Material Procurement and Experimental Procedures	54
3.2.1.1 Control Alloy	55
3.2.1.2 Laboratory Crucibles	56
3.2.1.3 Special Firing of Laboratory Crucibles	59
3.2.1.4 Standard Laboratory Technique for Evaluating Ceramic Crucibles	61
3.2.1.5 Additional Crucible Evaluations	66
3.2.1.6 Chemical Analysis Techniques	67
3.2.1.7 Mold Material Investigations	68

TABLE OF CONTENTS (Continued)

		Page
3.2.2	Results and Discussion - Crucible/Mold Materials	70
3.2.2.1	Task I Crucible Investigations	70
3.2.2.2	Task II Crucible Investigations	78
3.2.2.3	Task III Crucible Investigations	91
3.2.2.4	Mold Investigations	100
3.3	Summary - Phase I	105
3.4	Selection of Materials for Phase II Casting Development Activities	106
3.4.1	Alloys	107
3.4.2	Crucible	107
3.4.3	Mold Facecoat Material	107
3.5	Casting Trial "A"	108
3.5.1	Material Procurement	108
3.5.1.1	Alloy	108
3.5.1.2	Melting Crucibles	122
3.5.1.3	Thermocouple Protection Tubes	123
3.5.2	Mold Development	124
3.5.2.1	Material Procurement	124
3.5.2.2	Facecoat Investigations	126
3.5.2.3	Test Mold Fabrication	127
3.5.3	Foundry Activities	130
3.5.3.1	Mold Fabrication	132
3.5.3.2	Casting Process	132
3.5.3.3	Nondestructive Evaluation of Castings	139
3.5.3.4	Heat Treatment of Cast Tensile Samples	141
3.5.3.5	Tensile Test Evaluation	141
3.5.3.6	Chemical Analysis Results	143
3.5.3.7	Microstructure Evaluation	147
3.5.3.8	Hardness	158
3.5.4	Summary - Casting Trial "A"	158
3.6	Casting Trial "B"	159
3.6.1	Selection of Materials	160
3.6.1.1	Alloy	160
3.6.1.2	Melting Crucible	160
3.6.1.3	Mold Systems	161
3.6.2	Material Procurement	161
3.6.2.1	Alloy	161
3.6.2.2	Melting Crucible Fabrication	166
3.6.2.3	Thermocouple Protection Tube Fabrication	166
3.6.3	Mold Development	167
3.6.4	Foundry Activity	168

TABLE OF CONTENTS (Continued)

	Page
3.6.4.1 Mold Fabrication	168
3.6.4.2 Casting Process and Parameters	171
3.6.4.3 Nondestructive Evaluation of Castings	175
3.6.4.4 Heat Treatment of Cast Tensile Samples	178
3.6.4.5 Tensile Test Evaluations	178
3.6.4.6 Chemical Analysis Evaluation	182
3.6.4.7 Microstructural Evaluations	184
3.6.5 Summary - Casting Trial "B"	192
3.7 Summary - Phase II	195
4.0 CONCLUSIONS AND RECOMMENDATIONS	198
4.1 Conclusions	198
4.2 Recommendations	199
APPENDIX A - Chemical Analysis Results	200
APPENDIX B - Compilation of Tensile Properties	205
APPENDIX C - Compilation of Phase I Ingot Alloy Microstructures	224
APPENDIX D - Fabrication and Materials for Crucible/Mold Investigations	252
APPENDIX E - Experimental Mold Facecoat Slurry Compositions and Properties	262
APPENDIX F - Initial Selection of Ceramic Materials	280
APPENDIX G - Detailed Description of Investment Casting Procedures	284
REFERENCES	289

LIST OF ILLUSTRATIONS

Figure No.	Title	Page
1	Program Flow Diagram	5
2	Schematic for Phase I, Alloy Selections	9
3	Cutting Schematic for Transverse Ingot Slices and Test Samples	11
4	Typical As-Melted Ingot Microstructures for Several Alloy Systems	27
5	Typical Heat Treated Ingot Microstructures for Several Alloy Systems	29
6	Typical Microstructure From As-Melted 4.5-Inch-Diameter Ti-Cu Ingots	44
7	Typical Microstructures of Annealed (1560°F-1hr-FC) Material From 4.5-Inch-Diameter Ti-Cu Ingots	46
8	Relationship Between Elongation and Yield Strength of Ti-Cu Alloys	48
9	Experimental Melting Points of Titanium-Copper Alloys Compared With Liquidus Temperatures From the Literature	52
10	Appearance of Typical Laboratory Crucibles in a Range of Sizes and Fabrication Techniques Procured During Phase I Ceramic Investigations	58
11	Standard Arrangement for Thermal Treatment of Ceramic Crucibles	60
12	Side and Top Views of the Special Fired Crucibles Used in Task II Melting Experiments	63
13	Induction Furnace Used for Laboratory Melting Experiments	64
14	Standard Melt Run Experimental Arrangement, Which is Placed Within an Induction Coil for Heating of the Tantalum and Carbon Susceptors	65
15	Typical Microstructure of Ti-2.7Be Melts Conducted in Crucibles of Y_2O_3, Y_2O_3·15Ti, ThO_2 and Heavy Rare Earth Mixed Oxides	74
16	Alpha Case Contamination of the Surface of Ti-2.7Be Melts Made in Three Crucibles	75
17	Typical Microstructures at the Crucible/Melt Interface for Laboratory Melts of Ti-2.7Be Alloy in Y_2O_3, HREMO, and ThO_2 Crucibles	86
18	Typical Microstructures at the Crucible/Melt Interface for Laboratory Melts of Ti-10Cu, Ti-9Fe-0.03Y and Ti-16Cu Alloys in Y_2O_3 Crucibles	90
19	Microstructure of Y_2O_3·15Ti Crucibles (Task III, Group 2) Fired at Various Temperatures	96
20	Microstructures of HREMO·8Ti Crucibles (Task III, Group 2) Fired at Various Temperatures	97
21	Ingot Sectioning Diagram and Sample Locations for Ti-13Cu and Ti-13Cu-4.5Ni Alloys Used in Phase II Casting Trials	110
22	Typical Microstructures of the Phase II Ti-13Cu and Ti-13Cu-4.5Ni Alloys in the As-Melted and in the Annealed Conditions	112
23	Typical Microstructures of the Phase II Ti-13Cu Alloy (Heat 20056) Showing the Effect of Various Aging Treatments After High Temperature Annealing	113

LIST OF ILLUSTRATIONS (Continued)

Figure No.	Title	Page
24	Typical Microstructures of the Phase II Ti-13Cu-4.5Ni Alloy (Heat 25057) Showing the Effect of Various Aging Treatments After High Temperature Annealing (1760°F-1 hr-ac)	114
25	High-Cycle Fatigue Resistance of Heat-Treated Ingot Material for Ti-13Cu and Ti-13Cu-4.5Ni Alloys	118
26	Process Flow Diagrams for the Preparation of HREMO and Heavy Rare Earth Concentrates (HREC)	125
27	Appearance of Wax Pattern and Experimental Ceramic Investment Mold Used for Evaluation of Candidate Mold Materials	129
28	Flow Diagram for Casting Trial "A" Illustrating Sequence of Events Leading to Castings Poured Into ACC Molds But Not Into Experimental Low-Reactivity Molds as Originally Scheduled	131
29	Typical Appearance of Experimental Molds (Composition CC2) Illustrating Severe Spalling of Facecoats in Cup Area. Molds Fired at 1900°F for 1 Hour Were All Unusable for Further Casting Operations.	133
30	Appearance of Several Casting Trial "A" Ti-13Cu (P8, P10, P11) and Ti-13Cu-4.5Ni (P12, P13, P14, P15) Castings. Alloys Induction Melted in the Y_2O_3 Coated Y_2O_3·15Ti Crucible and Poured Into ACC Zircon Facecoat Mold System. Pour 15 is the Remains of the Melting Crucible With the Final Charge Solidified in Place.	137
31	Typical Appearance of Test Bar Cluster Casting	140
32	Plot of Alloy Oxygen Content Versus Yield Tensile Strength for Ti-13Cu and Ti-13Cu-4.5Ni in the As-Cast Condition	146
33	Microstructure of Ti-13Cu Cast Into ACC Standard Zircon Mold System	148
34	Microstructure of Ti-13Cu-4.5Ni Cast Into ACC Standard Mold System (Zircon)	149
35	Microstructure of Ti-13Cu-4.5Ni Alloy Cast Into ACC Zircon Mold System. Casting is the GTCP660 Cooling Fan and Microstructures Are of a Blade.	151
36	Electron Microprobe X-Ray Images of Second Phase Particle in Cast Ti-13Cu-4.5Ni Alloy After Melting in a Y_2O_3·15Ti Crucible During Casting Trial "A: (Pour 5)	152
37	Microstructure of Fracture Surfaces of Ti-13Cu Alloy Tensile Specimens Illustrating Shrinkage(S) and Porosity(P) in Top Figure and Inclusion Defects (Arrow) in Bottom Photo	153
38	Microstructure of Ti-13Cu-4.5Ni Alloy Solidified in Y_2O_3·15Ti Melting Crucible	155
39	Interior Microstructures of Y_2O_3·15Ti Plus Y_2O_3 Layer Crucible After Use for Casting Trial "A"	156
40	Microstructure of Y_2O_3·15Ti Plus Yttria Layer Crucible (No. 3) After Casting Trial "A" at Side Wall, Located Above But Near Melt Line	157

LIST OF ILLUSTRATIONS (Continued)

Figure No.	Title	Page
41	Typical Microstructures of the Phase II Ti-13Cu-1.5Al Alloy in the As-Melted and Heat Treated Conditions	164
42	Flow Diagram for Casting Trial "B"	169
43	Appearance of Various Molds Fabricated for Use in Casting Trial "B"	170
44	Appearance of Trial "B" Castings	173
45	Appearance of Ti-13Cu-1.5Al Alloy Cast Into the Howmet Monograf Mold (P-19)	176
46	Appearance of Ti-13Cu-4.5Ni Alloy Cast Into Experimental Y_2O_3-Potassium Silicate Mold (P-18)	177
47	Typical Microstructures of Cast Ti-13Cu-4.5Ni Alloy Illustrating Surface Structures Resulting From Two Mold Systems	185
48	Typical Microstructures of Cast Ti-13Cu-1.5Al and Ti-13Cu Alloys. Illustrates Surface Structures Resulting From Contact With Three Mold Systems.	187
49	Plot of Alloy As-Cast Microhardness as a Function of Distance From the Cast Surface for Alloys Cast Into Several Mold Systems	188
50	Typical Microstructures for Cast Ti-13Cu-1.5Al in the As-Cast, HIP, and Heat Treated Conditions	189
51	Typical Microstructures for Cast Ti-13Cu-4.5Ni in the As-Cast, HIP and Heat Treated Conditions	190
52	Typical Microstructures of As-Fabricated $Y_2O_3 \cdot 15Ti$ Melting Crucible Fired at 3000°F	193
53	Typical Microstructures of $Y_2O_3 \cdot 15Ti$ Crucible (Fired at 3000°F) Used in Casting Trial "B"	194

LIST OF ILLUSTRATIONS

APPENDIX C

Figure No.		Page
C-1	As-Melted Microstructures of Task I Compositions (250X)	225, 226, 227
C-2	Heat Treated Microstructures of Task I Ingots (250X)	228, 229, 230 231, 232, 232
C-3	As-Melted Ingot Microstructures of Task II Compositions Excluding Be-Containing Alloys (250X)	234, 235
C-4	Heat Treated Task II Ingot Microstructures Excluding Be-Containing Alloys (250X)	236, 237, 238, 239
C-5	As-Melted Ingot Microstructures of Ti-13Cu-3Al and Task III Compositions (250X)	240, 241, 242
C-6	Example of Duplex Heat Treatment Applied to the Ingot Ti-13Cu Composition (250X)	243
C-7	Heat Treated Ingot Microstructures of Ti-13Cu-3Al and Task III Compositions (250X)	244, 245, 246, 247, 248

LIST OF ILLUSTRATIONS APPENDIX C (Continued)

Figure No.	Title	Page
C-8	Ingot Microstructures of Beryllium Containing Task II Compositions (250X)	249
C-9	Heat Treated Ingot Microstructures of Beryllium Containing Task II Compositions (250X)	250, 251

LIST OF ILLUSTRATIONS
APPENDIX E

Figure No.	Title	Page
E-8-1	Appearance of Colal P-Alumina Facecoat Mold After Firing at 1900°F (1040°C)	276
E-8-2	Appearance of Y_2O_3-Silicate Facecoat Mold Fired at 1900°F (1040°C)	277
E-8-3	Appearance of Y_2O_3-Silicate and Facecoat Single Test Bar Molds	279

LIST OF TABLES

Table No.	Description	Page
1	Summary of Melting Point Determinations Performed on Selected Alloys	16
2	Property Summary of Best Phase I, Task I Alloy Compositions	25
3	Microstructure Features of Phase I, Task I Arc-Melted Compositions	26
4	Property Summary of Initial Best Phase I, Task II Alloy Compositions	33
5	Summary of Heat Treated Room Temperature Tensile Properties of Tasks I and II, Ti-Cu Alloys	36
6	Summary Room Temperature Properties for Phase I, Task III Alloys, Ti-13Cu, and Ti-13Cu-3Al Alloys	40
7	Room Temperature Tensile Properties of Five Alloys Before and After Thermal Exposure	43
8	Strength Consideration for Ti-Cu Alloy Development	50
9	Firing Procedures Used to Prepare Special Crucibles for Task II Melting Experiments	62
10	Chemical Analysis Results for Ti-2.7Be Alloy Melted in Task I Crucibles at Temperatures of 2870°F	73
11	The Influence of Temperature and Holding Time on the Contamination of the Ti-2.7Be Alloy	77
12	Chemical Analysis Results for Ti-2.7Be Alloy Melted in Phase I, Task II Crucibles at a Temperature of 2870°F	82
13	Comparison of Alloy Contamination Levels for Melts Made in Task I and Task II Crucibles	84
14	Influence of Crucible Materials on the Contamination of Low Melting Titanium Alloys	88
15	Chemical Analysis Results for Ti-2.7Be Alloy Melted in Phase I, Task III Crucibles at a Temperature of 2870°F	94
16	Results of Special Y_2O_3·15Ti Crucible Melt Run and Crucible Fabrication Summary	98
17	Task I of Phase II Arc-Melted Ingot Rockwell A Hardness and Tensile Properties Compared to Phase I Results	111
18	Property Data From Heat-Treated As-Melted Phase II Ingots of Ti-13Cu and Ti-13Cu-4.5Ni Compositions for Casting Trial "A"	116
19	Comparison of High Cycle Fatigue Data for Ingot Ti-Cu Alloys, Ti-6Al-4V, Ti-5Al-2.5Sn, Aluminum and Magnesium Alloys	119
20	Tensile Properties of Ingot Alloys Before and After Thermal Exposure	121
21	Facecoat Candidates Selected for Test Mold Fabrication	128
22	Casting Trial "A": Melting Data and Pour Parameters	136
23	Summary of Casting Trial "A" Tensile Properties for Ingot and Cast Ti-13Cu and Ti-13Cu-4.5Ni Alloys	142

LIST OF TABLES (Continued)

Table No.	Description	Page
24	Influence of Alloy Melting Point and Melting Crucible Composition on Cast Alloy Contamination	144
25	Property Data From Phase II Ingot of Ti-13Cu-1.5Al (Heat 25254) Alloy	163
26	Casting Trial "B": Melting Data and Pour Parameters	174
27	Tensile Property Summary for Ti-13Cu-1.5Al Alloy	180
28	Room Temperature Tensile Property Summary for Cast Ti-13Cu-4.5Ni Alloy	181

LIST OF TABLES
APPENDIX A

Table No.	Description	Page
A-1	Chemical Composition of Phase I Ingots	201
A-2	Chemical Compositions of Phase II Ingots Used for Casting Trials	202
A-3	Compilation of Chemical Analysis Results for Casting Trial "A"	203
A-4	Compilation of Chemical Analysis Results for Casting Trial "B"	204

APPENDIX B

Table No.	Description	Page
B-1	Summary of Room Temperature Tensile Properties and Hardness for All Phase I Alloys	206 through 216
B-2	Alloy Ti-13Cu: Compilation of Tensile Properties for Phase II, Task II Test Bar Castings	219
B-3	Alloy Ti-13Cu-4.5Ni: Compilation of Tensile Properties for Phase II, Task II Test Bar Castings	220
B-4	Tensile Properties (Room Temperature) for Bars Machined From Test Bar Casting Center Sprues	221
B-5	Additional Tensile Properties for Phase II, Task II Castings	222
B-6	Tensile Tests for Casting Trial "B"	223

LIST OF TABLES
APPENDIX D

Table No.	Description	Page
D-1	Fabrication and Properties of Crucibles Procured for Task I of Phase I	253
D-2	Fabrication and Properties of Crucibles Procured for Task II of Phase I	254
D-3	Fabrication and Properties of Crucibles Procured for Task III of Phase I	255
D-4	Firing Temperatures and Properties for Phase I Task III Crucibles	256
D-5	Chemical Composition and Properties for Several Lots of Yttrium-Oxide Used for the Program	257
D-6	Analytical Results for Several Lots of Titanium Powder Used for Crucible Fabrication	258
D-7	Fabrication History of Phase II, Casting Trial "A" Melting Crucibles	259
D-8	Fabrication History of Phase II, Casting Trial "B" Melting Crucibles	260
D-9	Properties of Heavy Rare Earth Concentrates Used for Laboratory Mold Investigations	261

LIST OF TABLES
APPENDIX E

Table No.	Description	Page
E-1	Group 2 Ceramic Mold Material Compositions and Properties	263
E-2	Influence of Firing Temperature on Properties of Group 3 Mold Facecoat Slurry Compositions	264
E-3	Compositions and Results for Group 4 Mold Facecoat Slurries Slip Cast Into Crucibles	265
E-4	Group Five Mold Facecoat Preparation and Properties	266, 267
E-5	Sintering Response of Group 5 Mold Compositions After Firing Bulk Samples at 1970°F for 1 Hour	268
E-6	Sintering Response of Group 5 Mold Compositions After Firing Bulk Samples at 2200°F	269
E-7	General Mold Fabrication Procedures	270, 271, 272
E-8	Experimental Mold Fabrication at AiResearch Casting Company	273 through 279

DEVELOPMENT OF TITANIUM ALLOY CASTING TECHNOLOGY

1.0 INTRODUCTION

Titanium casting production in the United States is limited to a few foundries, which all use skull melting in a water cooled copper crucible by the consumable and/or nonconsumable electrode method. Two basic casting process mold systems are used; ceramic investment molds using a nonreactive facecoat, and rammed graphite molds similar to those used for sand casting. Russian practice[1] involves consumable electrode melting into a graphite-lined, water-cooled copper jacket and molds fabricated from steel, graphite, alumina or sillimanite (Al_2SiO_5) lined with a graphite dispersoid.

At the present time, precision aerospace castings are expensive, due to high reject rates and rework efforts associated with quality problems. These quality problems relate directly to melting temperatures (~3000°F) and high reactivity of commercial titanium alloys. As a result, an objective of this program is to reduce titanium castings cost by using simpler and lower cost vacuum investment casting techniques, common to superalloy and steel foundries.

Conventional superalloy vacuum investment casting processes use induction melting in an uncooled ceramic crucible that provides accurate metal temperature control, melt thermal homogeneity, and molten metal superheating. In addition, significant

---

[1] Glasunov, S.G., "Precision Casting of Titanium, The Science, Technology, and Application of Titanium." Pergamon Press, New York, pp. 143-148, 1970.

preheating (2000°F) of ceramic molds is also possible with the conventional vacuum investment process, which reduces the temperature differential between the mold and molten alloy. These advantages contribute to improved casting quality, and result in minimum rejection rates and rework operation. However, the reactivity and melting temperature of existing commercial titanium alloys preclude the use of ceramic crucibles and mold materials normally employed in the vacuum investment casting process. Therefore, to use the conventional vacuum investment casting approach for producing low cost titanium castings, a low-melting titanium alloy, and an advanced, low-reactivity ceramic crucible and mold system, must be developed.

To achieve program objectives, development of a titanium alloy possessing good strength and adequate tensile ductility, while simultaneously displaying a sufficiently low melting temperature, was required. This would minimize the potential metal/ceramic reactions encountered in the casting operation. Attaining this objective was complicated by the fact that solute additions, made to reduce the melting point of titanium, result in formations of intermetallic compounds that reduce alloy ductility. To complement this low-melting alloy system, improved ceramic systems were also required. Prior work at AiResearch indicated that ceramic systems currently used in vacuum investment foundries were not adequate for melting or containing conventional titanium alloys and to a certain extent, low-melting titanium alloys. Therefore, development of cost-effective ceramic systems for melting crucibles and mold construction was pursued.

Successful completion of this program would develop technology that would provide a base to eventually allow any vacuum investment casting foundry to produce cast titanium components. This advancement would significantly reduce the cost of titanium castings, and result in the following benefits:

- Eliminate requirements for specialized melting equipment and processing techniques over those currently employed in vacuum investment foundries

- Provide greater capacity for production of titanium castings

- Promote significant manufacturing cost savings through replacement of selected cast and wrought titanium alloy parts

- Allow weight reduction by substitution for appropriate cast steel components

- Essentially eliminate corrosion problems (galvanic or general) currently experienced with magnesium and aluminum hardware

- Solve materials-related structural problems (creep) by replacing highly stressed magnesium and aluminum alloys

2.0 PROGRAM APPROACH

The overall program objective was to establish the materials technology necessary to develop a low cost approach for producing titanium alloy castings which further identified specific goals as listed below:

(a) Titanium Alloy - Development of a low melting (2200° - 2400°F) titanium alloy that would meet the minimum tensile properties shown below:

	UTS, ksi	YS, ksi	Elongation
o Room Temperature	100	90	5 percent
o 600°F	60	50	5 percent

(b) Crucible/Mold System - Development of ceramic materials and fabrication procedures for induction melting crucibles, and investment molds that result in minimum cast alloy contamination.

The original program was divided into three phases as shown in the flow diagram; Material Development, Casting Development, and Casting Optimization (see Figure 1). Under a revised program plan only the first two phases were conducted however, all three phases are briefly discussed below:

(a) Phase I, Material Development - This phase consisted of three sequential tasks involving concurrent alloy development and crucible/mold material investigations, which resulted in materials selection for Phase II casting development. Titanium alloy compositions with melting points ranging from 2400 - 2800°F, and anticipated room temperature tensile elongations of five percent, or greater, were evaluated. Tensile testing, chemical analysis, metallurgical evaluation and heat treatment studies were conducted with these alloys.

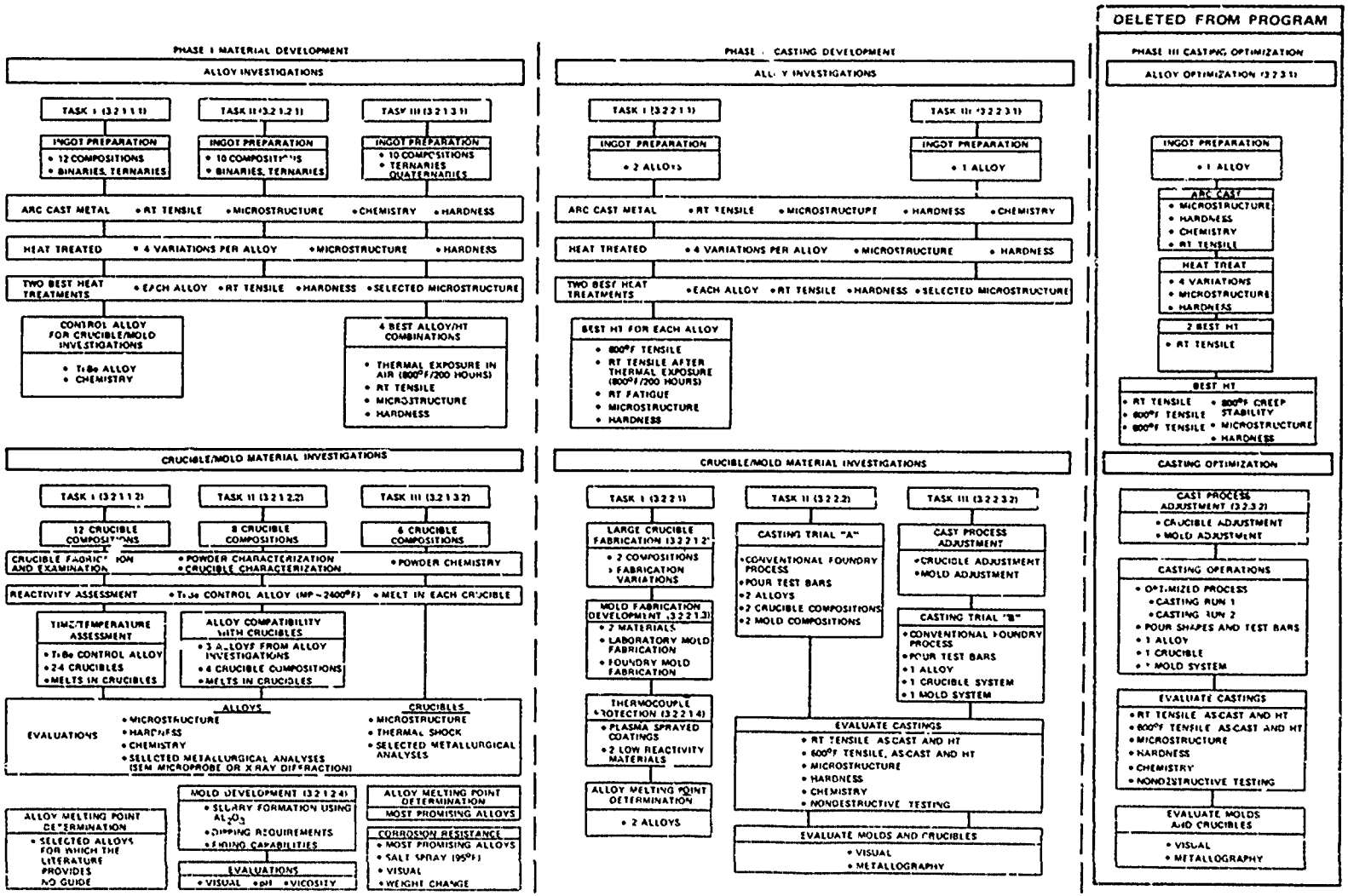


Figure 1. Program Flow Diagram.

Laboratory evaluation of potential low reactivity ceramic materials that could be used for melting crucibles and/or shell molds was also performed. Charges of a master low-melting (estimated 2570°F) titanium alloy (Ti-2.7Be) were melted in a variety of 1-inch diameter crucibles at standard conditions. These samples were then assessed for contamination using a combination of chemical analysis, metallography and hardness testing.

(b) Phase II, Casting Development - During this phase, the most promising titanium alloy and ceramic materials selected from Phase I were evaluated further as part of casting development activities. The selected alloys demonstrated a tolerance for contamination and displayed arc-melted ingot tensile ductilities of five percent or better. The crucible materials were selected on the basis of low reactivity and good thermal shock resistance, while the mold materials were allowed higher reactivity to minimize cost. In all cases, crucible and mold materials were selected to be cost-effective and not require sophisticated fabrication techniques to support the low-cost casting approach.

(c) Phase III, Casting Optimization - Phase III was to have consisted of a final casting operation using an optimized low-melting alloy and the most promising crucible and mold materials. In Phase III, complex shapes were to be cast to demonstrate process limits with respect to section size, contamination, and properties. Process reproducibility was to be assessed by casting two lots of samples followed by appropriate mechanical property and metallurgical evaluations. This phase was not conducted due to a revision in the program plan.

3.0 RESULTS AND DISCUSSION

The program was conducted as a two-phase effort to achieve the following objectives:

- o Phase I - Prepare and evaluate low-melting titanium alloys to identify systems with acceptable tensile properties (especially, ductility). Concurrent development and evaluation of candidate ceramic materials were also conducted for subsequent use as melting crucibles and mold facecoats in Phase II.

- o Phase II - Develop casting process requirements using the best alloys, crucibles and molds selected from Phase I work. Demonstrate the capability of meeting the program goals using the cast alloy(s).

The two major endeavors of Phase I consisted of alloy development and crucible/mold material investigations, which were each subdivided into three tasks and conducted in sequence (Figure 1). Alloy development (Section 3.1) was performed under subcontract by RMI Company and is discussed separately from the ceramic investigations (Section 3.2).

3.1 Phase I Alloy Development

The high-melting temperature (approximately 3000°F) and associated reactivity precludes the use of existing commercial titanium alloys with conventional investment casting ceramic systems. Pre-vious experimental work shows the feasibility of using conventional vacuum investment casting techniques for casting titanium alloys having significantly lower melting temperatures (approximately 2500°F). However, significant alloy development work was required to identify alloys that display the proper combination of melting temperature and mechanical properties.

With the above concept in mind, alloy additions to titanium can be primarily classified into the following two categories:

- Elements that produce significant reductions in melting temperature with varying impact on strength (iron, chromium, cobalt, nickel, copper, beryllium, manganese, and silicon).

- Elements that produce strength improvements with minimal impact on melting temperature (molybdenum, vanadium, columbium, tantalum, zirconium, aluminum, tin, oxygen and carbon).

Alloy investigations proceeded through three sequential tasks. This alloy development activity is summarized in Figure 2 showing the specific compositions evaluated in the three Phase I tasks. Initial alloy additions made to titanium were selected primarily on the basis of depressing the melting point without seriously degrading mechanical properties. Later ternary additions were made to some of the more promising low-melting alloys to improve strength and/or heat treatment response. This work resulted in the selection of two promising alloys for casting efforts of Phase II. Alloy development work discussion is divided into six sections as follows:

- Alloy Evaluation Procedure
- General Results
- Task I Investigations
- Task II Investigations
- Task III Investigations
- Discussion of Alloy Evaluations

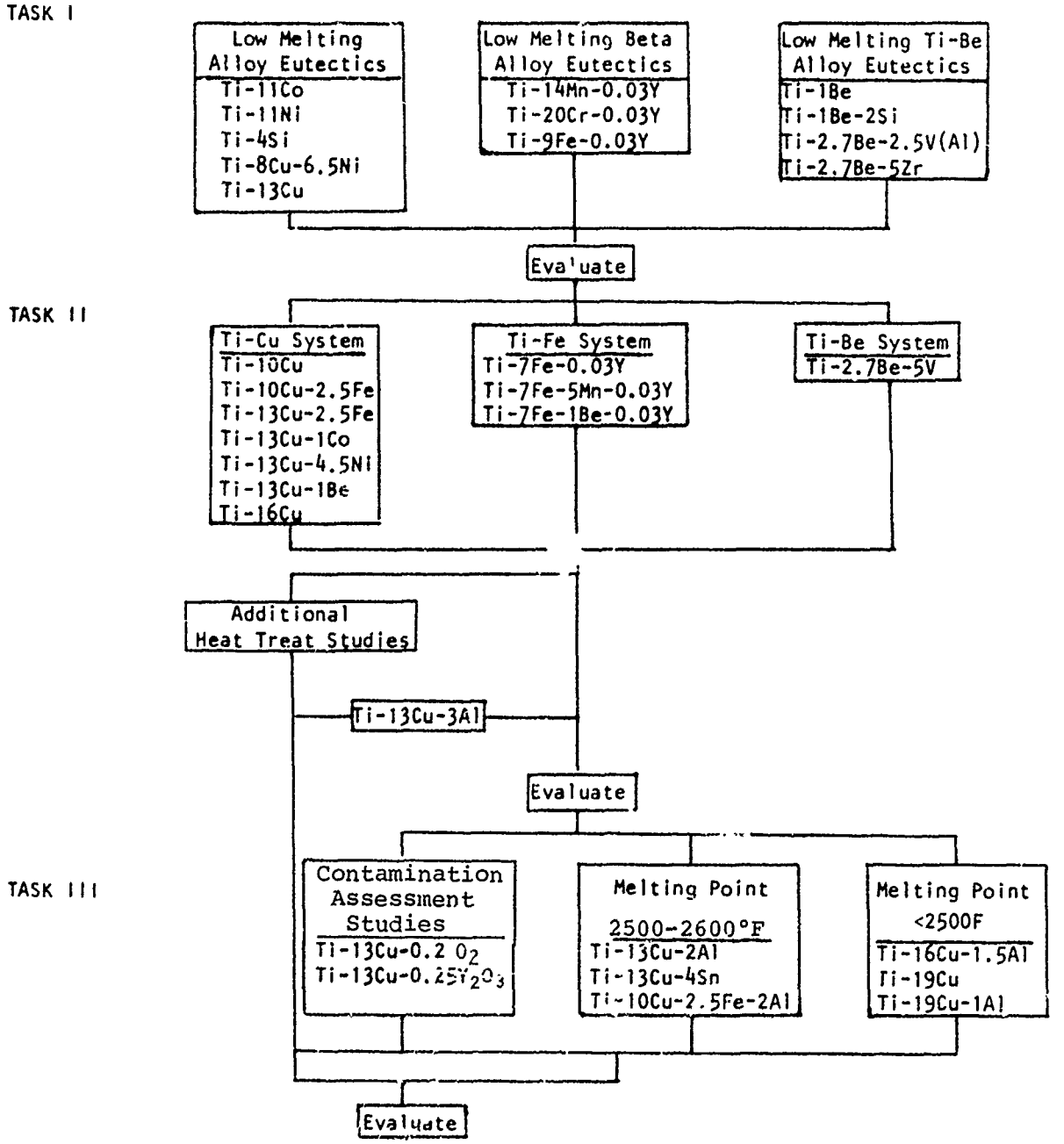


Figure 2. Schematic for Phase I, Alloy Selections.

3.1.1 Alloy Evaluation Procedures

Phase I alloy compositions were consumable-electrode arc melted under vacuum and remelted under argon (one atmosphere pressure). Exceptions were the Ti-13Cu and Ti-13Cu-1Be alloys which were arc melted a third time under argon. At the beginning of the program, all ingots were intended to be double-vacuum arc melted. However, arc control problems were experienced early in the second vacuum melting operation and the procedure was successfully changed to second-stage argon melting. The Ti-13Cu ingot (Heat 34029) was successfully double vacuum melted, but for consistency, was melted a third time under argon. Ti-13Cu-1Be (Heat 34267) showed segregation after second-stage melting, and was remelted under argon in an attempt to improve homogeneity. There was no evidence of cracking in any arc melted ingot, and therefore, slow cooling after melting, to prevent cracking, was not needed.

Final arc-melted ingots weighed approximately 17 pounds and were 4.5-inches in diameter by approximately 6 inches high. A larger 30-pound Ti-2.7Be (Heat 24038) control alloy ingot was melted to supply sufficient material for all Phase I crucible/melt studies (further discussed in Section 3.2.1.1).

After melting, ingots were sectioned for evaluation as shown in Figure 3. Transverse Section A was etched and a visual interpretation of the macrostructure for each ingot was recorded. Samples for hardness, oxygen and hydrogen analyses, and as-melted ingot tensile blanks were cut from slice A. As-melted ingot properties were considered as an important indicator of mechanical properties the alloys would exhibit in the cast condition. Chips saved from machining tensile blanks were used for chemical analysis samples to determine major alloying elements and remaining residual elements (Phase I chemical analysis results are compiled in Appendix A, Table A-1). Samples for hardness and metallography evaluation were heat treated using various time-temperature parameters and were ground to remove oxidation products. Slice B was

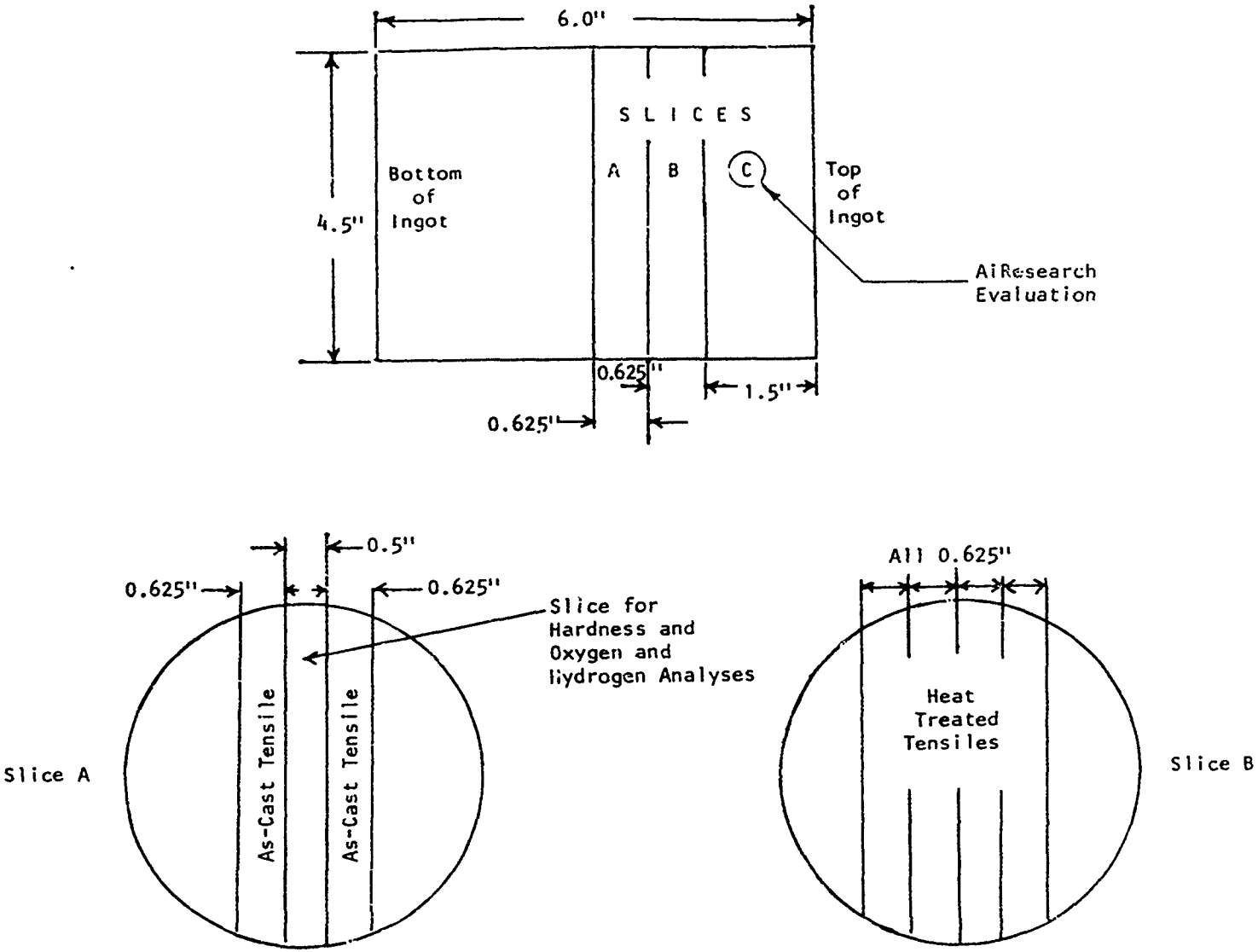


Figure 3. Cutting Schematic for Transverse Ingot Slices and Test Samples.

cut into four tensile blanks for heat treatment studies and tensile testing of the heat treated material. The 1.5-inch thick slice C, was transmitted to AiResearch for crucible melt studies and melting point determinations in Phase I.

The metallurgical evaluation for Phase 1 consisted of hardness studies on the as-melted ingots and at least four heat treatments on each alloy. Heat treatments on alloys containing active eutectoid additions (Co, Ni, Cu, Be and Si additions) consisted initially of heating to, and furnace cooling from, temperatures corresponding to 50°F below the respective eutectic, peritectic, and eutectoid temperatures for the various compositions. This was followed by long time exposure at temperatures below the alloys respective eutectoid temperature. Temperature selection for the sluggish eutectoid alloys (Cr, Fe and Mn additions) were generally based on heat treating above the respective beta transus or below the eutectoid temperatures. After heat treatment at the higher temperature, these alloys were furnace cooled, air cooled or water quenched. Aging treatments were conducted below the eutectoid temperatures. Based on hardness data and microstructure examination, at least two heat treatments were chosen for each composition and used to determine the heat-treated tensile properties. Complete hardness and tensile results for Phase I compositions are compiled in Appendix B, Table B-1. As-melted and heat treated microsturctures for all Phase I alloys are shown in Appendix C.

Thermal exposure tests were also conducted on five Phase I alloys to evaluate metallurgical stability and oxidation resistance. Two tensile samples from each alloy were exposed at 800°F for 200 hours in air. After exposure, the samples were tested at room temperature, with the surface oxide layer intact.

Melting points were determined for selected Phase I alloys by heating a small sample of the alloy in vacuum, under a partial

argon pressure. Initial and final melting temperatures were measured with an optical pyrometer. Some variability in these temperatures was observed due to slight reaction between the alloy and support plate (tantalum). However, it was estimated that reliability was within +45 and -20°F of the true liquidus temperature.

Densities for selected Phase I alloys were determined by water displacement. Salt spray corrosion tests, per ASTM Specification B117, were also conducted on selected Phase I compositions. One side of each alloy sample was polished to a metallographic finish at the beginning of the exposure and a scratch placed in the surface to locate a specific area. Microstructural examination of this area, and weight measurements were made periodically during an exposure of up to 1960 hours.

3.1.2 General Results

Observations applicable to alloy compositions, evaluated during Phase I, are presented in the following sections. Included are arc-melted ingot structure, chemical analyses, alloy melting point, salt spray corrosion and density. Specific results obtained in each of the three individual Phase I tasks are discussed in subsequent sections.

3.1.2.1 Ingot Structure

Generally, etched transverse slices, from the center of each ingot, exhibited equiaxed grains throughout the as-melted cross section. Several ingots had columnar grains from 0.06 to 1.5 inches in length extending in from the outside edge toward the equiaxed grains in the center. The Ti-13Cu-1Be ingot had the longest columnar grains. The second longest columnar grains were observed in the Ti-11Co ingot with columnar grains also found in all ingots containing 2.7 percent beryllium, and the beta alloy eutectics, which contained manganese, chromium and iron. The smallest equiaxed macro-grain (<1/64 inch) was found in the

Ti-13Cu-1Be alloy. All silicon-containing ingots had small equiaxed grain sizes (1/64 inch) as did the Ti-19Cu ingot. The largest equiaxed grains (up to 1/8 inch) were found in the low-melting beta alloys containing major amounts of manganese, chromium, and iron. All remaining ingots had equiaxed grain sizes between those discussed above. The equiaxed grain size of the majority of Ti-Cu compositions were 1/32 inch.

Etched ingots showed a melting pattern, which is evidence of macrosegregation, in the ingots containing 1 percent beryllium and in Ti-11Co, Ti-11Ni, Ti-9Fe-0.03Y, and Ti-14Mn-0.03Y. A melting pattern also existed in Ti-8Cu-6.5Ni and Ti-19Cu ingots. Other copper-containing ingots were free of this pattern indicating good melting behavior and freedom from gross alloy segregation.

3.1.2.2 Chemical Analyses

Chemical analyses of Phase I ingots (Appendix A, Table A-1) indicates that actual compositions agreed well with goals. Residual elements, carbon, nitrogen, and iron (except when iron was an alloying element) were normal and consistent within Phase I ingots. Oxygen content was 0.10 percent and greater, when major metallic additions were made as powder or flake. Oxygen was intentionally increased in Ti-13Cu (Heat 24273) and Ti-13Cu-0.25 Y_2O_3 (Heat 24281) ingots and the analyzed oxygen contents of these compositions agreed with the goal formulations. Hydrogen was not determined on all the ingots because low-melting titanium compositions had a tendency to promote loss of the platinum analytical susceptors. Initial hydrogen results were within the ranges expected for titanium ingots. Most low-melting compositions contained alloying additions in far greater amounts than typical for conventional titanium alloys. Standard analytical procedures for these elements are accurate at the usual lower levels, but the accuracy had not been established for the higher concentrations. However, analytical results for the major addition agreed reasonably well with formulated goals.

3.1.2.3 Alloy Melting Points

Most alloys had significantly lower melting points than originally estimated (Table 1). Copper-bearing alloys had melting points 45 - 85°F lower than predicted from the phase diagrams. For this reason, as well as the promising properties displayed by these alloys, most melting point experiments were performed on copper-bearing alloys.

Greater discrepancies were observed between predicted, and measured, melting points of ternary alloys, as compared with binary systems. Adding 4.5 percent nickel appeared more potent in depressing the melting point (188°F) than suggested from phase diagrams (120°F). Iron at 2.5 percent appeared predictable (78°F measured versus a phase diagram estimate of 90°F), but the measured effects of 1 percent cobalt (24°F) and 3 percent aluminum (18°F) were less than expected (60°F and 35°F, respectively) from phase diagrams.[2,3,4] These results indicate complex interactions with ternary and higher alloy systems with some potential for synergistic effects.

3.1.2.4 Salt Spray Corrosion

Salt spray corrosion tests conducted on selected alloys indicated that only minor weight changes occurred, with no significant microstructural evidence of corrosion observed after exposure for 1960 hours. All alloys appeared to have salt spray corrosion resistance similar to the Ti-6Al-4V control alloy.

---

(2) Hansen, M., "Constitution of Binary Alloys", McGraw-Hill, New York, 1958.

(3) Elliott, R.P., "Constitution of Binary Alloys", First Supplement, McGraw-Hill, New York, 1965.

(4) Shunk, F.A., "Constitution of Binary Alloys", Second Supplement, McGraw-Hill, New York, 1969.

TABLE 1

SUMMARY OF MELTING POINT DETERMINATIONS PERFORMED ON SELECTED ALLOYS

Alloy Composition		Number of Tests	Measured Melting Point °F*		Liquidus (°F) From Phase Diagrams**
Nominal	Analyzed		Liquidus	Eutectic or Solidus	
Ti-14Mn-0.03Y	12.5Mn	3	2695 ±30	(2515)	2805
Ti-1Be	1.2Be	3	2800 ±20	(2550)	2815
Ti-1Be-2Si	1.2Be, 2.0Si	3	2660 ±55	(2580 ±20)	2655
Ti-2.7Be	2.7Be	4	2600 ±40	(2175 ±50)	2570
Ti-10Cu	10.3Cu	3	2725 ±20	2580 ±30	2770
Ti-13Cu	13.1Cu	3	2613 ±20	2460 ±100	2680
Ti-13Cu-3Al	12.8Cu, 3.2Al	3	2595 ±30	2235 ±50	2645
Ti-13Cu-1Co	13.6Cu	2	2595 ±30	2200 ±30	2620
Ti-13Cu-2.5Fe	13.6Cu, 2.4Fe	2	2570 ±20	2165 ±40	2570
Ti-16Cu	16.3Cu	2	2515 ±20	2190 ±40	2600
Ti-8Cu-6.5Ni	7.8Cu, 6.6Ni	4	2515 ±20	(2350 ±20)	2675
Ti-13Cu-4.5Ni	13.7Cu, 4.5Ni	2	2425 ±20	2020 ±20	2560
Ti-19Cu	-	2	2417 ±20	2020 ±30	2510

*Melting points in parentheses are questionable.
**Based upon analyzed composition.

3.1.2.5 Density Measurements

Density measurements were made on a significant number of Phase I alloys. Most alloy systems of interest (lowest melting temperatures and those meeting mechanical property goals) had densities ranging from 0.17 to 0.18 lb/in^3, which were approximately 8 percent above that of Ti-6Al-4V.

3.1.3 Task I - Investigations

Phase I evaluation under this contract consisted of three sequential tasks that allowed continued alloy optimization toward achieving contract goals. Low-melting alloys, evaluated in Task I, included; eutectics (Ti-Ni, Ti-Cu, Ti-Cu-Ni, and Ti-Si); low-melting beta eutectics (Ti-Mn and Ti-Fe); Ti-Cr; and several Ti-Be eutectics that were hypoeutectic in composition.

3.1.3.1 Alloy Selection

The following twelve low-melting binary and ternary titanium alloy compositions were selected for Task I evaluation:

Group A	Group B	Group C
Ti-11Co	Ti-14Mn-0.03Y	Ti-1Be
Ti-13Cu	Ti-20Cr-0.03Y	Ti-1Be-2Si
Ti-11Ni	Ti-9Fe-0.03Y	Ti-2.7Be-2.5V-0.3Al
Ti-4Si		Ti-2.7Be-5Zr
Ti-8Cu-6.5Ni		

These compositions were as lean in alloy content as considered reasonable to enhance meeting program mechanical property goals. As a result, alloy melting points (2500 - 2850°F) were higher than the desired 2400°F maximum. Depending on the degree of reactivity and mechanical properties displayed by these alloys,

subsequent alloy additions could be made to further depress melting temperatures. The basis for selection of Task I alloys is as follows:

(a) Group A - Low-Melting Eutectics: Hypereutectoid Alloys

- Ti-11Co (Estimated Melting Point 2500°F) - The Ti-Co system has a low eutectic temperature of 1870°F (eutectic composition is Ti-28Co) and previously displayed low hardness[5,6] with one source[6] reporting exceptionally high ductility (75 percent elongation). At higher cobalt levels, embrittlement was encountered due to formation of the Ti_2Co[6] intermetallic, and at lower cobalt contents formation of omega was thought to cause low ductility.[7] Retained beta was reported in the Ti-Co system, after rapid quenching.[5,8,9] After slow cooling from below the eutectoid temperature, a pearlitic structure was reported for a Ti-9.9Co alloy.[10]

---

(5) Molchanova, E.K., "Phase Diagrams of Titanium Alloys", Daniel Davey & Co., Inc., New York, N.Y., 1965.

(6) Yakymyshyn, F.W., et al, "The Relationship Between the Constitutional and Mechanical Properties of Titanium-Rich Alloys of Titanium and Cobalt". Preprint of Forty-Second Annual Convention of the ASM, October, 1960, No. 198.

(7) Fedotov, S.G., et al, "The Physical Properties of Binary Alloys of Titanium in the Quench-Hardened State". Translation, NASA Scientific and Technical Information Facility, 1966 (N66-32990).

(8) Kolachev, B.A., and Livano, V.A., "Relationship of Structures Formed on Quenching Titanium Alloys to Equilibrium Phase Diagrams", Physical Metallurgy of Titanium. I.I. Kornilov, Editor, Science Publishing House, Moscow, 1964, NASA Technical Translation, NASA TT F-338, November, 1965, pp 67.

(9) Orrell, F.L., Jr., and Fontana, M.D., "The Titanium-Cobalt System", ASM Transactions, Vol. 47, 1955, pp 554-563.

(10) Mack, David J., "Nonferrous Eutectoid Structures", Metallography, Structures and Phase Diagrams, American Society for Metals, Metals Park, Ohio, 1973, Metals Handbook, Vol. 8.

- o Ti-13Cu (Estimated Melting Point 2700°F) - The Ti-Cu system has a low reported eutectic temperature at 1750°F (at a composition of a Ti-50Cu) and the beta phase is not retained at room temperature by quenching.[11] Hardness of beta-quenched specimens increased with copper content, but no minimum was reported. However, heat treatment, particularly slow cooling, was effective in altering hardness. Holding just below the eutectoid temperature and furnace cooling was reported to produce a pearlitic structure for a Ti-7Cu alloy.[9]

- o Ti-11Ni (Estimated Melting Point 2700°F) - Like the Ti-Cu system, eutectic temperature in the Ti-Ni system is near 1750°F (at Ti-27Ni). Retained beta was reported in a Ti-8Ni alloy after quenching from the beta phase field.[8,12] At nickel contents of 7 percent, and less, omega was observed[12] with low ductility reported for this alloy,[13] while at higher nickel contents somewhat better ductility was obtained. Previous RMI evaluations of Ti-17Ni compositions showed limited ductility (1 percent elongation) for annealed samples. Therefore, an alloy with 11 percent nickel appeared to offer the best opportunity for this system.

---

(11) Holden, F.C., et al, "Heat Treatment and Mechanical Properties of Ti-Cu Alloys". AIME Transactions, Vol. 203, 1955, pp 117-125,

(12) Margolin, Harold, et al, "Titanium-Nickel Phase Diagram". AIME Transactions, Vol. 197, 1953, pp 243-247.

(13) Kalabukhova, S.V., and Mikheev, V.S., "Investigation of Mechanical Properties of Ti-Mo-Ni Alloys". Translation National Lending Library for Science and Technology, November, 1970 (N71-36904).

- o Ti-4Si (Estimated Melting Point 2700°F) - Silicon is the most active beta eutectoid element that can be added to titanium (eutectic composition is at Ti-8.5Si and 2425°F) but the beta phase is not retained upon quenching. Hardness of Ti-Si alloys increased linearly with increasing silicon content.[14] At the 4 percent silicon level, a hardness of 311 Vickers and 6 percent tensile elongation were reported.[15]

- o Ti-8Cu-6.5Ni (Estimated Melting Point 2700°F) - Earlier RMI evaluation indicated that several Ti-Cu-Ni system composition displayed low hardness before and after annealing, as well as low melting points. The melting point of this ternary composition should be similar to those of Ti-11Ni and Ti-13Cu binary alloys, which were also included in Task 1.

(b) Group B - Low-Melting Beta Alloys

- o Ti-14Mn-0.03Y (Estimated Melting Point 2780°F) - This composition is hypoeutectoid with the eutectic composition at Ti-40Mn and 2150°F. Minimum hardness is believed to occur in the Ti-Mn system near 13 percent manganese[16] with the beta phase completely retained at this point. The omega phase forms at lower manganese concentrations, while at higher levels eutectoid decomposition

---

(14) Hansen, M., et al, "The Titanium-Silicon System", Transactions of the ASM, Vol. 44, 1952, pp 518-538.

(15) Epremian, E., "The Phase Diagram and Properties of Titanium-Silicon Alloys". Office of Naval Research, London, Technical Report ONRL-61-53, May, 1953.

(16) Maykuth, D.J., et al "The Titanium-Manganese, Titanium-Tungsten, and Titanium-Tantalum Phase Diagrams", Battelle Memorial Institute. Prepared for Wright Air Development Center, AF Technical Report 6516, Part 2, July, 1959.

reduces ductility. Independent studies at RMI showed modest ductility for Ti-14Mn (4.5 percent elongation) with improvement obtained by adding yttrium. Other experimental work indicated that heat treatment would provide improved ductility in alloys of this system.[17]

- Ti-20Cr-0.03Y (Estimated Melting Point 2820°F) - The Ti-Cr system (contains no eutectic) has a relatively high liquidus temperature of 2550°F at Ti-46Cr. This system, like those of Ti-Mn and Ti-Fe, exhibits sluggish eutectoid decomposition. The Ti-20Cr composition is the only beta alloy studied that is a hypereutectoid. A 100 percent metastable beta phase was retained after quenching a Ti-9Cr alloy from the beta phase field, but omega has been detected in binary alloys of less than 9 percent chromium.[5] Minimum hardness was reported for a Ti-20Cr alloy,[18] and a Ti-18Cr alloy quenched from the beta field reportedly displayed 31 percent tensile elongation.[19] Ti-15Cr alloy weldments displayed 4.5 percent tensile elongation, which was improved to 10 percent by heat treatment.[20] The Ti-20Cr composition selected for

(17) Holden, F.C., "Heat Treatment, Structure, and Mechanical Properties of Ti-Mn Alloys", AIME Transactions, Vol. 200, 1954, pp 169-184.

(18) Fontana, M.G., "Titanium-Chromium Binary Alloys", Ohio State University Research Foundation. Prepared for United States Air Force, Air Material Command, AF Technical Report No. 5946, May, 1950.

(19) Douglass, R.W., et al, "Metallurgical and Mechanical Characteristics of High-Purity Titanium Base Alloys", Battelle Memorial Institute, for Wright Air Development Division, WADC Technical Report 59-595, March, 1960.

(20) Meyer, Herbert M., and Rostoker, William "Study of Effects of Alloying Elements on the Weldability of Titanium Sheet", Armour Research Foundation, for Wright Air Development Center, Technical Report 53-230, May, 1953.

This program had a moderately high melting point (2820°F, but was expected to display good ductility.

- Ti-9Fe-0.03Y (Estimated Melting Point 2700°F) - This binary system is similar to the preceding two beta alloys in that 100 percent beta can be retained. This composition is hypoeutectoid with the eutectic at Ti-29Fe at a temperature of 1985°F. At less than 5 percent iron, omega phase occurred during cooling from the beta phase field[21] and ductility of a cast Ti-6.2Fe alloy was reported as 2.3 percent.[22] Minimum hardness was reported for Ti-10Fe after quenching from the beta field.[5] Previous RMI evaluation showed an early generation beta alloy, Ti-1Al-8V-5Fe, had good ductility after cooling from the beta field. Beta content of this alloy was equivalent to 7 percent iron.

(c) Group C - Low-Melting Ti-Be Alloy Eutectics: Hypoeutectoid Alloys

- Ti-1Be (Estimated Melting Point 2850°F)) - The eutectic composition is estimated to be near Ti-7Be [2,3,4,23,24] at 1800°F. Prior studies conducted at RMI and AiResearch revealed moderate ductility (2 to 4 percent) for Ti-Be alloys containing 2 to 5 percent beryllium (melting points

---

(21) Petrova, L.A., "Metastable Phases in the Alloys of Titanium with β-Alloying Metals", Titanium Alloys for Modern Technology, N.P. Sazhin, et al, NASA Technical Translation NASA TT F-596, March, 1970, pp 138-152.

(22) Hehner, N., et al, "Mechanical Properties of Cast Titanium-Iron and Titanium-Aluminum-Iron Alloys", Frankford Arsenal, Philadelphia, Pa., Report No. R-1416, November, 1957.

(23) Kaufman, L. and Nesor, H., "Computer Analysis of Alloy Systems", Technical Report ARML-TR-73-56, Manlabs, Inc., March 1973.

(24) Hunter, D.B., "The Titanium-Beryllium Phase Diagram up to 10 Wt-Pct Be", AIME Trans., V. 236, P. 900, June 1966.

of 2100 - 2700°F). The 1-percent beryllium composition was selected to obtain optimum ductility. If improved ductility was achieved, this composition would serve as a base for subsequent alloy modification.

- Ti-1Be-2Si (Estimated Melting Point 2690°F) - Adding silicon was expected to improve strength and lower the melting point of the above Ti-1Be alloy.

- Ti-2.7Be-2.5V-0.3Al (Estimated Melting Point 2500°F) - Earlier RMI and AiResearch work indicated Ti-2.7Be alloys achieved moderate ductility (3 percent). In addition, RMI studies also indicated vanadium additions improved Ti-2.7Be alloy strength substantially, without altering ductility. Vanadium promoted beta phase formation and was expected to provide the opportunity for obtaining improved ductility through heat treatment. The small aluminum addition was made because of the desirability to add vanadium as a vanadium-aluminum master alloy.

- Ti-2.7Be-5Zr (Estimated Melting Point 2500°F) - RMI studies also showed that zirconium additions to Ti-Be alloys, also improved strength but more important, appeared to improve ductility. Because of this possibility, the addition of zirconium was explored.

3.1.3.2 Results

Evaluation of Task I as-melted compositions showed that six of the twelve compositions had low as-melted ductility (less than 2 percent elongation) including Ti-11Co, Ti-11Ni, Ti-9Fe-0.03Y,

Ti-1Be-2Si, Ti-2.7Be-5Zr, and Ti-2.7Be-2.5V-0.3Al (complete tensile results in Appendix B, Table B-1). Ti-4Si, Ti-14Mn-0.03Y, Ti-8Cu-6.5Ni, and Ti-1Be alloys had modest tensile elongation (average of 1.9 to 4.0 percent). Ti-13Cu and Ti-20Cr-0.03Y displayed the best ductilities, which averaged 10 and 5 percent elongation, respectively (Table 2). These latter two compositions nearly met all the contract room temperature mechanical property goals in the as-melted condition.

In heat treated conditions, the Ti-20Cr-0.03Y alloy exhibited zero ductility after having shown promising as-melted ductility. After heat treatment, only alloys from the Ti-Cu and Ti-Be systems showed promise for meeting contract ductility goals (Table 2). However, alloys from both systems were low in strength and higher in melting point than desired. The Ti-13Cu alloy appeared to have more than adequate ductility while the Ti-8Cu-6.5Ni showed, with the heat treatments investigated, moderate ductility, increased strength and a lower melting point than Ti-13Cu. The moderate Ti-8Cu-6.5Ni alloy ductility was encouraging in that this alloy had one of the lowest measured melting points 2515°F of any Task I composition.

The twelve Task I alloy as-melted ingot microstructures, are shown in Appendix C, Figure C-1. Table 3 describes major microstructural features of the various compositions. For the first five (Group A) compositions, good ductility was associated, with a uniform pearlitic microstructure, and a discontinuous beta grain boundary as typified by Ti-13Cu and Ti-8Cu-6.5Ni (Figure 4). For the three Group B beta alloy eutectics, good as-melted ductility was associated with relatively clean beta grain boundaries and a secondary phase that did not contain sharp features as typified by Ti-20Cr-0.03Y (Figure 4). For beryllium-containing compositions (Group C) the best ductility was also associated with a uniform pearlitic structure, and a discontinuous grain boundary as shown by the Ti-2.7Be-5Zr alloy (Figure 4).

TABLE 2

PROPERTY SUMMARY OF BEST PHASE I, TASK 1 ALLOY COMPOSITIONS

Heat No	Nominal Composition	Actual or Estimated Melting Point,F	Room Temperature Tensile, As-melted UTS ksi	YS ksi	El %	RA %	Heat Treatments	Room Temperature Tensile Heat Treated, UTS ksi	YS ksi	El %	RA %
24106	Ti-1Be	2800[1]	87	72	3	2	1775F-1hr-FC	66	48	8	7
			84	68	3	2		64	49	6	5
							1775F-1hr-FC to	62	52	3	2
							1400F-4hr-AC	67	53	6	4
34029	Ti-13Cu	2613[1]	104	82	10	10[2]	1760F-1hr-FC	74	58	5	6
			105	82	10	12		74	59	5	5
							1560F-1hr-FC	85	62	13	16
								83	59	14	20
24107	Ti-2.7Be-5Zr	2570	92	80	1	-2	1775F-1hr-FC	54	49	5	3
			93	80	1	-3		52	48	4	1
							1775F-1hr-FC to	58	52	4	2
							1400F-4hr-AC	55	50	4	1
24108	Ti-2.7Be-2.5V-0.3Al	2570	92	87	1	-3	1775F-1hr-FC	85	74	2	<1
			96	82	1	-3		83	75	2	<1
							1775F-1hr-AC +	80	80	2	-4
							1400F-4hr-FC	93	79	2	1
24032	Ti-8Cu-6.5Ni	2515[1]	114	92	2	2[2]	1725F-1hr-FC	97	71	4	5
			114	84	6	6		97	71	4	6
							1450F-1hr-FC	95	64	6	8
								98	66	5	4[2]
PROGRAM GOALS		2400	100	90	5			100	90	5	

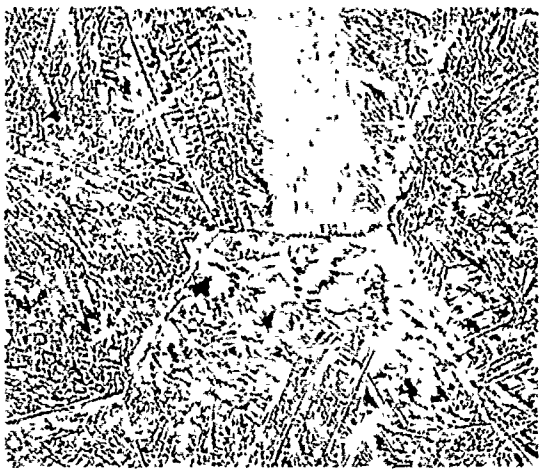
1. Experimentally determined
2. Broke at or near gage mark
3. Broke in shank of tensile

TABLE 3

MICROSTRUCTURE FEATURES OF PHASE I, TASK I ARC-MELTED COMPOSITIONS

Composition	Arc-Melted Ductility	ASTM Grain Size	Major Feature in Matrix	Grain Boundary	Secondary Feature in Matrix	Minor Feature in Matrix
Ti-xCo	Poor	6 - 1/2	Single phase constituent concentrated as islands at or near beta grain boundary	Very fine and relatively clean	Extremely fine pearlitic-type structure	Very small spheroid phase
Ti-13Cu	Good	00 - 1/2	Pearlitic-type structure	Discontinuous and width of one platelet		
Ti-11Ni	Poor	2 - 4	Clusters of single-phase constituent originating from grain boundary	Some continuous single-phase constituent	Large platelets of single phase constituent	Extremely fine-grained two-phase structure
Ti-4Si	Limited	2 - 4	Single-phase large needle-like precipitate	Almost continuous "Chinese Script" eutectic	Small spheroid phase	
Ti-8Cu-6.5Al	Limited	6 - 1/2	Pearlitic- ype structure coming out at grain boundary and extending into interior of grain	Discontinuous	Harder and appears as an extremely fine grained two-phase structure	
Ti-9Fe-.3Si	Poor	00	Small needle-like secondary phase	Needle-like phase is concentrated at and perpendicular to grain boundary. Denuded area away from grain boundary	Concentration of needle-like phase	Small spheroid phase
Ti-14Mn-.3Si	Limited	00	Sharp featured lath-like phase	Relatively clean with a discontinuous spheroid phase in grain boundary	Concentration of lath-like phase	Small spheroid phase
Ti-20Cr-0.03C	Good	00	Small-rounded secondary phase approaching a spheroid shape	Relatively clean	Concentration of rounded secondary phase	Even smaller spheroid phase
Ti-1Be	Limited	1 - 2	Pearlitic-type structure	Discontinuous secondary phase	Small pepper-like secondary phase	
Ti-1Be-Zr	Poor	3 - 4	Clusters of rounded secondary particles in a beta grain	Continuous phase with secondary particles	Small pepper-like secondary phase	
Ti-2.7Be-5Zr	Poor	5	Rounded secondary particles in beta grain	Continuous eutectic phase with discontinuous secondary particles	Concentration of a gray-colored phase at the grain boundaries extending inward to the grain	Small spheroid phase
Ti-2.7Be-2.5V-0.3Al	Poor	3 - 5	Small lath-like feature inside grain	Large width of continuous eutectic	Small spheroid phase	

[1] At subgrain boundaries in the beta grains



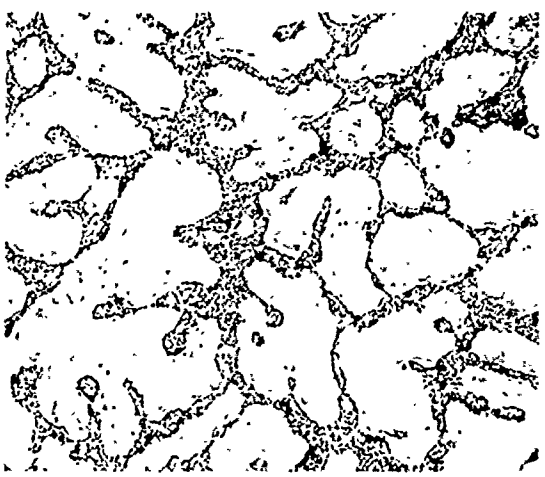
(a) Ti-13Cu (8726)
Heat 34029



(b) Ti-8Cu-6.5Ni (8735)
Heat 24032



(c) Ti-20Cr-0.03Y (8798)
Heat 24037



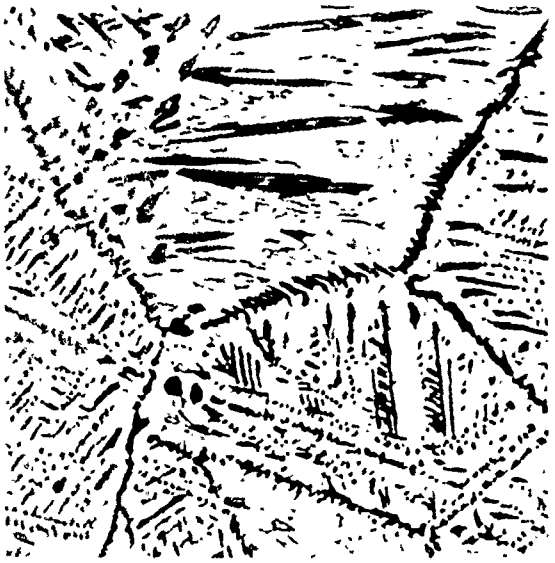
(d) Ti-2.7Be-5Zr (8992)
Heat 24107

Figure 4. Typical As-Melted Ingot Microstructures for Several Alloy Systems. (250X).

All heat treated microstructures for Task 1 alloys are presented in Appendix C, Figure C-2. The standard Kroll's etch developed reasonable microstructural features for these wide ranges of composition. Microstructures of heat treated samples were more uniform than those for the as-melted condition (Figure 5). Secondary phases generally have less alignment, after heat treatment, and tend to become rounded with lower heat treatment temperatures producing smaller secondary phase particles. All the alloys except the beta eutectics (Group B, Section 3.1.3.1), appear to have less continuous grain boundaries after heat treatment, while beta eutectics have very narrow grain boundaries. In the overaged condition, the Ti-20Cr-0.03Y alloy had a concentration of fine second phase particles around the beta grain boundary, which may be responsible for the low tensile ductility in this condition (Figure 5). As with arc-melted material, good tensile ductility on heat treating is associated with the formation of uniform microstructural features and discontinuous beta grain boundaries (Ti-13Cu and Ti-8Cu-6.5Ni alloys, Figure 5).

Hardness data for heat treated Task I ingots (also compiled in Appendix B) were generally lower than that for the as-melted ingot material, especially after furnace cooling from annealing temperatures. This lower hardness implied reduced strength and possible increased ductility.

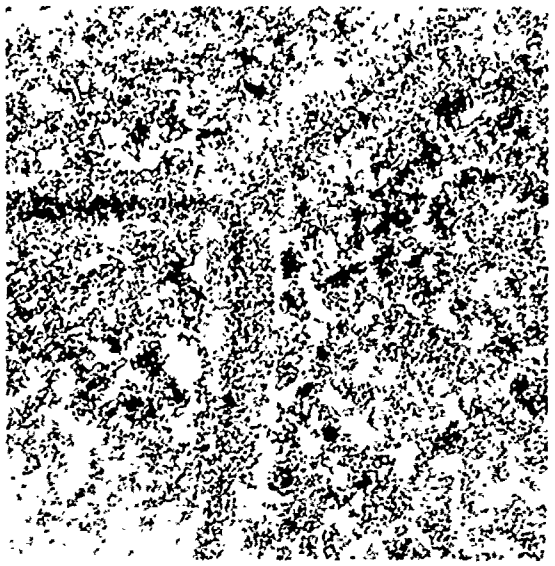
Task I alloys evaluation results specifically identified the copper bearing alloys as the most promising for obtaining low-melting points, while maintaining good tensile ductility. Microstructures for these alloys also indicated directions for future heat treatment activities to obtain the best combination of strength and ductility.



(a) Heat 34029 (8775)
Ti-13Cu
1760°F-1Hr-FC



(b) Heat 24032 (9258)
Ti-8Cu-6.5Ni
1450°F-1Hr-FC



(c) Heat 24037 (9264)
Ti-20Cr-0.03Y
1190°F-48Hr-AC



(d) Heat 24107 (9274)
Ti-2.7Be-5Zr
1775°F-1Hr-FC

Figure 5. Typical Heat Treated Ingot Microstructures for Several Alloy Systems.

3.1.4 Task II, Investigations

3.1.4.1 Alloy Selection

Based on Task I results alloys selected for Phase II consisted of the: Ti-Cu system; beta titanium alloys (Ti-Fe system) and Ti-2.7Be-5V alloy. Specific alloy compositions and selection basis are listed below:

Ti-Cu System	Ti-Fe System	Ti-Be System
Ti-10Cu	Ti-7Fe-0.03Y	Ti-2.7Be-5V
Ti-10Cu-2.5Fe	Ti-7Fe-5Mn-0.03Y	
Ti-13Cu-2.5Fe	Ti-7Fe-1Be-0.03Y	
Ti-13Cu-1Co		
Ti-13Cu-1Be		
Ti-13Cu-3Al		
Ti-16Cu		

(a) Ti-Cu System - Both Task I alloys containing copper displayed good ductility in as-melted ingot form as well as in a heat-treated condition. For this reason, the Ti-Cu system was selected as the primary candidate for further investigation, using a variety of elements to decrease the melting point and/or improve strength. This philosophy resulted in the five Ti-13Cu ternary compositions, all of which had estimated melting points near or lower than 2600°F. Ti-13Cu-4.5Ni was considered a more promising lower melting point variant of the Ti-8Cu-6.5Ni alloy, which had shown good properties in Task I. Ternary additions of iron, cobalt, beryllium and aluminum were made to increase strength, and decrease the melting point of the base Ti-10Cu and Ti-13Cu alloys.

(b) Ti-Fe System - No beta alloy from Task I (Ti-9Fe, Ti-20Cr, Ti-14Mn) showed attractive ductility at the composition levels evaluated. However, further evaluation of the best of the three alloys was considered desirable at a reduced alloy content, in an effort to obtain improved ductility. The Ti-Fe system was selected for further evaluation over the Ti-Cr and Ti-Mn systems because of:

- o Better heat treatment response.
- o Iron being a more effective melting point depressant.
- o Greater promise for higher strength.

A 7-percent iron content (MP - 2740°F) was chosen since this was considered below the level at which significant eutectoid compound formation occurred during aging. This composition (Ti-7Fe) afforded the greatest potential for obtaining improved ductility.

A 5-percent manganese addition of the Ti-7Fe binary was expected to depress the melting point to near 2680°F. The third alloy in this group involved a 1-percent beryllium addition (Ti-7Fe-1Be) to depress the melting point to near 2570°F. The choice of 1-percent beryllium was based on the reasonable ductility shown by the Task I Ti-1Be alloy. Like the Task I beta alloys these alloys contained a 0.03 percent yttrium addition, which has produced improved ductility in commercial and experimental titanium alloys.

(c) Ti-Be System - The last composition selected for Task II was the Ti-2.7Be-5V alloy, which had an estimated melting point of 2545°F and had shown promising ingot

ductility in earlier work. Vanadium was added as an elemental addition rather than as an aluminum-master alloy addition as in Task I. Compared to the Task I Ti-2.7Be alloys, the above alloy had a higher beta content (5 percent versus 2.0 percent vanadium) and no alpha stabilizing elements.

3.1.4.2 Initial Tensile Property Evaluations

Complete tensile and hardness results for the Task II alloys are shown in Appendix B. The Task II investigations continued to indicate the Ti-Cu system was superior to other alloy systems for achieving the contract goals.

Several of these alloys met or closely approached the room temperature mechanical property goals in the as-melted ingot or heat treated conditions. However, only one heat treat condition of one of the three Ti-7Fe system alloys met these goals after the initial heat treatment study. This alloy (Ti-7Fe-0.03Y), had an estimated melting point of 2740°F, which was considered too high compared to the Ti-Cu alloys. The Ti-Cu alloys displayed the best room temperature tensile properties of Task II alloys (summarized in Table 4). The Ti-10Cu alloy (actual melting point of 2725°F) met the room temperature tensile property goals in the as-melted condition and several alloys including Ti-13Cu-2.5Fe and Ti-13Cu-1Co approached these goals.

In the heat treated condition all alloys suffered reductions in strength but experienced improved ductility. The Ti-13Cu binary was used as a base to determine the effect of several ternary additions on properties. Evaluation of these alloys in the as-melted form as well as the heat treated condition showed the 2.5 percent iron addition resulted in the largest yield strength increase, 13-15 ksi in the Ti-13Cu base and 2-29 ksi in the Ti-10Cu base. A cobalt addition of 1.0 percent gave a small yield strength increase (2-5 ksi) and nickel had mixed effects

TABLE 4

PROPERTY SUMMARY OF INITIAL BEST PHASE I, TASK II ALLOY COMPOSITIONS

Heat No.	Nominal Composition	Actual or Estimated Melting Point, F	Room Temperature Tensile, As-melted UTS ksi	YS ksi	El %	RA %	Heat Treatments	Room Temperature Tensile Heat Treated, UTS ksi	YS ksi	El %	RA %
24220	Ti-10Cu	2725[1]	136	102	7	10	1760F-1hr-FC	107	75	10	10
			133	100	5	9		107	80	10	8
							1560F-1hr-FC	81	61	22	27
								82	61	24	27
24219	Ti-10Cu-2.5Fe	2680	148	128	2	3	1760F-1hr-FC	112	80	6	5
			156	132	4	5		112	78	8	7
							1560F-1hr-FC	106	77	14	12
								105	70	12	12
24221	Ti-13Cu-1Co	2595[1]	106	86	5	10	1760F-1hr-FC	81	63	6	4
			110	88	8	9		74	63	4	3
							1560F-1hr-FC	91	62	10	7
								89	62	10	8
24219	Ti-13Cu-2.5Fe	2570[1]	122	98	4	2	1760F-1hr-FC	77	70	5	3
			126	97	4	3		85	72	1	-[2]
							1560F-1hr-FC	100	75	6	4
								97	73	5	3
24264	Ti-13Cu-3Al		147	-	-	-	1560°F-1hr-FC	122	104	10	11
			143	-	-	-		118	106	5	6
24217	Ti-16Cu	2515[1]	97	75	9	10	1760F-1hr-FC	70	56	4	2
			97	76	9	12		74	56	5	2
							1560F-1hr-FC	82	56	9	9
								84	58	10	9
24224	Ti-13Cu-4.5Ni	2425[1]	92	78	-	-[2]	1760F-1hr-FC	75	59	3	<2
			103	76	6	4		78	62	3	<2
							1560F-1hr-FC	89	63	5	3
								87	65	5	3
PROGRAM GOALS		2400	100	90	5	-	--	100	90	5	-

1. Experimentally determined
2. Broke at or near gage mark

on yield strength over the base Ti-13Cu alloy strength. Ti-13Cu-4.5Ni alloy (Task II) had a lower melting point, strength, and possibly ductility than the Ti-8Cu-6.5Ni alloy (Task I). Comparing Ti-16Cu to Ti-10Cu (Table 4) showed a melting point reduction of over 200°F for the higher copper alloy, but displayed reductions in strength and ductility for all conditions evaluated.

Results (Table 4) for the Ti-13Cu-3Al composition were encouraging in that the yield strengths, after annealing at 1560°F and furnace cooling, were considerably above (45 ksi) the Ti-13Cu level as well as above the room temperature tensile yield strength goal of 90 ksi. Furthermore, the alloy had 8 percent average elongation in this heat treat condition. However, the lack of ductility in the as-melted condition indicated 3 percent aluminum was too high and a lower level would be more desirable.

Continued heat treatment studies on the 2.7 percent beryllium alloys (Appendix B, Table B-1) did not result in any improvements in ductility or strength over the conditions evaluated in Task I. The Task II beryllium containing alloys Ti-13Cu-1Be, Ti-7Fe-1Be-0.03Y, and Ti-2.7Be-5V, all had estimated melting points at or higher than the previous Task I Ti-8Cu-6.5Ni composition (MP=2515°F) as well as lower tensile ductilities, rendering these three beryllium containing compositions much less desirable.

3.1.4.3 Additional Tensile Property Evaluations

Several of the Task I and Task II Ti-Cu compositions approached the room temperature mechanical property goals. However, actual castings would be of varying sizes and cross sections, which would introduce variable cooling rates with a possible variation in properties. Therefore, a heat treatment was desirable to eliminate variations in strength or ductility caused by varied

cooling rates. Considerable effort was made to evaluate the effect of cooling rate, solution annealing temperature, and aging time and temperature parameters using the various Ti-Cu compositions. Most of this work was based on hardness data with the majority of the effort on the Ti-13Cu, Ti-16Cu, and Ti-13Cu-3Al alloys.

Increased cooling rates and duplex heat treatments were found to be effective in increasing the tensile strength and/or hardness of alloys from the Ti-Cu system. Therefore, all of the Ti-Cu compositions were further evaluated primarily using duplex heat treatments in an effort to obtain improved tensile properties (tensile and hardness data compiled in Appendix B, Table B-1). The exception was the Ti-10Cu alloy, which exceeded the room temperature tensile goals in the as-melted condition. A summary of these room temperature tensile results for the duplex heat treated alloys is listed in Table 5.

The binary Ti-13Cu and Ti-16Cu alloys nearly achieved the room temperature tensile goals after the duplex treatment and suggested that higher copper contents (lower melting points) should be evaluated. Several of the ternary compositions met or exceeded the room temperature tensile property goals after duplex heat treating with the Ti-13Cu-4.5Ni alloy nearly meeting all these goals including a melting point of 2400°F. Ti-13Cu-3Al exceeded the room temperature goals in the annealed condition (Table 5), which suggested further effort be expended in adding alpha stabilizing elements to Ti-Cu compositions.

3.1.4.4 Microstructural Evaluation

The as-melted and heat treated Ti-Cu binary alloy microstructures were similar to the structures observed during Task I (Figures 4 and 5). The Ti-10Cu alloy microstructure exhibited the greatest variation from that considered typical for the Ti-Cu alloys with no obvious grain pattern, but a slight

TABLE 5

SUMMARY OF HEAT TREATED ROOM TEMPERATURE TENSILE PROPERTIES OF TASKS I AND II, Ti-Cu ALLOYS

Heat No.	Nominal Composition	Actual or Estimated Melting Point,F	Annealed[2] Tensile Properties				Duplex Heat Treated[3] Tensile Properties			
			UTS ksi	YS ksi	El %	RA %	UTS ksi	YS ksi	El %	RA %
24220	Ti-10Cu	2725[1]	81 82	61 61	22 24	27 27	[4] 136 133	102 100	7 5	10 9
24219	Ti-10Cu-2.5Fe	2680	106 105	77 70	14 12	12 12	151	124	5	3
34029	Ti-13Cu	2613[1]	85 83	62 59	13 14	16 20	118	88	10	12
24221	Ti-13Cu-1Co	2595[1]	106 105	77 70	14 12	12 12	110 114	92 87	8 9	6 10
24264	Ti-13Cu-3Al	2595[1]	122 118	104 106	10 6	11 6[5]	146	128	7	7
24219	Ti-13Cu-2.5Fe	2570[1]	100 97	75 73	6 5	4 3	123 130	102 102	3 4	5 6
24217	Ti-16Cu	2515[1]	82 84	56 58	9 10	9 9	110 112	91 92	4 5	6 8
24032	Ti-8Cu-6.5Ni	2515[1]	95 98	64 66	6 5	8 4[5]	120 112	83 79	8 6	9 7
24224	Ti-13Cu-4.5Ni	2425[1]	89 87	63 65	5 5	3 3	119	104	4	6
PROGRAM GOALS		2400	100	90	5		100	90	5	

1. Experimentally determined.
2. Eutectoid Temperature + 100°F (1560°F)-hr-FC at 100°F/hr to 900°F-AC.
3. Best duplex heat treatment in approaching goals with good strength-ductility combination; for specific heat treatment, see Appendix B, Table B1.
4. As-melted properties
5. Broke at or near gage mark.

subgrain pattern was evident. This heat treated Task II, Ti-Cu alloy microstructure appeared more uniform (Appendix C, Figure C-4, a through l) compared to as-melted ingot microstructures (Appendix C, Figure C-3, a through f). The secondary phases generally had less alignment after heat treatment and tended to form a rounded shape and lowering the heat treatment temperature from 1760° to 1560°F produced a smaller particle size.

The as-melted Ti-Fe alloy microstructures appeared quite different from the Ti-Cu alloys. The Ti-7Fe-0.03Y and Ti-7Fe-5Mn-0.03Y alloys had martensitic alpha in the interior of the grain with an oriented, lathe-like features along the grain boundaries. Microstructures of the Ti-7Fe-0.03Y alloy in the beta annealed plus furnace cooled and solution treated plus aged conditions were typical of beta titanium alloys treated in these conditions. Both of these alloys developed microstructural "sharp" features, which were associated with the poor tensile ductilities.

Microstructures of the as-melted and heat treated Ti-2.7Be-5V alloy were similar to those observed for Task I beryllium containing alloys and did not indicate additional avenues for improvement of tensile properties.

3.1.5 Task III, Investigations

Based on encouraging Task II results, only Ti-Cu compositions were selected for evaluation in Task III. The major heat treatments of interest were the annealed (1560°F-1 hr-FC at 100°F/hr to 900°F-AC) and the duplex heat treatment (solution at 1760°F for 1 hour, air cool, and age) conditions.

3.1.5.1 Alloy Selections

Alloys chosen for Task III evaluations and the basis for making these selections were as follows:

Group A	Group B	Group C
Ti-13Cu-0.2 Oxygen	Ti-13Cu-2Al	Ti-16Cu-1.5Al
Ti-13Cu-0.25 Y_2O_3	Ti-13Cu-4Sn	Ti-19Cu
	Ti-10Cu-2.5Fe-2Al	Ti-19Cu-1Al

(a) Group A - This group of alloy compositions contained oxygen and yttrium oxide additions to the Ti-13Cu composition to determine their effect on mechanical properties of the Ti-Cu system. Both were contaminants expected to occur during casting due to reactions between molten metal and crucible or mold ceramics. The 0.2 percent oxygen level was based upon the maximum limit specified for current aerospace titanium castings as well as a reasonable expectation of what the program casting process may promote. The level of yttrium oxide was selected at 0.25 percent based upon the typical melt contamination levels encountered during the laboratory ceramic evaluations (Section 3.2).

(b) Group B - The second group of compositions selected were those that had estimated melting points between 2500°F and 2600°F and required strength improvements. Aluminum, tin and iron appeared to be favorable alloy additions and were chosen for more extensive evaluation. In addition to reducing density, aluminum substantially improved strength without sacrificing ductility. Close comparison of properties for the Ti-13Cu and Ti-13Cu-3Al alloys indicated a better

strength-ductility relationship in the aluminum-containing alloy. A Ti-13Cu-2Al composition was selected for Task III in order to decrease the high strength and improve the ductility. Ti-10Cu-2.5Fe alloy from Task II was modified with 2 percent aluminum in an effort to retain maximum ductility at the higher strength levels while simultaneously reducing the melting point from the iron addition. A third alloy was selected (Ti-13Cu-4Sn) with tin added on the same basis as aluminum; that is, to obtain solid-solution strengthening of the alpha phase but at a reduced level.

(c) Group C - The third group of compositions selected were those that had melting points less than 2500°F. However, the large amount of alloying required to obtain such low liquidus temperatures increased the probability of obtaining low tensile ductility. The binary Ti-19Cu was evaluated, even though it was within the eutectic field, because considerable ductility had been previously observed with the Ti-16Cu alloy. Aluminum additions to Ti-16Cu and Ti-19Cu binary alloys were also made to increase strength while maintaining ductility.

3.1.5.2 Tensile Property Evaluation

All hardness and tensile properties for the Task III alloys are compiled in Appendix B. Table 6 contains a summary of tensile data for these compositions, as well as comparative Task II data for the Ti-13Cu and Ti-13Cu-3Al alloys and showed several compositions met the program room temperature tensile goals of 90 ksi yield strength and 5 percent elongation. Good ductility (greater than 2 percent) was achieved in the as-melted condition for all compositions with the exception of alloys which contained aluminum additions of 2 percent or more. The Ti-10Cu-2.5Fe-2Al composition had particularly high as-melted strength

TABLE 6

SUMMARY ROOM TEMPERATURE PROPERTIES FOR PHASE I, TASK III ALLOYS, Ti-13Cu, AND Ti-13Cu-3Al ALLOYS

Heat No	Nominal Composition	Actual or Estimated Melting Point,F	Tensile Properties											
			As-melted				Annealed[2]				Duplex Heat Treated[3]			
			UTS ksi	YS ksi	El %	RA %	UTS ksi	YS ksi	El %	RA %	UTS ksi	YS ksi	El %	RA %
24227	Ti-10Cu-2.5Fe-2Al	2665	175 170	168 160	2 2	4 4	132 131	106 106	7 7	4 7				
34029	Ti-13Cu (Task I)	2613[1]	104 105	82 82	10 10	10[4] 12	85 83	62 59	13 14	16 20	118	88	10	12
24273	Ti-13Cu-0.2 O	2613	132 120	109 102	3 3	2 2	95 95	72 72	5 4	6 4	122 125	102 100	5 5	5 6
24281	Ti-13Cu-0.25Y_2O_3	2613	104 102	76 76	9 7	11 9	87 86	56 54	10 12	16 17	106 104	77 75	8 8	3[4] 9
24275	Ti-13Cu-2Al	2600	143 163	138 148	1 1	-[4] -[4]	104 106	92 92	12 12	14 14	127 126	104 106	7 6	8 7
24264	Ti-13Cu-3Al (Task II)	2595[1]	147 143	-- --	-- --	-- --	122 118	104 106	10 6	11 6[4]	146	128	7	7
24276	Ti-13Cu-4Sn	2590	118 116	100 99	8 8	9 11	95 94	78 77	8 9	10 10	115	106	8	10
24278	Ti-16Cu-1.5Al	2500	113 114	97 97	4 4	5 5	94 94	79 78	4 6	6 4	122 120	112 113	5 3	5 5
24279	Ti-19Cu	2417[1]	87 90	65 65	4 4	4 3	69 68	53 52	1 4	-[4] 3	92 97	74 80	4 4	2 3
24280	Ti-19Cu-1Al	2410	98 95	80 73	3 3	2 3	86 90	65 68	5 5	7 6	97 101	79 78	4 4	3 5
PROGRAM GOALS		2400	100	90	5		100	90	5		100	90	5	

1. Experimentally determined
2. 1560F-1hr-FC @ 100F/hr to 900F-AC
3. Best duplex heat treatment in approaching goals with good strength-ductility combination; for specific heat treatment, see Appendix B, Table B1.
4. Broke at or near gage mark

(164 ksi yield strength) and consequently low ductility. However, the three compositions (Ti-10Cu-2.5Fe-2Al, Ti-13Cu-2Al, and Ti-13Cu-3Al), which had high strength in the as-melted condition, met the program room temperature tensile goals after annealing. Increasing copper content was found to decrease the strength when the alloy was annealed above the eutectoid temperature. In this condition, other elements added to the Ti-Cu binary compositions tended to minimize the reduction in strength.

Tensile results showed the alloys exhibited very favorable heat treatment response. Duplex heat treatments could be used to produce a range of strengths and ductilities depending on the aging temperature and time selected. Based on the normal strength-ductility relationships, the ductility of many of these compositions could be improved by adjusting the strength to a lower level. However, with the Ti-19Cu composition, water quenching from the annealing temperature (instead of air cooling) was required to obtain strength levels comparable to the other duplex heat treated Ti-Cu alloys.

Data from Ti-Cu compositions that contained alpha stabilizers were especially encouraging, particularly aluminum additions. On the basis of as-melted ductilities, 2 percent aluminum in the Ti-13Cu composition was excessive, although in heat treated conditions ample ductility was obtained at 2 and 3 percent aluminum levels. In addition to the apparent benefits of aluminum on strength, melting point, and density, an improvement in fluidity may also be obtained when casting the alloy[25].

Data in Table 6 also show minor losses in ductility and strength when 0.25 percent Y_2O_3 was added to the Ti-13Cu alloy. However, when 0.2 percent oxygen was added to the Ti-13Cu alloy,

(25)Magnitskiy, O. N., "Casting Properties of Titanium Alloys", 1968. Translation by Foreign Technology Division, Wright-Patterson Air Force Base, Ohio. FTD-HT-23-386-69, April 1970.

an appreciable loss in ductility was observed and this was not recovered effectively by heat treatment. The oxygen containing Ti-13Cu alloy tensile properties were increased as expected and met the program goals.

3.1.5.3 Influence of Thermal Exposure on Tensile Properties

Table 7 contains pre- and post-thermal exposure tensile results for five heat treated compositions. The thermal exposure consisted of exposing machined tensile specimens at 800°F for 200 hours in air and then tensile testing at room temperature with the surfaces intact. The alloys selected covered a composition range that was necessary to select alloys for Phase II. The binary Ti-16Cu alloy showed a slight instability as evidenced by a loss in strength, whereas Ti-Cu compositions with aluminum, iron, and nickel additions were stable. The Ti-13Cu-2.5Fe, Ti-13Cu-4.5Ni, and Ti-13Cu-2Al alloys showed slight gains in ductility with the Ti-13Cu-4.5Ni alloy also experiencing an increase of 10 ksi in yield strength. The addition of ternary elements to the binary Ti-Cu alloy appeared to provide improved and acceptable alloy thermal stability.

3.1.5.4 Microstructural Evaluation

Microstructures of the as-melted and heat treated Task III (also Ti-13Cu-3Al) compositions are assembled in Appendix C. Additions of aluminum, tin, and oxygen to Ti-13Cu resulted in a finer transformed product within the beta grains of as-melted ingot. The as-melted microstructure of the Ti-19Cu alloy appeared similar to those for the Ti-13Cu and Ti-16Cu alloys (Figure 6). Aluminum additions to the 16 and 19 percent copper compositions did not refine the transformation product compared to the respective binary bases. The yttria-containing Ti-13Cu composition microstructure contained light-gray colored secondary particles, which tended to have a square shape. These

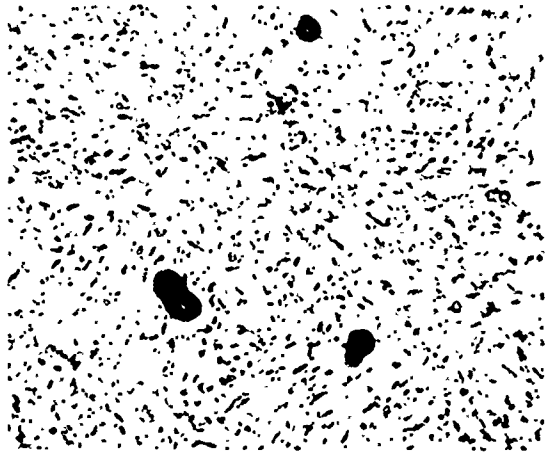
TABLE 7

ROOM TEMPERATURE TENSILE PROPERTIES OF FIVE ALLOYS BEFORE AND AFTER THERMAL EXPOSURE

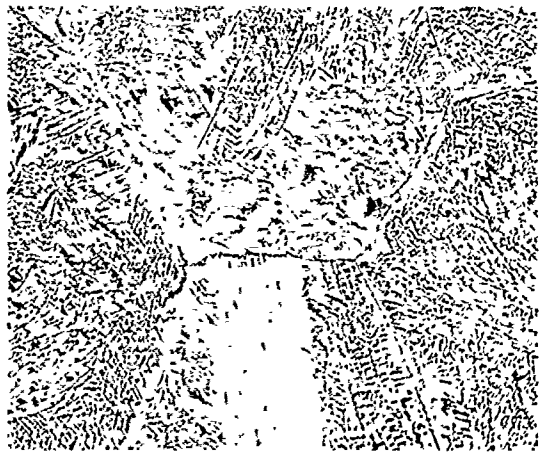
Heat No.	Composition	Heat Treatment	As-Heat Treated				Heat Treated and Exposed			
			UTS ksi	YS ksi	El %	RA %	UTS ksi	YS ksi	El %	RA %
24217	Ti-16Cu	1760F-1hr-AC + 1400F-8hr-AC	112 108	91 92	6 6	6 8	97 94	71 69	6 7	6 7
24275	Ti-13Cu-2Al	1560F-1hr-FC	104 106	92 92	12 12	14 14	106 107	87 90	14 13	17 18
24278	Ti-16Cu-1.5Al	1760F-1hr-AC + 1450F-16hr-AC	122 120	112 113	5 3	5 5	122 124	109 115	4 4	4[2] 4
24218	Ti-13Cu-2.5Fe	1760F-1hr-AC + 1400F-8hr-AC	123 130	102 102	3 4	5 6	128 130	96 101	4 6	6 6
24224	Ti-13Cu-4.5Ni	1760F-1hr-AC + 1400F-8hr-AC	108	82	5	6	106 105	90 88	7 6	5 5

1. Exposed at 800°F for 200 hours and tested with oxide surface layer intact

2. Broke outside gage mark



(a) HEAT 24220 Ti-10Cu 9435



(b) HEAT 34029 Ti-13Cu 8726



(c) HEAT 24217 Ti-16Cu 9432



(d) HEAT 24279 Ti-19Cu 9583

Figure 6. Typical Microstructure From As-Melted 4.5-Inch-Diameter Ti-Cu Ingots (250X).

particles are similar in appearance to those observed in Ti-2.7Be melts made in yttria containing crucibles during the ceramic investigation portion of the program (see Section 3.2).

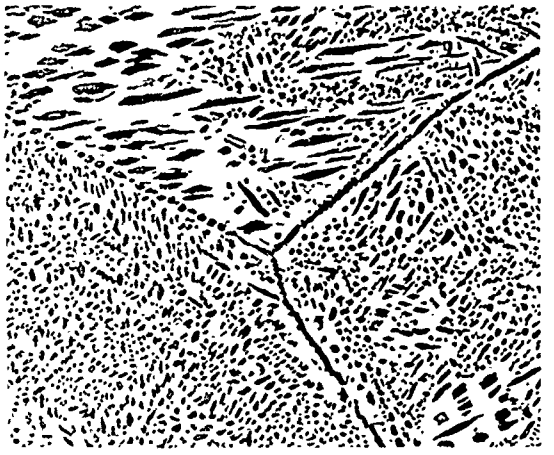
The annealed (1560°F-1 hr-FC at 100/hr to 900°F-AC) microstructures for all the copper containing compositions except Ti-13Cu-3Al appear similar (Figure 7). After heat treatment, the size of the Ti_2Cu precipitate was increased at the prior beta grain boundary and within the grains. In the annealed condition, Ti-13Cu-3Al had a microstructure similar to that of the annealed Ti-10Cu alloy, that is, one primarily composed of spherical agglomerates. Microstructures from the duplex heat treated compositions, including Ti-13Cu, have in comparison a finer lamellar product and a decrease or absence of Ti_2Cu precipitates at the prior beta grain boundaries. This fineness of the lamellar products was believed responsible for the higher strength obtained with the duplex heat treatments compared to the annealed condition.

3.1.6 Discussion of Alloy Evaluation

At the end of Task I of Phase I, the Ti-Cu system was the most attractive for further exploitation to meet the program goals. Therefore, during the remaining tasks in Phase I, major emphasis was placed on the Ti-Cu system, with additional effort involving beryllium-containing and low-melting beta eutectic alloys. The Ti-7Fe-0.03Y alloy tensile ductility met the program goals and exceeded that of an earlier Task I composition. However, the melting point of this beta alloy was excessive (above 2700°F) and efforts to lower the melting point by 5 percent manganese (2680°F) or 1 percent beryllium (2570°F) additions reduced the tensile ductility to unacceptable levels. Further work in Task II with a Ti-2.7Be-5V alloy (MP=2570°F) did not result in improved properties over the Task I compositions and the addition of 1 percent beryllium to the Ti-13Cu alloy (MP=2506°F) resulted



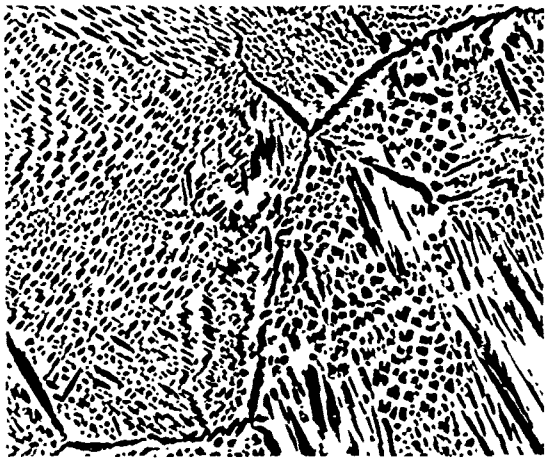
(a) HEAT 24219 9471
Ti-10Cu



(b) HEAT 34029 8776
Ti-13Cu



(c) HEAT 24217 9461
Ti-16Cu



(d) HEAT 24279 9609
Ti-19Cu

Figure 7. Typical Microstructures of Annealed (1560°F-1Hr-FC) Material From 4.5-Inch-Diameter Ti-Cu Ingots (250X).

in both low strength and low ductility. The above trends all supported early decisions to concentrate efforts on the Ti-Cu system.

Ti-Cu alloys met or nearly met the room temperature tensile goals in one or more conditions (as-melted, annealed, or duplex heat treated) as shown in Figure 8. Hardness data from other duplex heat treatments consisting of various aging temperature-time parameters applied to Ti-Cu compositions indicated flexibility for varying the strength of these alloys (Appendix B, Table B-I). Data suggests these alloys exhibit very good heat treatment response, which should result in an even better combination of yield strength and ductility for many of the Ti-Cu alloys.

Early investigations on Ti-Cu alloys indicated that high strength[11,26,27,28] could be obtained but with attendant low ductility.[11,26,28] However, data from this program demonstrated excellent ductility (6 to 23 percent elongation) with Ti-10Cu, Ti-13Cu, and Ti-16Cu alloys in the as-melted or annealed conditions, and adequate ductility (4 percent elongation) for similar conditions with the Ti-19Cu composition.

The duplex heat treatment applied to the Ti-Cu alloys resulted in higher strengths compared to annealed material. The ductility of these heat treated Ti-Cu alloys was, on a strength-ductility comparison, as good as or better than the ductility

---

(26) Buchanan, K.M., et al, "Titanium-Based Casting Alloys", British Non-Ferrous Metals Research Assn., for Procurement Executive, Ministry of Defense, Final Report, S295/11, July 1973.

(27) Williams, J. C., "An Electron Microscopy Study of the Phase Transformations in Ti:Cu Alloys", PhD dissertation, University of Washington, 1968. Available University Microfilms Inc., Ann Arbor, Michigan, 69-13, 640.

(28) Bunshah, R.F., and Margolin, H., "Microstructure and Mechanical Properties of Ti-Cu-Al and Ti-Cu-Al-Sn Alloys", Transactions of the American Society for Metals, Vol. 51, 1959, pp 961-980.

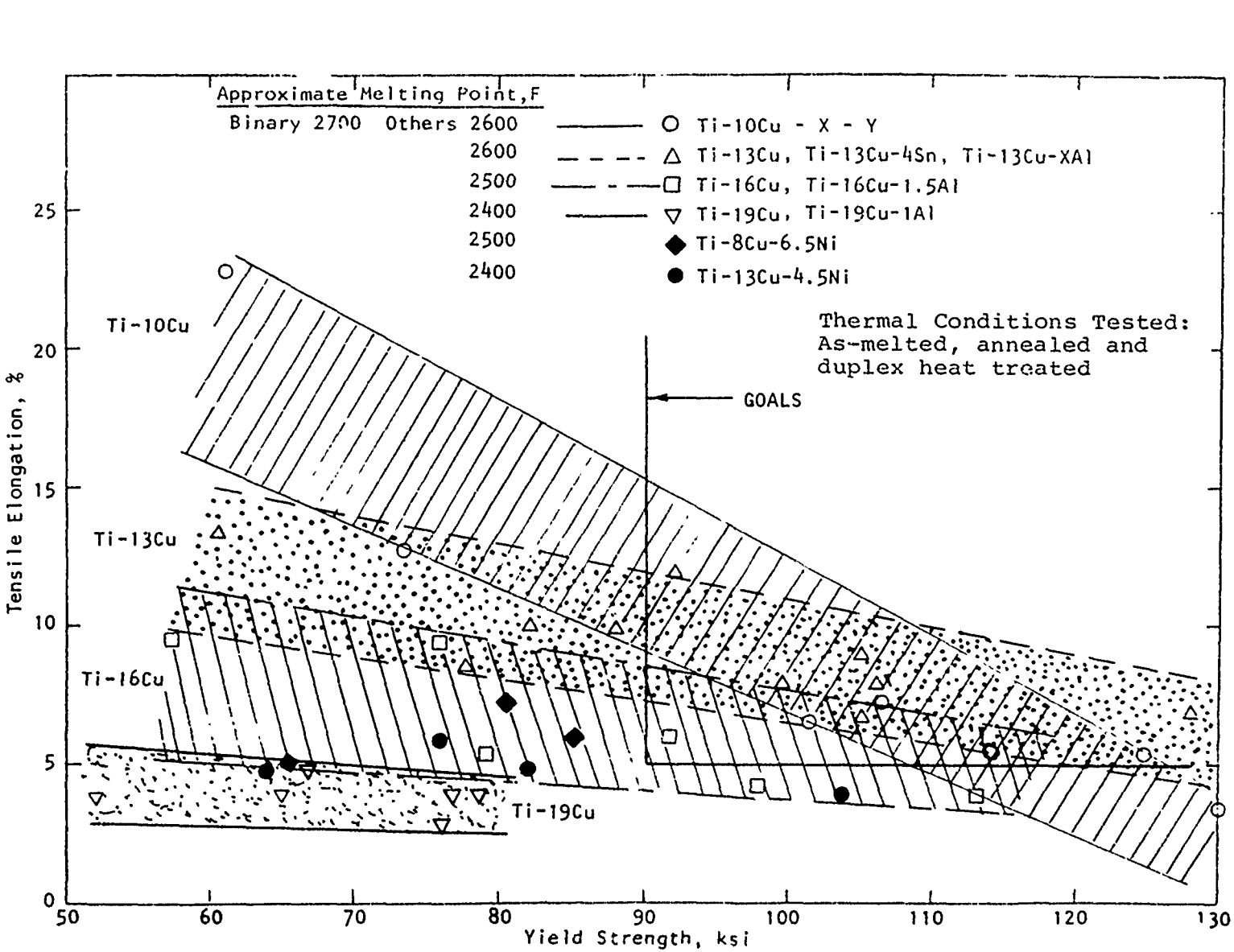


Figure 8. Relationship Between Elongation and Yield Strength of Ti-Cu Alloys.

associated with annealed Ti-Cu compositions (Tables 5 and 6). Aging the Ti-Cu alloys after rapid cooling from the beta or beta-plus-compound field provided the flexibility for achieving desired strength and ductility levels in these alloys. Microstructures of duplex heat treated alloys, compared to annealed material, consisted of a finer lamellar structure with a decrease or absence of Ti_2Cu precipitates at the prior beta grain boundaries. The subsequent microstructural analyses in Phase II as-melted Ti-Cu alloys showed that as the aging temperature increased, coarseness of the lamellar structure increased and was accompanied by decreased strength and a general improvement in ductility.

Strength increases over the Ti-Cu binaries for the annealed ternary and quaternary Ti-Cu alloys appeared to result from solid-solution strengthening of the alpha phase by the added elements. Table 8 shows the influence of these alloy elements on strength and melting point of the Ti-Cu base alloy. Data derived in this program on alloys in the annealed condition and compared with literature values[29] show the alpha stabilizers, aluminum and tin, resulted in greater alpha solid-solution strengthening than expected. Iron, a sluggish eutectoid beta element, resulted in less strengthening than expected and the active eutectoid beta elements nickel and cobalt resulted in no appreciable strengthening. The unexpected poor strengthening from the addition of the nickel and cobalt suggests that these elements may be interacting with copper, which is also an active eutectoid element, and forming complex compounds such as Ti_x-Cu_y-Ni_z or Ti_x-Cu_y-Co_z during the eutectoid reaction.

---

(29) Seagle, Stan R., "Principles of Alloying Titanium, Lesson 3, Titanium and Its Alloys, Course 27". Edited by Harold D. Kessler, Metals Engineering Institute, American Society for Metals, 1968.

TABLE 8

STRENGTH CONSIDERATION FOR Ti-Cu ALLOY DEVELOPMENT

o ESTIMATED YIELD STRENGTH OF BASE PHASES

Phase	Yield Strength, ksi
Alpha Solid Solution Hardened by Copper	∿65
Ti_2Cu	∿28

o EFFECT ON MELTING POINT AND THE ALPHA SOLID-SOLUTION STRENGTHENING EFFECT OF OTHER ALLOYING ELEMENT

Element	Decrease in Melting Point From Ti-Cu Binary Compositions	Increase in Strength	
		Contract Data[1]	Literature
Aluminum	6F/1%	15 ksi/1%	9 ksi/1%[2]
Tin	<5F/1%	4.5 ksi/1%	2.5 ksi/1%[2]
Iron	31F/1%	5.6 ksi/1%	10 ksi/1%[2]
Nickel	42F/1%	1 ksi/1%	6 ksi/1%[3]
Cobalt	18F/1%	2 ksi/1%	8 ksi/1%[2]

1. Based on change in yield strength of annealed compositions
2. Reference 29
3. Estimated

The aging mechanism for the complex Ti-Cu alloys is thought to be similar to that of the Ti-Cu binary alloys. After duplex heat treatment the complex Ti-Cu alloy microstructure consisted primarily of finer lamellar spacing than obtained with the annealed complex Ti-Cu alloys. This finer lamellar structure and the solid solution hardening of the alpha phase by the alloy additions both contributed to the superior strength of the complex Ti-Cu alloys compared to the binary alloys. An examination of the aging cycles employed for Ti-Cu alloys (Appendix B, Table B-1) indicates the Ti-Cu binary alloys require lower aging temperatures than the complex Ti-Cu alloys to obtain equivalent strength and hardness. A shift in phase boundaries in the Ti-Cu system appears to occur with the addition of alloying elements and appears to change the time-temperature-transformation (TTT) relationships. This shift would explain the differences in aging kinetics observed between the complex Ti-Cu and Ti-Cu binary compositions.

Copper was very effective in decreasing the liquidus temperatures of titanium with approximately a 34°F decrease for each weight percent added. Experimental melting point data (Figure 9) showed equally good agreement, but somewhat lower liquidus temperatures than estimated and published for the Ti-Cu phase diagram[4]. Experimental melting points of higher-copper titanium alloys by Buchanan[26] follow reasonably well an extension of melting points of the lower copper titanium alloys determined in this study. The Ti-40Cu alloy melting point, as determined by Smeltzer and Compton,[30] also agreed with an extension of the liquidus temperature line shown in Figure 9. All ternary alloying additions to the Ti-Cu system that were evaluated, resulted in further reduction in melting temperatures (Table 8).

---

[30] Smeltzer, C.E., and Compton, W.A., "Titanium Braze System for High Temperature Applications", First Interim Technical Report, Solar Division of International Harvester Co., AF Contract F33615-74-C-5118, August 1974.

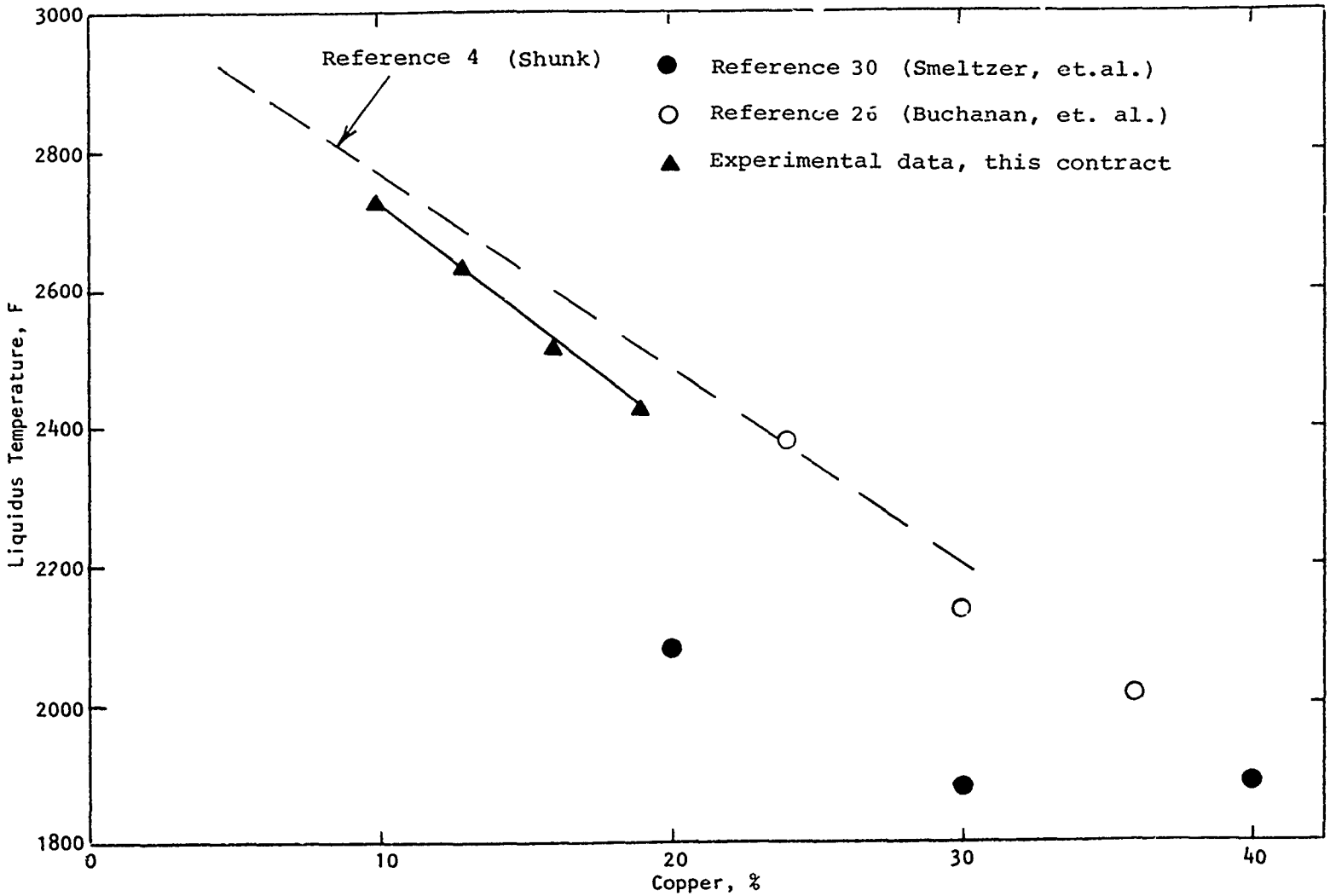


Figure 9. Experimental Melting Points of Titanium-Copper Alloys Compared With Liquidus Temperatures From the Literature.

3.1.7 Summary - Alloy Development

Several approaches were investigated during Phase I to achieve an alloy displaying a desirable combination of melting point and tensile properties. The alloys evaluated included low-melting eutectics (Ti-Ni, Ti-Cu, Ti-Co, and Ti-Si), beta eutectics (Ti-Mn and Ti-Fe), and Ti-Cr and Ti-Be alloys. The most promising alloys contained copper as the main melting point depressant; thus, the emphasis during the latter portion of Phase I was placed on titanium alloys containing copper as the principal alloying element. The annealed binary copper alloy strength levels, while low, were increased by a duplex heat treatment, involving aging below the eutectoid temperature after a solution treatment. Both alpha (Al, Sn) and beta stabilizers (Fe, Ni, Co) were added to the Ti-Cu alloys to increase strength and/or to further depress the melting point. The alpha stabilizing elements were found to provide good strength improvements while maintaining better ductility than beta stabilizers. The following eight Ti-Cu base alloys, which had melting points ranging from 2515°F to 2630°F, exhibited room-temperature tensile properties that met the program goals in various heat treated conditions:

Ti-10Cu-2.5Fe	Ti-13Cu-4Sn
Ti-10Cu-2.5Fe-2Al	Ti-13Cu-1Co
Ti-13Cu-2Al	Ti-13Cu-0.2 oxygen
Ti-13Cu-3Al	Ti-16Cu

The Ti-13Cu-4.5Ni alloy was particularly attractive due to a low melting point (2425°F) and near attainment of program tensile goals (104 vs 90 ksi yield strength and 4 vs 5 percent elongation, respectively). Thermal exposure tests (200 hours/800°F) conducted on five binary and ternary alloys to evaluate metallurgical stability and oxidation resistance indicated alloys containing either iron, nickel, or aluminum were very stable and experienced no loss in ductility or strength.

3.2 Phase I Crucible/Mold Material Investigations

The previous section (3.1) was concerned with the development of low melting point titanium alloys. The present section (3.2) is devoted to the evaluation of ceramic materials, which could be applied to the fabrication of melting crucibles and mold facecoats. Evaluation of ceramic materials in Phase I was conducted by the following general procedure:

- Procure small crucibles of each ceramic material.
- Melt a charge of a low melting titanium control alloy in the crucible under controlled and repeatable laboratory conditions.
- Chemically analyze the alloy melt for contamination and by metallography evaluate the crucible/melt interface for degree of reaction.
- Compare chemical analysis, microstructures and hardness data in order to identify the better (lower reactivity) ceramic materials.

Evaluation of materials for crucible and mold applications was consistent throughout Phase I, and the fabrication and laboratory techniques used for all three Phase I tasks are discussed in a single section (3.2.1). Results and discussion are contained in one section (3.2.2) and are reviewed in the sequence, in which the investigations occurred.

3.2.1 Material Procurement and Experimental Procedures

Evaluation of the candidate ceramic materials was accomplished by analyzing melts of a control alloy in small crucibles fabricated from various ceramics. These analyses involved

chemical analysis for contaminates as well as hardness testing and metallography to detect metal/ceramic interactions. In order to accomplish this evaluation, standard and consistent techniques were used throughout Phase I including a control alloy (Ti-2.7Be), crucible fabrication approaches, and melting procedures.

Near the end of Phase I, a limited mold development activity was initiated to provide assistance in the material selection for Phase II. This development included laboratory preparation of mold facecoat slurries, firing of dried samples, and an evaluation of the degree of sintering.

3.2.1.1 Control Alloy

The best approach to evaluate promising ceramics for crucible and mold applications would involve melting a control titanium alloy (low melting point) in candidate ceramic crucibles. Analysis of the resulting alloy melts (performed under consistent laboratory procedures) would provide reliable data necessary to the identification of the best ceramics. On the basis of prior work, the Ti-Be system appeared to offer the most promising properties for the program and was therefore also chosen for the control alloy. The Ti-2.7Be alloy composition was selected based upon a melting point (2570°F) intentionally above the goal for the program (2400°F). The higher melting point provided a conservative approach toward ceramic selection as well as experimental alloy selection for later casting efforts.

One thirty-pound ingot (4.5-in. diameter) of the Ti-2.7Be (nominal) alloy was double consumable vacuum melted at RMI Company to provide sufficient material for all Phase I melting experiments. The chemical composition of this material is

reported in Appendix A (Table A-2) showing a Be content quite near the target composition and low oxygen at 0.079 wt-percent (determined by vacuum fusion analysis).

Also, as a result of the toxic nature of beryllium, master alloy processing and melt runs were monitored for beryllium contamination. Handling beryllium-containing alloys may present a health hazard, particularly in operations that create respirable particulate matter. As a result, a portion of this program was devoted to surveillance of operations such as melting, casting, cutting, and polishing for airborne and surface concentrations of beryllium. The National Institute for Occupational Safety and Health (NIOSH) has prepared a recommended standard covering the occupational exposure to beryllium. Key sections in this standard deal with the following:

- Work place air
- Medical surveillance
- Marking of packages and areas where exposure is possible
- Protective equipment and clothing
- Informing employee of hazards
- Work practices
- Sanitation practices
- Monitoring and records management

The above areas were recognized and implemented at RMI Company and AiResearch during the activities involving all beryllium containing alloys.

3.2.1.2 Laboratory Crucibles

Laboratory crucibles were fabricated by a variety of techniques such as cold press and sinter, isostatic press and sinter, hot pressing, reaction bonding or pyrolytic deposition.

Crucibles were primarily a nominal 1-inch diameter by 1-inch high, but a few were as large as 2-inch diameter by 2-inch high (Figure 10). Crucibles were purchased from various suppliers as detailed in Appendix D with fabrication parameters and properties. Chemical analyses of several lots of yttria used to fabricate crucibles are also given in Appendix D (Table D-4).

Two special materials were procured during the Phase I and included the Heavy Rare Earth Mixed Oxide (HREMO) and Light Rare Earth Mixed Oxide (LREMO). The materials were concentrates of respective ores, the HREMO coming from the mineral Xenotime ($Y_2O_3 \cdot P_2O_5$) while the LREMO material is obtained from the mineral Basnasite [(Ce,La,Dy)F CO_3]. Composition ranges for these two concentrates are shown below:

HREMO

	Percentage	
Y_2O_3	58 - 63	Other rare earth oxides, 5-15 percent; non-rare earth oxides (CaO, Al_2O_3, TiO_2), 6 percent maximum
Dy_2O_3	5 - 12	
Yb_2O_3	5 - 7	
Er_2O_3	5 - 7	
Gd_2O_3	3 - 6	
CeO_2	1 - 5	

LREMO

CeO_2	65 - 90	Other rare earth oxides, 5-20 percent; non-rare earths, 0.5 percent
La_2O_3	10 - 33	
Nd_2O_3	5 - 12	
ThO_2	0 - 10	

Both of these materials were used for crucible fabrication, while only the HREMO material was used for mold development during the program.

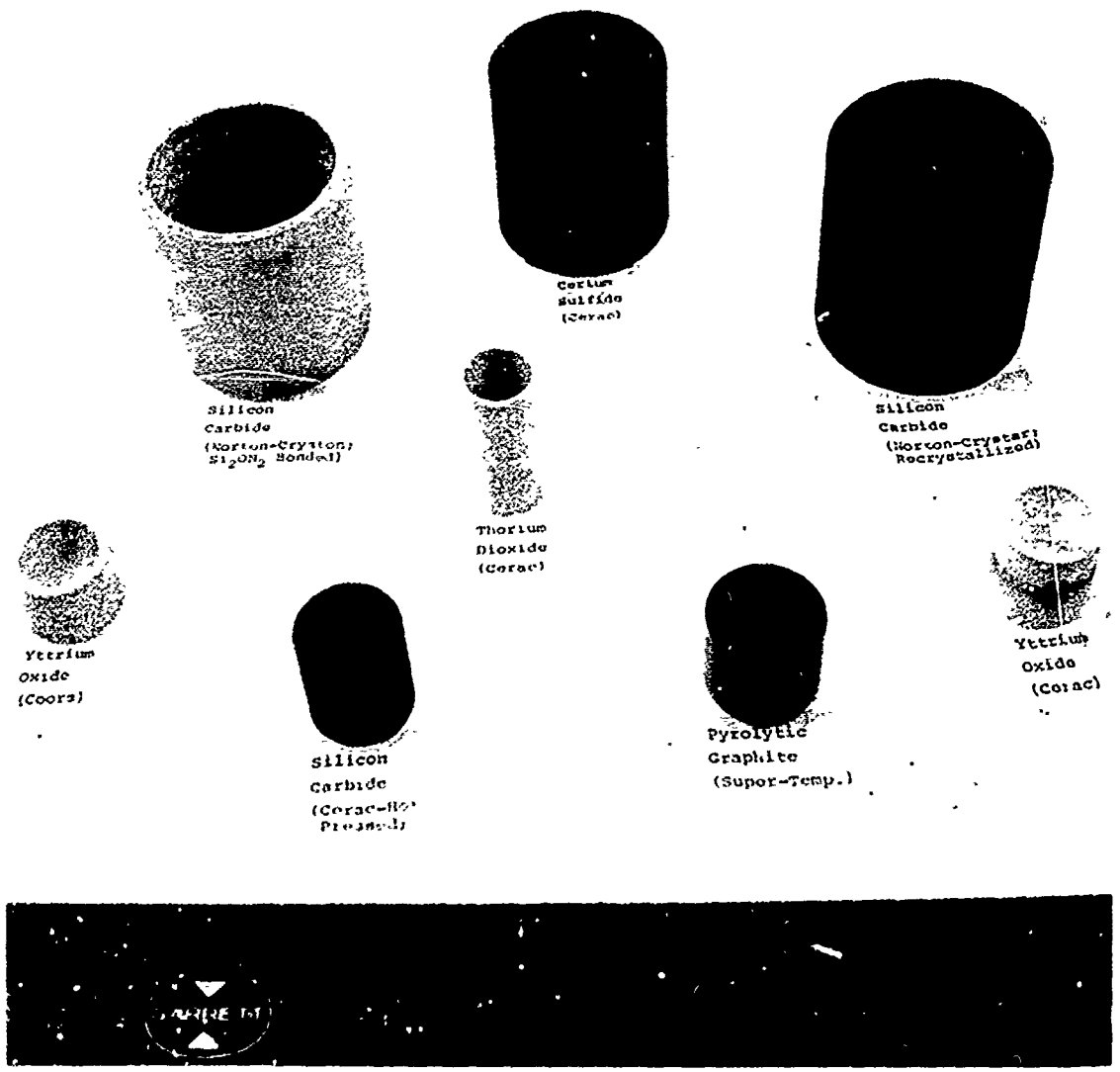


Figure 10. Appearance of Typical Laboratory Crucibles in a Range of Sizes and Fabrication Techniques Procured During Phase I Ceramic Investigations.

3.2.1.3 Special Firing of Laboratory Crucibles

In addition to evaluating crucibles in the as-received condition from suppliers, it was important to assess the effect of crucibles in other fired conditions. In particular, it has been reported(31,32) that low oxygen stoichiometry in yttria was beneficial in reducing contamination. In addition, the fabrication of titanium containing ceramics involved a firing operation for which there were no previous guidelines. Therefore, special firing procedures were required to produce the low oxygen stoichiometry crucibles as well as define appropriate firing for titanium modified ceramic compositions.

3.2.1.3.1 Low Oxygen Crucibles

Efforts were made to promote low oxygen stoichiometry in several crucibles by refiring at high temperatures (greater than 2940°F) under various conditions as follows:

(a) Several Y_2O_3, ThO_2 and HREMO crucibles were coated on the inside surface with a carbon-acetone slurry, dried, and then fired.

(b) HREMO and Y_2O_3·15Ti crucibles were fired without the presence of the carbon coating.

These crucibles were refired in argon by induction heating of a graphite susceptor using the arrangement shown in Figure 11. Judging by weight losses of the crucible due to firing, some

---

(31) S. R. Lyon, Personal Communication, August 21, 1973.

(32) Lyon, S. R., S. Inouye, C. A. Alexander, and D. E. Niesz, "The Interaction of Titanium with Refractory Oxides," Titanium Science and Technology, Volume 1, Edited by R. I. Jaffee and H. M. Burte (1973) 271-284.

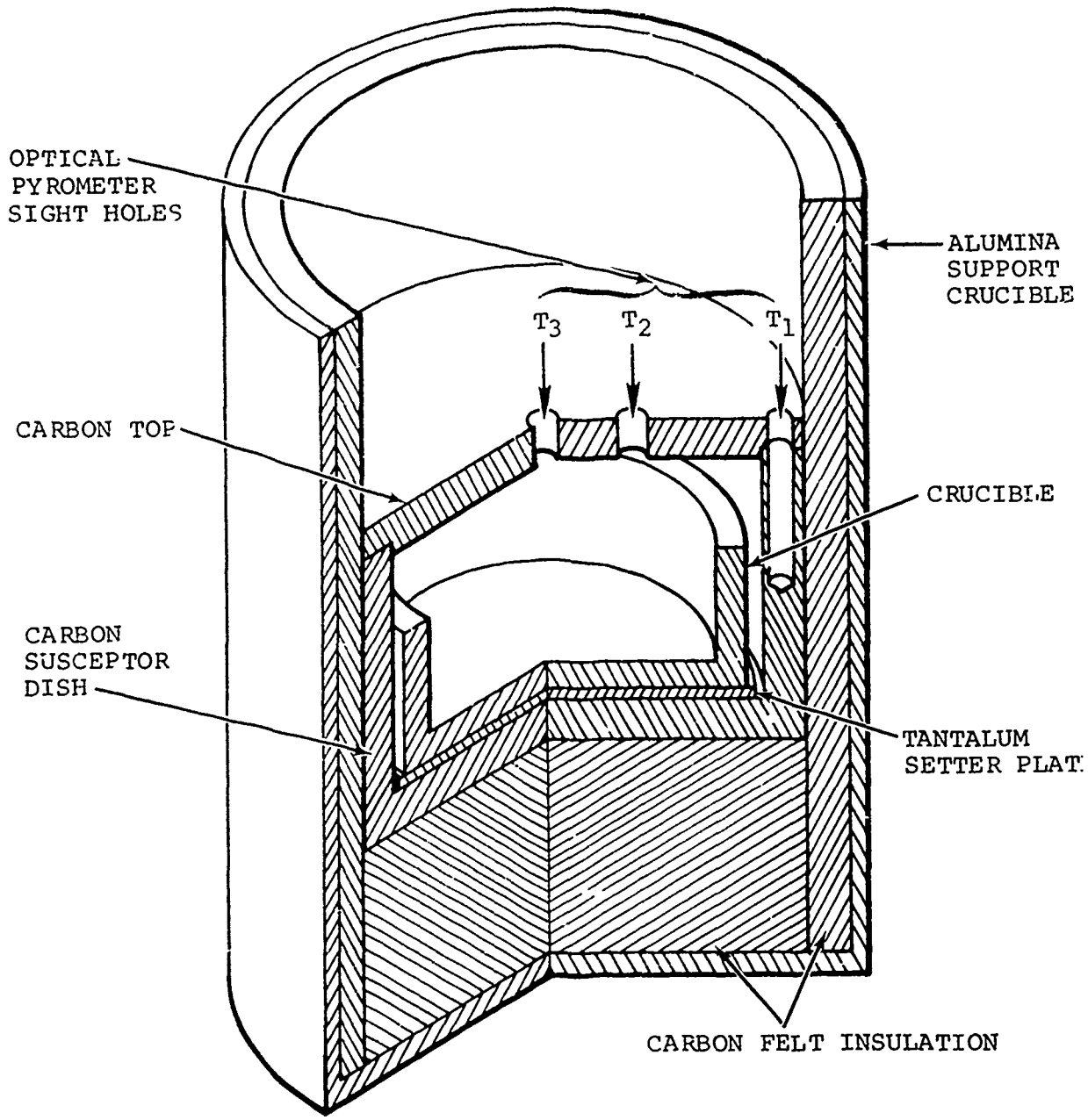


Figure 11. Standard Arrangement for Thermal Treatment of Ceramic Crucibles. The Set-Up is Placed Within Induction Heating Coils and Optical Pyrometer Temperature Measurements Made Through T_2 on Crucible Inside Wall.

decrease in oxygen stoichiometry (discussed further in Section 3.2.2.2) has occurred as shown in Table 9. Degradation occurred primarily at the higher firing temperatures for the Y_2O_3 crucibles (Figure 12).

3.2.1.3.2 Titanium-Modified Crucibles

Several of the titanium modified crucibles procured for Task III were given firing treatments in addition to the initial 3000°F firing at Coors Porcelain Co. The setup shown in Figure 11 was used to induction heat the carbon susceptor and obtain the necessary high temperature. Table 9 also presents firing conditions for titanium modified crucibles given additional firing treatments.

3.2.1.4 Standard Laboratory Technique for Evaluating Ceramic Crucibles

The candidate crucible/mold materials were evaluated by melting a 10-gram charge of the Ti-2.7Be control alloy in crucibles and holding for 10 minutes at a temperature of 2870°F (300°F above the alloy melting point). The experimental setup was placed in a vacuum chamber and induction heated (Figure 13). The arrangement shown in Figure 14 was used for Tasks II and III, whereas the Task I melts were made without the top lid and insulation. Temperatures were measured with a Pt/Pt-10 percent Rd thermocouple located at the position shown in Figure 14. Estimates, from a calibration melt of 1018 carbon steel (MP=2774°F), indicated crucibles were 50°F lower in temperature than the thermocouple-indicated temperature during Task I, whereas the deviation was not as large for later melts (near 20°F). However, thermocouple-indicated temperatures are quoted throughout the report.

TABLE 9

FIRING PROCEDURES USED TO PREPARE
SPECIAL CRUCIBLES FOR TASK II MELTING EXPERIMENTS

Crucible	Carbon Coating	Firing Treatment	Estimated Stoichiometry*
Y_2O_3-14	Yes	3100°F/12 min/Argon	$Y_2O_{2.99}$
-39	Yes	3320°F/13 min/Argon	$Y_2O_{2.97}$
-52	Yes	3220°F/10 min/Argon	$Y_2O_{2.97}$
ThO_2-D3	Yes	2940°F/20 min/Argon	$ThO_{1.93}$
-D4	Yes	3165°F/14 min/Argon	$ThO_{1.96}$
-D5	Yes	3220°F/15 min/Argon	$ThO_{1.95}$
HREMO-2	Yes	3075°F/12 min/Argon	$RE_2O_{2.96}$
-4	No	3385°F/12 min/Argon	$RE_2O_{2.93}$
-7	Yes	3245°F/13 min/Argon	$RE_2O_{2.94}$
Y_2O_3.15Ti-1	No	3355°F/11 min/Argon	(0.11% loss)
-2	No	3190°F/11 min/Argon	(0.034% loss)
-4**	No	3190°F/11 min/Argon	(0.008% gain)
-5	No	3200°F/14 min/Argon	(0.012% loss)

* Based upon crucible weight loss from firing

** Firing set-up different from that used for all other crucibles shown in Figure 12 in that the carbon top was replaced with an open cylinder of Cb metal with an I.D. the same as the carbon dish.

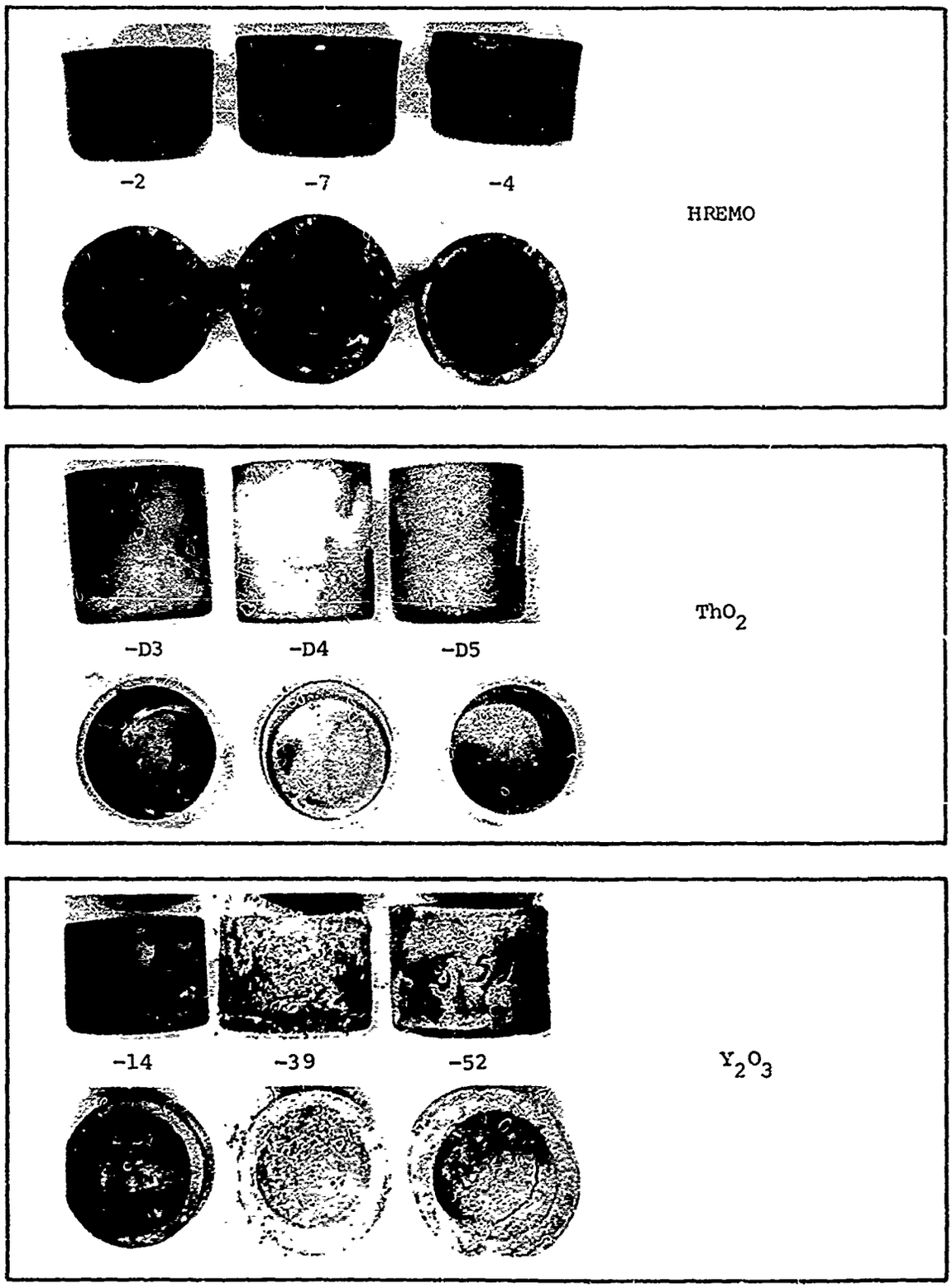


Figure 12. Side and Top Views of the Special Fired Crucibles, Used in Task II Melting Experiments.

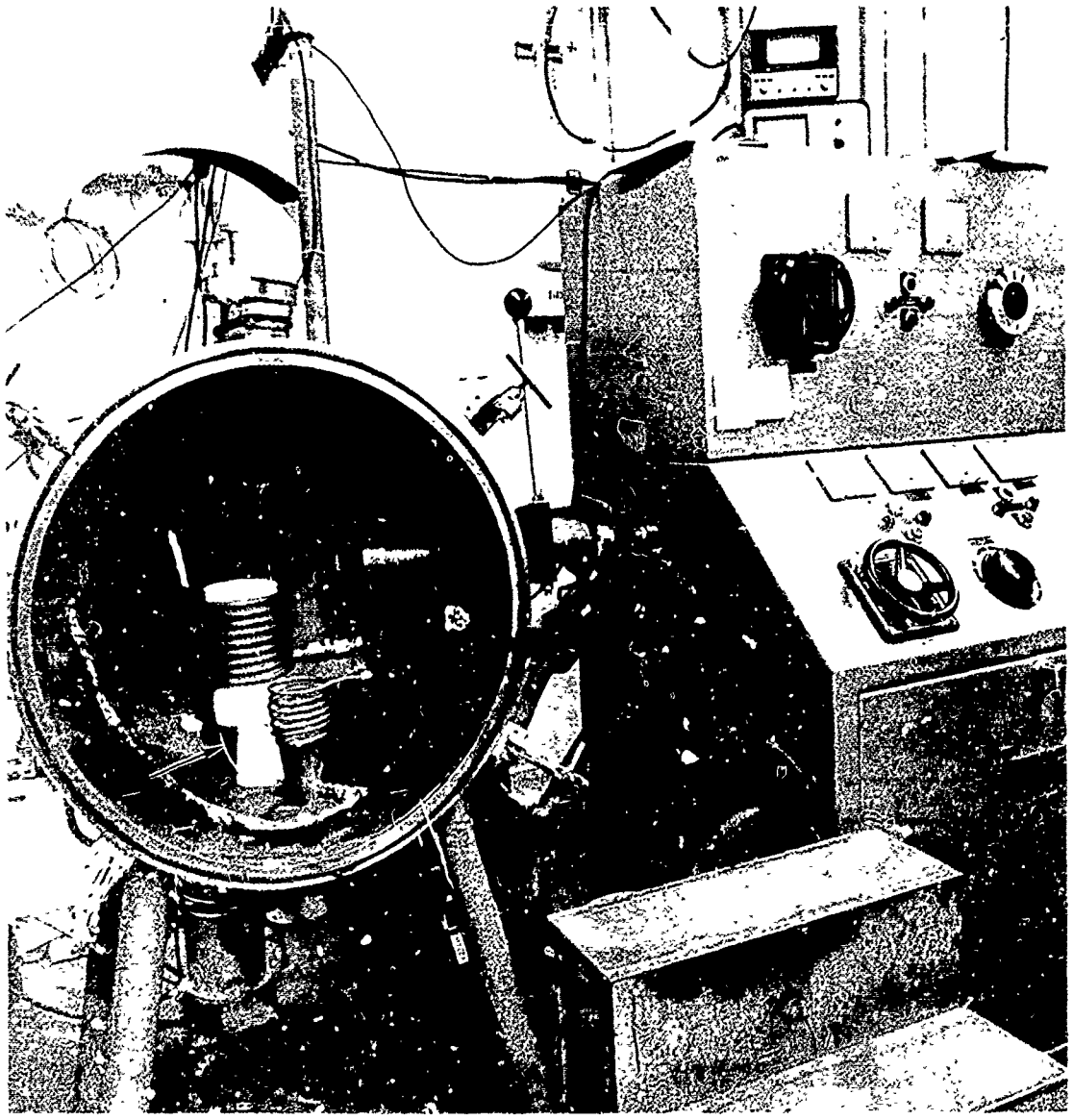


Figure 13. Induction Furnace Used for Laboratory Melting Experiments. Melting Experiment Set-Up is Located in the Large Coils (Note Thermocouple at Arrow). Samll Coils Contained the Set-Up for Crucible Firing.

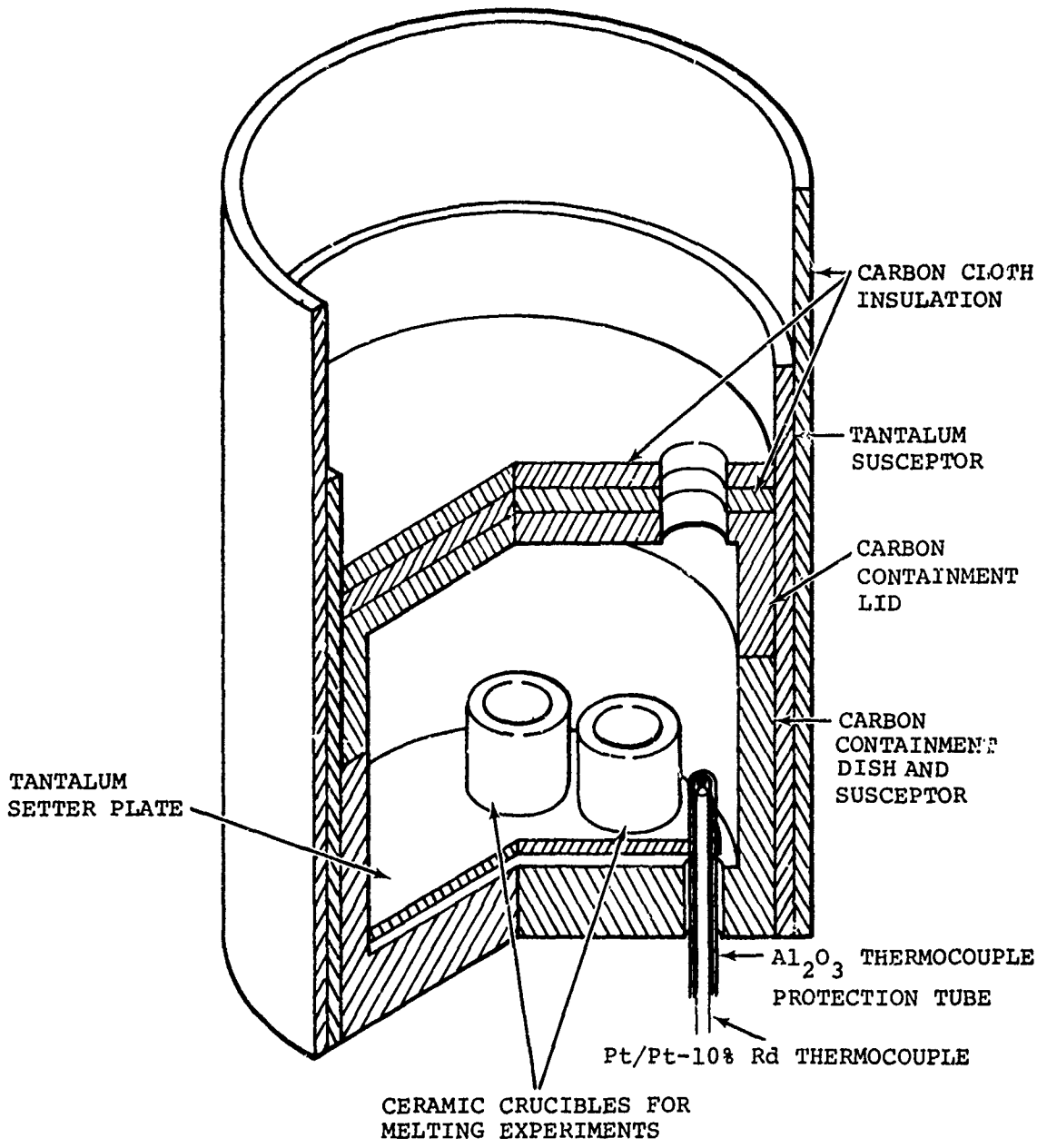


Figure 14. Standard Melt Run Experimental Arrangement Which is Placed Within an Induction Coil for Heating of the Tantalum and Carbon Susceptors.

Several crucibles (3-5) were included in each melt run to allow uniform comparisons of reactivity. A yttrium oxide crucible and alloy charge was included in each melt run to provide a run-to-run correlation. Vacuum atmospheres in the 0.1 to 1.0 micron range were maintained during the melts except for one run which was conducted in argon at a partial pressure of 5-inches of Hg. This argon run included CaO, CaO·15Ti and MgO crucibles, all of which had shown excessive metal boiling and spitting during previous vacuum runs.

After the melt run, the entire setup was cooled in vacuum at a rate of approximately 4000°F/hour for the Task I and 1300°F/hour for the Tasks II and III melts. These slower cooling rates for the later melts were partially due to the improved laboratory melting setup, (included the lid arrangement that also reduced thermal gradients) which kept the crucibles intact.

After cooling to near room temperature, crucibles, with the solidifed control alloy were removed from the susceptor dish, photographed, weighed and examined. The crucible plus melt was then sectioned to provide a combined metal/ceramic metallography sample and the remainder of the melt used for chemical analysis. The metallography sample containing both crucible and melt was then evaluated for crucible/melt reactions, metal bulk microstructure changes and hardness.

3.2.1.5 Additional Crucible Evaluations

Standard melt runs (Section 3.2.1.4) were primarily used to assess the relative level of reactivity to molten titanium of the various ceramics evaluated. It was also necessary to determine the degree of influence exerted by time and temperature on contamination of melts. Therefore, variations in time and temperature from the standard run were conducted in a series of

additional melt runs. Evaluation procedures used for melts and crucibles were identical to those described previously for the standard run.

As the alloy development progressed (Section 3.1), other binary systems (Ti-Cu and Ti-Fe) began to appear more promising than the Ti-Be system. Melt runs were therefore required to assess crucible contamination of these other alloy systems in order to anticipate any serious deviation from results gained by using the Ti-2.7Be control alloy to assess crucible performance. Several melt runs were conducted using low melting alloys (Ti-10Cu, Ti-16Cu and Ti-9Fe) as well as the control alloy. These alloys were placed in various crucibles and run using the standard technique but at temperatures 200°F above the particular alloy melting point as opposed to the 300°F used for standard runs. A control sample, consisting of the Ti-2.7Be alloy in Y_2O_3 crucible, was included in each additional melt run.

3.2.1.6 Chemical Analysis Techniques

Since excessive oxygen can be deleterious to the mechanical properties of titanium, it was monitored for all laboratory crucible melts. One-gram samples of laboratory melts (Ti-2.7Be alloy) were analyzed by the neutron activation technique (IntelCom Rad Tech, San Diego, CA). This technique had indicated, during previous AiResearch studies, higher oxygen values than standard vacuum fusion techniques particularly, for samples containing refractory oxides. To establish the control alloy oxygen content, several Ti-2.7Be rolled bar samples were analyzed for oxygen by neutron activation (0.16 percent) and vacuum fusion (0.11 percent) techniques. The neutron activation value was used as baseline for estimating oxygen contamination of Ti-2.7Be melts made in crucibles during Phase I.

From neutron activation data, analyzed values for oxygen are estimated within $\pm$0.06 percent of the actual amount. This scatter is quite high and may relate to contamination associated with sample preparation, variations in oxygen in the bar stock, or inherent difficulties in the neutron activation analytical process.

Chemical analysis of other elements (including rare earths and some oxygen analyses) was conducted on 1-gram samples submitted to National Spectographic Laboratories (Cleveland, OH). Samples were submitted with the surface reaction zone intact on the material but with adhering crucible material removed.

3.2.1.7 Mold Material Investigations

Fabrication of investment molds does not involve pressing and firing (greater than 2900°F) approaches used for crucibles. The mold fabrication requires non-toxic ceramics that can be handled in stable liquid slurries and can be fired at lower temperatures (2000°F). The low temperature capability common to the superalloy investment casting industry for mold sintering places a restriction on the materials that may be used for the low reactivity facecoat. Current practice involves using silica as a binder aid as well as a primary material (silicates). The silicates ($ZrSiO_2$ primarily) were known to promote excessive contamination of even the low melting titanium alloys and therefore required replacement with other low reactivity binders and primary materials.

Crucible melt evaluations identified promising low reactivity materials, and several were considered for use in mold facecoats. Evaluations were therefore required in order to adapt the low reactivity ceramics to the mold fabrication process with primary objectives of developing proper slurry properties and low temperature sinterability (2000°F). Mold facecoat investigations involved the preparation of aqueous slurries of HREMO or

alumina with a variety of sintering aids and approrpriate wetting and antifoam agents (specific compositions are given in Appendix E (Tables E-1, E-2, and E-3). Processing of slurries involved:

(a) Mixing by hand, lightning mixer or ball mill techniques

(b) Drying the slurry in bulk, thin layers or slip cast on the inside of small crucibles

(c) Firing of dried slurries in air or argon at temperatures from 1900°F to 2450°F

(d) Evaluating the fired mass for sintering quality

Investigation during Phase I involved the evaluation of four groups of facecoat compositions:

(a) Group 1 - Organic binder used, bulk samples evaluated

(b) Group 2 - Contained CaF_2, LiF and SiO_2 sintering aids, bulk samples evaluated

(c) Group 3 - Contained CaF_2 and SiO_2 sintering aids, bulk and thin layer samples evaluated

(d) Group 4 - Contained organic binder or CaF_2 and SiO_2 in large quantities, slip cast layers evaluated

3.2.2 Results and Discussion - Crucible/Mold Materials

Phase I crucible/mold material evaluations were conducted by evaluating titanium alloy melts in small ceramic crucibles of various materials. This was the primary technique for screening materials, which would be acceptable in the casting process as either induction melting crucibles or low reactivity facecoacs for investment molds.

A limited effort also involved the evaluation of slurries and various binder agents which would produce low temperature (near 2000°F) sintering of appropriate material candidates for mold facecoats.

3.2.2.1 Task I Crucible Investigations

Literature surveys and previous AiResearch efforts identified several promising materials for possible use in crucible and mold applications. These materials were selected based upon one or more of the following criteria (specific details are discussed in Appendix F):

- Low reactivity with molten titanium alloys
- Adequate thermal shock resistance
- Reasonable cost
- Ease of fabrication

The materials chosen were as follows:

Y_2O_3	CaO
Y_2O_3·15Ti (wt.-%)	CaO·15Ti
ThO_2	MgO
Dy_2O_3	SiC
La_2O_3	Pyrographite
CeS	

HREMO (Heavy Rare Earth Mixed Oxide)
LREMO (Light Rare Earth Mixed Oxide)

Crucibles were successfully fabricated from all of the above candidates except La_2O_3. Several different fabrication approaches were attempted with the La_2O_3, but no sound crucibles could be produced primarily due to its hygroscopic nature. As a result, no evaluation of La_2O_3 crucibles was conducted.

Examination of the remaining crucibles visually and by metallography (where appropriate) indicated all were reasonably dense and well bonded except the CaO·15Ti, Y_2O_3·15Ti, and to a limited degree CaO. Most crucibles ranged from 85-97 percent of theoretical density, and were considered representative of good material.

3.2.2.1.1 Crucible Storage Evaluation

Most crucibles were not adversely affected by open storage (humidity ranged from 4 to 36 percent). However, the CaO containing compositions and the La_2O_3 were completely disintegrated by exposure to ambient air in approximately one-months time. Of special significance is that the MgO and the LREMO crucibles performed well under ambient storage conditions.

3.2.2.1.2 Standard Crucible Evaluation

Eleven Task I standard melt runs were performed with a variety of crucibles included in each run. All crucibles used in melt runs were able to contain the Ti-2.7Be control alloy with no through-wall penetrations except in areas where a crack existed prior to melting. The Y_2O_3 and LREMO crucibles showed a tendency for thermal shock cracking, but this occurred during cooling of the melt and did not result in metal loss.

Chemical analysis results of the solidified control alloy melts are summarized for each crucible composition in Table 10. The Y_2O_3 and $Y_2O_3 \cdot 15Ti$ were the best compositions for limiting contamination of the alloy. HREMO crucibles demonstrated the next best performance, and due to relatively low cost, appears promising. The ThO_2, CaO, and Dy_2O_3 also displayed reasonable indications of low reactivity. The remainder of the candidate materials all showed either excessive oxygen contents or large amounts of other crucible elemental contamination.

Microstructures indicate that a variety of second phases were produced in alloy melts. The second phases generally appeared blocky, as shown in Figure 15 for melts made in Y_2O_3, $Y_2O_3 \cdot 15Ti$, ThO_2 and HREMO crucibles. The LREMO crucible did not promote significant second phase formation, but severe second phase formation occurred in melts conducted in Dy_2O_3, CeS and pyrographite. The presence of these second phases could affect the cast alloy mechanical properties.

Melts made in the Y_2O_3 base systems consistently showed less microstructural evidence of contamination than any of the other crucible materials. Melts made in HREMO crucibles, in addition to the blocky internal second phases, displayed microstructural contamination of the metal surface adjacent to the crucible to a depth of 120-200 mils. Melts in LREMO, MgO and $CaO \cdot 15Ti$ crucibles showed an alpha case in addition to extensive internal contamination (Figure 16). Melts in SiC exhibited severe surface contamination, while minor surface contamination but heavy internal contamination was observed for melts in pyrographite. Melts in CeS, CaO, ThO_2 and Dy_2O_3 all showed internal microstructural contamination but an absence of surface alpha case.

Bulk hardness measurements made on melts from each crucible/mold material ranged from a low of $R_A 58$ for Y_2O_3 to a high of $R_A 87$ for the SiC melt. Starting ingot alloy hardness was $R_A 51$.

TABLE 10

CHEMICAL ANALYSIS RESULTS
FOR Ti-2.7Be ALLOY MELTED IN TASK I
CRUCIBLES AT TEMPERATURES OF 2870°F

Crucible Material	Number Of Melts	Oxygen Increase (wt-%)		Increase In Other Elements (wt-%)		
		Range	Average	Element	Range	Average
Y_2O_3	7	0.06-0.14	0.09	Y	0.07-0.26	0.19
Y_2O_3.15Ti	2	0.11-0.13	0.12	Y	0.18-0.20	0.19
ThO_2	3	0.46-0.64	0.57	Th	0.70-0.80	0.63
Dy_2O_3	2	0.83-1.07	0.95	Dy	0.30-0.67	0.48
La_2O_3	None	--	--	--	--	--
LREMO	1	--	3.10	R.E.	--	0.027
HREMO	2	0.44-0.52	0.47	R.E.	0.07-0.29	0.16
CaO	3	0.52-0.71	0.59	Ca	0.002-1.07	0.37
CaO.15Ti	2	0.58-1.54	1.06	Ca	<0.001-0.007	0.004
MgO	3	3.03-4.02	3.41	Mg	0.003-0.004	0.004
CeS	1	0.02-0.03	0.03	Ce S	- -	0.56 0.19
Pyro-graphite	2	0.01-0.03	0.02	C	0.56-0.60	0.58
SiC	1	--	0.02 loss	Si C	-- --	7.51 5.83

*Average oxygen content of alloy was 0.16 wt-%. Oxygen analyses performed by neutron activation, others by wet chemical, spectro chemical, or spectrographic.

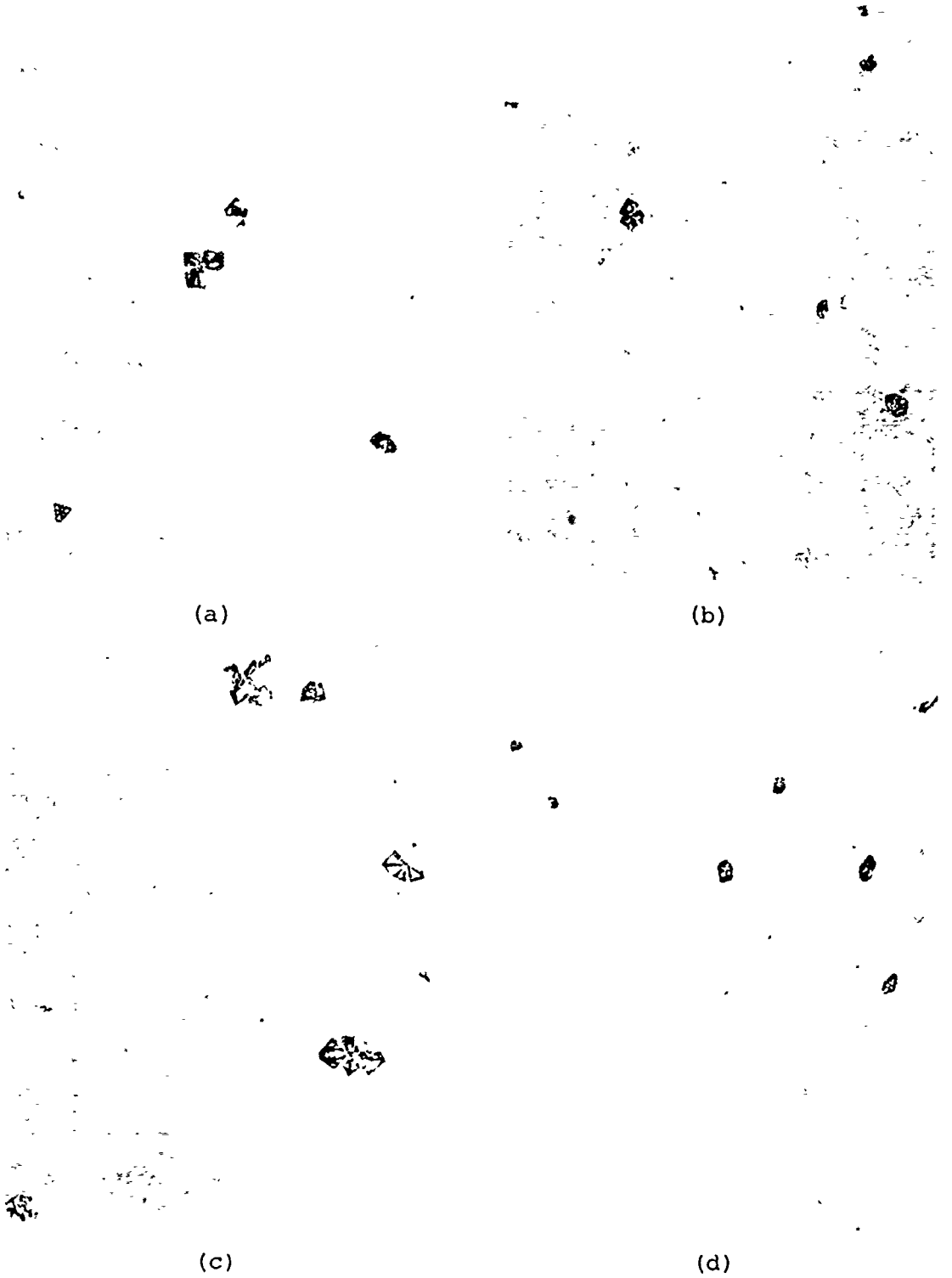


Figure 15. Typical Microstructure of Ti-2.7Be Melts Conducted in Crucibles of Y_2O_3(a), Y_2O_3·15Ti(b), ThO_2(c) and Heavy Rare Earth Mixed Oxides (d). All Show Large Blocky Gray Inclusions. (As-Polished 100X).



(a) MELT IN LREMO CRUCIBLE (IC-10)



(b) MELT IN CaO.15Ti CRUCIBLE (IC-7)



(c) MELT IN MgO CRUCIBLE (IC-7)

Figure 16. Alpha Case Contamination of the Surface of Ti-2.7Be Melts Made in Three Crucibles. The Alpha Case is the Solid White Layer in (a) and (c) Whereas it is the Porous Appearing Layer in (b) (100X).

Most of the crucible materials produced alloy melt hardnesses in the low 60's, indicating various degrees of internal contamination from reactions with the various crucible materials.

Microhardness measurements were also made on melts made in several of the better crucible materials (Y_2O_3, ThO_2 and HREMO). Measurements were made primarily to determine; (1) if significant contamination was present on the melt surface adjacent to the crucible material and, (2) the relative hardness of the second phase particles which developed in the melt as a result of metal/crucible reaction. Edge hardness (1-mil from edge) did not significantly differ from internal hardness indicating an absence of severe near-surface contamination. The true hardness of second phase particles was difficult to assess due to shape and size, but were found harder (407 KHN) than the metal matrix (209 KHN).

3.2.2.1.3 Temperature/Time Evaluations

Melt runs were performed to determine the effect of molten metal temperature and hold times on melt contamination with the more promising crucible materials. Chemical analysis of these melts (Table 11) indicated that increasing the metal temperature promoted increased contamination. The influence of hold time was not readily observed, except possibly by hardness changes (Table 11) since hold times (3 to 10 minutes) were not far enough apart to promote discernible differences. These times were initially chosen to reflect the typical time range expected during actual casting operations. However, the typical melting time actually experienced during Phase II casting efforts was closer to 20 minutes.

3.2.2.1.4 Summary - Task I

Y_2O_3, both as the pure material and in the titanium modified form, resulted in the lowest titanium melt contamination.

TABLE 11

THE INFLUENCE OF TEMPERATURE AND HOLDING TIME ON THE CONTAMINATION OF THE Ti-2.7Be ALLOY

Conditions and Results	Influence of Temperature Metal Held at Melting Point (M.P.) for 4-min	Influence of Temperature M.P. + 200°F 10 Min	Influence of Time M.P. + 300°F 3 Min	Standard Run M.P. + 300°F 10 Min	Influence of Temperature M.P. + 460°F 10 Min
Run Number	IC-1	IC-12	IC-16	IC-4,-5,-6,-7,-10	IC-9
Temperature (°F)	2510	2774	2879	2870	3030
Time at Temperature (Min)	4	10.4	3.4	10	9
Time Above 2550°F (Min)	0	19	19	23	32
Time Above 1850°F (Min)	78	43	49	56	58
Y_2O_3 Crucible					
O_2 Increase (Wt-%)	0.11	0.03	0.09	0.08	0.14
Y Increase (Wt-%)	0.13	0.07	0.23	0.16	0.26
Hardness Increase R_A	10	7.5	6.5	10.0	--
Yttria Particle Size in Metal Microstructure (Mils)*	0.5	1.3	2-5	1.8	--
ThO_2 Crucible					
O_2 Increase (Wt-%)	0.32	0.46	--	0.62	0.64
Th Increase (Wt-%)	1.00	0.73	--	0.70	0.80
Hardness Increase R_A	11.5	11.5	--	12.5	--
Thoria Particle Size in Metal Microstructure (Mils)*	2	1.7	--	2	--
Pyrographite Crucible**					
O_2 Increase (Wt-%)	--	0.02	0.14	0.07	0.00
C Increase (Wt-%)	--	0.63	0.96	0.58	1.01
Hardness Increase R_A	--	7.5	8.0	8.0	--
Carbide Particle Size in Metal Microstructure (Mils)*	--	14	16	25	--
Hremo Crucible					
O_2 Increase (Wt-%)	0.19	--	--	0.44	0.51
Rare Earth Increase (Wt-%)	0.29	--	--	0.07	0.12
Hardness Increase R_A	11.5	--	--	11.5	--
Rare Earth Particle Size in Metal Microstructure (Mils)*	0.6	--	--	1.7	--

* Diameter for Y_2O_3 and ThO_2 and Length for Carbide

** Standard run taken as average of runs IC-4 and IC-5; the M.P. + 460°F values are from run IC-13

The Y_2O_3·15Ti composition did not show the expected reactivity improvement over Y_2O_3 (it was however equivalent) and microstructures suggested it was fired at too low a temperature (3000°F). However, the titanium modified composition did show much improved thermal shock resistance to the pure Y_2O_3.

The ThO_2, HREMO, and CaO compositions showed good promise for limiting contamination of the melt. The ThO_2 and HREMO were projected at a cost of $7-11/pound for the raw powder compared to Y_2O_3 at $30, while CaO was much lower in cost ($0.70/pound).

Other materials, Dy_2O_3, LREMO (Light Rare Earth Mixed Oxides), CaO·15Ti and MgO all showed high oxygen contamination or severe second phase formation in the microstructure (pyrographite, SiC and CeS), and therefore none of the above was considered promising for further investigations.

3.2.2.2 Task II Crucible Investigations

The following crucible/mold compositions were included in the Task II investigation (properties compiled in Appendix D, Table D-2):

Y_2O_3 (control from Task I fabrication)
Y_2O_3 (substoichiometric)
ThO_2 (substoichiometric)
HREMO (substoichiometric)
Y_2O_3·15Ti (wt-%)
Y_2O_3·8Ti (wt-%)
HREMO·15Ti (wt-%)
Y_2O_3 Slip cast into a SiC crucible
CaO

Crucibles evaluated in the substoichiometric condition (Y_2O_3, ThO_2 and HREMO) were purchased according to the same specifications for similar Task I crucibles. Various thermal treatments were then employed to reduce the oxygen stoichiometry as previously described (Section 3.2.1.3.1).

Titanium modifications of Y_2O_3 and HREMO materials were considered promising from Task I results, especially from the standpoint of improved thermal shock resistance. The $Y_2O_3 \cdot 8Ti$ composition was selected in order to evaluate a lower titanium content and was based upon results of research conducted at Battelle Columbus Laboratories[33] indicating titanium in excess of 25 atomic-percent (6.5 weight-percent) was required to saturate the Y_2O_3 with titanium. Reductions in titanium below this level were not considered promising due to an expected loss in thermal shock resistance. The fifteen percent titanium addition to HREMO was made based upon the acceptable Task I performance of the $Y_2O_3 \cdot 15Ti$ composition.

Slip casting a layer of Y_2O_3 on the inside of a SiC crucible was intended to take advantage of the good reactivity displayed by Y_2O_3 and the excellent thermal shock resistance of SiC. Calcia (CaO) was selected for further evaluation primarily because of its low cost, moderate reactivity and good thermal shock resistance.

Most of the Task II crucibles arrived in sound condition from the suppliers, the Y_2O_3 coated SiC crucible being the exception. The Y_2O_3, slip cast into a SiC backup crucible, underwent a reaction during sintering, which appeared to convert the Y_2O_3 to a carbide. This reaction combined with the structural deterioration of the SiC backup crucibles eliminated this

(33) McCoy, L. G., N. M. Griesenauer, C. A. Alexander, T. R. Wright and D. E. Niesz, Interaction Between Titanium and Y_2O_{3-x}, Research on Metallurgical Synthesis, AFML-TR-72-238, Part II, January 1974.

composition from further consideration during the program. However, the philosophy of applying a low-reactivity material (Y_2O_3) to a thermal shock resistant substrate remains attractive for future efforts.

A HREMO·15Ti crucible, fired at 3100°F (at Coors) developed severe cracking and degradation as time passed under dessicated storage. The Y_2O_3·15Ti and Y_2O_3·8Ti crucibles also developed very light cracking with time but not severe enough to prohibit further evaluation. Lower temperature (3000°F) fired crucibles of the above three compositions were intact and did not appear to be degrading with time. Subsequent firing of single crucibles under low thermal gradient conditions at equivalent temperatures (at AiResearch) did not promote cracking. These cracking problems were associated with the containment atmosphere purity and/or thermal gradients during firing of multiple crucibles by the supplier.

3.2.2.2.1 Special Firing of Laboratory Crucibles

Initial attempts to produce sound Y_2O_3 crucibles of low stoichiometry were not successful due to severe degradation of the crucibles. The degradation included fracturing of the solid crucible as well as the formation of a powder. However, the results of these thermal treatments showed that weight losses and blackening of yttria crucibles were effected by heating to 3100°F or above in close proximity to carbon (either in vacuum or argon). This blackening has been associated with reduced oxygen stoichiometry[32], and the weight losses[32,34]

[34] Alexander, C.A., N.M. Griesenauer, D.P. Moak, L.D. McCoy, and D.E. Niesz, "Evaluation of Refractory Oxide Crucible Material for Induction Melting of Titanium", AFML-TR-72-238 (1972) 76-93.

indicate the crucibles could have compositions ranging from $Y_2O_{2.98}$ to $Y_2O_{2.92}$. Efforts to resolve differences in lattice parameters between white Y_2O_3 (supposedly stoichiometric in composition) and black material (supposedly substoichiometric) were unsuccessful by X-ray diffraction. Chemical analysis for oxygen was also inconclusive and no verification of stoichiometry could be obtained.

Firing at temperatures greater than 3270°F were also found to affect the Y_2O_3 crucible adversely, promoting severe cracking and degradation. Firing conditions were subsequently established for rendering the Y_2O_3, ThO_2 and HREMO crucible compositions black (substoichiometric) as well as for the Y_2O_3·15Ti material, and several intact crucibles prepared for subsequent melting experiments. The refiring used for the Y_2O_3·15Ti composition was not to reduce stoichiometry but to increase crucible density and promote a more complete reaction between the Y_2O_3 and the metallic titanium.

3.2.2.2.2 Standard Crucible Evaluation

Visual appearance of Task II crucibles after melt runs varied from intact to shattered. From this inspection, an assessment of thermal shock resistance was made with the titanium-modified compositions exhibiting the greatest resistance to cracking followed in order by CaO, HREMO, ThO_2, and Y_2O_3. The Y_2O_3·15Ti crucible was much superior to the HREMO·15Ti composition. Blistering of the HREMO·15Ti crucible after the melt run indicated the titanium content was too high since the unmodified HREMO crucible did not blister. Chemical analysis results for Task II crucible melts, summarized in Table 12, indicated the Y_2O_3 composition continued to demonstrate the best performance. The HREMO and ThO_2 compositions exhibited next best performance, although displaying about twice the oxygen contamination as Y_2O_3.

TABLE 12

CHEMICAL ANALYSIS RESULTS
FOR Ti-2.7Be ALLOY MELTED IN PHASE I, TASK II
CRUCIBLES AT A TEMPERATURE OF 2870°F*

Crucible Material	Number of Melts	Oxygen Increase (wt-%)		Increase in Other Elements (wt-%)		
		Range	Average	Element	Range	Average
Y_2O_3	5	0.08-0.21	0.16	Y	0.10-0.20	0.16
Y_2O_3-LS**	2	0.11-0.13	0.12	Y C	0.16-0.17 0.014-0.022	0.17 0.018
ThO_2-LS**	2	0.24-.37	0.31	Th	1.40-1.49	1.45
HREMO-LS**	3	0.21-0.32	0.27	Rare Earths	0.15-0.23	0.20
HREMO-15Ti	1	-	1.70	Rare Earths	-	0.09
Y_2O_3.8Ti	1	-	0.68	Y	-	0.08
Y_2O_3.15Ti	2	0.55-0.73	0.65	Y	0.06-0.19	0.11
CaO (½" dia.)	1	-	1.41	Ca	-	0.005
CaO (2" dia)***	1	-	1.52	Ca	-	0.003

*Average oxygen content of alloy was 0.16 wt-percent. Oxygen analyses performed by neutron activation, others by wet chemical, spectrochemical, or spectrographic. The Ti-2.7 Be alloy has a melting point of 2570°F and was placed within 1-inch nominal crucibles (4 cc volume) as a 10-gram charge.

**LS refers to crucibles with the thermal treatments designed to produce low stoichiometry (oxygen).

***The large crucible was charged with about 100 grams of alloy and lost 85 percent during melting. The amount remaining in the crucible was nearly equivalent to the amount in the small CaO crucible and would be expected to show equivalent contamination effects.

The titanium modified ceramic compositions showed quite high levels of oxygen contamination and low levels of yttrium or/and rare earth contamination (Table 13). These oxygen levels, when compared to the Task I, $Y_2O_3 \cdot 15Ti$ crucible results (0.12 percent O_2 and 0.19 percent Y increases), indicated that the Task II crucibles contaminated the melt to a greater extent. Rechecking the crucible manufacturer's (Coors Porcelain Co.) fabrication procedures established Task I crucibles had been fired in argon while the Task II crucibles were fired in a very poor vacuum (about 200-microns pressure without argon purging). This poor vacuum could increase the oxygen content of the titanium metal in Task II crucibles as well as prevent the Y_2O_3 from going substoichiometric in oxygen. Both of these effects would be expected to increase the reactivity of the crucible toward the molten titanium alloy, thereby causing higher melt oxygen contamination.

A comparison of analytical results between Tasks I and II is given in Table 13. This data indicates several trends as follows:

- Apparent lower stoichiometry in the Y_2O_3 did not improve its contamination performance.
- Apparent lower stoichiometry in the Task II ThO_2 and HREMO compositions showed marked improvements in oxygen contamination over stoichiometric, Task I crucibles (about 40 percent less contamination) but with higher metallic contamination.
- A slight decrease in alloy melt contamination (lower O_2 but higher metallic contamination) occurred when the $Y_2O_3 \cdot 15Ti$ crucible was refired at higher temperatures (3200°F) in argon at AiResearch, indicating higher firing temperatures may be useful.

TABLE 13

COMPARISON OF ALLOY CONTAMINATION LEVELS FOR MELTS MADE IN TASK I AND TASK II CRUCIBLES

Crucible *	Contamination Increase (wt-percent)			
	Oxygen		Crucible Metallic	
	Task I	Task II	Task I	Task II
Y_2O_3	0.09	0.12 **	0.19	0.14 **
Y_2O_3-LS ($Y_2O_{2.98}$)	--	0.12	--	0.17
ThO_2	0.57	--	0.63	--
ThO_2-LS ($ThO_{1.96}$)	--	0.31	--	1.45
HREMO	0.47	--	0.16	--
HREMO-LS ($RE_2O_{2.95}$)	--	0.27	--	0.20
Y_2O_3·15Ti (Fired 3000°F)	0.12	0.73	0.19	0.06
Y_2O_3·15Ti (Fired > 3180°F)	--	0.65	--	0.11
CaO (1-in. diam)	0.59	1.41	0.37	0.004

*LS refers to thermal treated crucibles to obtain low stoichiometry as estimated in parenthesis.

**This value obtained for two melts made in same runs as the Y_2O_3-LS crucibles.

- Melt outgassing and contamination were considerably higher for Task II melts in CaO, possibly due to inadequate firing or the higher melt run vacuum levels.

Microstructural examination of alloy melts showed the formation of second phase particles in all melts made in Y_2O_3, ThO_2, and HREMO crucibles. This was consistent with Task I results. These particles were located primarily in the eutectic areas of the microstructure. Melts made in Y_2O_3 showed no evidence of a contaminated case (Figure 17a), although a variety of crucible surface textures were observed in contact with the melt. Melts made in the HREMO crucible also did not exhibit surface contamination, although moderate infiltration of the melt into the crucible was intermittently observed (Figure 17b). The surface of the melt adjacent to the ThO_2 crucible (Figure 17c) showed light alpha case formation as well as some internal contamination.

Melts made in the Y_2O_3 crucibles displayed only slight evidence of microstructural contamination. Both the ThO_2 and HREMO melts showed microstructures indicating higher contamination than $_2O_3$ melt (this was consistent with analytical results). The [illegible]nium modified crucible compositions all produced heavier contamination of the melt matrix.

3.2.2.2.3 Alloy/Crucible Compatibility Evaluation

Special melt runs conducted to evaluate the compatibility of the most promising alloy systems and crucibles were made. This evaluation would allow deviations in performance of crucibles due to melts of other alloy compositions (than the control alloy) to be anticipated. Task I alloy development work indicated the Ti-Cu and Ti-Fe systems were most promising and therefore Ti-9Fe (melting point of 2700°F), Ti-10Cu (MP=2725°F),



(a) Y_2O_3-37 ETCHED



(b) HREMO-4, FIRED AT 3390°F IC-21)



(c) ThO_2-D5, FIRED AT 3220°F WITH CARBON COAT (IC-23)

Figure 17. Typical Microstructures at the Crucible/Melt Interface for Laboratory Melts of Ti-2.7Be Alloy in Y_2O_3, HREMO, and ThO_2 Crucibles. Note the Absence of Alpha-Case on Melts in Y_2O_3 and HREMO but its Presence for the Melt in ThO_2. (Etched, 250X).

and Ti-16Cu (MP= 2575°F) were selected for the compatibility study. The crucible materials selected were Y_2O_3, ThO_2, HREMO, and Y_2O_3·15Ti. The melt runs were made with the standard setup at temperatures approximately 200°F above the melting point of the alloy under test. A control sample was included in each run and consisted of the Ti-2.7Be alloy in a Y_2O_3 crucible. Chemical analyses (Table 14) conducted on samples from each melt indicated the following trends:

- The Y_2O_3 material remained the best material for limiting the contamination in melts of all alloys.
- Alloys with lower melting points displayed, in general, lower contamination when melted with an equal amount of superheat.
- Lower absolute temperature also gave less contamination.
- The Ti-Cu and Ti-Fe alloys displayed lower contamination than the Ti-2.7Be control alloy when melted in Y_2O_3 crucibles.
- Ti-Cu and Ti-Fe alloys displayed higher oxygen and lower metallic contamination than the Ti-2.7Be control alloy when melted in ThO_2 and HREMO crucibles.
- Effect of the Y_2O_3·15Ti crucible on the contamination of various alloys could not be clearly established due to the limited amount of data.

TABLE 14

INFLUENCE OF CRUCIBLE MATERIALS ON THE CONTAMINATION OF LOW MELTING TITANIUM ALLOYS*

	Run Temp (°F)	Ti Alloy	Contamination (wt-%) of Alloys Melted in Crucibles							
			Y_2O_3		$Y_2O_3 \cdot 15Ti$		HREMO		ThO_2	
			O_2	Other	O_2	Other	O_2	Other	O_2	Other
Task I Results	2870	2.7 Be	0.25	Y-0.19	0.28	Y-0.19	0.63	RE-0.16	0.73	Th-0.63
Task II Results										
IC-20	2866	2.7 Be	0.36	Y-0.17	0.89	Y-0.06	--	--	--	--
Ti-10Cu	2948	2.7 Be	0.36	Y-0.32	--	--	--	--	--	--
(IC-22)		10 Cu	0.31	Y-0.29	--	--	0.82	RE-0.18	0.63	Th-1.34
Ti-16Cu	2740	2.7 Be	0.25	Y-0.14	--	--	--	--	--	--
(IC-24)		16 Cu	0.16	Y-0.21	0.50	Y-0.06	0.47	RE-0.10	--	--
Ti-9Fe	2904	2.7 Be	0.40	Y-0.34	--	--	--	--	--	--
(IC-25)		9 Fe	0.28	Y-0.05	--	--	0.82	RE-0.02	0.56	Th-0.35

*Oxygen values are as-analyzed rather than as increases above the as-received ingot, oxygen analyses in table performed by neutron activation (NA).

Microstructural examination of melts for the Ti-Cu and Ti-Fe alloys in the Y_2O_3 crucibles showed no apparent surface contamination (Figure 18). All three alloys exhibited similar second phase particle formation to that previously observed in the Ti-2.7Be alloy melts.

Bulk hardness measurements for the three alloys melted in Y_2O_3 showed increases, which were consistent with the increase in oxygen contamination.

3.2.2.2.4 Summary - Task II

Results from this task supported previous trends, which showed that Y_2O_3 is the best material for limiting contamination (0.16 percent O_2) of low-melting titanium alloy melts. As judged by oxygen contamination, HREMO (0.27 percent O_2) and ThO_2 (0.30 percent O_2) were next best with titanium modified Y_2O_3 third (0.7 percent O_2).

Lowering the apparent oxygen stoichiometry was not of significant benefit for Y_2O_3 but was effective in reducing oxygen contamination of melts made in HREMO and ThO_2 (by nearly 50 percent). Microstructural examination showed the continued presence of the blocky second phase particles in the low stoichiometry versions of the Y_2O_3, HREMO and ThO_2 crucible melts.

Higher oxygen contamination of melts in titanium modified Y_2O_3 were observed for crucibles fabricated in Task II (0.73 percent) than for those fabricated in Task I (0.12 percent). The reason for this behavior was not identified but was attributed to crucible firing procedure.

Thermal shock resistance of the more promising ceramic systems was judged to range from fair to poor with Y_2O_3 exhibiting the poorest performance. However, titanium modification of



(a) Ti-10Cu MELT AT 2948°F IN Y_2O_3 (-11)



(b) Ti-9Fe MELT AT 2904°F IN Y_2O_3 (-53)



(c) Ti-16Cu MELT AT 2740°F IN Y_2O_3 (-42)

Figure 18. Typical Microstructures at the Crucible/Melt Interface for Laboratory Melts of Ti-10Cu, Ti-9Fe-0.03Y and Ti-16Cu Alloys in Y_2O_3 Crucibles.

the ceramics significantly improved the thermal shock properties without seriously degrading reactivity.

Contamination of other titanium alloys (Ti-Cu and Ti-Fe binaries) were found comparable to that of the Ti-2.7Be control alloy melted in the more promising crucible/mold materials. As a result, scale-up of these type alloys to casting operations was not expected to present any serious incompatibilities.

3.2.2.3 Task III Crucible Investigations

The following compositions and fabrication parameters were selected for the Task III crucible evaluations:

- o Y_2O_3 (control from Task I fabrication)
- o $Y_2O_3 \cdot 15Ti$, as received (fired at 3000°F)
- o $Y_2O_3 \cdot 15Ti$ refired at temperatures above 3200°F
- o HREMO·8Ti, as-received (fired at 3000°F)
- o HREMO·8Ti, refired at temperatures above 3175°F

Task I and II work identified Y_2O_3 as the least reactive ceramic material, but its relatively high price ($30/lb) limits its attractiveness for mold applications. However, Y_2O_3 is the prime candidate for melting crucibles, but the thermal shock resistance (TSR) of Y_2O_3 is poor and requires improvement. The most promising approach toward improving the TSR is by the addition of titanium, which would then allow repeated crucible usage in the casting process. Task II results indicated there was no appreciable difference in reactivity between the two titanium modified Y_2O_3 compositions (8 percent and 15 percent Ti) evaluated. The $Y_2O_3 \cdot 15Ti$ composition was therefore selected in Task III to obtain maximum TSR and these crucibles were evaluated in the as-received condition (fired at 3000°F in argon) as

well as after refiring at a higher temperature ($\geq$3355°F). Evaluation of these crucibles in a higher fired condition was undertaken to improve the reactivity of the crucible, hopefully to attain the low melt contamination levels observed for the Task I crucibles.

Evaluation of the titanium modified HREMO system was continued since the HREMO material had demonstrated the potential for low melt contamination and is substantially cheaper ($11/lb) than Y_2O_3. In an effort to approach the reactivity level of the basic HREMO system, while maintaining the TSR obtained by titanium modification, a lower titanium content (8 percent) was selected. Evaluations were performed on crucibles of this material in the as-received (fired in argon at 3000°F) and in the refired (in argon at $\geq$3175°F) conditions. Evaluation of higher fired conditions were necessary to identify the best conditions for low reactivity performance of the crucible.

The initial crucibles of both compositions (Y_2O_3·15Ti and HREMO·8Ti) were received in poor condition and considered unsuitable for program evaluation. All crucibles were black and rough as opposed to the gray, smooth appearance of crucibles from the previous two tasks. Crucibles of both compositions exhibited spalling, and/or extreme blistering (HREMO·8Ti). Discussions with the vendor (Coors Porcelain Co.) indicated excessive temperatures and heating rates were attained during firing due to temperature measurement problems. This was attributed to fogging of the furnace sight glass, due to the large number of crucibles (11) fired, compared to previous tasks (3-4 crucibles). As a result, erroneous optical pyrometer temperature measurements were obtained with the actual firing temperature estimated to have been in excess of 3000°F. This fogging phenomenon, had been observed at less severe levels by Coors during previous firings and was considered typical for titanium modified compositions.

A second lot of crucibles were processed by Coors and were delivered in good condition. The second crucible firing was conducted using combined thermocouple and pyrometer temperature measurements with only 4-5 crucibles fired in each lot.

Several crucibles were refired, at AiResearch prior to melt runs (approach previously described in Section 3.2.1.3.2), using higher temperatures (to 3685°F) than the initial 3000°F firing at Coors (crucible appearances and properties are presented in Appendix D, Table D-4).

3.2.2.3.1 Standard Crucible Evaluation

Chemical analyses of the Task III melt runs are shown in Table 15. Yttria control crucibles included in these runs were again rated as the best for minimizing oxygen contamination of low-melting titanium melts with greater reactivity resulting from modification of the Y_2O_3 with titanium. Oxygen analyses were again contrary to the low oxygen contamination (0.12 percent) observed for melts in Y_2O_3·15Ti crucibles fabricated during Task I of the program (the next section describes a further analysis of the contrary behavior).

The titanium modified HREMO crucible melts showed a 10 to 25 percent higher contamination level (0.63 percent oxygen) than the titanium modified Y_2O_3 crucible melts '0.50 percent oxygen). This was considered very good performance since the HREMO composition contains only 60 percent Y_2O_3 and would be cheaper than Y_2O_3 compositions.

Both titanium-modified materials exhibited reduced reactivity after firing at progressively higher temperatures (Table 15). The HREMO·8Ti composition fired at 3355°F showed melt contamination levels (0.46 percent O_2) which were nearly equivalent to the Y_2O_3·15Ti crucible (0.41 percent O_2) fired at the same temperature. No difference in thermal shock resistance

TABLE 15

CHEMICAL ANALYSIS RESULTS
FOR Ti-2.7Be ALLOY MELTED IN PHASE I, TASK III
AT A TEMPERATURE OF 2870°F

Crucible Material**	Number of Melts	Oxygen Increase (wt-%)		Increase In Other Elements (wt-%)		
		Range	Average	Element	Range	Average
Y_2O_3	2	0.18-0.19	0.19	Y	0.15-0.17	0.16
Y_2O_3·15Ti						
3000°F (As-Received)	1	-	0.50	Y	-	0.11
3355°F (Refired)	1	-	0.41	Y	-	0.09
3685°F (Refired)	1	-	0.36	Y	-	0.11
HREMO·8Ti						
3000°F (As-Received)	1	-	0.63	Rare Earths	-	0.16
3175°F (Refired)	1	-	0.55	Rare Earths	-	0.15
3355°F (Refired)	1	-	0.46	Rare Earths	-	0.13

*Average oxygen content of alloy was 0.16 wt-%.

**Temperatures listed beneath crucible material refers to the re-firing temperature used after fabrication. As received crucibles were fired at 3000°F.

was observed, and based upon the above melt contamination levels, these two compositions appear to be nearly equal in performance.

Metallographic examination of the melts made in both the Y_2O_3·15Ti and HREMO·8Ti crucibles continued to show second phase particles distributed throughout the metal. The size and number of these particles did not appear to be influenced by the crucible firing temperature. Melts made in both crucible materials also showed a relatively clean layer of metal adjacent to the crucible surface.

The influence of crucible firing temperature on the crucible microstructure is shown for Y_2O_3·15Ti (Figure 19) and HREMO·8Ti (Figure 20). As firing temperature was increased, both crucible compositions showed decreased porosity as well as microstructural changes in the titanium particles. HREMO·8Ti appears to show lower porosity than Y_2O_3·15Ti for equivalent firing conditions, indicating more complete sintering for the HREMO composition. Although it was not evaluated, the decrease in porosity would be expected to decrease thermal shock resistance.

Bulk hardness measurements of crucible melts were not made during Task III since previous work showed poor correlation between hardness and oxygen content.

3.2.2.3.2 Supplemental Y_2O_3·15Ti Crucible Evaluation

Chemical analysis of melts made in Y_2O_3·15Ti crucibles during the three tasks indicated different levels of contamination for each lot. In order to verify that experimental procedures were not responsible for this inconsistency, extra Y_2O_3·15Ti crucibles remaining from each of the three tasks, were run together in a single melt run. Lower reactivity was verified for Task I crucibles and fabrication parameters and properties did not readily explain the difference in performance (Table 16). The firing

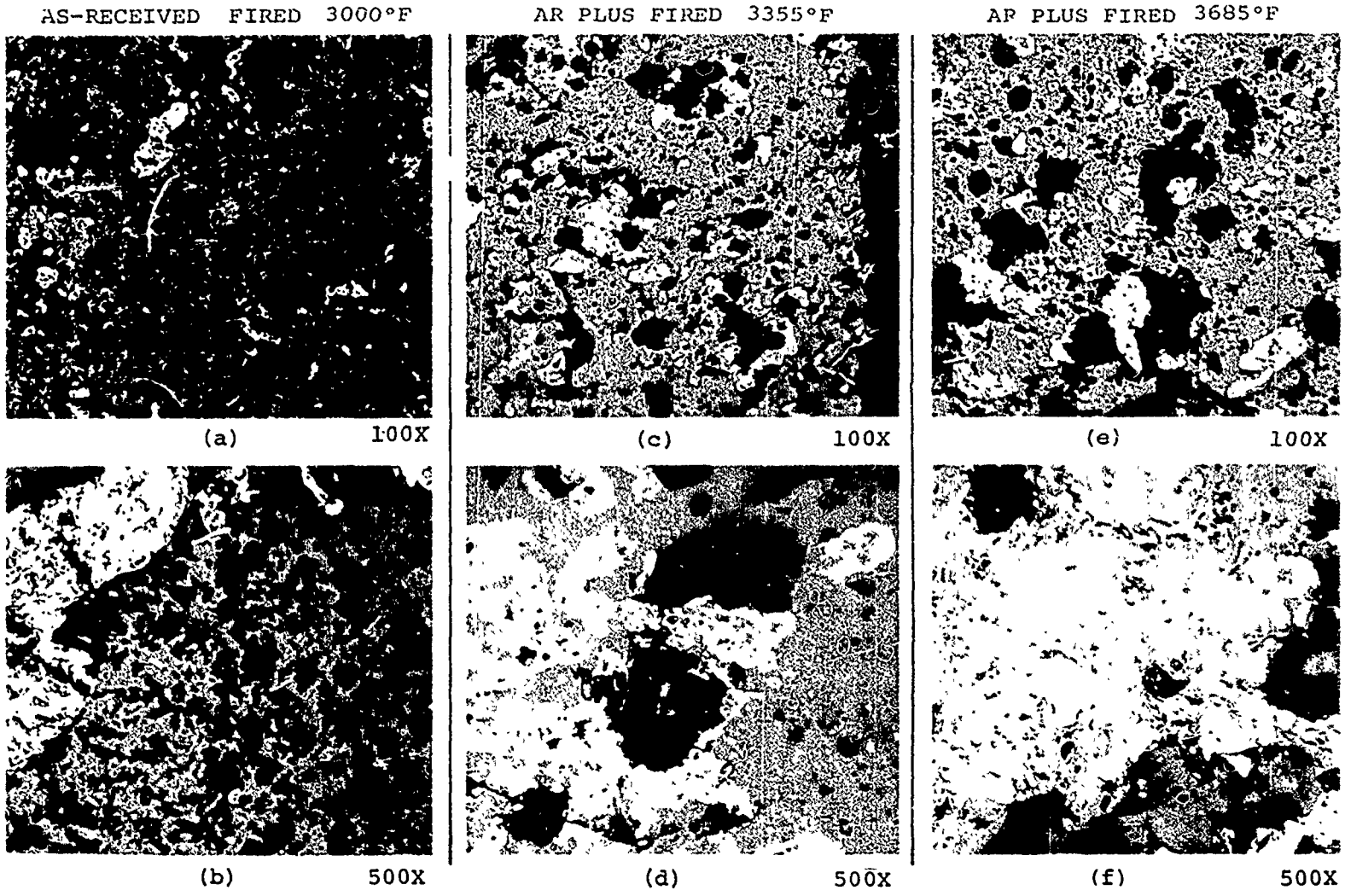


Figure 19. Microstructure of Y_2O_3·15Ti Crucibles (Task III, Group 2) Fired at Various Temperatures. Note the Densification of the Ceramic Structure (Grey) Due to Firing at 3355°F and Higher. Also Note the Structure Modification in the Titanium Particles (White). The Dark Areas are Voids or Epoxy Filled Voids.

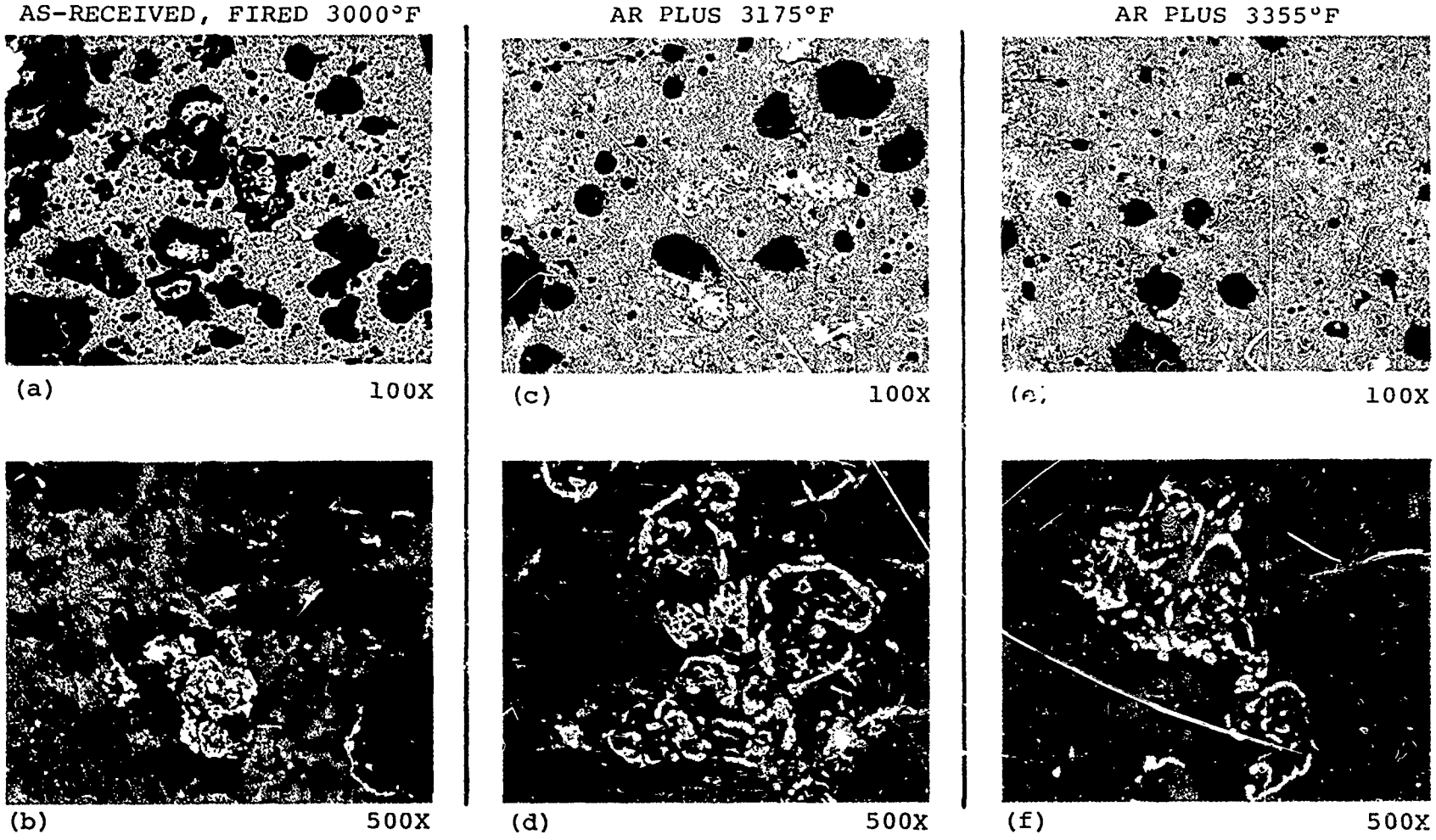


Figure 20. Microstructures of HREMO•8Ti Crucibles (Task III, Group 2) Fired at Various Temperatures. Note the Structure Modification in the Titanium Particles (White).

TABLE 16

RESULTS OF SPECIAL Y_2O_3·15Ti CRUCIBLE MELT RUN AND CRUCIBLE FABRICATION SUMMARY

	Y_2O_3·15Ti Crucibles Fabricated In		
	Task I	Task II	Task III (Group 2)
Contamination Increase (standard melt run IC-30)			
o Oxygen (wt-%)	0.22	0.61	0.41
o Yttrium (wt-%)	0.15	0.08	0.11
Fabrication Parameters and Properties			
o Green Density (lb/in^3)	0.078	0.062	0.083
o Firing - Temperature (°F)	3000**	3000	3000
- Time (hrs)	2	0.17	1
- Atmosphere	Argon	Vacuum (200 μ)	Argon
o Fired Density (lb/in^3)	0.119	0.088	0.126
o Fired Shrinkage (%)	14	9	11
o Fired Weight Gain (%)	0.6	2.3	4.5

*Melts were made in a crucible procured for each of the 3 tasks and run in a single Task III standard melt run. Oxygen content of the alloy charge was 0.16%.

**Firing may have been at higher temperature (near 3200°F).

temperature for Task I crucibles was believed higher (near 3200°F) than that quoted in (Table 16). Data in Table 15 indicated crucible firing temperatures in excess of 3685°F would be required to cause Task I crucibles to perform at the very low melt contamination levels observed. This high temperature (>3685°F) was considered too far above the estimated Task I crucible firing temperature (3200°F) to have been responsible for the good Task I crucible performance. Raw material analysis indicated the titanium powder used for Task I crucible fabrication was of slightly higher purity, showing lower values of Al, Mg and Si than the Ti powder used for Tasks II and III crucibles (Appendix D, Table D-6). Actual reasons for the superior performance of Task I, Y_2O_3·15Ti crucibles are not clear but it was shown that both fabrication parameters and raw material purity were important.

3.2.2.3.3 Summary - Task III

Pure Y_2O_3 continued as the best ceramic material for limiting contamination of molten titanium alloys. However, titanium modification of the Y_2O_3 is a preferred technique for melting crucible fabrication since this procedure provides superior TSR, with minimal increases in reactivity. Higher firing temperatures are also a desirable method of decreasing reactivity of titanium modified materials but may also produce lower thermal shock resistance. The titanium modified HREMO material demonstrated slightly greater reactivity than the comparable yttria system, but it may be a more desirable material due to its significantly lower raw material cost (70 percent lower).

Task III Y_2O_3·15Ti crucibles showed higher reactivity than did comparable Task I crucibles. The superior reactivity of Task I crucibles was verified by an additional melt run. Processing of crucibles, including a possible higher firing temperature, did not appear responsible for the superior performance of Task I Y_2O_3·15Ti crucibles. The better performance was attributed to

titanium powder purity where Task I powder showed lower levels of Al, Mg and Si.

3.2.2.4 Mold Investigations

Standard investment casting molds in general are not acceptable for casting low melting titanium alloys. Typical molds have a facecoat of zircon or alumina bonded with silica. The silica is especially undesirable due to reactivity with molten titanium, thereby contaminating the cast surface.

Silica is typically added to the facecoat slurry as ethyl silicate or colloidal silica. The colloidal silica acts as a suspending agent to produce a stable slurry, and as a binder to give the facecoat and mold adequate green strength during handling and de-waxing. After de-waxing, the mold is typically fired in the range of 1800° to 2100°F. The colloidal silica reacts chemically with the alumina or zircon to produce a sturdy mold and a hard, smooth facecoat which is resistant to spalling and moderate abrasion.

Crucible investigations had identified several ceramics possessing low reactivities with the titanium alloys. These ceramics were considered for mold applications and several investigations (four groups) were conducted in order to establish procedures for mold facecoat fabrication. Mold facecoat formulation was primarily directed at eliminating possible contaminants such as the silica binder. Facecoat formulation also involved substitution of a low reactivity material (HREMO) for current primary materials ($ZrSiO_4$ or Al_2O_3), while retaining the low temperature (2000°F) sintering capability of the molds. The above formulation goals, established mold facecoat evaluations as described in the following four investigations.

3.2.2.4.1 Group 1 Facecoat Evaluations

The goal of this group was to explore the problems that would arise in preparing a mold facecoat containing no silica.

Efforts involved the use of alumina as a flour material and an organic binder material (Methocel MC 4000) to provide slurry stability and facecoat green strength. Fifteen aqueous slurry compositions including the Methocel, anti-foam agent and a wetting agent were evaluated with the following conclusions:

- o An acceptable slurry could not be prepared without the use of wetting and antifoam agents.
- o A slurry containing approximately 80 percent solids 0.5 percent Methocel MC 4000, a wetting agent and an antifoam agent produced a very uniform facecoat having acceptable green strength.
- o Firing at 2000°F removed the Methocel binder but did not produce sufficient sintering, leaving a powdery facecoat that could be easily abraded.

This study concluded that acceptable slurry properties could be achieved using an organic rather than a colloidal silica binder. However, a fired facecoat was not produced with acceptable properties. This work established a need for inorganic sintering aids (CaO, SiO_2, etc.) for integrating the lower reactivity ceramics (Y_2O_3, ThO_2, HREMO, etc.) into the mold fabrication process.

3.2.2.4.2 Group 2 Facecoat Evaluations

The goal was to apply inorganic binders to facecoat formulation in order to obtain sintering at 2000°F. Additions of colloidal silica, CaF_2, and LiF were used to prepare slurries with HREMO and Al_2O_3 powders (called flour for mold making). Slurry preparation procedures and results used for Group 2 candidates are given in Appendix E, Table E-1. Colloidal silica, typically used in commercial mold systems, results in contamination when casting titanium. Silica was included in this investigation in reduced concentrations to replace the organic binder

(Methocel) to determine the minimum quantity that would permit sintering. CaF_2 was selected because of excellent fluxing properties and reasonable potential to permit sintering of either HREMO or Al_2O_3 at 2000°F. In addition, CaF_2 has been used as a protective cover slag in the Inductoslag process for melting conventional titanium alloys.[35] LiF was chosen due to its lower melting temperature and to expand the use of fluorides as sintering aids. Several slurries were evaluated with the following conclusions:

- Al_2O_3 slurries had good consistency and stability but required optimization of the solids content.
- The HREMO powder had a much smaller particle size and required a low solids content to produce a usuable slurry. In addition, the HREMO slurries had high pH and the viscosity changed with time, indicating a stability problem.
- Additions of colloidal silica to the HREMO and Al_2O_3 slurries promoted adequate green strength and sintering. However, there was a tendency for a greater degree of sintering at the surface of these samples, indicating a migration of SiO_2.
- Additions of CaF_2 and LiF significantly decreased the facecoat green strength.
- CaF_2 provided adequate sintering in concentrations from 5 to 25 weight percent.
- LiF was excessively volatile and while producing adequate sintering in Al_2O_3 did not in HREMO.

---

(35) Clites, P. G. and R. A. Beall, "Industoslag Melting of Titanium Scrap and Sponge," Metallurgical Society of AIME, Paper Selection A72-36, 1972.

Group 2 evaluation generally indicated adequate sintering of dried slurries in bulk form could be obtained using inorganic binders but that some segregation occurred causing non-uniform sintering behavior.

3.2.2.4.3 Group 3 Facecoat Evaluations

The goal was to optimize the HREMO slurry composition and evaluate its sintering behavior when slip cast on the inside of SiC and Al_2O_3 crucibles. Three slurries were evaluated (Appendix E, Table E-2) with the following conclusions:

- o HREMO slurry of 55 percent solids (95 percent HREMO, 5 percent CaF_2, Methocel, wetting and antifoam agents) had acceptable stability and good coating properties (composition CC-2).
- o Slurry viscosity instability and low solids content observed for Group 2 and 3 HREMO slurries appeared to be a function of the ultrafine HREMO particle size (<10-microns) and blending procedure.
- o Thin coatings of Group 3 slurries did not sinter adequately at 1950°F as was indicated by Group 2 experiments. The lack of sintering to a hard coating was attributed to binder migration and separation during the drying process.

3.2.2.4.4 Group 4 Facecoat Evaluations

The goal was to evaluate slurry formulations with higher binder contents than Groups 2 and 3 in order to promote sintering at 2000°F in thin layers. Slurry compositions (Appendix E, Table E-3) involved high binder contents (8 to 17 percent CaF_2, 4 to 17 percent colloidal silica, and 43 percent CaF_2 plus Al_2O_3) mixed with the HREMO powder and slip cast into crucibles. Evaluations of fired samples indicated the following:

- o These compositions did not sinter in thin layers at temperatures of 1900°F and 2190°F.

- o Selected samples, also did not sinter at temperatures as high as 2450°F in air or 2100°F in argon.

Group 4 facecoat formulation of high binder content did not improve the sintering characteristics of HREMO slurries beyond the level displayed for low binder contents evaluated in the other groups.

3.2.2.4.5 Summary - Mold Investigations

Investigations showed a need for binder additions to promote sintering of mold facecoats which contained a low reactivity material such as HREMO. Subsequent evaluations using CaF_2, LiF, and colloidal silica indicated these materials could, in some cases, promote sintering of the HREMO material. This sintering was, however, for dried slurries showing concentrations of these binders at surfaces, with bulk samples and thin layers generally not showing appreciable sintering.

As a result of the above experiments, it was apparent that further laboratory work was required to define adequate mold facecoat slurry compositions and preparation procedures. It was also believed that yttria would present identical problems to those experienced with HREMO (lack of sinterability at low temperature) due to the less reactive nature of yttria. These preliminary evaluations served to identify the following specific problem areas which required further investigation in Phase II mold development activities:

- o Facecoat slurry stability

- o Low temperature (2000°F) facecoat sintering aids

3.3 Summary - Phase I

Phase I alloy development was successful in identifying alloys of the Ti-Cu system as having low melting temperatures (2600°F or less) combined with desirable tensile properties. Eight Ti-Cu alloys ranging in melting temperatures from 2515° to 2625°F, demonstrated tensile properties, which met the room temperature goals of the program. These eight alloys included the following:

Ti-10Cu-2.5 Fe	Ti-13Cu-4Sn
Ti-10Cu-2.5Fe-2Al	Ti-13Cu-1Co
Ti-13Cu-2Al	Ti-13Cu-0.2 oxygen
Ti-13Cu-3Al	Ti-16Cu

The room temperature tensile property goals (100 ksi UTS, 90 ksi YS and 5 percent elongation) were achieved in the above alloys using a variety of heat treatments with the most effective being a solution and age cycle. Two additional alloys Ti-13Cu-4.5Ni and Ti-16Cu-1.5Al, were also considered promising, due to their lower melting temperatures (2425° and 2500°F, respectively) and near goal tensile properties.

Thermal exposures applied to several alloys indicated the Ti-Cu alloys require at least third element additions to obtain thermal stability. Salt spray corrosion testing of selected alloys to 1960 hours indicated all of the Ti-Cu alloys were at least equivalent to a Ti-6Al-4V control alloy sample.

Evaluations were conducted on Ti-Cu alloys having intentional additions of oxygen and yttrium which were expected as contaminants from the casting process. A Ti-13Cu-0.2 oxygen alloy displayed the expected strength increase with a corresponding loss in ductility compared to the Ti-13Cu baseline alloy. A Ti-13Cu-0.25 Y_2O_3 alloy exhibited slight decreases in strength and ductility, but ductility was considerably better than the oxygen containing alloy.

Crucible/mold investigations identified the more promising ceramic materials for use as melting crucibles and mold facecoats in investment casting of low-melting titanium alloys. The best material for limiting contamination of melts was pure Y_2O_3, followed by the HREMO material and ThO_2. Titanium modified versions of Y_2O_3 and HREMO, displayed improved thermal shock resistance compared to the basic oxides and the reactivity of these modified compositions was acceptable. Other materials such as Dy_2O_3, CaO and pyrographite promoted moderate contamination levels in melts and were considered marginal for future applications. Fabrication procedures and material purity also appeared to influence the reactivity performance of the ceramic systems.

Laboratory mold development activities indicated a need for further work to identify binder systems, which would promote low temperature (2000°F) sintering of these low reactivity ceramic materials.

3.4 Selection of Materials for Phase II Casting Development Activities

Phase II involved the application of technologies, established in Phase I toward the development of a casting process consistent with the objectives of the program. Two casting trials were conducted in Phase II with appropriate chemical, mechanical property and metallurgical evaluations of castings. Phase I results allowed a selection (by joint decision of the AFML project engineer and AiResearch and RMI representatives) of the following alloys, melting crucibles and mold facecoat compositions for initial evaluation in casting Trial "A":

- Alloys - Ti-13Cu and Ti-13Cu-4.5Ni
- Crucibles - Y_2O_3·15Ti and Y_2O_3·15Ti with a Y_2O_3 surface layer
- Mold Facecoats - HREMO and the AiResearch Zircon ($ZrSiO_4$) system

The basis for these selections are reviewed in the following sections.

3.4.1 Alloys

The Ti-13Cu alloy was selected primarily on the basis of good ingot tensile ductility, which would provide maximum tolerance for potential contamination from the casting operation. This binary system would then provide a good base for further alloy additions. However, the melting point (2630°F) of the binary composition was in excess of the 2400°F maximum desired for the program.

The Ti-13Cu-4.5Ni alloy had a melting point (2425°F) commensurate with the program objectives, but the demonstrated ingot tensile properties were marginal with respect to the program goals. However, the results of casting these two alloys would help define the influence of alloy melting temperature on contamination levels and, mechanical properties. This data would allow selection of an improved alloy for casting Trial "B".

3.4.2 Crucible

Yttria is the best material for crucibles from a reactivity standpoint, but displays very poor thermal shock resistance. In order to obtain a good combination of reactivity and thermal shock resistance, Y_2O_3•15Ti was selected as the primary crucible material. However, in an effort to exploit the low reactivity of the yttria material, Y_2O_3•15Ti crucibles were also used as substrates to which a pure yttria layer was applied on the inner surfaces.

3.4.3 Mold Facecoat Material

During casting, a mold is in contact with molten metal for a short time and therefore facecoat materials would not have to be as inert as crucible materials. Low cost mold construction materials are required since investment molds are not reusable.

HREMO material was established as the next least reactive material compared to pure yttria, but with only 30 percent of the cost, and was therefore considered the prime candidate for the mold facecoat. Phase I efforts, failed to define adequate binders for sintering the HREMO material and other desirable materials (such as yttria or thoria) were expected to have similar sintering problems.

The current AiResearch mold system which utilizes a $ZrSiO_4$ facecoat was selected as the second candidate material. This would be the lowest cost approach but one that was expected to result in higher contamination of the cast alloy. However, the contamination of a low-melting titanium alloy by a conventional mold system was not known. This assessment of the worst situation would allow final mold material decisions for subsequent program efforts.

3.5 Casting Trial "A"

Alloys, melting crucibles, and thermocouple protection tubes were procured for the casting effort. Limited evaluation of the alloy ingot material was also conducted to provide a baseline for comparison with cast alloys. Since mold facecoat construction had been identified as a major problem during Phase I, additional development activity was performed in this area.

3.5.1 Material Procurement

3.5.1.1 Alloy

One-hundred-pound ingots of the Ti-13Cu and Ti-13Cu-4.5Ni compositions were arc-melted to supply material for Casting Trial "A". These ingots were larger (8-inch diameter) than those evaluated during Phase I (4.5-inch). Melting practice was equivalent to Phase I procedures and metallurgical evaluation of the materials followed the procedures in Section 3.1.2. Additional mechanical property testing included smooth rotating-beam fatigue and 600°F tensile of the two as-melted alloys in the optimum heat treated condition.

After melting, the ingots were sectioned transversely as shown in Figure 21. Samples of as-melted material from both ingots were supplied to the Air Force Materials Laboratory. Both ingots were sampled for chemical analysis, hardness, metallography, and mechanical properties in the locations also shown in Figure 21.

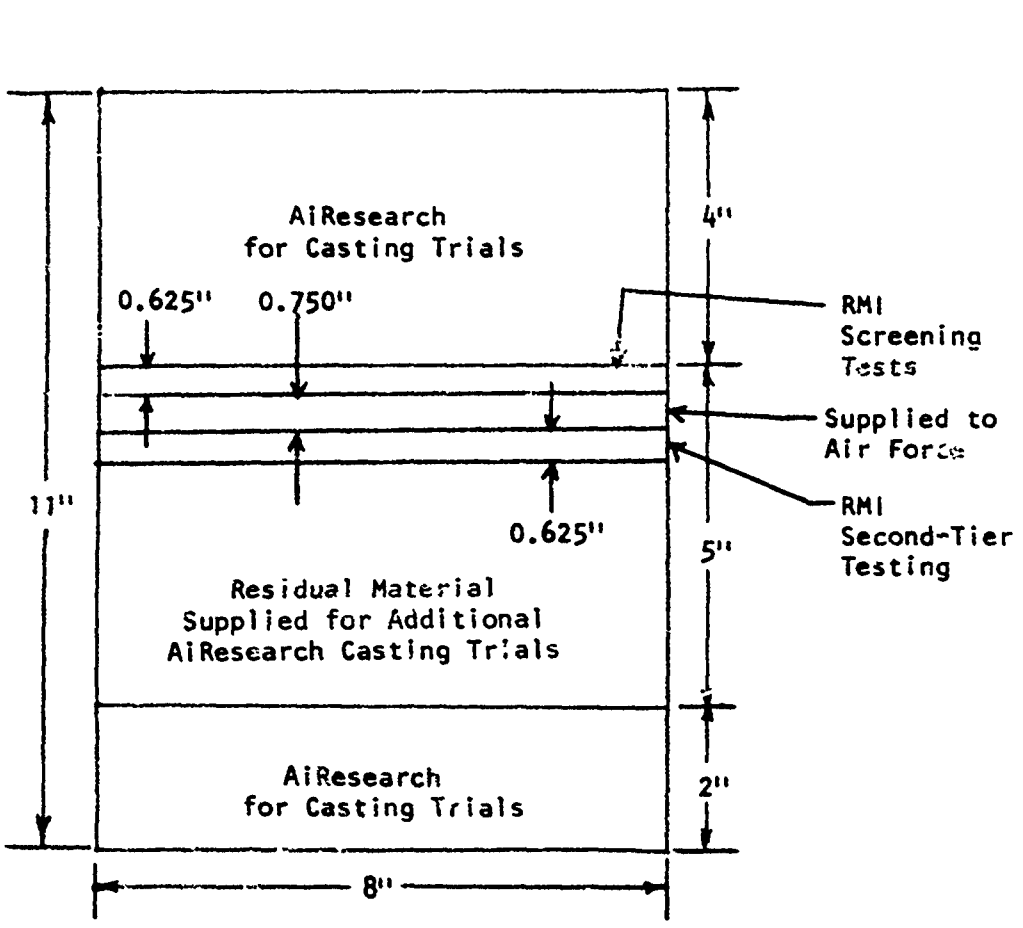
Ingot compositions agreed closely with the aim formulations (Appendix A, Table A-2) and oxygen contents of these Phase II heats (0.052 percent) were slightly lower than similar Phase I ingots (0.078 and 0.094 percent).

Examination of etched macro slices cut transversely through ingot centers showed equiaxed macro grains. Both ingots showed grain sizes (1/32 inch) similar to those obtained from the smaller 4.5-inch Phase I ingots.

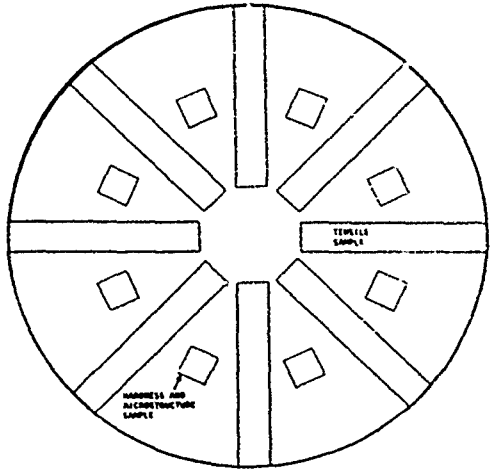
Hardness data and radial tensile properties are presented in Table 17 for the Ti-13Cu and Ti-13Cu-4.5Ni alloys from Phase II and Phase I. The larger as-melted Phase II ingots have slightly lower hardness, yield and ultimate strengths, and equivalent ductility, to the smaller ingots. This lower hardness and strength of the larger as-melted ingots is associated with a slower cooling rate during ingot solidification. Upon heat treatment, the two larger ingots developed equivalent strengths to the smaller ingots of the same composition, indicating differences in oxygen level did not significantly influence tensile properties.

Typical microstructures are presented for both compositions in Figures 22, 23, and 24. Several pertinent observations, relating to as-melted and annealed structural features of these materials are listed below:

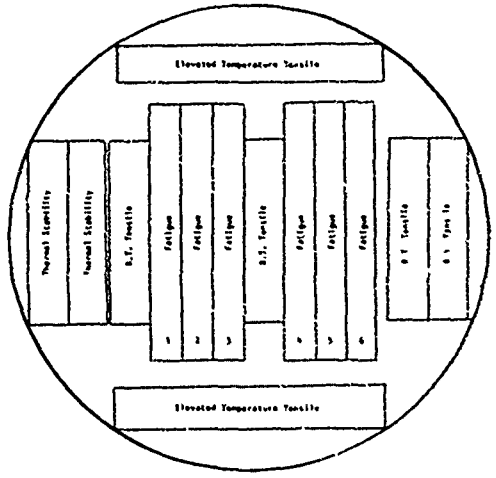
- Both of the larger ingots show: more porosity, a larger average beta-grain size, better defined Ti_2Cu precipitates, and less uniform lamellar structure than Phase I ingots, all attributed to size effects rather than compositional differences.



(a) Ingot Sectioning Diagram



(b) Initial Sample Locations



(c) Second Tier Sample Locations

Figure 21. Ingot Sectioning Diagram and Sample Locations for Ti-13Cu and Ti-13Cu-4.5Ni Alloys Used in Phase II Casting Trials.

TABLE 1/

TASK I OF PHASE II ARC-MELTED INGOT ROCKWELL A HARDNESS AND TENSILE PROPERTIES COMPARED TO PHASE I RESULTS

Heat No.	Nominal Composition	Heat Treatment	Rockwell A Hardness		Phase II[5]				Phase I			
			Phase II	Phase I	UTS ksi	YS ksi	El %	RA %	UTS ksi	YS ksi	El %	RA %
25056	Ti-13Cu	As-Cast	57.1	58.3[1]	94 91	66 63	10.0 9.0	15.9 13.9	104 105	82 82	10.5 10.0	9.7[1,2] 11.6[1]
		1560F-1hr-FC @100F/hr to 900F-AC	53.7	53.3[1]	78 82	60 60	15.5 13.0	18.2 16.3	85 83	62 59	13.0 14.0	16.0[1] 20.0[1]
		1760F-1hr-AC	71.1	69.9[1]								
		1760F-1hr-AC + 1450F-8hr-AC			102 100	82 80	11.0 10.0	12.3 11.7	106	82	10.0	11.0[1]
		1760F-1hr-AC + 1300F-8hr-AC	63.5	64.1[1]	112 116	84 87	5.5 5.5	6.2 5.4[2]	118	88	10.0	12.0[1]
		1760F-1hr-AC + 1300F-8hr-AC + 900F-8hr-AC	63.5		114 114	82 85	6.0 6.0	5.8[2] 6.3[2]				
		1760F-1hr-AC + 1250F-8hr-AC	65.0	65.6[1]					118 114	88 88	6.0 6.0	8.6 8.3
		1760F-1hr-AC + 1200F-8hr-AC	63.9	69.1								
3057	Ti-13Cu-4.5Ni	As-Cast	56.5	57.3[3]	88 89	62 56	4.0 4.0	7.9 6.2	92 103	78 76	-- 6.0	--[2,3] 4.3[3]
		1560F-1hr-FC @100F/hr to 900F-AC	54.7	56.3[3]					89 87	63 65	5.0 5.0	2.4[2,3] 2.3[3]
		1760F-1hr-AC	68.4	70.5[3]								
		1760F-1hr-AC + 1560F-8hr-AC			96 96	77 78	4.0 4.0	2.8[2] 4.8	102	77	4.0	3.0[3]
		1760F-1hr-AC + 1450F-8hr-AC	63.5	63.5[3]	96 97	73 72	6.0 5.0	6.3 5.2	98	74	4.0	4.0[3,4]
		1760F-1hr-AC + 1450F-8hr-AC + 900F-8hr-AC			95 94	72 72	6.5 5.5	4.8[2] 4.4[2]				
		1760F-1hr-AC + 1450F-8hr-AC + 850F-24hr-AC			91 89	69 70	4.0 4.0	8.5 3.3[2]				
		1760F-1hr-AC + 1375F-8hr-AC	65.1						119	104	4.0	6.0[3]
		1760F-1hr-AC + 1375F-8hr-AC + 900F-8hr-AC	65.3									
		1760F-1hr-AC + 1275F-8hr-AC	66.2									

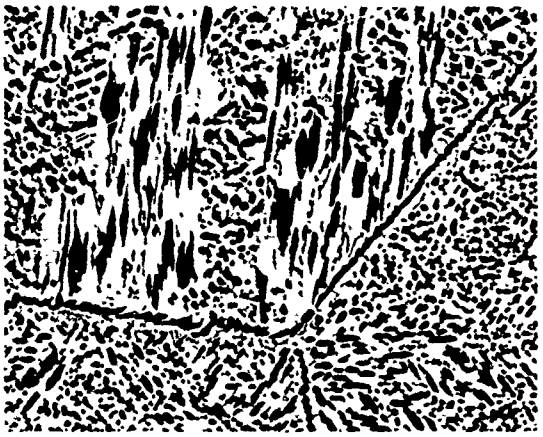
1. 4.5-inch-diameter ingot, Heat 34029
2. Broke at or near gage mark
3. 4.5-inch-diameter ingot, Heat 24224
4. 1760F-1hr-AC + 1475F-8hr-AC
5. Mid Radial Speciman direction and location

AS-MELTED

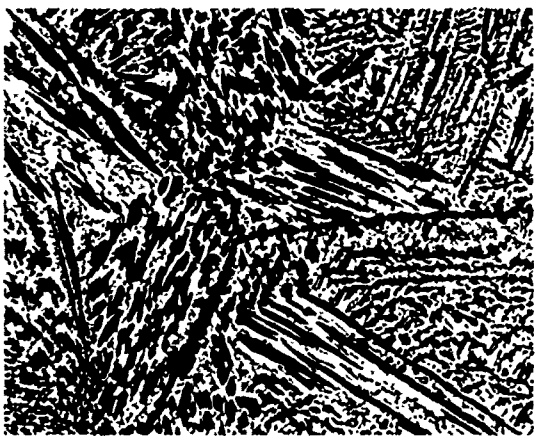


(a) Heat 25056 5-265
Ti-13Cu

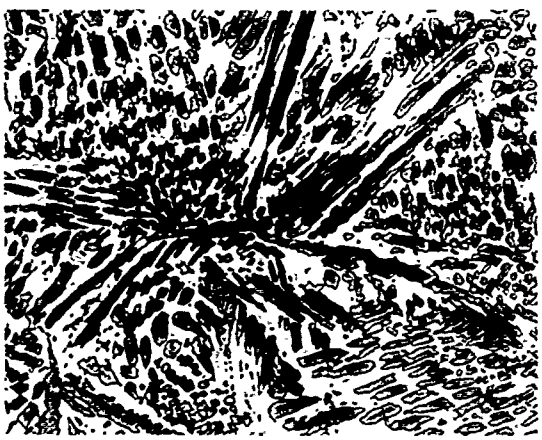
ANNEALED 1560F-1Hr-FC
AT 100F/hr to 900F-AC



(c) Heat 25056 5-266
Ti-13Cu

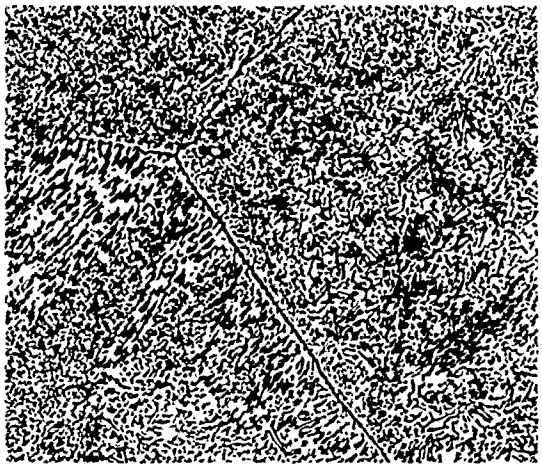


(b) Heat 25057 5-270
Ti-13Cu-4.5Ni

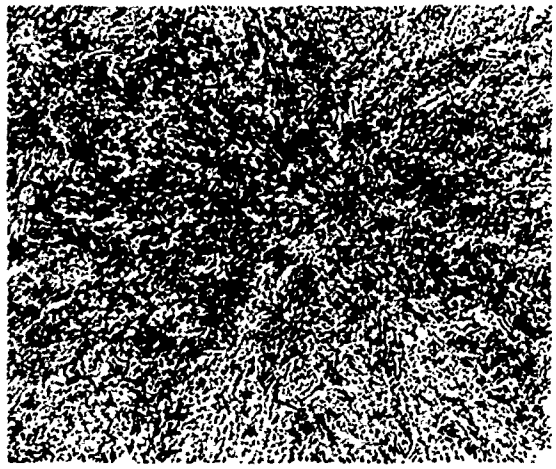


(d) Heat 25057 5-271
Ti-13Cu-4.5Ni

Figure 22. Typical Microstructures of the Phase II Ti-13Cu and Ti-13Cu4.5Ni Alloys in the As-Melted and in the Annealed Conditions.



(a) 1450F-8 hr-AC 5-323



(b) 1300F-8 hr-AC + 900F-8 hr-AC 5-267

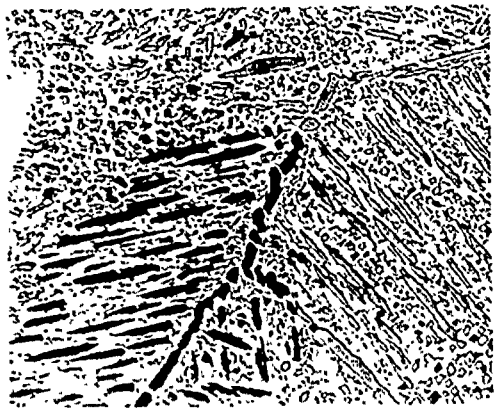


(c) 1250F-8 hr-AC 5-269

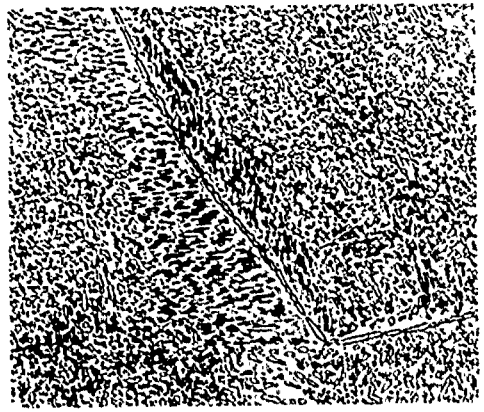


(d) 1200F-8 hr-AC 5-268

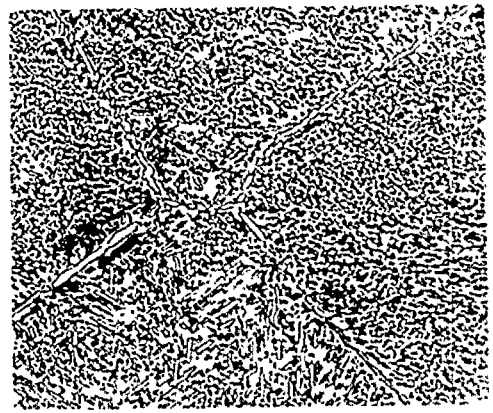
Figure 23. Typical Microstructures of the Phase II Ti-13Cu Alloy (Heat 25056) Showing the Effect of Various Aging Treatments After High Temperature Annealing (1760°F-1 Hr-AC).



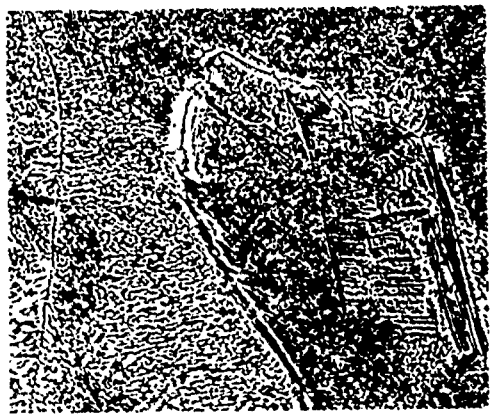
(a) 1560F-8 hr-AC 5-325



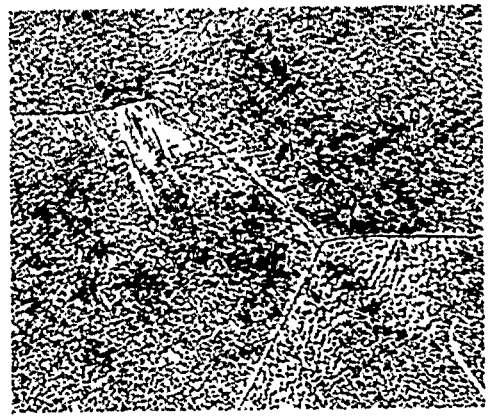
(b) 1450F-8 hr-AC 5-274



(c) 1450F-8 hr-AC + 900F-8 hr-AC 5-324



(d) 1375F-8 hr-AC + 900F- 8 hr-AC 5-272



(e) 1275F-8 hr-AC 5-273

Figure 24. Typical Microstructures of the Phase II Ti-13Cu-4.5Ni Alloy (Heat 25057) Showing the Effect of Various Aging Treatments After High Temperature Annealing (1760°F-1 Hr-AC).

- For both alloys, the 1560°F anneal improved the definition of microstructural features and gave a coarser lamellar structure than in the Phase I ingots.

For both Phase II compositions, lower aging temperatures after solution annealing (1760°F-1hr-AC), resulted in finer eutectoid product and nonuniform microstructures. The Ti-13Cu-4.5Ni alloy generally showed coarser eutectoid structures at equivalent aging temperatures. Aging both alloys at 1450°F gave microstructures similar to the annealed condition, but included narrower Ti_2Cu precipitates at the prior beta grain boundaries and smaller Ti_2Cu precipitation within grains. Based on the above evaluations, a duplex heat treatment was selected for both alloys for subsequent mechanical property determinations. Tensile tests evaluated a variety of heat treatments (Table 17) and indicated the strengths of duplex treated material from Phase I and II compositions were equivalent when heat treated similarly. However, when the Phase II Ti-13Cu alloy was aged at 1300°F, it displayed approximately the same strength but about half the ductility of similar Phase I material. Lower ductility in the Phase II Ti-13Cu material was related to a less uniform microstructure in the larger ingots (Phase II).

On the basis of the above evaluations, the duplex heat treatment (1760°F anneal followed by the 1450°F age) was selected for second tier mechanical property testing of Phase II Ti-13Cu and Ti-13Cu-4.5Ni ingots. Second tier evaluations included additional room temperature tensile tests, and 600°F tensile properties and room temperature rotating-beam fatigue tests.

Sample location within the as-melted ingot showed a minor influence (up to 12 ksi strength and 5 percent elongation) on room temperature tensile properties for duplex annealed material (Table 18). These property differences did not indicate that orientation effects would be a problem for the two alloys in the cast condition. Aging Ti-13Cu-4.5Ni at a lower temperature

TABLE 18

PROPERTY DATA FROM HEAT-TREATED AS-MELTED PHASE II INGOTS OF Ti-13Cu AND Ti-13Cu-4.5Ni COMPOSITIONS FOR CASTING TRIAL "A"

Heat No.	Nominal Composition	Type of Test	Location and Specimen Direction[1]	Heat Treatment	UTS (ksi)	YS (ksi)	El (%)	RA (%)
25056	Ti-13Cu	Room Temp. Tensile	Mid Radial	1760F-1hr-AC+ 1450F-8hr-AC	102 100	82 80	11.0 10.0	12.3 11.7
		Room Temp. Tensile	Edge Tangential	1760F-1hr-AC+ 1450F-8hr-AC	100 100	74 74	12.0 10.0	15.5 6.7[2]
		Room Temp. Tensile	Mid Tangential	1760F-1hr-AC+ 1450F-8hr-AC	100	72	12.0	14.6
		Room Temp. Tensile	Center	1760F-1hr-AC+ 1450F-8hr-AC	98	70	12.5	12.6
		600F Tensile	Edge Tangential	1760F-1hr-AC+ 1450F-8hr-AC	74 75	44 49	13.0 16.0	25.2 25.5
		High-Cycle Fatigue (R = -1.0)	Random Tangential	1760F-1hr-AC+ 1450F-8hr-AC	30 ksi Endurance Limit (10^7 cycles)			
25057	Ti-13Cu-4.5Ni	Room Temp. Tensile	Mid Radial	1760F-1hr-AC+ 1450F-8hr-AC	96 97	73 72	6.0 5.0	6.3 5.2
		Room Temp. Tensile	Edge Tangential	1760F-1hr-AC+ 1450F-8hr-AC	99 99	71 73	4.0 7.0	5.8 10.5
		Room Temp. Tensile	Mid Tangential	1760F-1hr-AC+ 1450F-8hr-AC	98	70	5.5	8.2
		Room Temp. Tensile	Center	1760F-1hr-AC+ 1450F-8hr-AC	89	66	2.0	9.[illegible][2]
		Room Temp Tensile	Mid Radial	1760F-1hr-AC+ 1375F-8hr-AC	108 104	99 91	5.0 3.5	4.4 7.9
		600F Tensile	Edge Tangential	1760F-1hr-AC+ 1450F-8hr-AC	86 82	50 41	15.0 13.0	24.0 23.4
		High-Cycle Fatigue (R = -1.0)	Random Tangential	1760F-1hr-AC+ 1450F-8hr-AC	30 ksi Endurance Limit (10^7 cycles)			

[1] As cut from a transverse slice from the center of 8-inch-diameter, arc-cast ingot

[2] Broke at or near gage mark

(1375°F) increased the alloy strength sufficiently to meet room temperature program goals while ductility (4.2 percent) dropped slightly below the goal (5 percent).

The 600°F tensile properties of Ti-13Cu and Ti-13Cu-4.5Ni were similar (Table 18). The 46 ksi average yield strength of both alloys was close to the program goal of 50 ksi, and the ductilities (14 percent elongation) were well above the 5 percent goal. The 600°F yield strength is about 63 percent of the room temperature yield strength for both compositions. For comparison the 600°F yield strength for wrought, Ti-6Al-4V is approximately 68 percent of the room temperature yield strength.

The smooth rotating-beam fatigue endurance limits for the Ti-13Cu and Ti-13Cu-4.5Ni alloys were 30 ksi (Figure 25). Analysis of the data showed no consistent relationship between failures and specimen location in the ingot. Fracture surface examination of the broken fatigue specimens showed evidence of porosity up to 0.01-inch diameter in size. On several specimens, porosity was identified as probable fatigue initiation sites. However, fracture analysis was difficult because the fatigue surfaces were damaged prior to final failure.

Table 19 lists endurance limits of other cast titanium alloys[36, 37] along with data[38] from aluminum and magnesium castings at a stress ratio of R = -1.0. The limits at R = -1.0

---

(36) Brown, Robert A., "Precision Casting of Titanium". Lecture 11-A; paper presented at New York University Titanium Course, September 8-11, 1969.

(37) McClaren, S.W., et al, "Processing, Evaluation, and Standardization of Titanium Alloy Castings". LTV Aerospace Corporation for Air Force Materials Laboratory, Wright-Patterson Air Force Base, Ohio. Technical Report TR-68-264, April 1, 1969.

(38) Brown, R.A., et al, "Production, Properties and Applications of Precision Titanium Castings". Paper presented at Fall Meeting of AIME, Detroit, Michigan, October 18-21, 1971.

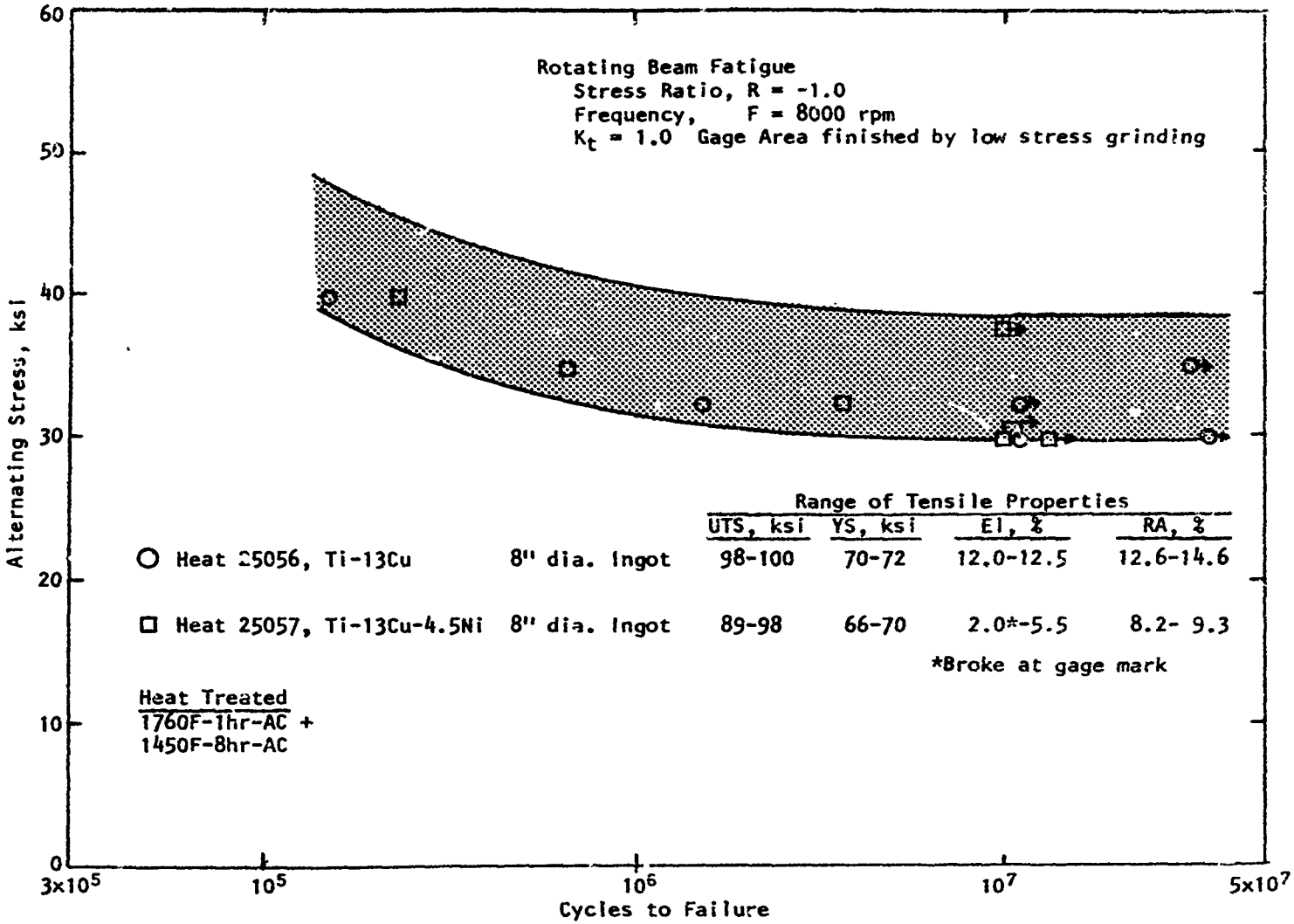


Figure 25. High-Cycle Fatigue Resistance of Heat-Treated Ingot Material for Ti-13Cu and Ti-13Cu-4.5Ni Alloys.

TABLE 19

COMPARISON OF HIGH CYCLE FATIGUE DATA
FOR INGOT Ti-Cu ALLOYS, Ti-6Al-4V,
Ti-5Al-2.5Sn, ALUMINUM AND MAGNESIUM ALLOYS

Alloy	Endurance Limit, ksi at R = -1.0	UTS (ksi)	Ratio of Endurance Limit to UTS
Ti-13Cu	30	99	0.30
Ti-13Cu-4.5Ni	30	94	0.32
Investment Cast Low Oxygen Ti-6Al-4V Ref. 36	35	108	0.32
Ti-6Al-4V Ref. 37	55	138	0.40
Ti-5Al-2.5Sn Ref. 37	39	120	0.32
Aluminum Alloy Ref. 38	7*	66	0.11
Magnesium Alloy Ref. 38	5*	43	0.12

*Estimated

for the aluminum and magnesium castings are estimated from values established at different stress ratios, following the procedures described by Dieter.[39] Fatigue performances of alloys are often compared on the basis of endurance strength divided by ultimate strength. This ratio for the program Ti-13Cu and Ti-13Cu-4.5Ni ingot material (0.30 to 0.32) is similar to other cast titanium alloys and is significantly higher than for aluminum and magnesium castings (0.11 to 0.12).

Table 20 presents tensile properties for Ti-13Cu and Ti-13Cu-4.5Ni Phase II ingot material after a 200-hour thermal stability exposure at 800°F (surface oxide layer intact), as well as previous Phase I results for comparison. The ductilities of Phase II alloys were not significantly affected by the thermal exposure, and only slight decreases occurred in the yield strength of Ti-13Cu (6 ksi) and in the ultimate strength of Ti-13Cu-4.5Ni (9 ksi).

In summary, scaling-up the Phase I compositions from 4.5- to 8-inch ingots produced the following variations, which affected microstructures and therefore, tensile properties:

- o A slower cooling rate of the 8-inch ingots resulted in lower as-melted strengths than in the 4.5-inch ingots.
- o A greater incidence of porosity was evident in the larger as-melted ingots.
- o The 8-inch ingots contained larger as-melted micro grains than 4.5-inch ingots. It is believed that the larger grains resulted in less uniform structures and reduced tensile ductility.

---

(39) Dieter, George E., Jr., "Mechanical Metallurgy," McGraw-Hill Book Company, New York, 1961, pp 324-325.

TABLE 20

TENSILE PROPERTIES OF INGOT ALLOYS BEFORE AND AFTER THERMAL EXPOSURE

Heat No.	Composition	Heat Treatment	Room Temperature				Room Temperature After 800F - 200hr Exposure[2]			
			UTS ksi	YS ksi	El %	RA %	UTS ksi	YS ksi	El %	RA %
Phase I										
24217	Ti-16Cu	1760F-1hr-AC + 1400F-8hr-AC	112 108	91 92	6 6	6 8	97 94	71 69	6 7	6 7
24275	Ti-13Cu-2Al	1560F-1hr-FC	104 106	92 92	12 12	14 14	106 107	87 90	14 13	17 18
24278	Ti-16Cu-1.5Al	1760F-1hr-AC + 1450F-16hr-AC	122 120	112 113	5 3	5 5	122 124	109 115	4 4	4[1] 4
24218	Ti-13Cu-2.5Fe	1760F-1hr-AC + 1400F-8hr-AC	123 130	102 102	3 4	5 6	128 130	96 101	4 6	6 6
24224	Ti-13Cu-4.5Ni	1760F-1hr-AC + 1400F-8hr-AC	108	82	5	6	106 105	90 88	7 6	5 5
Phase II										
25056	Ti-13Cu	1760F-1hr-AC + 1450F-8hr-AC	100 100	74 74	12 10	16 7[1]	98 98	67 69	9 12	15 18
25057	Ti-13Cu-4.5Ni	1760F-1hr-AC + 1450F-8hr-AC	99 99	71 73	4 7	6 10	88 93	71 68	3 4	4 6

1. Broke at or near gage mark
2. Tested with oxide layer intact

- o The higher aging temperatures after solution annealing were effective in obtaining more uniform microstructures and greater ductility but lower strength.

- o Oxygen and other compositional differences did not appear to influence tensile properties.

3.5.1.2 Melting Crucibles

Four melting crucibles (3.5-inch diameter by 8-inch high) were fabricated by Coors for use in casting Trial "A". All four crucibles were cold isostatic pressed from a mixture of Y_2O_3 plus 15 weight-percent titanium (yttria characterized in Appendix D, Table D-5, lot 4 and the titanium in Appendix D, Table D-6, lot 3). A pure yttria layer was slip cast onto the inside surface of two crucibles prior to firing. This was generally successful except several small runs and flaws developed near the top edge of one crucible where the slip was poured out. Processing parameters and physical data are given in Appendix D, Table D-7 for these crucibles (numbers 1 through 4) as well as for two small control crucibles that were fired in the same run as the No. 4 large crucible.

The four large crucibles were received in good condition, except Crucible No. 1 exhibited an outside surface layer near the bottom that was spalling. This layer was identified as Y_2SiO_5, by X-ray diffraction, and spectrographically contained high yttrium and silicon with minor titanium. The silicon contamination source was not verified, but may have resulted from previous silicon contamination of the firing furnace. As a precaution the two crucibles without the yttria coating were grit blasted to remove a small amount of the inside surface to eliminate potential melt contamination.

The yttria coated crucibles displayed some coating darkening, which may have been due to reaction with titanium in the crucible body that rendered the coating substoichiometric. Carbon contamination from furnace fixturing was also observed at

the bottom of one yttria coated crucible (No. 2). Therefore, crucibles No. 3 (yttria layer) and No. 4 (Y_2O_3·15Ti) were selected for use in Casting Trial "A".

3.5.1.3 Thermocouple Protection Tubes

Previous casting efforts at AiResearch using low melting titanium alloys indicated optical pyrometer measurement of melt temperature was difficult due to metal fogging of the furnace site port. Therefore, direct thermocouple measurement of melt temperatures during the program casting trials was required. The reactivity of titanium precludes the use of conventional thermocouple assemblies, which use sheath materials such as Inconel 600, tantalum, platinum or various oxide or silicate ceramics. Phase I work identified Y_2O_3 as a low reactivity material, which would be satisfactory for thermocouple protection tubes as well as the melting crucibles. However Y_2O_3 was not sufficiently thermal shock resistant and Y_2O_3·15Ti tubes were much too expensive to fabricate protection tubes for the program. Therefore, the concept of applying a thin layer of Y_2O_3 to the outside of a suitable protection tube by plasma spray techniques was pursued.

As a result, thermocouple protection tube substrates of three ceramic compositions (silica, alumina, and mullite) were plasma sprayed with yttria (Y_2O_3) powder by Plasmadyne (Santa Ana, California). Preliminary plasma spray efforts had indicated standard production yttria powder had too small a particle size (<20-microns) to permit proper feeding of the plasma gun. As a result, a coarse (35 percent was + 325 mesh) yttria powder (Appendix D, Table D-5, Lot 792) was procured from Molybdenum Corporation of America (Louviers, Colorado). Test samples were sprayed with a 10-mil thick layer of yttria and showed excellent adherence.

Thermal shock tests were conducted to determine the more durable substrate/coating combinations. A coated tube of each

composition was inserted into a furnace at elevated temperatures, (up to 2250°F), allowed to soak for a minimum of 15 minutes and then removed into ambient air. Visual inspection identified the alumina substrate as the best material. Tendencies for spalling of the yttria layer were observed with all the substrates, but the overall results were sufficiently encouraging to use all three combinations for Casting Trial "A".

3.5.2 Mold Development

As previously discussed (Paragraph 3.2.1.7), investigations of binder materials for mold facecoats identified the following requirements:

(a) Promote sintering of the facecoat system at 2000°F

(b) Provide slurry stability

(c) Result in minimal contamination of titanium metal

(d) Display a lack of toxicity

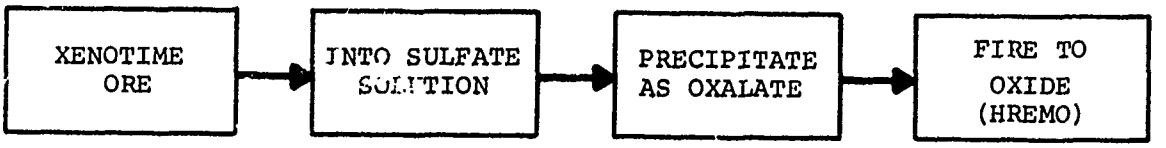
These requirements provided direction to the extensive mold facecoat investigations and material selections discussed in the following sections.

3.5.2.1 Material Procurement

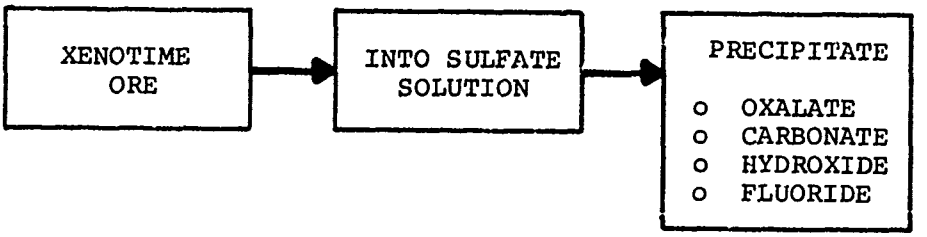
HREMO material previously used in the program was typically 60 percent yttria with the balance consisting of other rare earth oxides and a low non-rare earth impurity content (less than 6 percent CaO or TiO_2). The HREMO powder was produced from a sulfate solution of Xenotime ore by precipitating as an exalate and firing to an oxide as shown in Figure 26 (Process A). Since HREMO displays the desired low reactivity but presents considerable difficulty in sintering, several other forms of the heavy rare earth concentrate (HREC) were selected for investigation on the basis of:

(a) Improved low temperature sinterability

HREMO, PROCESS A



HREC, PROCESS B (LOW PURITY)



HREC, PROCESS C (HIGH PURITY)

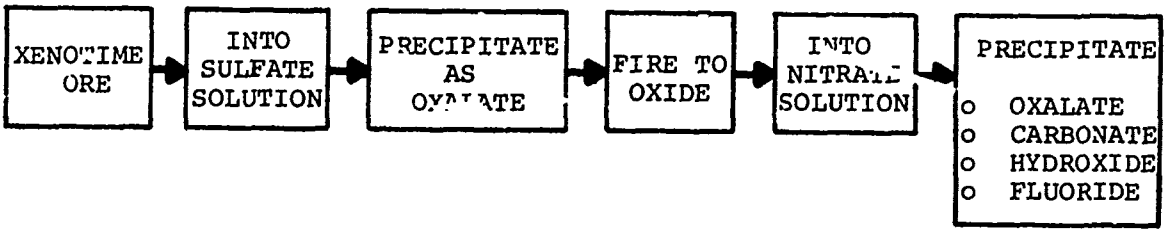


Figure 26. Process Flow Diagrams for the Preparation of HREMO and Heavy Rare Earth Concentrates (HREC).

(b) Conversion to the oxide (HREMO) at low temperatures

(c) Acceptable chemical and thermal stability

The four selected HREC materials (oxalate, carbonate, hydroxide and fluoride) were procured from Research Chemicals, Inc. (Phoenix, Arizona) at two purity levels. The two purity levels for each material were obtained by variations in processing (Figure 26). The first process (Process B) involved a single precipitation of four concentrates and produced the lowest purity. The four concentrates produced by Process C involved a duplex precipitation which produced higher purity materials (Appendix D, Table D-9). These eight HREC were then used either as low percentage additives to the HREMO material in an effort to improve sinterability, or as the primary facecoat material, which could then be fired to the oxide.

3.5.2.2 Facecoat Investigations

Additional oxide and silicate materials were also procured for evaluation as sintering aids. Various combinations of these sintering aids with HREMO and HREC materials were prepared as water slurries, air dried and fired (procedure given in Appendix E, Table E-4). Bulk samples were fired at 1970°F (Appendix E, Table E-5) for 1 hour with several compositions also fired at 2200°F for 17 or 64 hours (Appendix E, Table E-6).

Samples were dimensioned and weighed before and after firing with the density, shrinkage and weight changes calculated. Very few compositions exhibited adequate sintering as judged by relative hardness after firing, but the following trends were apparent:

(a) The most effective sintering aids were TiO_2, CaF_2, $CaO \cdot SiO_2$, and colloidal silica.

(b) The heavy rare earth carbonate appeared to sinter more readily than the other materials. The impure material (Process B) was noticeably superior.

(c) The heavy rare earth oxalate compositions evolved excessive amounts of gas during firing, which rendered them unsinterable.

(d) In general, the HREMO material was more difficult to sinter than the HREC materials.

(e) Many compositions, when fired at the higher temperature (2200°F) showed considerable improvement compared to firing at 1970°F.

(f) Several compositions that sintered, were either lower purity materials or fluorides (that would not convert to the oxide) and therefore, were considered less desirable for use as mold facecoats because of expected higher reactivity.

3.5.2.3 Test Mold Fabrication

The best sintering compositions (Table 21) were selected as candidates for fabrication of test molds at the AiResearch Casting Company, in Torrance, California. Slurries of each of these compositions were ball milled (alumina mill and balls) for a minimum of 16 hours prior to dipping of the wax patterns. All slurries were thixotropic to various degrees, which resulted in poor facecoat quality. However, three test molds were constructed from each of the first six compositions listed in Table 21 using zircon sand as the stucco material (Figure 27). These test molds were completed using conventional mold back-up construction materials employed at the AiResearch Casting Company. After drying and dewaxing, visual examination revealed only facecoat compositions H, CC2 and Group 2, No. 7 were firm and

TABLE 21

FACECOAT CANDIDATES SELECTED
FOR TEST MOLD FABRICATION

Code		Est. Y_2O_3 (%)	Solids (%)	Estimated Sinter Temp.	Shrink-age (%)
P	60% HREMO + 40% TiO_2 in 1/2% Methocel Solution	36	67	1970°F	6
H	75% HREMO + 25% TiO_2 in 10% Colloidal SiO_2 Solution	43	71	1970°F	10
6G	80% HREC-Carbonate + 20% Silene EF (16 $CaO.SiO_2$) in 1/2 Methocel Solution	46	46	2200°F	84
*CC-2 (Group3)	95% HREMO + 5% CaF_2 in 15% Colloidal SiO_2 Solution	55	55	1970°F	10
**Gr. 2 No. 7	100% HREMO in Colloidal SiO_2 Solution (15% or 22%)	55	70	2200°F	--
7H	75% HREC-HYDROXIDE + 25% TiO_2 in Colloidal SiO_2 Solution (10%)	26	73	2200°F	44
6H	75% HREC-Carbonate + 25% TiO_2 in Colloidal SiO_2 Solution (10%)	26	71	1970°F	69
6F	90% HREC-Carbonate + 10% CaF_2 in 1/2% Methocel	51	42	1970°F	74

*Composition evaluated in Phase I (Appendix E, Table E-2).

**Composition evaluated in Phase I (Appendix E, Table E-1).



Figure 27. Appearance of Wax Pattern (Left) and Experimental Ceramic Investment Mold (Center) Used for Evaluation of Candidate Mold Materials. Fired Mold Face coats Were Either Intact (Right Bottom) or were cracked and Spalled (Right Top).

coherent in the green state. A mold of each facecoat composition was then fired by the following techniques:

(a) Inserted from room temperature directly into a 1900°F, furnace, held one hour, and withdrawn into ambient air.

(b) Inserted slowly into a furnace at 2160°F, held one hour, and withdrawn slowly into ambient air.

(c) Inserted into a furnace at 1200°F, furnace heated to 1925°F, held 64 hours, furnace cooled to 1060°F, and withdrawn into ambient air.

After firing, facecoats were observed not to sinter to the same degree observed for previous bulk samples (Figure 27). This poor sintering of thin layers had been observed in the Phase I mold development activity and is attributed to a lack of a satisfactory sintering aid. The sintered condition of all three mold facecoat compositions was nearly equivalent, but composition CC2 was selected for use in Casting Trial "A" because of more consistent fabrication behavior. In order to improve slurry stability, sufficient HREMO material of a larger particle size was procured from Research Chemicals, Inc., for Casting Trial "A" to help remedy the thixotropic behavior.

3.5.3 Foundry Activities

The casting trial was conducted at the AiResearch Casting Company (ACC) in Torrance, California. This trial, depicted in Figure 28, was to have consisted of induction melting the Ti-13Cu and Ti-13Cu-4.5Ni alloys in the Y_2O_3·15Ti and Y_2O_3·15Ti plus yttria layer crucibles and casting both alloys into test bar molds fabricated with the experimental facecoat material (HREMO) and conventional ACC molds with a zircon ($ZrSiO_4$) facecoat. However, no castings were made with the experimental molds due to mold problems described in the following Section.

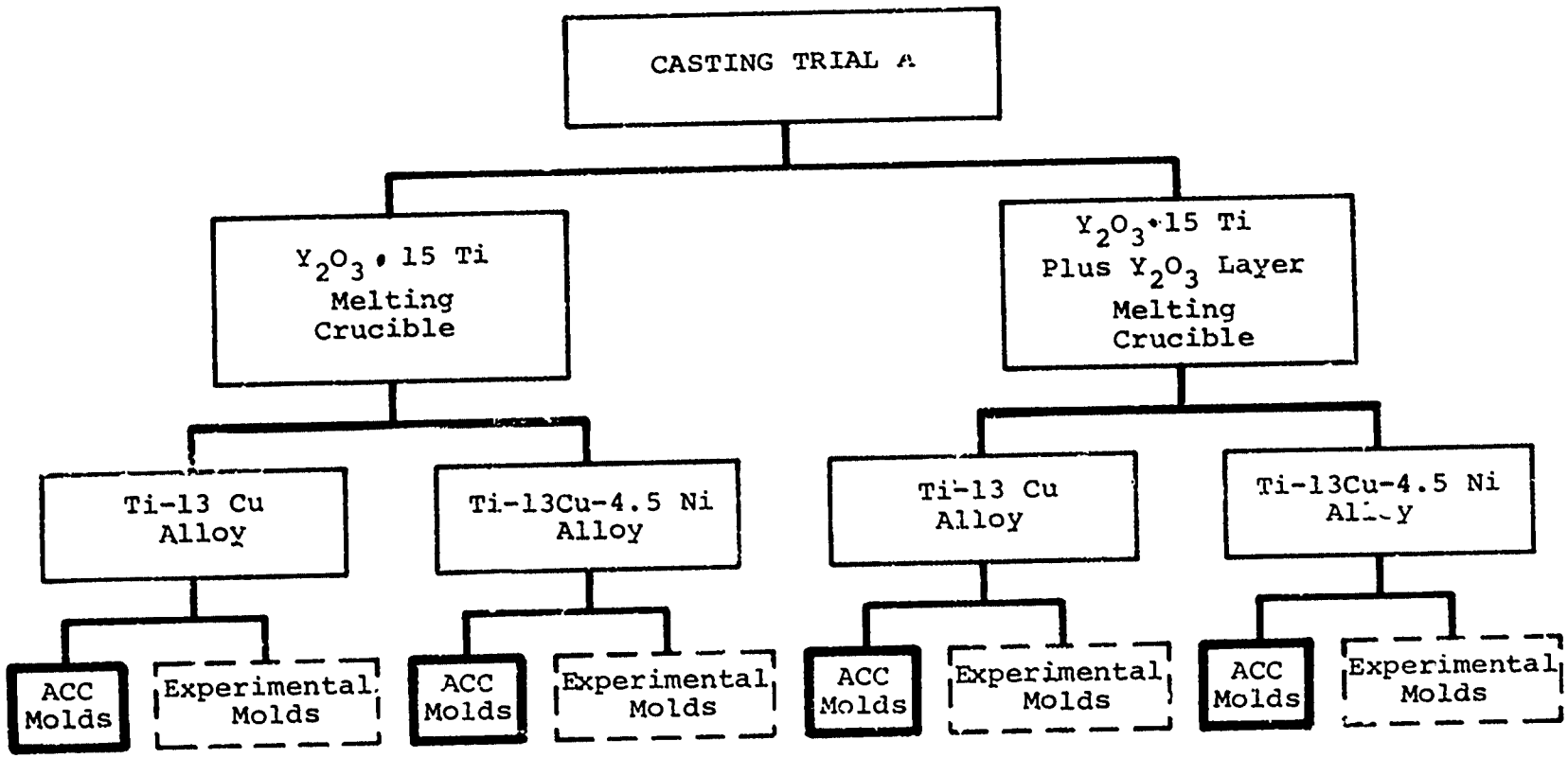


Figure 28. Flow Diagram for Casting Trial "A" Illustrating Sequence of Events Leading to Castings Poured into ACC Molds but not into Experimental Low-Reactivity Molds (Dashed Lines) as Originally Scheduled.

3.5.3.1 Mold Fabrication

The ACC standard and experimental molds were prepared using conventional approaches (fabrication procedures are given in Appendix E, Table E-7). The facecoat used for experimental molds (Composition CC2) consisted of 85 percent HREMO, 4 percent CaF_2, and 11 percent colloidal silica. No acceptable molds (Figure 29) were obtained with this system due to the recurrence of problems observed during previous laboratory mold development activities. The primary problem areas were:

(a) Thixotropic behavior of slurry which resulted in lack of facecoat adherence to wax pattern and uneven facecoat thickness

(b) Facecoat cracking caused by excessive shrinkage resulting from low slurry solid content

(c) Lack of adequate sintering at the 1900°F (16 hours) firing temperature

(d) Lack of bond between the facecoat and backup material

The above problem areas were associated with the small particle size of the HREMO powder as well as the CaF_2 binder not promoting adequate sintering. The HREMO powder, procured in a large particle size range, was agglomerated and did not provide the desired slurry consistency nor eliminate slurry thixotropic behavior.

3.5.3.2 Casting Process

The casting effort was organized to demonstrate capabilities in the following areas:

- Ceramic crucibles can be used to induction melt low-melting titanium alloys.

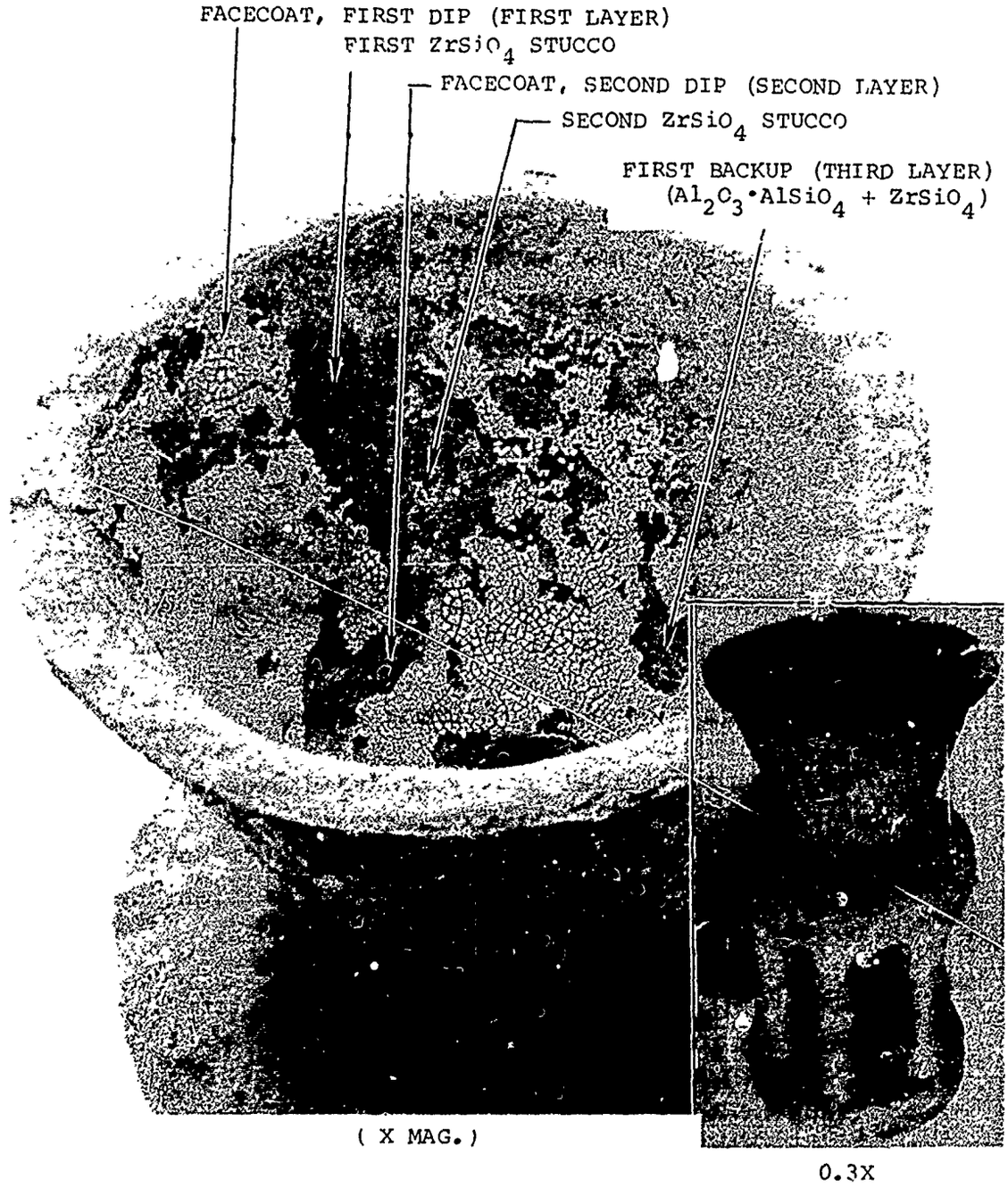


Figure 29. Typical Appearance of Experimental Molds (Composition CC2) Illustrating Severe Spalling of Facecoats in Cup Area. Molds Fired at 1900°F for 1-Hour Were all Unusable for Further Casting Operations.

- Low-melting titanium alloys can be cast into conventional molds without excessive contamination of the cast surface.

- Low melting titanium alloys which display acceptable contamination levels and tensile properties approaching ingot material can be cast.

In the process of establishing these capabilities, uniform process conditions were used including metal pour temperature, vacuum levels, melting times, induction power input, uninsulated molds (conventional zircon facecoat composition), mold preheat temperature, and casting cooling rate after pour. The casting procedure is detailed in Appendix G and generally consisted of the following steps:

- Bake out melting crucible under vacuum.

- Hand load metal charge into crucible (furnace opened to ambient conditions at this time).

- Pump furnace down to 5-microns vacuum

- Melt ingot material slowly to avoid excessive spitting.

- After metal is fluid, make initial power setting, and measure melt temperature using an immersion thermocouple.

- Make final power setting to reach pour temperature (melting point plus 200°F).

- Transfer mold to vacuum furnace after preheating in air at 1950°F.

- Withdraw thermocouple after temperature has stabilized and then pour metal.

- Cool casting under vacuum for 25 to 35 minutes before removing into air.

- Allow casting to cool in air. Remove metallographic samples with mold material intact.

- Break out casting and light grit blast to remove mold material.

A total of fifteen vacuum-induction melts were made during a two-day casting effort. The following castings and test samples were obtained:

- Nine test bar clusters (ACC mold)

- One cooling fan (P/N 969249-11); ACC mold

- Two pours in pyrolytic carbon crucibles (1-inch diameter x 5-inch)

- One pour into a ZrO_2 crucible (3.5-inch diameter x 8-inch)

- One melt of Ti-13Cu-4.5Ni alloy solidified in the $Y_2O_3 \cdot 15Ti$ melting crucible

- One melt of Ti-13Cu-4.5Ni alloy solidified in the yttria layer melting crucible

Specific details for casting Trial "A" melting operations are listed in Table 22 and the appearance of typical castings is shown in Figure 30. A review of the casting parameters (Table 22) indicates most conditions were relatively uniform although the following pours deviated from typical conditions:

TABLE 22

CASTING TRIAL "A": MELTING DATA AND POUR PARAMETERS

MELT NUMBER	MELTING CRUCIBLE*	MOLD SHAPE	TITANIUM ALLOY	TOTAL WEIGHT (lb) CHARGE	TOTAL WEIGHT (lb) INGOT	AVG. % OF INGOT SURFACE IRREGULARITIES**	MOLD MATERIAL	MELTING POWER ON (%)	MELTING POWER (kW)	TIME (min)	POUR POWER (kW)	POUR POWER OFF (%)	MELTING TEMP. (°F)	POUR TEMP. (°F)	SOLIDUS TEMP. (°F)	TIME TO POUR (sec)	AT POUR	REMARKS
P1	Y_2O_3-15Ti	Bars	-13Cu	5.8	5.2	12	Silica	19	19	-	9	--	2800 ±50	1538	-	<5		Crucible cracked
P2		Bars		6.1	3.1	30	Alumina	12	11	11	7.5	15-20	2820 ±20	1539	>1554	<5		
P3		Carbon Crucibles		5.0	0	14	Mullite	11	12	8	<12	15-18	2818 10	1538	>1554	4-7		
P4		Carbon Crucibles		3.5	1.0	33	Mullite	~10	7	5	10	15	2820 ±10	1549	1552	5-6	6	
P5		Bars	-13Cu -4.5Ni	5.6	5.5	18	Alumina	11	18	13	9	15-20	2625 ±25	1440	>1490	4-6	4	Ingot has center crack
P6		Bars		8.0	5.5	22	Silica	17	21	8	~10	12-16	2630 ±15	1443	>1468	3-5	3	Ingot has center crack. Hot leak rate = 85 µ/m. Cold = 9.5 µ/m.
P7		Charge solidified in cruc.		3.2	--	33	Silica	6	16 to power off	12 to power off	7-9	15-20	--	--	>1404	3-6	3	Cold leak rate = 14 µ/m.
P8	Y_2O_3-15 + Y_2O_3 layer	Bars	-13Cu	6.3	5.8	27	Silica	16	61	50	13	15-20	2930 ±15	1610	--	15 to 1000	55	Mold, S-SCTB, insulated. Crucible clean-out. Hot leak rate 60 µ.
P9		Pour into Z_rO_2 Crucible		4.3	--	39	None	13	14	5	12	15-30	~2900	1590	--	3-7	7	Cold leak rate = 20 µ/m. Hot = 85 µ/m.
P10		Bars		5.9	5.6	13	Mullite	7	12	10	--	11-20	2820 ±10	1549	>1554	4-8	4	Ingot has center crack
P11		Bars		5.3	4.7	12	Silica	9	18	14	12	12-15	~2900	~1590	--	4 to 1000	--	T/C prot. tube stuck in crucible
P12		Impeller	-13Cu -4.5Ni	5.4	5.5	35	None	11	11	5	13	--	~2930	~1610	--	6-10	6	Mold preheat to 1825°F, insulated
P13		Bars		5.1	5.0	11	Alumina	10	10	6	10	--	2630 ±10	1443	1510	3	3	Ingot has center crack
P14		Bars		6.0	5.8	19	Mullite	11	14	8	--	15	2625 ±20	1440	--	4	4	Ingot has center crack
P15		Charge solidified in cruc.		5.3	--	35	Pour in Mullite Poured	~7	9 to power off	6 to powr off	10	--	--	--	1466	5	5	Cold leak rate = 15 µ/m.

*First melting crucible (Y_2O_3-15Ti) baked out 2 hours at 1615°F under vacuum and cooled overnight prior to ingot loading.

Second melting crucible (Y_2O_3-15Ti + Y_2O_3 layer) baked out 1.1 hours at 1615°F under vacuum and cooled 7 min. prior to ingot loading. Hot leak rate was 24 µ/m. without molten metal

**Ingot surface may contain impurities or vary in composition from bulk of ingot and therefore may relate to final casting composition and properties.

***Note the sum of times listed in the 1st and 3rd columns is the total time the metal is being heated and melted.

****Alloy melting points are: Ti-13Cu 2615°F and Ti-13Cu-4.5Ni 2425°F.

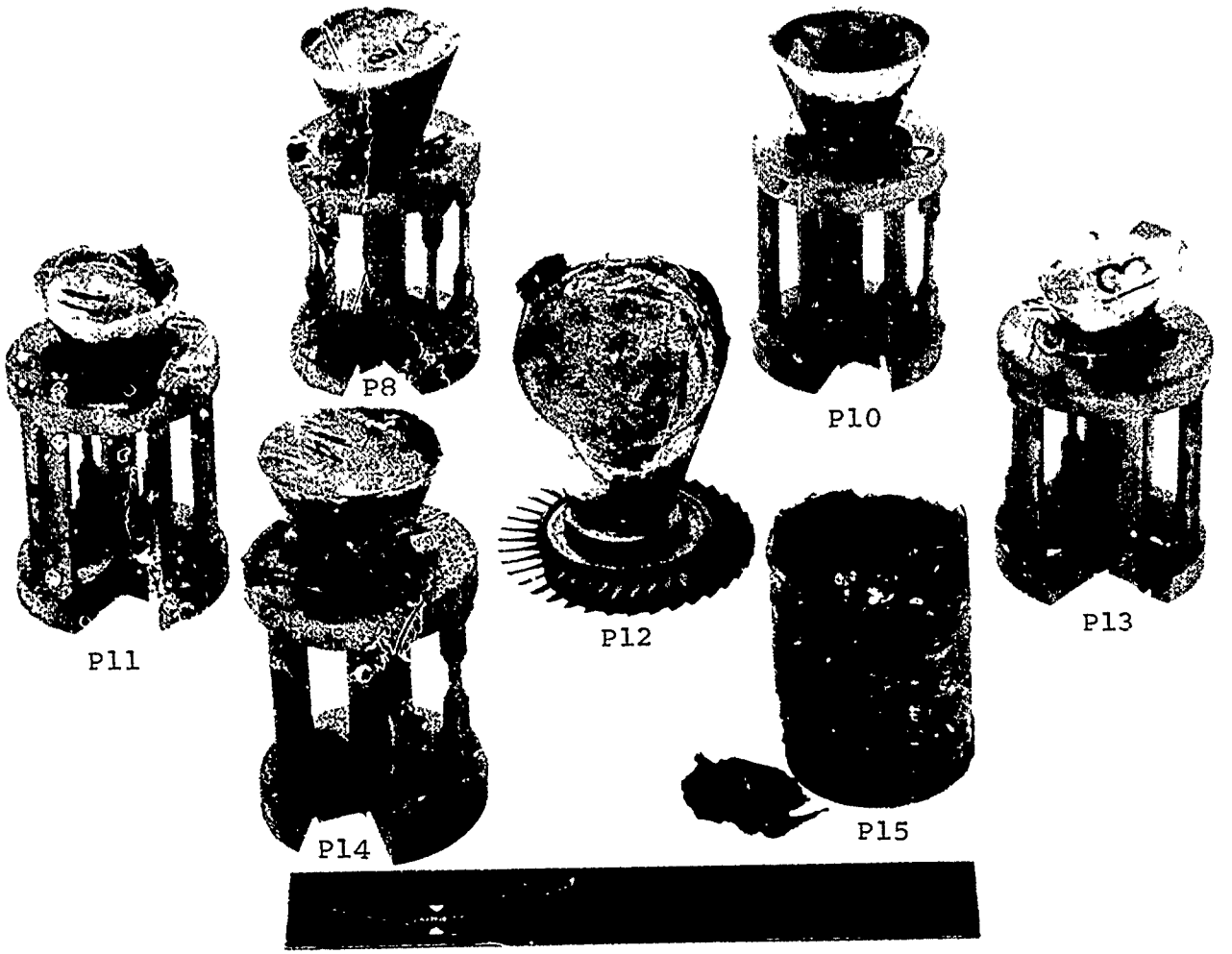


Figure 30. Appearance of Several Casting Trial "A" Ti-13Cu (P8, P10, P11) and Ti-13Cu-4.5Ni (P12, P13, P14, P15) Castings. Alloys Induction Melted in the Y_2O_3 Coated Y_2O_3·15Ti Crucible and Poured into ACC Zircon Facecoat Mold System. Pour 15 is the Remains of the Melting Crucible With the Final Charge Solidified in Place.

- Pour 8 was held molten for a longer time, at higher temperature, and under poorer vacuum levels (to 1000 microns) during backout of new crucible which had not been outgassed prior to the start of casting activities.

- Casting 11 was poured at a higher temperature (approximately 270°F above alloy melting point) and under poor vacuum conditions (up to 1000 microns). The high pressure level during melting resulted from a loss of a portion of the ceramic thermocouple protection tube into the melt.

Of the test bar castings, Pour 10, with the Ti-13Cu alloy and Pour 13, with the Ti-13Cu-4.5Ni alloy, appeared to have been conducted under the best melting conditions (minimum melting time and uniform parameters). The balance of the castings were poured under very similar conditions, but some parameters, not monitored in the process, caused differences in the castings. These parameters were:

- Maximum metal temperature was not monitored during melting in order to minimize thermocouple protection tube degradation.

- Mold temperature at the time of metal pour varied since molds were not insulated and the mold transfer time from preheat furnace to casting furnace was not monitored. The mold temperature would influence cast surface contamination, gas porosity, and the degree of micro-shrinkage, all of which would affect mechanical properties.

Ingot material used for each melt consisted of a variety of section sizes, and this precluded using the ingot loading device. Repeated opening of the melt chamber, to load the alloy, contributed to higher potential contamination levels than would be expected under production conditions.

The melting crucibles (Y_2O_3·15Ti and Y_2O_3·15Ti plus a Y_2O_3 layer) showed a low degree of wetting by molten titanium alloys. However, the yttria coated crucible visually showed slightly more wetting and erosion than the uncoated crucible. Both crucibles showed extensive cracking as a result of the repeated melting operations but satisfactorily contained the molten metal.

Standard zircon molds contained the molten titanium alloys with no occurrence of metal runout. However, a rapid rise in vacuum pressure was observed immediately after each mold was poured indicating a significant mold/metal reaction (gas porosity on the surface of these castings verified this reaction).

The three types of yttria coated thermocouple protection tube substrates (alumina, mullite and silica) appeared capable of providing adequate short-time (3 to 5 minutes) protection from the melt. Alumina and mullite substrates were far superior to silica tubes but were not totally satisfactory due to cracking and spalling of the yttria coating.

3.5.3.3 Nondestructive Evaluation of Castings

Visual and X-ray examination indicated the presence of gas porosity in all test bar castings (zircon mold) to varying degrees. The porosity was generally more predominant in the lower gate and primarily located on top surfaces. Porosity was negligible on surfaces of the cast-to-size test bars but was quite apparent on the surfaces of the 1/2-inch round bars (Figure 31). Castings of the lower melting Ti-13Cu-4.5Ni alloy (2425°F) generally exhibit lower porosity than the Ti-13Cu alloy (2630°F) castings. Gas porosity in these castings, appeared to be primarily due to mold/metal reaction.

The ability of the Ti-13Cu-4.5Ni alloy to fill the very thin blades (0.060 inch) of the cooling fan cast in Pour 12 was encouraging.

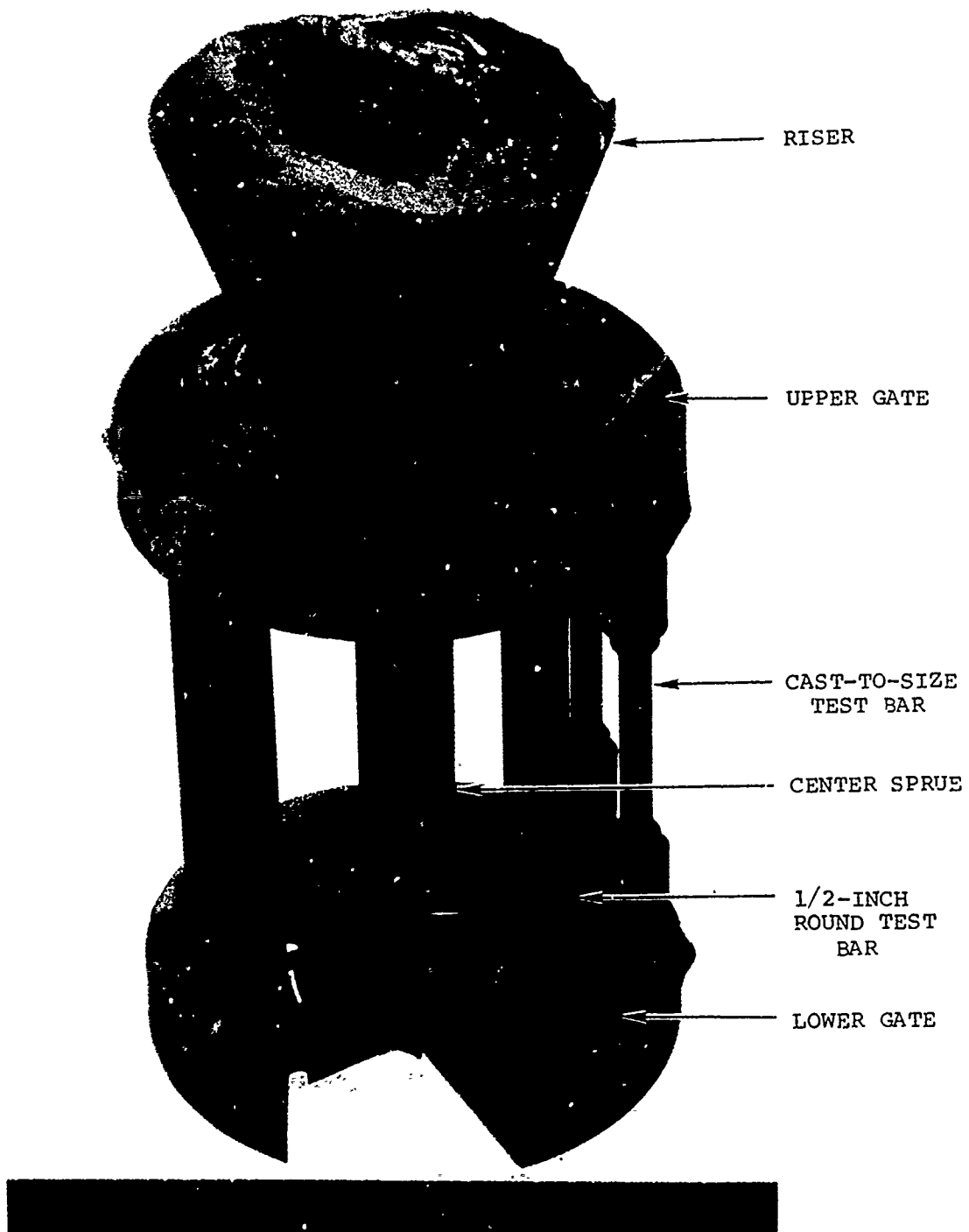


Figure 31. Typical Appearance of Test Bar Cluster Casting. Note the Presence of Gas Voids on Top Surfaces of Upper and Lower Gates (Arrows). This Porosity is not Evident on Bottom Surfaces (Pour 14).

3.5.3.4 Heat Treatment of Cast Tensile Samples

The 1/2-inch round and cast-to-size test bars were removed from all castings, X-ray radiographed for soundness and then several bars selected for heat treatment prior to tensile testing. Cast bars were heat treated using the optimum treatment defined by RMI ingot evaluations (Section 3.5.1.1): 1760°F/1 hour/air cool plus 1450°F/8 hours/air cool.

Most of the tensile samples were heat treated in a steel capsule filled with argon and water quenched in an effort to simulate an air cool rate. Control samples, in the form of Ti-13Cu ingot material were also included in the capsule in order to verify the heat treatment. Evaluation of this control material indicated low strength and high ductility compared to RMI processed material, suggesting an overaged condition (data in Appendix B, Tables B-2, B-3 and B-5). Tensile data for the two cast alloys in the heat treated condition are therefore typical of an overaged condition.

3.5.3.5 Tensile Test Evaluation

A variety of cast samples were used for tensile property evaluation including 1/2-inch rounds, 3/4-inch round center sprues, cast-to-size bars and round slugs removed from alloy solidified in melting crucibles. Test data for all tensile samples as well as fracture surface examination results are compiled in Appendix B (Tables B-2 through B-5).

The test results (summarized in Table 23) were encouraging since both alloys showed the ability of producing cast tensile properties, which were equivalent to the best ingot properties obtained at room temperature and only slightly lower than the 600°F results (Table 23). Generally, the best results were observed with cast material from which the contaminated surface layer had been removed. However, even cast material with the

TABLE 23

SUMMARY OF CASTING TRIAL "A" TENSILE PROPERTIES FOR INGOT AND CAST Ti-13Cu AND Ti-13Cu-4.5Ni ALLOYS

Alloy	Test Temp.	Form	As-Melted or As-Cast					Heat-Treated[1]				
			No. of Tests	UTS (ksi)	YS (ksi)	EL. (%)	RA (%)	No. of Tests	UTS (ksi)	YS (ksi)	EL. (%)	RA (%)
Ti-13Cu	R.T.	Ingot[2]	2	92	64	9	15	4	99	72	12	14
		CSTB	2	88	77	2	4	3	83	78	3	6
		Machined 1/2" Round	2	98	87	3	6	3	96	75	10	13
	600°F	Ingot[2]	-	-	-	-	-	2	74	46	14	25
		CSTB	-	-	-	-	-	-	-	-	-	-
		Machined 1/2" Round	1	67	44	9	18	4	64	43	11	24
Ti-13Cu-4.5Ni	R.T.	Ingot[2]	2	88	59	4	7	5	98	72	5	7
		CSTB	3	89	71	2	4	2	79	70	2	3
		Machined 1/2" Round	4	102	75	7	7	4	84	67	3	5
	600°F	Ingot[2]	-	-	-	-	-	2	84	45	14	24
		CSTB	-	-	-	-	-	1	77	41	12	18
		Machined 1/2" Round	3	77	40	20	28	4	77	38	20	28
Program Goals	R.T. 600°F			100 60	90 50	5 5			100 60	90 50	5 5	

[1] 1760°F/1 hr/air cool plus 1450°F/8 hrs/air cool

[2] Phase II ingot properties

as-cast surface present displayed reasonable ductility (2-3 percent). This was encouraging since common titanium casting surface cleaning procedures such as chemical milling were not employed. It was also observed that, for the Ti-13Cu alloy, the heat-treated machined bar properties (Table 23, boxed-in values) were equal to comparable ingot heat-treated properties, while the properties of the Ti-13Cu-4.5Ni alloy were equivalent in the as-cast condition (Table 23 boxed-in values). This indicates that differences in heat treatment response can be expected between ingot and cast material.

A variety of defects were observed (20X magnification) on tensile specimen fracture surfaces. This included gas voids, microporosity, and inclusions. In addition, fracture surfaces of samples from both alloys exhibited considerable amounts of cleavage fracture in as-cast and heat-treated specimens tested at room temperature, with the Ti-13Cu-4.5Ni alloy generally showing larger areas of cleavage. Samples tested at 600°F exhibited reduced amounts of cleavage for both alloys with the Ti-13Cu material showing an absence of cleavage.

3.5.3.6 Chemical Analysis Results

Each Trial "A" casting (including charges solidified in crucibles; Pours 7, 9, and 15) was analyzed for bulk oxygen and yttrium. Bulk samples of selected castings were also analyzed for possible mold contaminants (Zr, Si, Na, and Al) or alloy solute elements (Cu and Ni). Analytical samples, in all cases, were removed from one end of a tensile bar of the various castings. No gating, sprues or riser sections were sampled for analysis. Complete analytical results are presented in Appendix A, Table A-3.

A summary of the oxygen and yttrium results are listed in Table 24 and showed that castings of the lower melting alloy (Ti-13Cu-4.5Ni) experienced less contamination than the Ti-13Cu

TABLE 24

INFLUENCE OF ALLOY MELTING POINT AND MELTING CRUCIBLE COMPOSITION ON CAST ALLOY CONTAMINATION

Melting Crucible	Ti-13Cu MP = 1434°C (2613°F)			Ti-13Cu-4.5Ni MP = 1330°C (2425°F)		
	Pour	Oxygen (%)	Yttrium (%)	Pour	Oxygen (%)	Yttrium (%)
Y_2O_3·15Ti	1	0.26	0.44	5	0.21	0.28
	2	0.28	0.49	6	0.19	0.26
	Avg	0.27	0.47	Avg	0.20	0.27
Y_2O_3·15Ti Plus Y_2O_3 Layer	10	0.29	0.50	13	0.18	0.27
	11	0.40	0.54	14	0.28	0.37
	Avg	0.35	0.52	Avg	0.23	0.32

NOTE: 1. Analyses are for the test bar castings.

2. Oxygen analyzed by Neutron activation and Yttrium by spectrochemical.

alloy. Data in this table also suggests that castings made from melts in the Y_2O_3·15Ti crucible experience contamination levels comparable to those made with the yttria layer crucible.

Surface contamination of four Trial "A" castings was determined by analyzing lathe turnings which included 0.010-inch layer from the surface. The surface oxygen contents for these samples were near 0.7 percent for the Ti-13Cu alloy and 0.55 percent for the Ti-13Cu-4.5Ni alloy. This again illustrated the higher reactivity of the higher melting point alloy (Ti-13Cu). This level of oxygen on the cast surface of both alloys would contribute to the lower ductility displayed by bars tested with the cast surface intact.

Metal poured into a pyrolytic carbon crucible (Pour 4) was analyzed for carbon contamination. Carbon was analyzed at 0.006 percent for the bulk material and 0.03 percent for the surface (approximately 0.06-inch-thick sample). These carbon levels were considerably less than bulk analyses observed for Phase I Ti-2.7Be alloy laboratory melts made in the same crucibles (0.58 percent). This relationship illustrated the possibility of using more reactive materials for mold construction compared to melting crucible materials. As a result, the possibility of using high density carbon as mold material appears attractive.

Copper and nickel analyses were also made on cast samples of both alloys. Variations from the analyzed ingot composition were observed but were not considered unusual and it did not appear that solute losses due to volatilization during melting were significant. Generally, other elements (mold contaminants) in bulk samples were present at quite low levels. Cast surface analyses for Zr, Al and Si contamination were not performed.

A correlation between oxygen content and yield strength of cast material also was established (Figure 32). The free oxygen values of Figure 32 were calculated by subtracting the amount of oxygen used in forming Y_2O_3, from the analyzed oxygen (total oxygen).

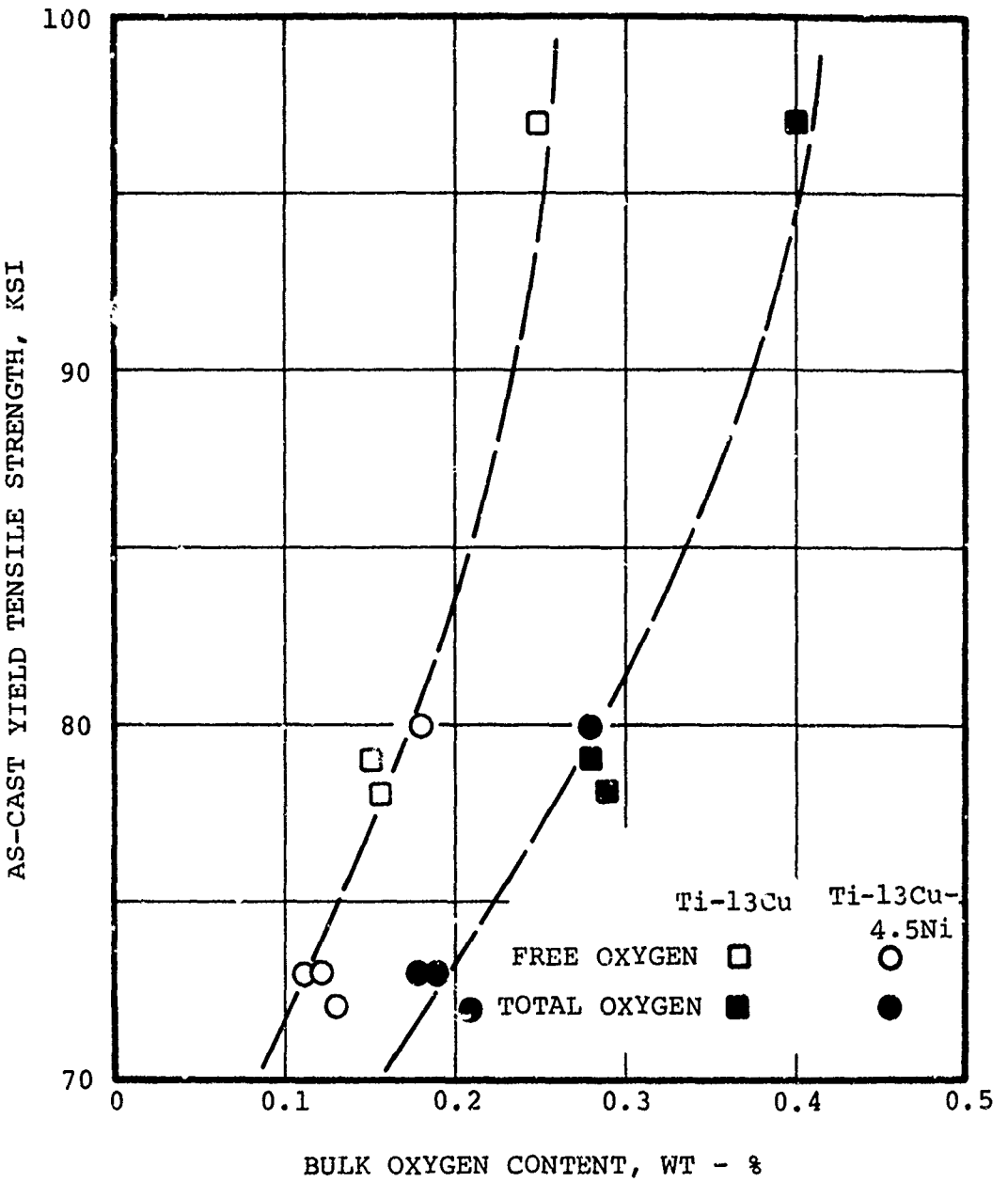


Figure 32. Plot of Alloy Oxygen Content Versus Yield Tensile Strength for Ti-13Cu and Ti-13Cu-4.5Ni in the As-Cast Condition.

During the program, various samples were analyzed for oxygen, by vacuum fusion (VF) and neutron activation (NA) techniques to determine the acceptability of neutron activation. There was correlation between VF and NA oxygen analyses although NA results generally were slightly higher. Metal that contained yttrium (probably as Y_2O_3) also displayed higher oxygen contents when analyzed by NA as compared to VF. Earlier AiResearch work showed similar trends and indicated that metal containing elements such as zirconium and thorium which form very stable oxides, display higher oxygen values when analyzed by NA. This suggested that analysis of total oxygen may be by neutron activation with analysis of free oxygen by vacuum fusion.

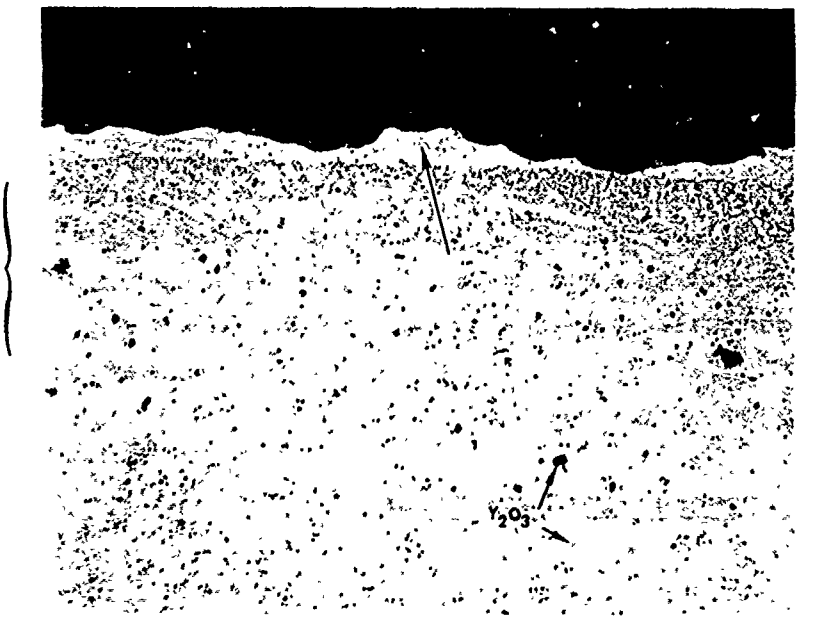
3.5.3.7 Microstructure Evaluation

Metallography samples were evaluated to characterize material from the casting operation in the following areas:

- Casting surface contamination
- Tensile samples
- Melts solidified in crucibles
- Melting crucibles

3.5.3.7.1 Casting Surface Contamination

Samples from the various Trial "A" castings were evaluated for surface microstructural changes, which were associated with contamination rather than influence of surface cooling rates. Castings made in zircon molds showed alpha-case and a diffusion zone (Figures 33 and 34). The higher melting alloy Ti-13Cu, (Figure 33) showed more alpha case contamination (2.3 mils) than did the lower melting alloy, which showed a layer 1.4 mils deep. Metal solidified in the Y_2O_3·15Ti melting crucibles show no alpha-case while metal poured into the ZrO_2 crucible showed high contamination (alpha-case and diffusion zone). Metal poured into the pyrocarbon crucibles showed very low surface microstructural contamination.

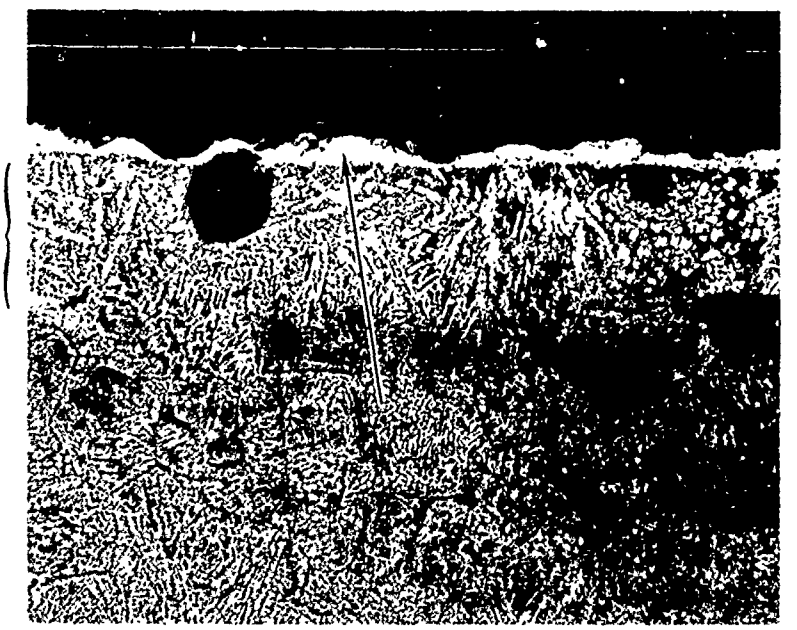


(A) TYPICAL SURFACE 100X

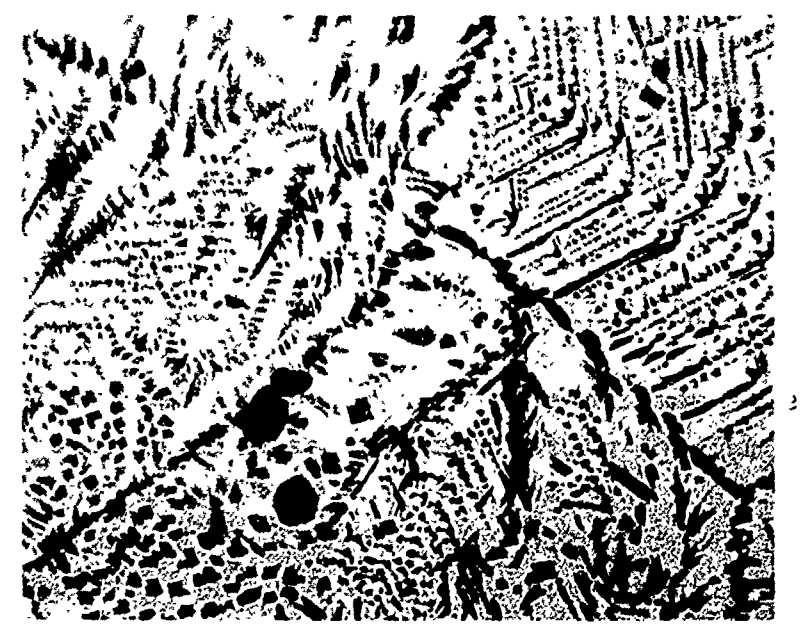


(B) TYPICAL INTERIOR 450X

Figure 33. Microstructure of Ti-13Cu Cast into ACC Standard Zircon Mold System. Note Alpha Case (at Arrow) and Indication of Diffusion as Well as Y_2O_3 Inclusions (Bottom Gate of Pour 2).



(A) TYPICAL SURFACE 100X



(B) TYPICAL INTERIOR 450X

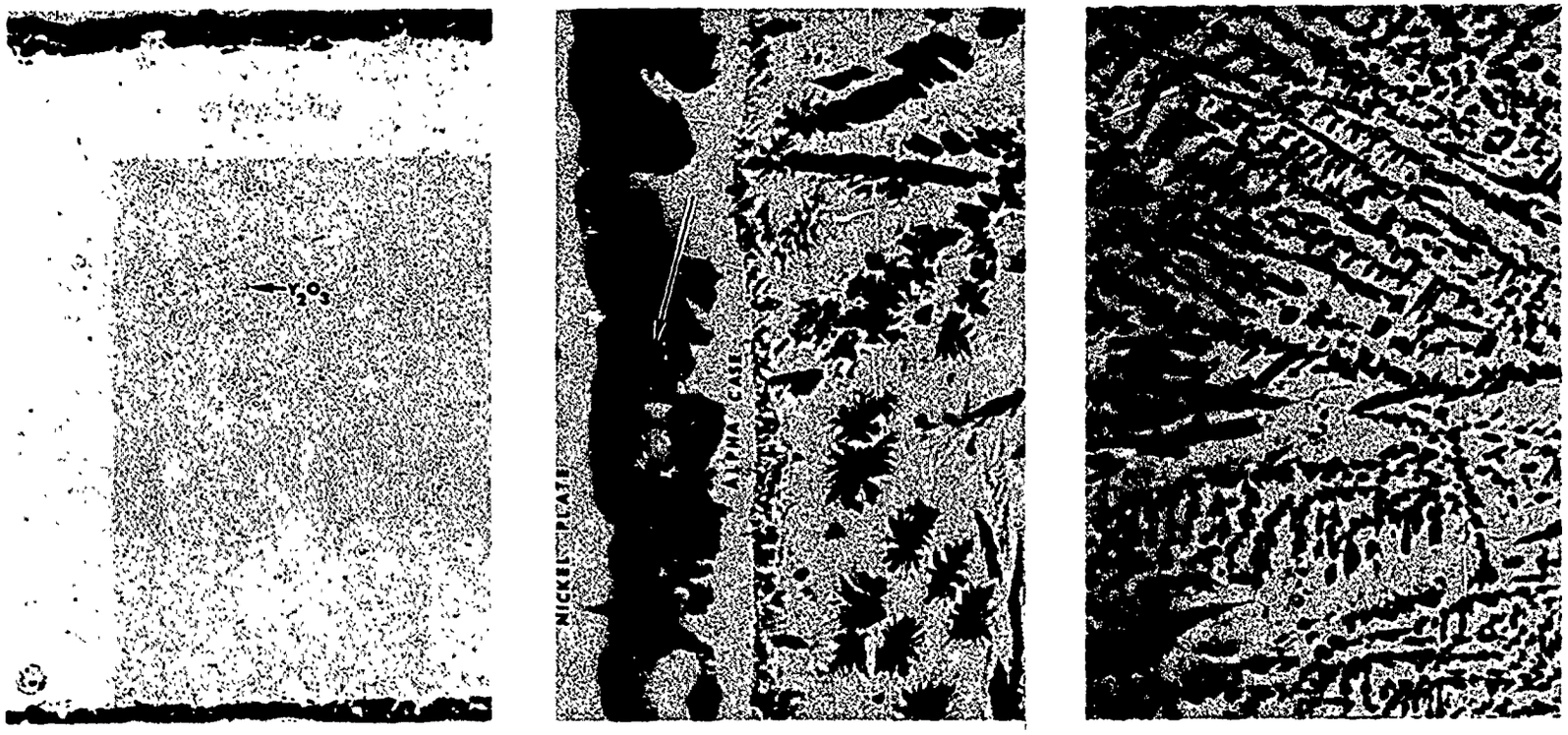
Figure 34. Microstructure of Ti-13Cu-4.5Ni Cast Into ACC standard Mold System (Zircon). Note Alpha Case (Arrow) and Indication of Diffusion Zone (Bracket) (Bottom Gate of Pour 5).

A blade section of the cooling fan casting (Pour 12) made from the Ti-13Cu alloy was evaluated to provide an assessment of the microstructure for a thin section (0.060-inch-thick). The microstructure (Figure 35) was well defined in the interior indicating a relatively slow cooling rate with an alpha-case of 1.5 mils at the surface. The diffusion zone appeared much smaller (0.4-3.0 mils) compared to that (7 mils) displayed by 3/4-inch thick cast sections from the same alloy. The yttria particle size and distribution in the thin blade (Figure 35) were also less than observed for 3/4-inch thick sections (Figure 34).

A sample of cast Ti-13Cu-4.5Ni alloy was evaluated at the Air Force Materials Laboratory, to identify the above suspected yttria second-phase particles (Figures 33 and 34) typically observed after melting in yttria crucibles. Electron microprobe evaluation indicated the particles to be high in yttrium, with negligible amounts of Ti, Cu, Al, or Ni (Figure 36). This analysis indicated these blocky second phase particles are basically yttria. Quantimet measurement of the particles indicated a quantity equivalent to 0.37 percent by volume (0.39 weight-percent). This compared favorably to the analyzed yttrium content of 0.28 percent, which would convert to 0.35 weight-percent if present as yttria.

3.5.3.7.2 Tensile Samples

Tensile specimens were examined to evaluate the effect of heat treatment on microstructure, as well as to characterize the fracture path. Cast material for both Trial "A" alloys had a beta grain size of ASTM 2.5. Ti-13Cu typically developed a finer cast microstructure (Figure 33) than the Ti-13Cu-4.5Ni alloy (Figure 34) duplicating structure trends previously described (Section 3.5.1.1) for arc-melted ingot. A variety of defects were also observed in most tensile samples including porosity, microshrinkage and inclusions (Figure 37).



(A) BLADE SECTION (100X) (B) MOLD INTERFACE (450X) (C) INTERIOR (450X)

Figure 35. Microstructure of Ti-13Cu-4.5Ni Alloy Cast into ACC Zircon Mold System. Casting is the GTCP660 Cooling Fan and Microstructures are of a Blade. Note Alpha Case and Entrapment of Mold Materials (Arrow) as Well as Y_2O_3 Inclusions.Pour 12 (12-1).

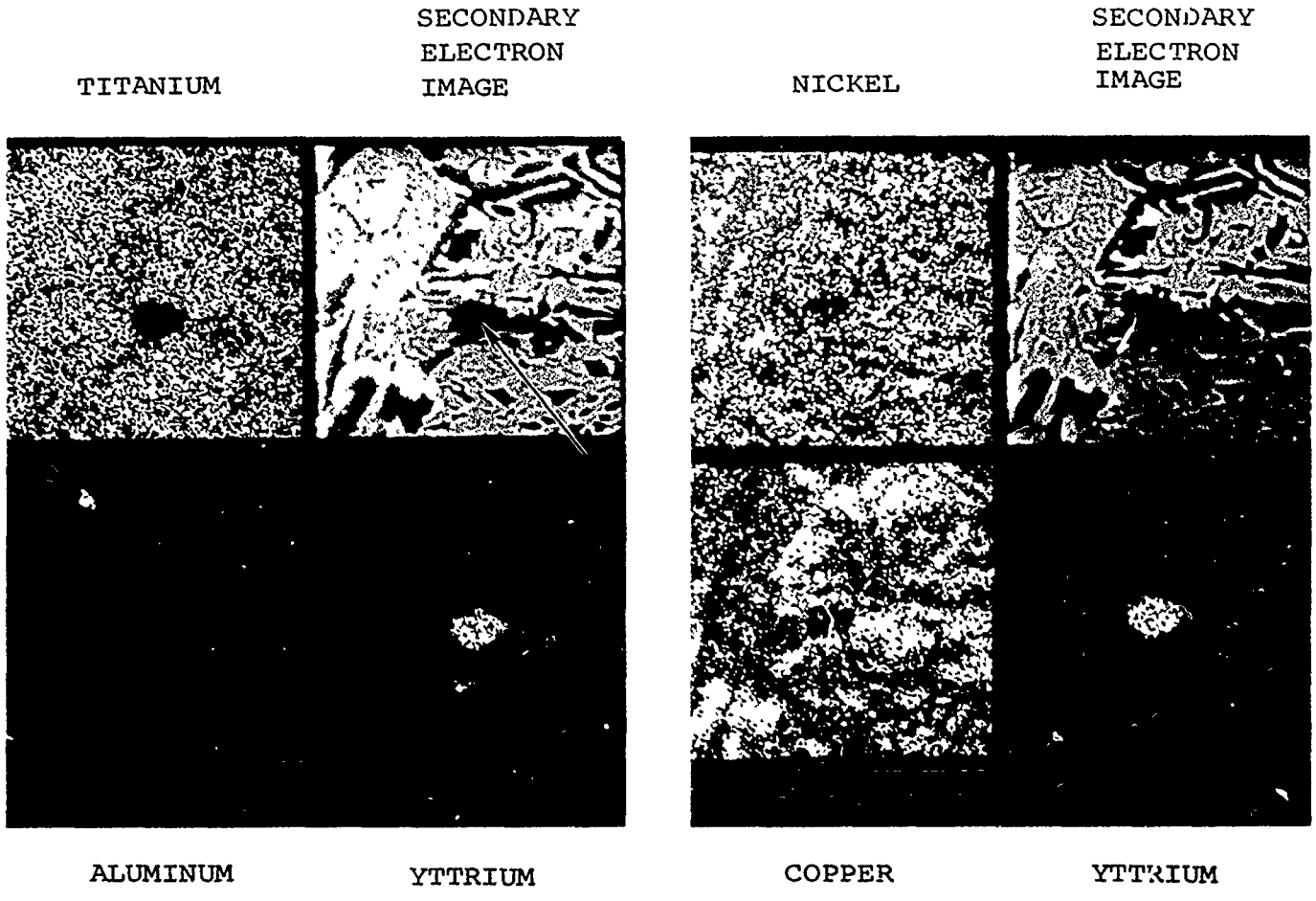
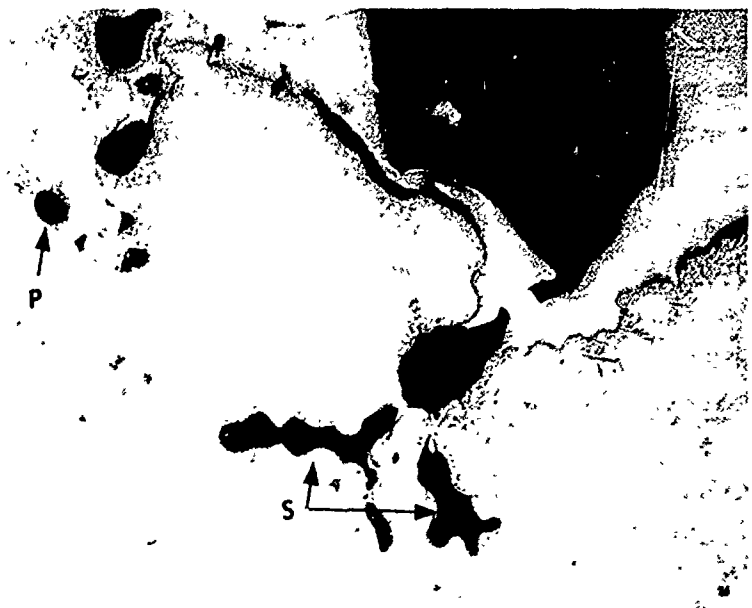


Figure 36. Electron Microprobe X-Ray Images of Second Phase Particle (Arrow) in Cast Ti-13Cu-4.5Ni Alloy After Melting in a Y_2O_3•15Ti Crucible During Casting Trial "A" (Pour 5). Note the High Yttrium Content and Absence of Other Elements.



(A) AS CAST, MACHINED BAR, SAMPLE 1-5 200X



(B) AS-CAST, CSTB SAMPLE 8-3 500X

Figure 37. Microstructure of Fracture Surfaces of Ti-13Cu Alloy Tensile Specimens Illustrating Shrinkage(S) and Porosity(P) in Top Figure and Inclusion Defects (Arrow) in Bottom Photo.

3.5.3.7.3 Melts Solidified in Crucibles

Melts of Ti-13Cu-4.5Ni solidified in each of the Y_2O_3·15Ti melting crucibles developed the microstructures shown in Figure 38. No alpha case was observed for either melt and a diffusion zone if present was difficult to define microstructurally. The general alloy microstructure was also quite coarse and well defined when compared to that for the bottom gate of a test bar casting (Figure 34) or a thin section such as the cooling fan blade (Figure 35).

3.5.3.7.4 Melting Crucibles

Microstructures of the two crucibles used for casting Trial "A" were evaluated with the following observations:

- Both crucibles, after use for induction melting, showed a heterogeneous structure in the wall which appeared to be associated with wall location and titanium concentration variations (Figure 39).

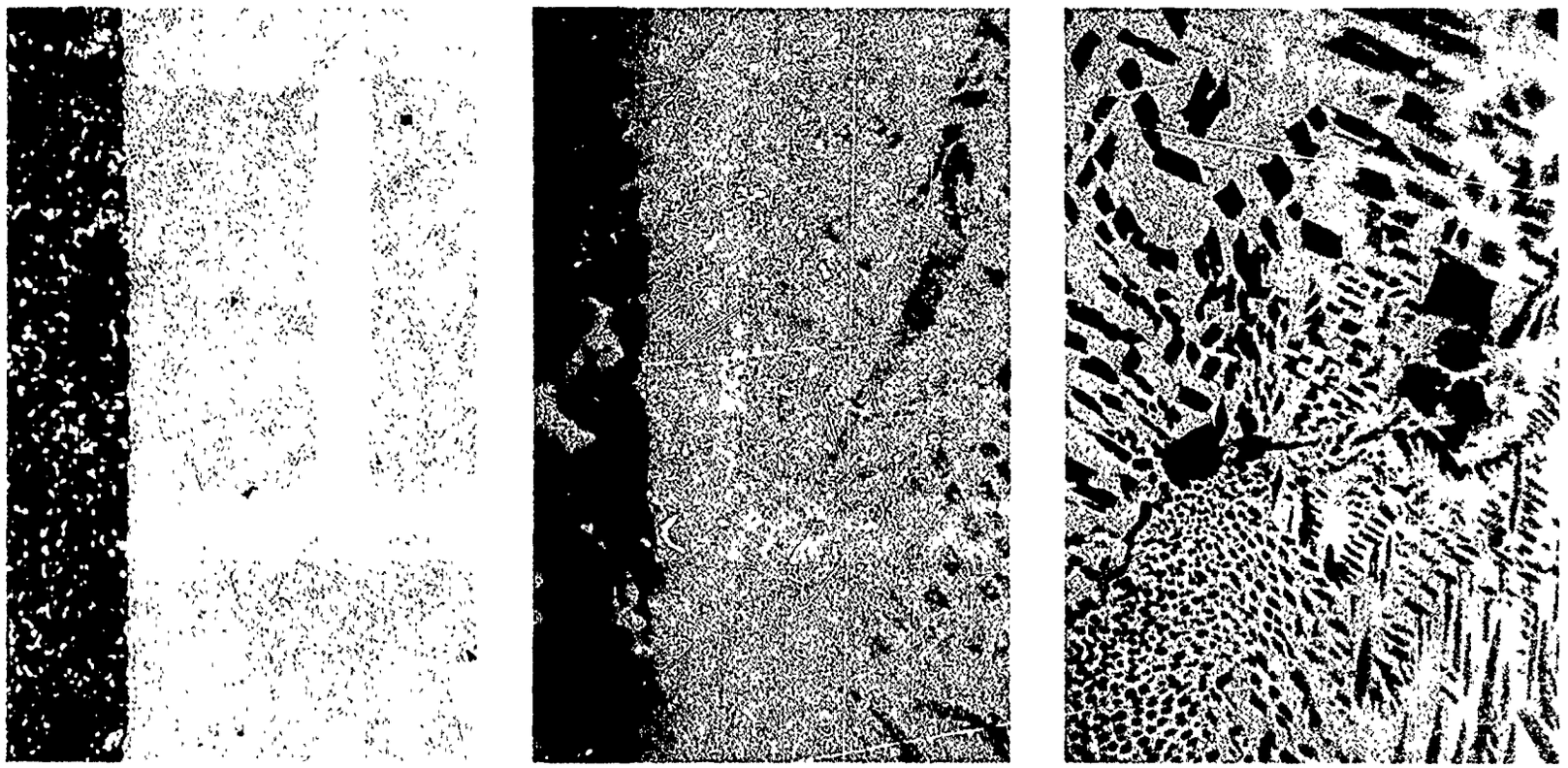
- Crucible material above the melt showed titanium particle structure changes and volume fraction reduction.

- Below the melt line, the crucibles showed reasonably intact titanium particle structure and concentration.

- Both crucibles contained interconnected porosity as evidenced by titanium infiltration from the melt (Figure 40B).

- The yttria layer, when present on the crucible, prevented this titanium infiltration (Figure 40A).

Microstructures of the melting crucibles appear to undergo changes as a result of melting operations, which may or may not



(A) CRUCIBLE-METAL INTERFACE (100X)

(B) CRUCIBLE-METAL INTERFACE 450X

(C) METAL INTERIOR (450X)

Figure 38. Microstructure of Ti-13Cu-4.5Ni Alloy Solidified in Y_2O_3·15Ti Melting Crucible. Note Lack of Second Phase Precipitation in Alloy Near Crucible - Metal Interface but Presence in Interior. Pour 7 (7-2-2)

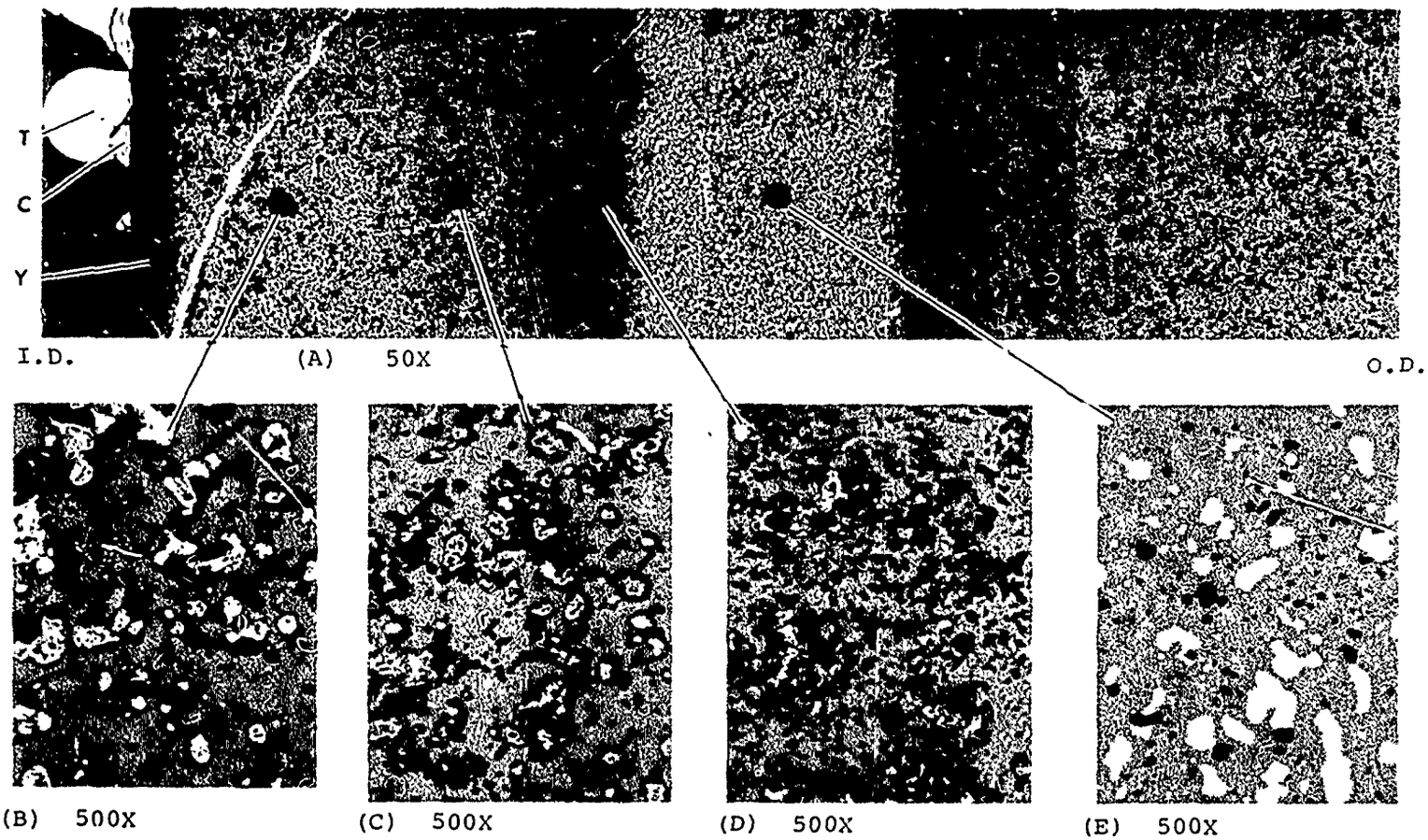
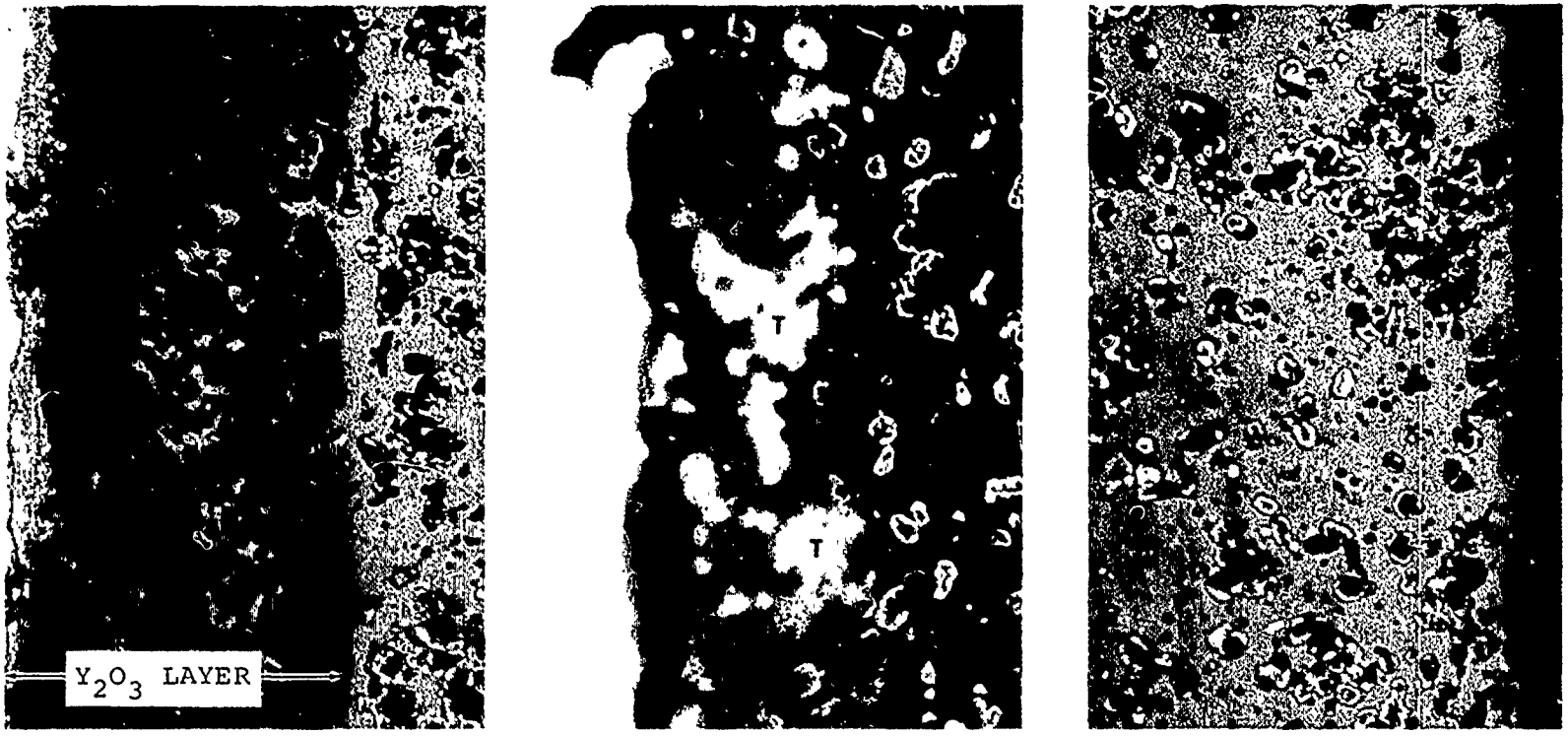


Figure 39. Interior Microstructures of Y_2O_3·15Ti Plus Y_2O_3 Layer Crucible (No. 3) After use for Casting Trial "A". Wall is Located Above but Near Melt Line. Note Y_2O_3 Layer at Y, Suspected Copper Metal Splatter at C, and Ti Alloy Splatter at T.(C-2)



(A) I.D. EDGE WITH YTTRIA LAYER (450X) (B) I.D. EDGE SHOWING TITANIUM ALLOY INFILTRATION (450X) (C) O.D. EDGE (450X)

Figure 40. Microstructure of Y_2O_3•15Ti Plus Yttria Layer Crucible (No. 3) After Casting Trial "A" at Side Wall, Located Above but Near Melt Line. Note Yttria Layer Microstructure in (A), Titanium Infiltration (T) in (B) and General Structure of ID in (A) and (B) and OD in (C). (C-2)

affect the reactivity or thermal shock behavior of the crucible. Microstructures of a typical crucible in the as-fabricated condition are included in the Section 3.6 discussions for Casting Trial "B".

3.5.3.8 Hardness

Trial "A" hardness tests were conducted on a wide variety cast specimens but the results were influenced considerably by cast section size, metal soundness, thermal treatment, cooling rates and oxygen contamination. Some trends appear to exist between these factors and hardness, but a useful correlation such as hardness/oxygen or hardness/strength was not apparent.

3.5.4 Summary-Casting Trial "A"

Casting Trial "A" was conducted using two low-melting alloys (Ti-13Cu and Ti-13Cu-4.5Ni), which were induction melted in two ceramic crucibles (Y_2O_3·15Ti and Y_2O_3·15Ti with a Y_2O_3 layer). Castings were made in a high reactivity, conventional superalloy mold system (zircon facecoat). The resulting castings were evaluated by visual, NDT, metallographic, chemical analysis and tensile tests for comparison to ingot metal properties.

The casting trial was successful and demonstrated feasibility in two significant areas, (1) low-melting titanium alloys can be induction melted in an appropriate ceramic crucible and, (2) the resulting castings display acceptable contamination levels and tensile properties.

The properties of both alloys nearly met program room temperature tensile goals in both ingot and cast material. Alloys with the cast surface intact did not display ductility equivalent to internal metal but exhibited reasonable tensile elongation (2-3 percent). Limited rotating beam fatigue testing also indicated an endurance limit near 30 ksi (10^7 cycles) for ingot material of both alloys in the heat treated condition which was considered promising.

The melting crucibles (Y_2O_3·15Ti and Y_2O_3·15Ti plus an Y_2O_3 layer) performed equivalently well in spite of considerable thermal shock cracking. Acceptable melt contamination levels were observed in Trial "A" castings which ranged from 0.18 to 0.36 percent oxygen and 0.19 to 0.55 percent yttrium. Lower contamination levels were also observed for the lower melting Ti-13Cu-4.5Ni alloy (2425°F) compared to the Ti-13Cu alloy (2630°F).

Additional mold development was required to permit successful application of low reactivity ceramic materials. The experimental mold system having a facecoat of the HREMO material (plus CaF_2 and SiO_2 binder aids) could not be successfully fabricated due to poor slurry properties and lack of sintering. Castings poured into higher reactivity molds (zircon) displayed good fill and adequate internal soundness, but exhibited considerable surface porosity attributed to mold/metal reactions. No difficulty was encountered in containing the molten metal with this mold system, further demonstrating the benefits of a low-melting titanium alloy system.

3.6 Casting Trial "B"

Casting Trial "A" established the feasibility of applying materials developed in Phase I to the production of investment castings. The low-melting titanium alloys induction melted in a ceramic crucible were shown to have the capability for producing acceptable ductility and strength in cast metal; however, strength was below the program goals. Fabrication problems associated with the experimental mold system and cast surface contamination required further improvement in the investment molds. These results lead to the selection of materials for Casting Trial "B" as follows and discussed in the next section (3.6.1):

Alloy:	Ti-13Cu-1.5Al
Melting Crucible:	Y_2O_3·15Ti
Mold System:	Howmet Moncgraf graphite



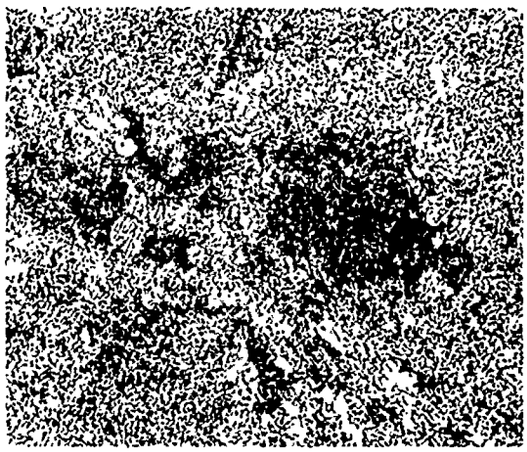
(a) AS-MELTED 5-902



(b) 1560F-1 hr-FC AT 600F/HR TO 900F-AC 5-904



(c) 1560F-1 hr-FC AT 100F/hr TO 900F-AC 5-903



(d) 1760F-1 hr-AC + 1450F-16 hr-AC 5-905

Figure 41. Typical Microstructures of the Phase II Ti-13Cu-1.5Al Alloy in the As-Melted and Heat Treated Conditions.

crucibles appeared nearly equivalent and the lower cost, less complex crucible material (Y_2O_3·15Ti) was selected for further evaluation.

3.6.1.3 Mold Systems

The AiResearch Casting Company (ACC) standard mold system was used exclusively during Trial "A" due to problems encountered in fabricating the experimental mold system. The ACC system produced mold/metal reaction, which promoted a contaminated cast surface that reduced the tensile ductility in both alloys. In order to demonstrate the total casting concept, the four leading titanium casting foundries in the United States were contacted with respect to furnishing molds for program casting efforts. The Howmet Corporation Monograf mold system (graphite facecoat) was selected on the basis of foundry response and ability to meet the program schedule. In addition, experimental facecoat development was continued using oxide ceramics in an effort to prepare low-reactivity mold systems.

3.6.2 Material Procurement

Alloys, melting crucibles and thermocouple protection tubes were procured for casting Trial "B" as discussed in the following sections.

3.6.2.1 Alloy

A 100-pound ingot of Ti-13Cu-1.5Al alloy was double-melted by RMI for ingot evaluation and for use in Casting Trial "B". In order to allow a correlation to Casting Trial "A" as well as an assessment of new mold systems, both of the Trial "A" alloys (Ti-13Cu and Ti-13Cu-4.5Ni) were also used for Trail "B" casting.

Evaluation of the as-melted Ti-13Cu-1.5Al ingot generally followed that described in Section 3.5.1.1 except for the inclusion of 600°F tensile tests and the exclusion of thermal stability tests. The ingot was sectioned similar to Trial "A" ingots (Figure 21) except that material for AFML and second-tier mechanical property testing was not included.

The chemical analysis of the Ti-13Cu-1.5Al ingot is listed in Appendix A (Table A-2). All residual elements (C, N, and Fe) were normal and consistent with previous Ti-Cu ingots. The oxygen at 0.06 percent was similar to that obtained for Phase II Ti-13Cu and Ti-13Cu-4.5Ni ingots.

Hardness and tensile results for the as-melted and heat-treated samples are given in Table 25. As expected, the Rockwell A hardness of the as-melted ingot (62.7) was greater than that of the Ti-13Cu ingot (57.1) and somewhat less than the higher aluminum (2-3 percent) Phase I Ti-Cu alloys (64.7). For as-melted material, the tensile yield strength of Ti-13Cu-1.5Al at 90 ksi was also greater than the 64 ksi level for the Ti-13Cu and Ti-13Cu-4.5Ni alloys (Table 17). The 1.5-percent aluminum addition also resulted in improved ductility for the as-melted Ti-13Cu-1.5Al alloy (3-percent elongation) compared to the previous Phase I, Ti-13Cu-2Al and Ti-13Cu-3Al ingots (1.0 and 0.0 percent elongation, respectively) as shown in Table 6. Additional ductility improvements were obtained in the Ti-13Cu-1.5Al alloy by heat treatment (Table 25) and the room temperature tensile goals of the program were met using the 1760°F-1 hr-AC plus 1450°F-16 hr-AC duplex cycle. The 600°F tensile properties for Ti-13Cu-1.5Al alloy in duplex heat treated condition were significantly improved over those of the previous Phase II alloys and also considerably above the program goals.

As-melted and heat treated microstructures from the 8-inch Ti-13Cu-1.5Al ingot are shown in Figure 41. The as-melted beta-grain size of this alloy was 0.017 inch, the same as noted for

TABLE 25

PROPERTY DATA FROM PHASE II INGOT OF
Ti-13Cu-1.5Al (HEAT 25254) ALLOY

Nominal Composition	Heat Treatment	Rockwell A Hardness	Type of Test	Location and Specimen Direction[1]	UTS ksi	YS ksi	El %	RA %
Ti-13Cu-1.5Al	As-Melted	62.7	Room Temp. Tensile	Mid-Radial	110 111	92 87	3.0 3.0	4.8 5.6
	1560F-1hr-FC @ 100F/hr to 900F-AC	59.0	--					
	1560F-1hr-FC @ 600F/hr to 900F-AC	59.8	Room Temp. Tensile	Mid-Radial	97 98	79 80	8.0 8.0	12.7 11.2
	1760F-1hr-AC	71.2	--					
	1760F-1hr-AC + 1300F-8hr-AC	67.6	--					
	1760F-1hr-AC + 1400F-8hr-AC	67.3	--					
	1760F-1hr-AC + 1400F-16hr-AC	65.5	--					
	1760F-1hr-AC + 1450F-8hr-AC	64.3	--					
	1760F-1hr-AC + 1450F-16hr-AC	64.6	Room Temp. Tensile	Mid-Radial	114 114	94 94	7.0 9.0	8.0 10.0
	1760F-1hr-AC + 1450F-16hr-AC	--	Room Temp. Tensile	Edge Tangential	114 115	89 91	10.0 10.0	15.2 14.2
	1760F-1hr-AC + 1450F-16hr-AC	--	600F Tensile	Edge Tangential	90 90	62 62	19.0 19.0	36.0 34.0

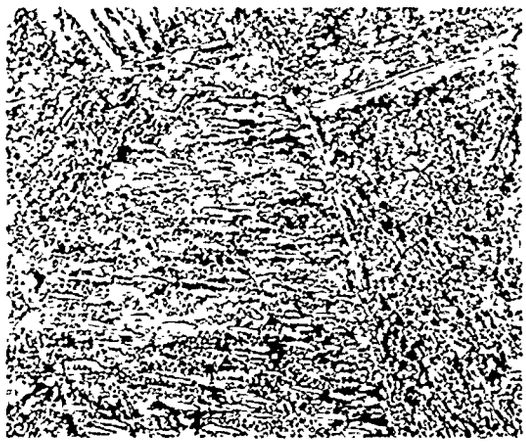
1. Cut from a transverse slice at center of the 8-inch-diameter ingot.



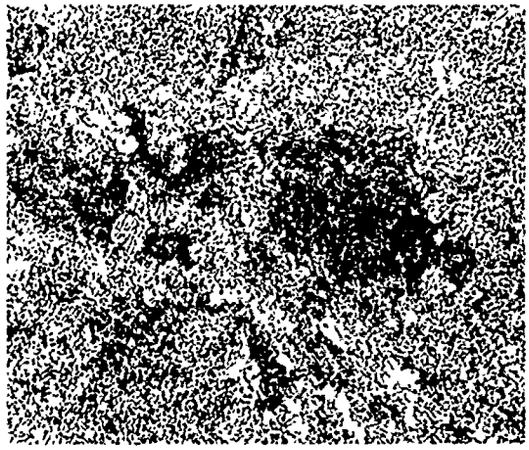
(a) AS-MELTED 5-902



(b) 1560F-1 hr-FC AT 600F/HR TO 900F-AC 5-904



(c) 1560F-1 hr-FC AT 100F/hr TO 900F-AC 5-903



(d) 1760F-1 hr-AC + 1450F-16 hr-AC 5-905

Figure 41. Typical Microstructures of the Phase II Ti-13Cu-1.5Al Alloy in the As-Melted and Heat Treated Conditions.

the previous 8-inch, Ti-13Cu-4.5Ni ingot. This grain size was a little larger than in smaller ingots of aluminum-containing Ti-13Cu alloys evaluated in Phase I (0.017 versus 0.010 inch). The as-melted microstructure of the Ti-13Cu-1.5Al alloy (Figure 41a) showed smaller eutectoid products than obtained in either of the previous Phase II, Ti-13Cu and Ti-13Cu-4.5Ni as-melted ingots (Figure 22, a and b). The finer eutectoid product in the Ti-13Cu-1.5Al alloy was consistent with that observed and in the Phase I aluminum bearing alloys.

Annealed microstructures for Ti-13Cu-1.5Al (Figure 41, b and c) were similar to those of Ti-13Cu and Ti-13Cu-4.5Ni (Figure 22, c and d) with the exception that smaller Ti_2Cu precipitates form within the prior beta grains of Ti-13Cu-1.5Al. Increasing the cooling rate after annealing Ti-13Cu-1.5Al resulted in less Ti_2Cu precipitation at the prior beta grain boundaries (Figures 41, b versus c). The microstructure of duplex heat treated Ti-13Cu-1.5Al material (Figure 41d) showed no evidence of prior beta grains or the fine eutectoid product. This structure was similar to that obtained for the Phase I duplex heat treated Ti-13Cu-2Al alloy (Appendix C, Figure C7f).

To further characterize properties, the modulus of elasticity was determined from load-versus-strain tensile curves at both room and 600°F using duplex heat treated Ti-13Cu-1.5Al ingot material. A room temperature value of 17.0×10^6 psi was obtained, which is consistent with those of commercial alpha-beta titanium alloys. However, it was higher than obtained with metastable beta titanium alloys (15.0×10^6 psi). The modulus of elasticity at 600°F was 14.8×10^6 psi which is higher than that of commercially-pure titanium (12.5×10^6 psi) at the same temperature.

These moduli data suggest, along with previous room and elevated temperature tensile data, thermal stability and fatigue results, that low-melting Ti-Cu alloys have the potential for substitution for other cast titanium and wrought titanium alloys.

However, additional mechanical property evaluations would be helpful for acceptance of cast Ti-Cu alloy products.

3.6.2.2 Melting Crucible Fabrication

Four $Y_2O_3 \cdot 15Ti$ melting crucibles (4 inch diameter by 8 inch high) were fabricated at Coors Porcelain Co. by cold isostatic pressing and firing at 3000°F for 4 hours in argon. The first crucible (No. 5) cracked during the firing cycle due to excessive thermal gradients. Subsequent firing operations produced crucibles in excellent condition, including for the first time the firing of two crucibles in one load. Fabrication data, (presented in Appendix D, Table D-8) indicated these crucibles (numbers 5 through 8) to be equivalent to those fabricated for Casting Trial "A".

3.6.2.3 Thermocouple Protection Tube Fabrication

Thermocouple protection tubes were plasma sprayed with yttria as had been done for Casting Trial "A". Five experimental groups were fabricated as follows:

(a) Alumina substrate tube; standard velocity gun, yttria coating, 4 mils thick. This was equivalent to the best performing system used in Casting Trial "A", but with a thinner yttria coating (Trial "A" tubes were sprayed to a thickness of 10 mils).

(b) Alumina substrate tube; high velocity gun, yttria coating, 2 mils thick.

(c) Alumina substrate tube; standard velocity gun, intermediate titanium coating, 1.5 mils thick and outer yttria layer, 4 mils thick.

(d) Beryllia substrate tube; standard velocity gun, yttria coating, 4 mils thick.

(e) Mullite substrate tube; high velocity gun, yttria coating, 2 mils thick.

After spraying, all tubes were in good condition and available for use in Casting Trial "B".

3.6.3 Mold Development

In a final effort to develop a promising low-reactivity ceramic mold system, several experimental mold facecoats of the following compositions were evaluated:

- Colal "P" binder (silica particles with alumina outer layer) plus HREMO.
- Titania plus Colal "P" and Colal "M" binders.
- Colal "P" binder plus yttria
- Colal "M" binder plus yttria
- Colal "M" binder plus alumina
- Colal "P" binder plus alumina
- Yttria plus a binder of yttria dispersed in potassium-silicate solution (Y_2O_3/K_2SiO_3)
- Yttria plus TiO_2 plus colloidal silica binder

The laboratory processing and evaluations were conducted in the same manner described previously. The Colal (Colal is described in Appendix E-8) compositions using HREMO and titania di?

not produce adequate slurries or sintering characteristics. All other facecoat compositions appeared to display acceptable slurry behavior, good facecoat green strength, and reasonable sintered hardness. The last three compositions from the above were selected for Casting Trial "B" mold fabrication.

3.6.4 Foundry Activity

Casting activity was again conducted at the AiResearch Casting Company (ACC) and organized as shown in the diagram in Figure 42. In order to allow a correlation to Casting Trial "A" as well as an assessment of new mold systems, both of the Trial "A" alloys (Ti-13Cu and Ti-13Cu-4.5Ni) were also used for Trial "B" casting. Three alloys were poured into a variety of molds to produce castings for metallurgical and mechanical property evaluations.

3.6.4.1 Mold Fabrication

In an effort to obtain castings with minimum surface contamination, a proven titanium casting mold system (Howmet-Monograf) was the primary choice for use in casting Trial "B". However, in addition to this and three experimental mold systems, a new commercial product (Remet Zirbind) and the previously used ACC zircon system were also included. The above six mold systems were prepared for Trial "B" casting activities shown in Figure 43 and listed below:

- Howmet Monograf; graphite construction
- Experimental Composition "Y"; Y_2O_3/K_2SiO_3 binder plus coarse yttria
- Experimental Composition "T"; Yttria plus Titania plus colloidal silica binder

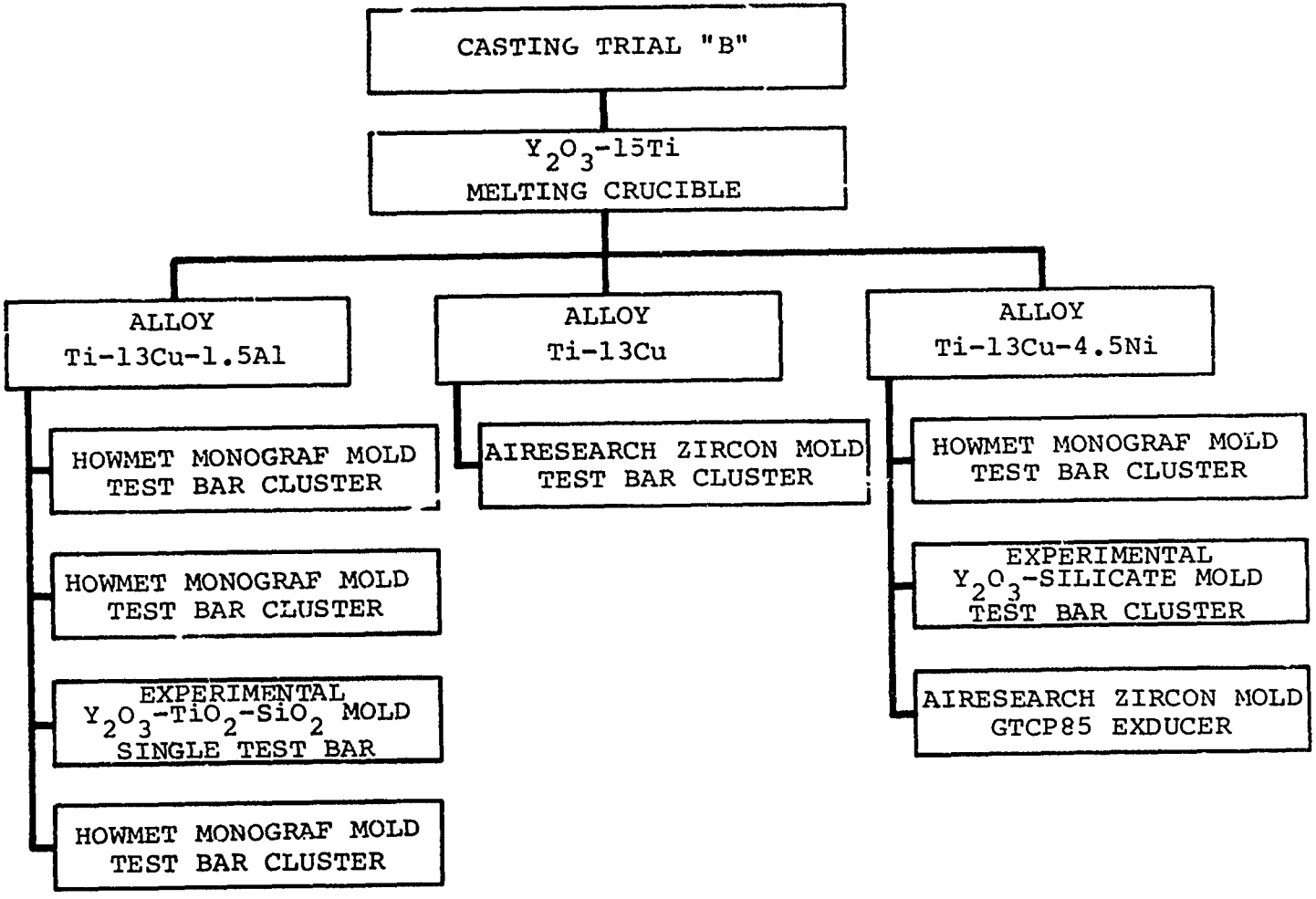


Figure 42. Flow Diagram for Casting Trial "B".

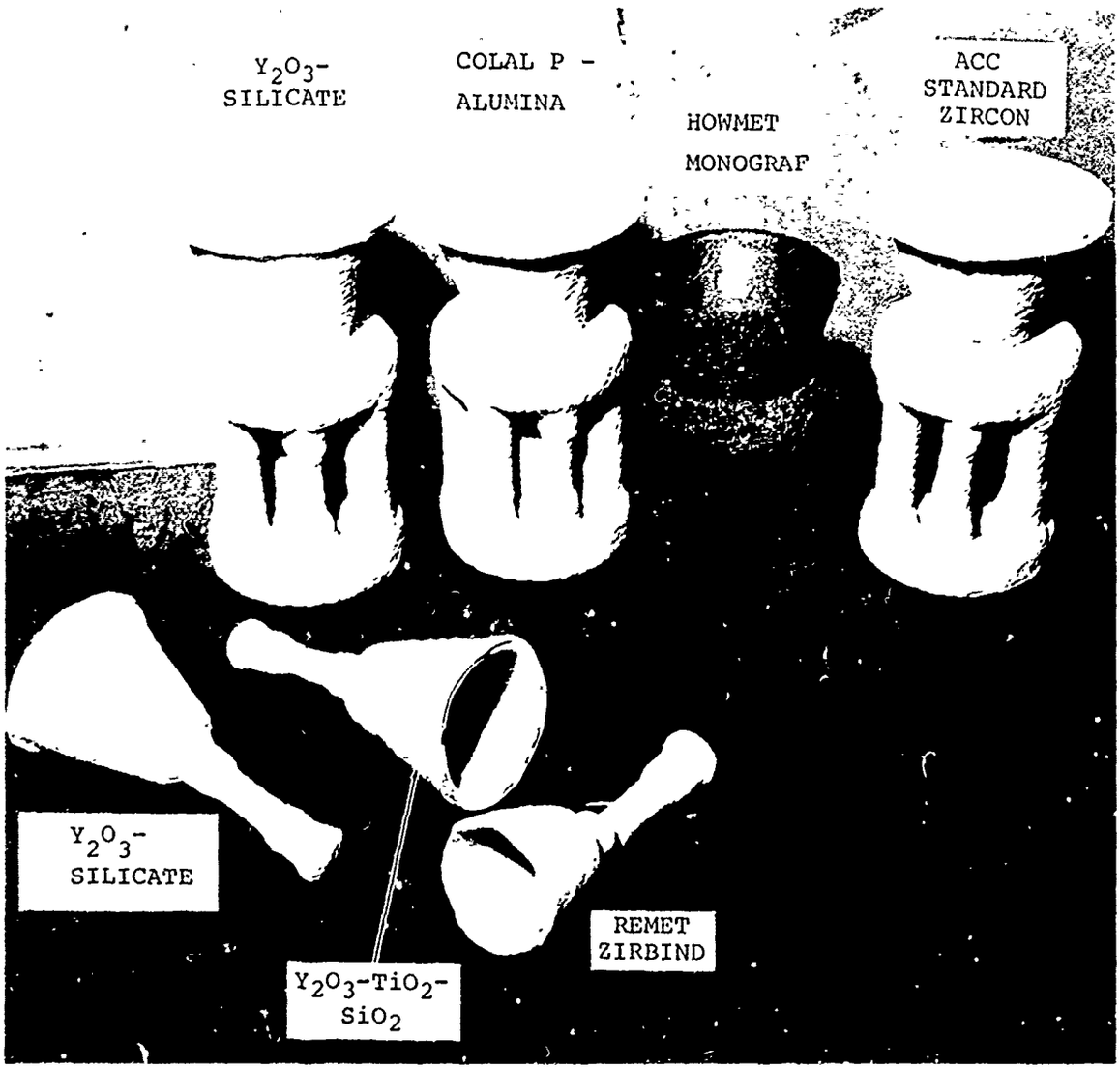


Figure 43. Appearance of Various Molds Fabricated for Use in Casting Trial "B". Note the Broken Remet Mold.

- o Experimental Composition "C"; Alumina plus Colal "P" binder

- o ACC Standard Zircon ($ZrSiO_4$)

- o REMET Zirbind; Zirconia (ZrO_2)

Experimental mold fabrication was successful and encouraging (fabrication procedures described in Appendix E, Table E-8). All slurries exhibited good characteristics and the completed molds exhibited firm facecoats in the green state and after firing at 1900°F in air. These results were much improved over those exhibited by the mold facecoats prepared for the Trial "A" casting effort using the HREMO material.

Mold facecoats prepared with Experimental Composition "C" were smooth and continuous with no voids or loose material. Yttria mold facecoat compositions ("Y" and "T") were somewhat rough due to voids in the facecoat surface. These voids originated during the facecoat dipping process, and appeared to be gas entrapment.

Test bar wax patterns were also transmitted to Howmet Corporation (Whitehall, Mich.) for Monograf mold fabrication and to REMET Corporation (Pompano Beach, FL) for "Zirbind" mold construction. The Howmet mold is a graphite system while the "Zirbind" mold is a zirconia facecoat and binder system. The Howmet molds were received in good condition while REMET molds broke during shipment and were not used in casting activities.

3.6.4.2 Casting Process and Parameters

The Y_2O_3•15Ti melting crucible (No. 7) was loaded into the induction coil box using a dry ceramic pack. The assembly was air baked, at approximately 200°F for 10 hours, before loading into the melting furnace.

Loading the first alloy charge, using the ingot loader, was difficult due to minimal clearance between the charge and crucible walls. As the melting operations continued during the day, the upper portion of the crucible became more restricted, due to metal solidification on the lip. This metal buildup was attributed to positioning the top of the crucible too far above the induction coils, thereby producing a relatively cold crucible lip that promoted metal solidification.

All molds were preheated in air prior to casting; the Howmet Monograf molds to 600°F with a minimum 4-hour preheat, and the ceramic molds to 1900°F with a minimum 8-hour preheat. Because of low preheat temperature, the Monograf molds were insulated with a Kao-wool blanket to minimize heat loss during transfer from preheat to pour (approximately 2 minutes). Ceramic molds were not insulated, and typical transfer time was approximately 1.3 minutes (mold temperature estimated to be near 1750°F at time of pour).

The casting procedure was similar to that used for Trial "A" with the following exceptions:

- Vacuum levels were slightly higher for Trial "B" (13-microns versus 4-microns).

- Metal charges were cleaner for Trial "B"; however, they were hand loaded into the crucible contrary to the planned use of the ingot loader.

A total of eight castings were poured as scheduled (Figure 44) with melting data and pour parameters given in Table 26. Unfortunately, two (P20 and P22) of the three Monograph test bar molds cast with the Ti-13Cu-1.5Al alloy experienced short casts.

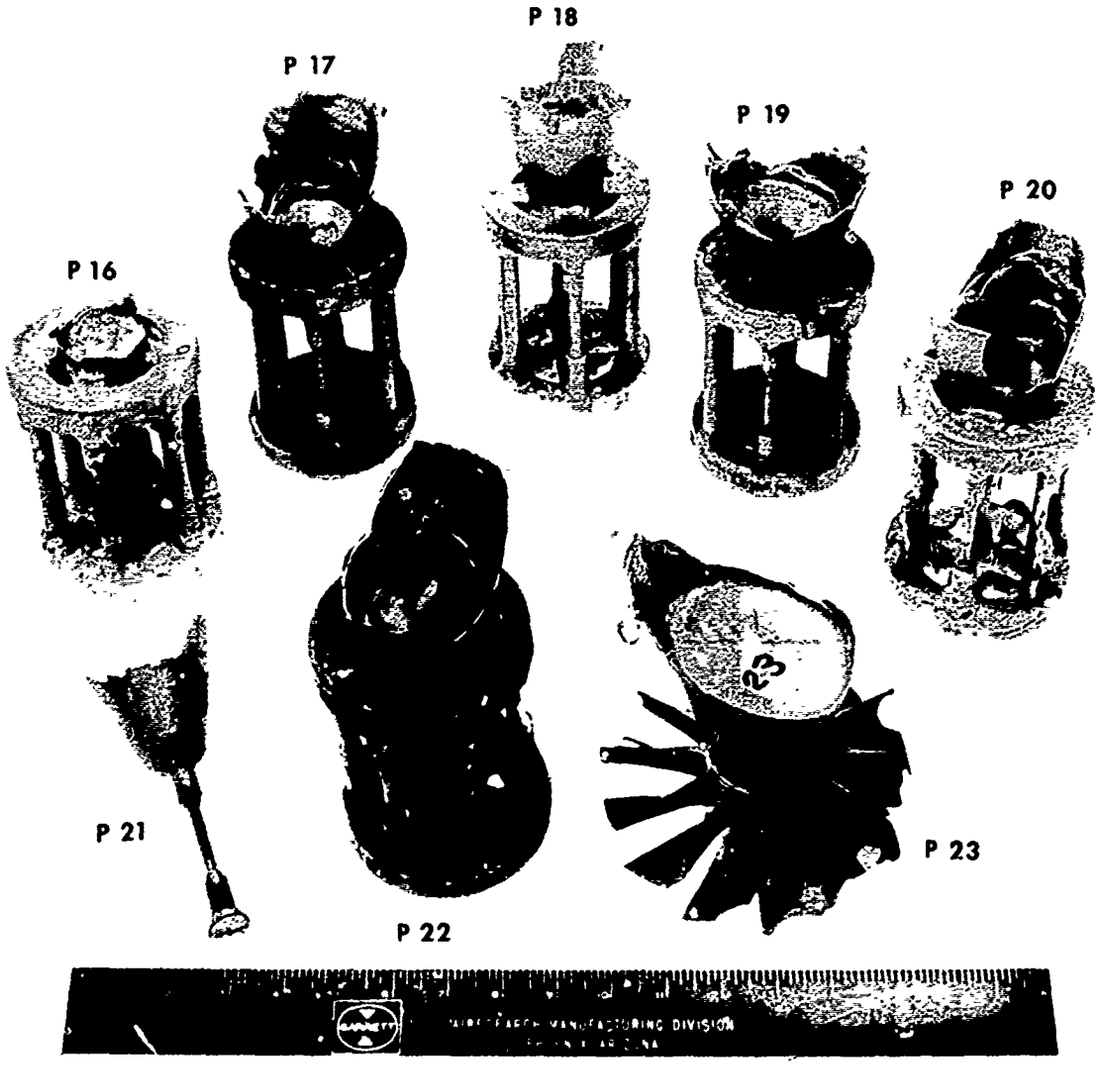


Figure 44. Appearance of Trial "B" Castings.

TABLE 26

CASTING TRIAL "B": MELTING DATA AND POUR PARAMETERS

MELT NUMBER*	SHAPE CAST	MOLD / PREHEAT	TITANIUM ALLOY**	METAL HEIGHT (LBS) CHARGED	METAL HEIGHT (LBS) CAST	AMOUNT OF INGOT SURFACE AREA (%) IN CHARGE ***	T/C PROTECTION TUBE	MELTING PARAMETERS* TIME (MIN)** POWER-ON TO MELT	START OF MELT TO POUR	100% MELT TO POUR	POWER (KW) TO HOLD POUR TEMP.	PEAK AFTER MELTING	TEMPERATURE AT POUR (°F)	TEMPERATURE AT POUR (°C)	TEMPERATURE EST. PEAK (°C)	VACUUM (μ) HIGH-LOW RANGE	VACUUM (μ) AT POUR	REMARKS
P16	Test Bar Cluster	Zircon 1900°F	-13Cu	6.9	4.4	0	Al_2O_3 (a1)	18	18	7	12	15	2815 ±15	1549	--	14-500	100	o Crucible induction coil box outgassing o Mold into air prematurely o Vacuum pressure increased to 120μ after pour
P17	Test Bar Cluster	Monograph Insulated 600°F	-13Cu -4.5Ni	5.0	5.0	0	Al_2O_3/Ti (c1)	14	--	14	10	21	2632 ±10	1445	>1505	13-15	13	o High reaction of T/C protection tube
P18	Test Bar Cluster	Y_2O_3/ K_2SiO_3 1900°F	-13Cu -4.5Ni	6.0	4.9	10	Mullite (d1)	12	18	15	--	20	2615 ±10	1435	>1530	10-15	10	o Vacuum remained at 10μ after pour
P19	Test Bar Cluster	Monograph Insulated 600°F	-13Cu -1.5Al	5.7	5.2	0	Al_2O_3 (a2)	14	16	11	12	20	2820 ±20	1550	--	13-25	13	o Vacuum pressure increased to 150μ after pour
P20	Test Bar Cluster	Monograph Insulated 600°F	-13Cu -1.5Al	5.0	2.8	0	Al_2O_3 (a3)	14	15	12	12	--	2810 ±20	1543	>1560	12-15	15	o Vacuum pressure increased to 130μ after pour o Thermocouple protection tube poured into mold
P21	Single Test Bar	Y_2O_3-TiO_2-SiO_2 1900°F	-13Cu -1.5Al	1.6	0.7	0	Al_2O_3 (a4)	12	9	7	15	20	--	--	--	10-13	10	o Temperature not measured o Vacuum pressure increased to 170μ after pour
P22	Test Bar Cluster	Monograph Insulated 600°F	-13Cu -1.5Al	4.5	3.5	0	Al_2O_3 (a4)	8	18	15	10	20	2834 ±20	1556	>1570	11-13	11	o Thermocouple protection tube poured into mold
P23	GTCP85 Exducer	Zircon 1900°F	-13Cu -4.5Ni	5.9	4.6	0	Al_2O_3 (e1)	7	11	8	10	20	--	--	--	10	10	o Vacuum pressure increased to 40μ after pour

*All melts made by induction heating in Y_2O_3-15Ti crucible No. 7.

**Alloy melting points are: Ti-13Cu-1.5Al = 2615°F: Ti-13Cu-4.5Ni = 2425°F.

***Ingot surface may contain impurities or vary in composition from bulk of ingot and therfore may relate to final casting composition and properties.

****The Sum of times listed in the first and third columns is the total time the metal was being heated and melted.

3.6.4.3 Nondestructive Evaluation of Castings

Castings P16 through P19, and P21 all filled completely. Pours P20 and P22 showed lack of fill due to short casts, while Pour 23 experienced misrun. Samples cast in the zircon mold (P16) showed few surface voids and good internal soundness, which were improvements over similar Trial "A" castings. Reasons for this improved soundness are not presently known.

All castings poured into Howmet Monograf molds showed a considerable number of surface cold shuts (Figure 45). This was associated with the low mold pre-heat temperatures compared to the ceramic molds. In addition, the two Howmet molds that filled completely (P17 and P19) also displayed heavy concentrations of centerline voids and shrinkage. As a result, no test bars of Ti-13Cu-1.5Al alloys from the Howmet molds were suitable for testing in the as-cast condition.

Pours into experimental molds, Y_2O_3/K_2SiO_3 (Figure 46) and Y_2O_3-TiO_2-SiO_2, (P21), showed excellent fill and surface integrity. However, P18 and P21 castings showed positive surface indications due to metal filling the previously discussed mold facecoat voids (Paragraph 3.6.4.1). Improved mold facecoat slurries would be expected to correct this condition. The P18 casting also showed excellent internal soundness.

The exducer casting (P23) made in a zircon mold showed misrun (lack of fill in the blade sections) but continued to demonstrate a capability for low-melting alloys to fill thin sections. Higher metal temperature or mold insulation, as were used in Trial "A" for casting the cooling fan would promote complete fill.

Thermocouple protection tubes performed satisfactorily although not as well as those used in Trial "A". In Trial "B",



Figure 45. Appearance of Ti-13Cu-1•5Al Alloy Cast into the Howmet Monograf Mold (P-19). Note Good Fill but Surface Cold Shuts (Arrows).

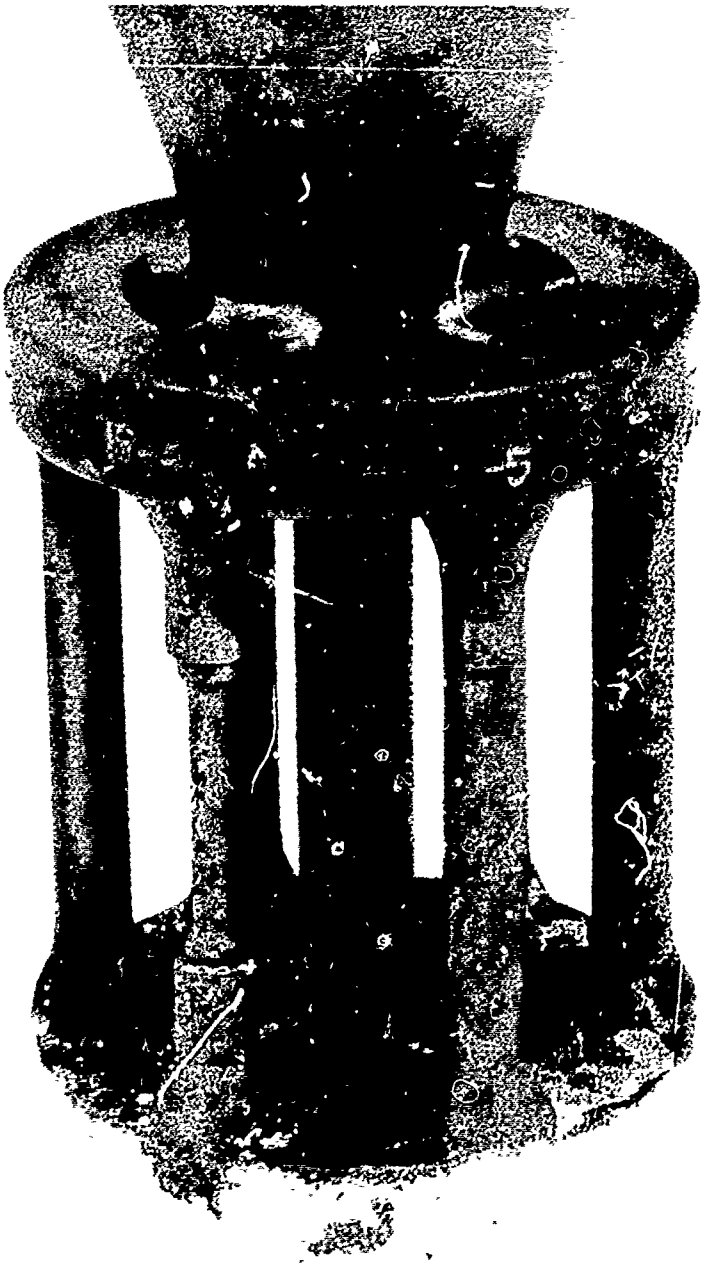


Figure 46. Appearance of Ti-13Cu-4.5Ni Alloy Cast into Experimental Y_2O_3-Potassium Silicate Mold (P-18). Noce Lack of Voids or Defects on Surface.

failure was by cracking of the substrate protection tubes where as in Trial "A" the primary failure was by spalling of the yttria coating.

3.6.4.4 Heat Treatment of Cast Tensile Samples

The preferred heat treatment for the Ti-13Cu-1.5Al alloy was established from tensile results obtained for ingot material, as below:

- o Solution at 1760°F for 1 hour and air cool
- o Age at 1450°F for 16 hours and air cool

This heat treatment was similar to that previously used for the Ti-13Cu and Ti-13Cu-4.5Ni alloys in Trial "A" and again used for these two alloys in Trial "B", namely:

- o Solution at 1760°F for 1 hour and air cool
- o Age at 1450°F for 8 hours and air cool

As mentioned earlier, all of the Ti-13Cu-1.5Al cast test bars from the Howmet molds had severe internal shrinkage rendering them unsuitable for testing. In order to remedy this situation, these bars as well as unacceptable cast bars of the Ti-13Cu-4.5Ni alloy (P17) were hot isostatically pressed (HIP). A HIP cycle of 1675°F (4 hours) 14.7 ksi was used. The HIP operation successfully closed the internal defects with the exception of one specimen where the internal defects were connected to the surface. The sound bars were subsequently tested in the as-HIP or HIP plus heat treat conditions using the above heat treatment cycles.

3.6.4.5 Tensile Test Evaluations

In order to adequately characterize the mechanical properties of the low-melting titanium alloys, as-cast and HIP test

bars from the Trial "B" castings were tensile tested at room temperature and 600°F. This included samples of the Ti-13Cu-1.5Al, Ti-13Cu-4.5Ni and Ti-13Cu alloys. The processing history and test results, including 20X examination of fracture surfaces are given for these bars in Appendix B, Table B-6. No test data is presented for the Ti-13Cu-1.5Al alloy (Table 27) in the as-cast condition due to a lack of acceptable castings; however, the available results indicated the following:

(a) Tensile properties of cast samples in the HIP plus heat treat condition meet the program goals with the exception of room temperature ductility, which was slightly low (4.7 versus 5.0 percent).

(b) The HIP operation did not degrade the heat treatment capability of this alloy with both strength and ductility of the cast plus HIP material improved by heat treatment.

(c) Cast plus HIP samples displayed higher strength and lower ductility at room temperatures compared to ingot material in both the as-melted and heat-treated conditions. This may be due to oxygen pick-up during the casting operation.

(d) At 600°F, the tensile properties of the cast plus HIP material were slightly superior to ingot samples in the heat treated condition.

A summary of room temperature tensile results for Ti-13Cu-4.5Ni alloy specimens from Casting Trial "B" are listed in Table 28 along with results from Casting Trial "A" for comparison. Various casting, specimen surface and heat treatment conditions are included and indicate the following:

TABLE 27

TENSILE PROPERTY SUMMARY FOR Ti-13Cu-1.5Al ALLOY

Condition*	Test Temperature (°F)	UTS (ksi)	YS (ksi)	Elongation (%)	RA (%)
As-Processed					
Ingot	75	110	90	3.0	5.2
Cast + HIP	75	111	100	2.3	5.2
Heat Treated (1760°/1450°F)					
Ingot	75	114	92	9	12.0
Cast + HIP	75	125	109	4.7	7.2
Program Goal	75	100	90	5	--
Ingot	600	90	62	19	35
Cast + HIP	600	95	66	19	32
Program Goal	600	60	50	5	--

*All bars tested with machined gage sections, all conditions at least duplicate tests.

TABLE 28

ROOM TEMPERATURE TENSILE PROPERTY SUMMARY
FOR CAST Ti-13Cu-4.5Ni ALLOY

Condition*	UTS (ksi)	YS (ksi)	Elongation (%)	RA (%)
As-Cast, Cast to Size Bars				
Trial A, Zircon Mold	89	71	2	4
Trial B, Howmet Mold				
-As Cast	83	71	0.3	2.8
-HIP	87	67	0.1	2.1
Trial B, Y_2C_3/K_2SiO_3 Mold	102	81	4.1	2.4
As-Cast, Machined Bars				
Trial A, Zircon Mold	102	75	7	7
Trial B, Howmet Mold				
-As Cast	97	70	1.4	2.4
-As HIP	92	68	4.5	4.0
Heat Treated, Machined Bars				
Trial A, Zircon Mold, 1760(1)/1450(8)	84	67	3	5
Trial B, Howmet Mold				
-As HIP	92	68	4.5	4.0
-HIP + 1760(1)/1450(8)AC	109	95	6.5	9.4
-HIP + 1760(1)/1450(8)FC	102	85	4.8	5.1
-HIP + 1760(1)/1560(1)AC	101	82	3.0	5.5
Program Goals	100	90	5.0	---

*All Trial B results are a single test, while Trial A results are an average of 2 or more tests. Temperatures given are in °F.

(a) Bars from the Y_2O_3/K_2SiO_3 mold tested in the as-cast condition with the cast surface intact displayed superior properties to similar specimens from Howmet and ACC-zircon molds.

(b) Ductility and ultimate strength of machined test bars were improved over those of comparable cast-to-size specimens indicating the impact of surface contamination on mechanical properties.

(c) As-HIP properties of cast-to-size and machined bars were not significantly improved over the properties of comparable as-cast specimens.

(d) Heat treatment (1760°F/1 hr + 1450°F/8 hr) of HIP castings was effective in increasing both strength and ductility to a level which exceeded the program goals

(e) Heat treatment response of the HIP material appears adequately sensitive to aging temperature and cooling rates.

A variety of defects were observed in fracture surfaces of most of the non-HIP bars from Trial "B". Porosity, microshrinkage and inclusions were similar to the Trial "A" castings. Microporosity was not evident in the samples, which had been HIPped. The fracture surfaces also exhibited varying amounts and degrees of cleavage but most of the trends observed for Trial "A" material were not apparent. However, cleavage fracture was not present in the Ti-13Cu-1.5Al alloy when tested at 600°F, where a corresponding increase in tensile ductility was observed.

3.6.4.6 Chemical Analysis Evaluation

Chemical analysis of bulk samples from castings generally reflected the influence of the melting process whereas surface

analyses correlated with mold systems. For the Ti-13Cu-4.5Ni alloy, bulk analyses (Appendix A, Table A4) for the Trial "B" ca castings were similar to Trial "A" castings reflecting consistency between melting procedures in the two trials; as below:

Ti-13Cu-4.5Ni	Oxygen (%)	Yttrium (%)
Trial "A"	0.21	0.28
Trial "B"	0.21	0.30

When the bulk oxygen and yttrium analyses of samples from both casting trials were grouped together, the impact of alloy melting point (P) and therefore metal pour temperature (P + 200°F) on contamination was apparent. The following results illustrate the lower contamination levels exhibited by the lower melting Ti-13Cu-4.5Ni alloy:

	Oxygen (%)	Yttrium (%)
Ti-13Cu and Ti-13Cu-1.5Al alloys (MP = 2620°F)	0.32	0.49
Ti-13Cu-4.5Ni alloy (MP = 2425°F)	0.21	0.29

This relation appeared to be reasonably consistent whereas a melting time versus contamination correlation was not observed for the time investigated. Therefore, maximum temperature during melting was vastly more important than time in controlling contamination of the melts. Analysis of surface layers (0.010 in. thick) from various castings of both trials indicated the Howmet molds promoted the lowest oxygen contamination (0.34 percent). With the same Ti-13Cu-4.5Ni alloy, the experimental Y_2O_3/K_2SiO_3 and ACC zircon molds produced oxygen contamination of 0.48 and 0.57 percent, respectively. The oxygen level obtained with the experimental mold system was very encouraging, especially since molds were preheated to 1900°F compared to 600°F for the Howmet mold.

Bulk chemistries also indicated alternating alloys during the casting process produced cross-contamination of castings in the range of 0.1 to 0.3 percent of Al or Ni. This behavior might be significant in effect on mechanical properties and therefore should be avoided in practice.

Nitrogen contamination was quite low for the melting process (0.019 percent) compared to an ingot level near 0.01 percent. Oxygen and yttrium therefore were the primary contaminants occurring during melting with the yttria primarily due to crucible degradation.

3.6.4.7 Microstructural Evaluations

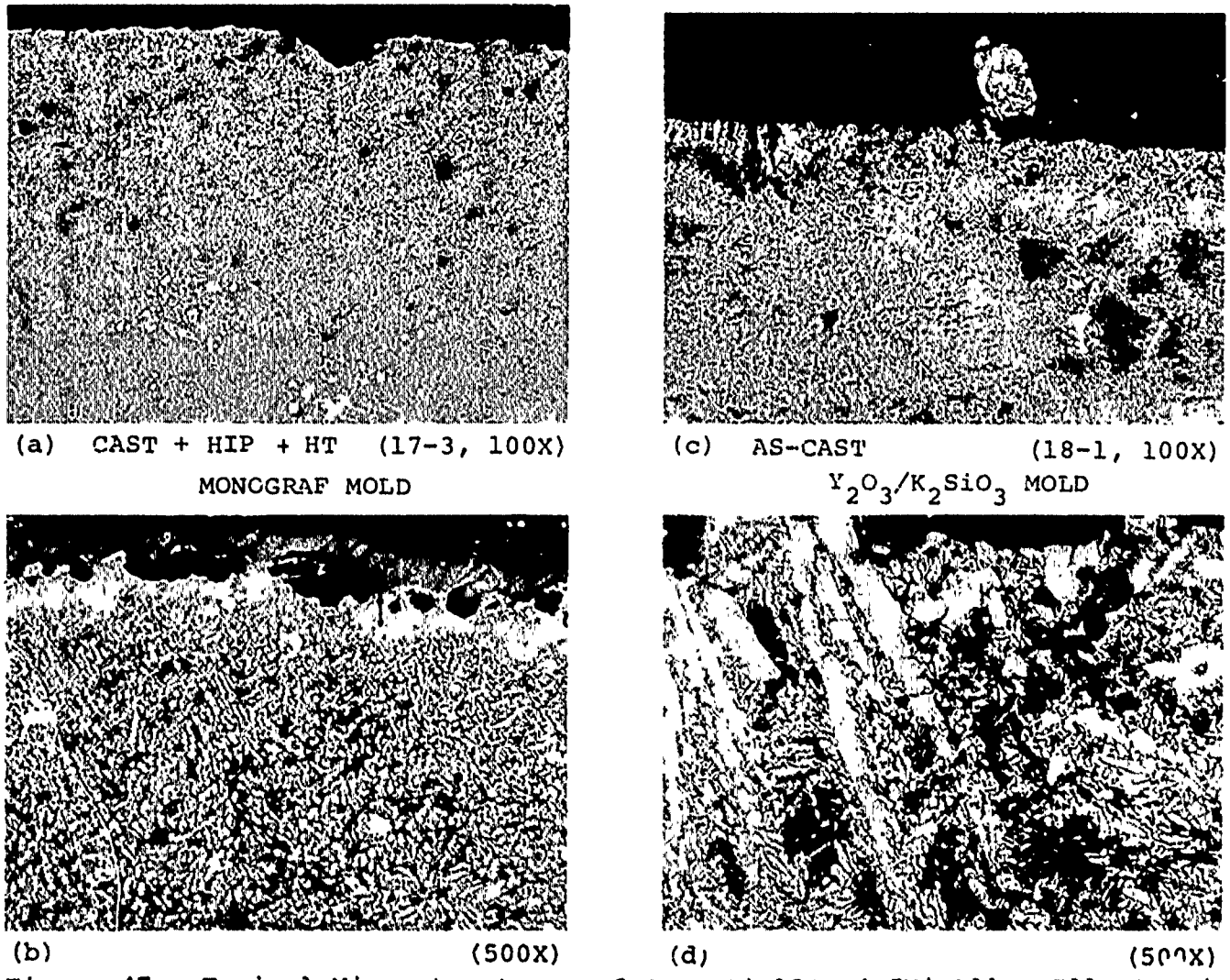
Microstructural evaluation of materials from Casting Trial "B" was separated into three groups for discussion:

- Surface structures
- Effect of HIP and heat treatment
- Structure of melting crucibles

3.6.4.7.1 Surface Structures

Structural differences were present to some degree in all castings. These structures were attributed to contamination effects, except for the apparent diffusion (Figure 47b) zone of metal cast in the Howmet-Monograf molds associated with a rapid cooling rate due to a low mold preheat temperature (600°F).

Examination of Ti-13Cu-4.5Ni alloy castings showed very low surface contamination from the Monograf mold and very encouraging levels from the experimental Y_2O_3/K_2SiO_3 mold (Figure 47). Alpha case from the Monograf mold was near 0.2 mils and was not



(a) CAST + HIP + HT (17-3, 100X)

MONOGRAF MOLD

(c) AS-CAST (18-1, 100X)

Y_2O_3/K_2SiO_3 MOLD

(b) (500X)

(d) (500X)

Figure 47. Typical Microstructures of Cast Ti-13Cu-4.5Ni Alloy Illustrating Surface Structures Resulting from Two Mold Systems. Note Alpha Case in (b) at Arrow and Diffusion Area in (c) at Arrow.

detected on cast metal from the Y_2O_3/K_2SiO_3 mold although intermittent contamination zones were observed to a depth of 2-5 mils.

Comparisons of cast surfaces for the Ti-13Cu and Ti-13Cu-1.5Al alloys (similar melting points and pour temperatures) allowed an assessment of the influence of other mold materials (Figure 48). When comparing alpha-case, the Monograf mold again promoted quite low surface contamination (0.2 mils) while the experimental Y_2O_3-TiO_2-SiO_2 mold developed a depth (1 mil) intermediate to the depth resulting from the zircon mold (2 mils). Both of the yttria bearing facecoat molds promoted less microstructural surface contamination of the cast metal than did the zircon mold. These molds appeared to have equivalent diffusion zone depths but the stabilized alpha zone from the Y_2O_3-TiO_2-SiO_2 facecoat (Figure 48) appeared to be more continuous suggesting greater facecoat reaction and higher contamination levels.

Surface contamination, as would be expected, did not appear to be limited to oxygen from microstructural features. Chemical analysis verified the presence of other contaminants Y, Si, Zr, and C depending upon the mold system. However, the primary contaminant was normally oxygen, which promoted the alpha stabilized structures for metal cast in ceramic molds; either alpha-case or coarse acicular alpha.

Microhardness measurements made on cast samples showed differences that were associated with the mold system (Figure 49). These results also indicated Monograph was the best mold system, followed closely by the experimental Y_2O_3/K_2SiO_3 mold. The reason for the low hardness very near the surface of alloy cast into the Monograf mold was not apparent. Both the zircon and Y_2O_3-TiO_2-SiO_2 molds produced much higher levels of surface hardness (contamination) than the above two systems. The hardness for cast samples from the zircon mold decreased rapidly while cast metal from the Y_2O_3-TiO_2-SiO_2 mold remained at relatively

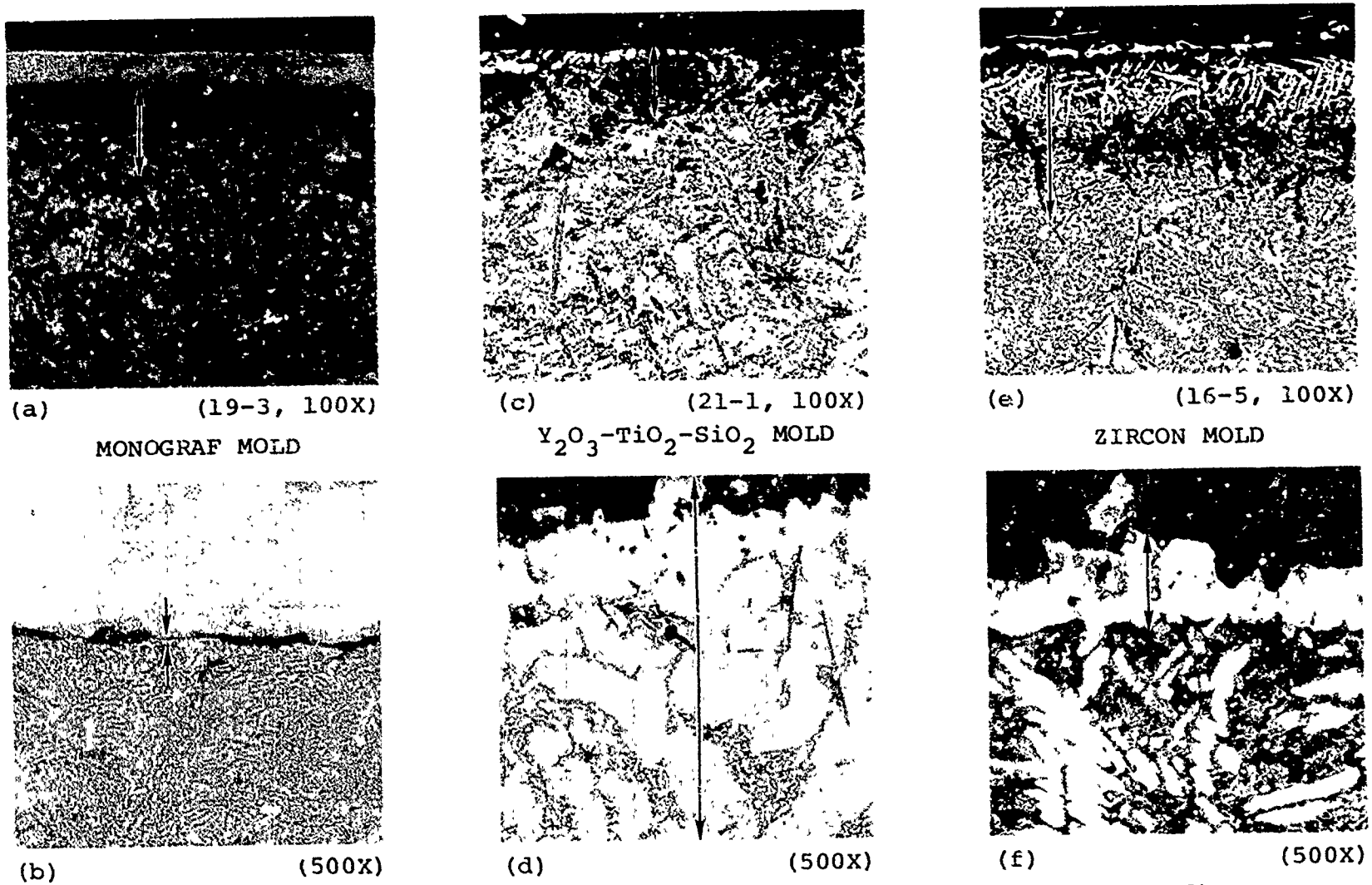


Figure 48. Typical Microstructures of Cast Ti-13Cu-1.5Al (a through d) and Ti-13Cu (e, f) Alloys. Illustrates Surface Structures Resulting From Contact With Three Mold Systems. Diffusion Zones and Alpha Case are Shown at Arrows

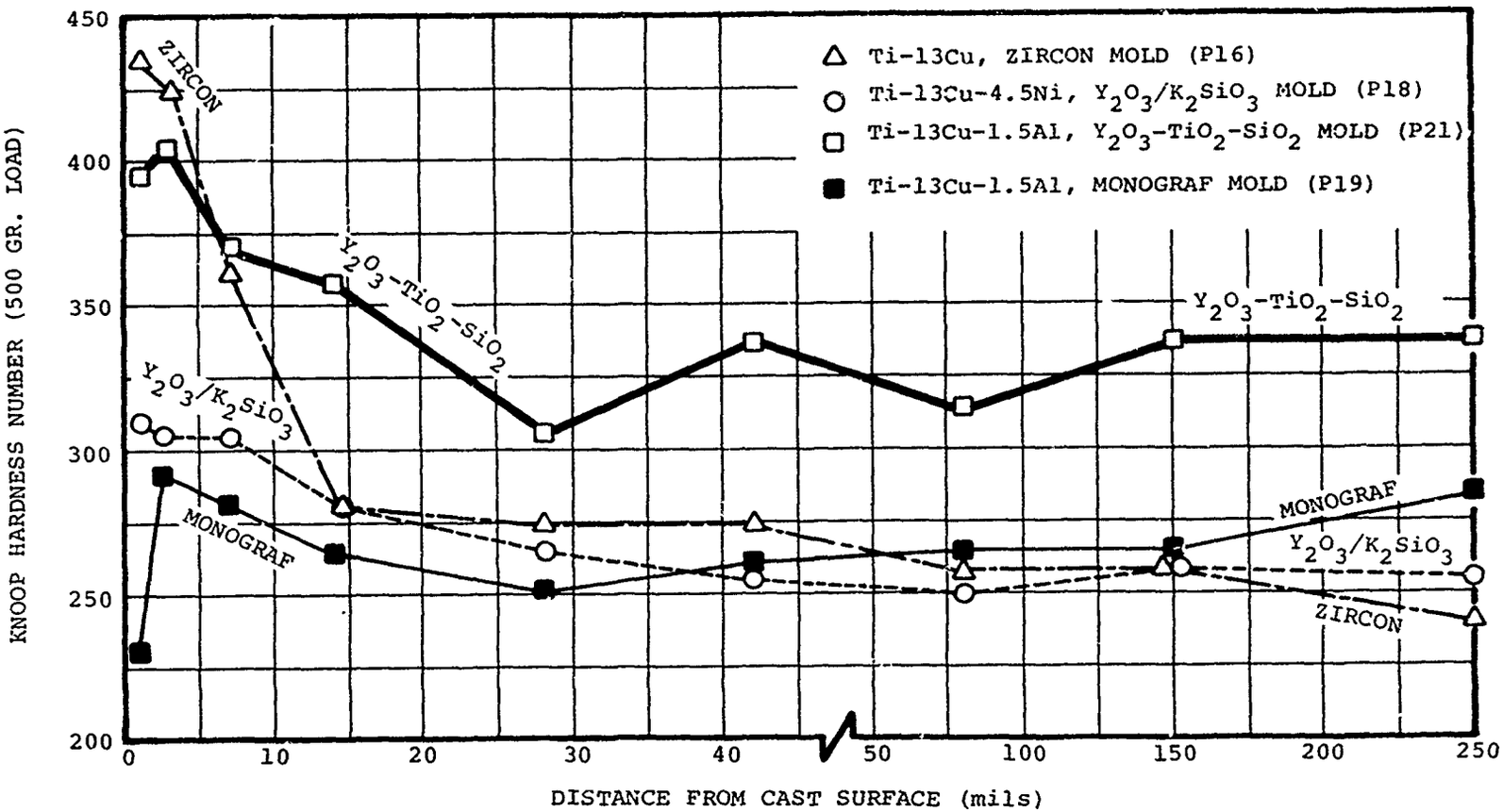


Figure 49. Plot of Alloy As-Cast Microhardness as a Function of Distance From the Cast Surface for Alloys Cast into Several Mold Systems.

high hardness levels indicating significant contamination through its entire cross section or higher strength levels due to the faster cooling rate. Thus, from cast alloy microstructure, hardness, and surface oxygen analysis the mold systems were rated on the basis of reactivity as follows:

Monograf Y_2O_3/K_2SiO_3	Best and nearly equivalent
Zircon Y_2O_3-TiO_2-SiO_2	Poorest and comparable, promoting about 2 to 3 times the surface contamination of the above.

The Y_2O_3/K_2SiO_3 mold system was considered the most promising material of the above due to the fact that a 1900°F preheat had been used compared to 600°F for the Monograf mold. This high pre-heat capability will ensure the production of high quality castings.

3.6.4.7.2 Effect of HIP and Heat Treatment

Hot isostatic pressing the Ti-13Cu-1.5Al and Ti-13Cu-4.5Ni cast bars altered the cast microstructures. Typical microstructures of these alloys in the as-cast, HIP, and HIP plus heat treated conditions are shown in Figures 50 and 51. Similar microstructural response was noted for both alloys which correlated with the observed tensile properties (Tables 27 and 28). The as-cast structures were coarsened to some extent by the HIP cycle (1675°F -4 hours), but a subsequent solution and age heat treatment refined the structure. In the HIP plus heat treat condition, the tensile strengths were improved over the as-HIP properties with both strength and ductility being improved for the Ti-13Cu-1.5Al alloy.

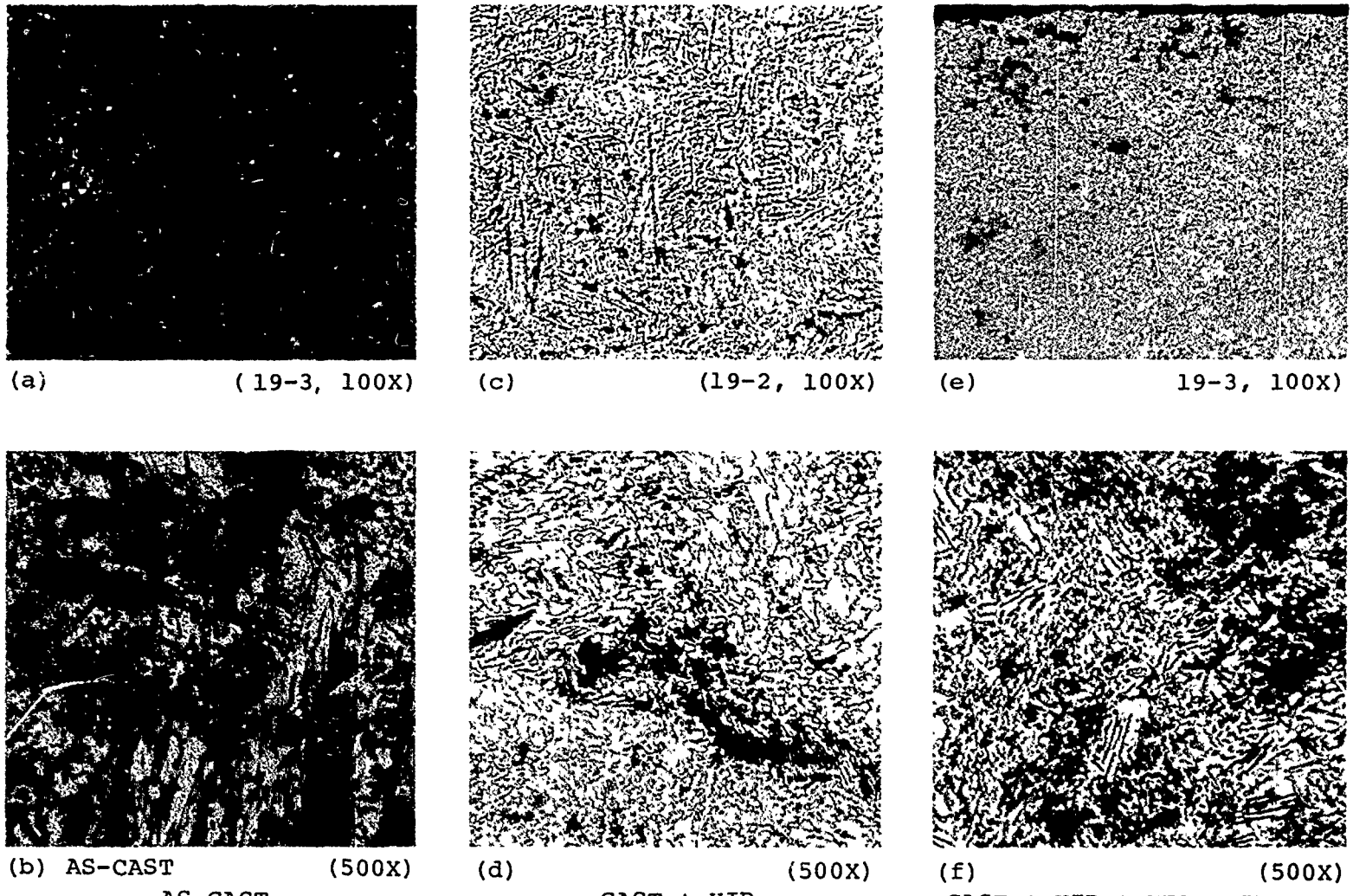
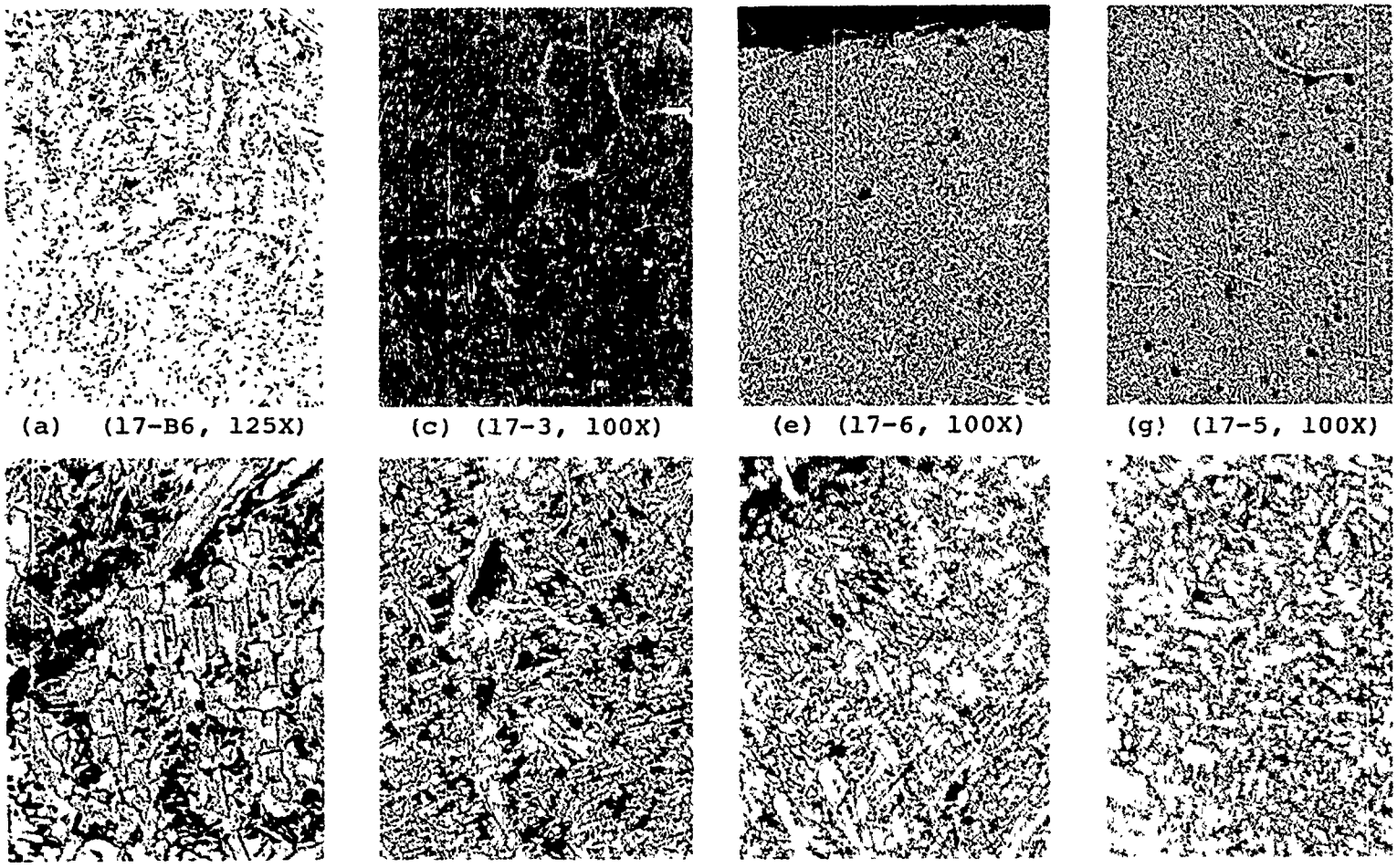


Figure 50. Typical Microstructures for Cast Ti-13Cu-1.5Al in the As-Cast, Hip, and Heat Treated Conditions. Note the Refinement of Structure After Heat Treatment (e, f) at 1760°F-1 Hr-AC Plus 1450°F-16 Hr-AC.



(a) (17-B6, 125X) (c) (17-3, 100X) (e) (17-6, 100X) (g) (17-5, 100X)

(b) (500X) AS-CAST (d) (500X) CAST + HIP + 1760/1450(AC) (f) (500X) CAST + HIP + 1760/1450(FC) (h) (500X) CAST + HIP + 1760/1560 (AC)

Figure 51. Typical Microstructures for Cast Ti-13Cu-4.5 Ni in the As-Cast, Hip and Heat Treated Conditions. Note the Effective Refinement of Cast Structure by the Heat Treatments.

3.6.4.7.3 Melting Crucibles

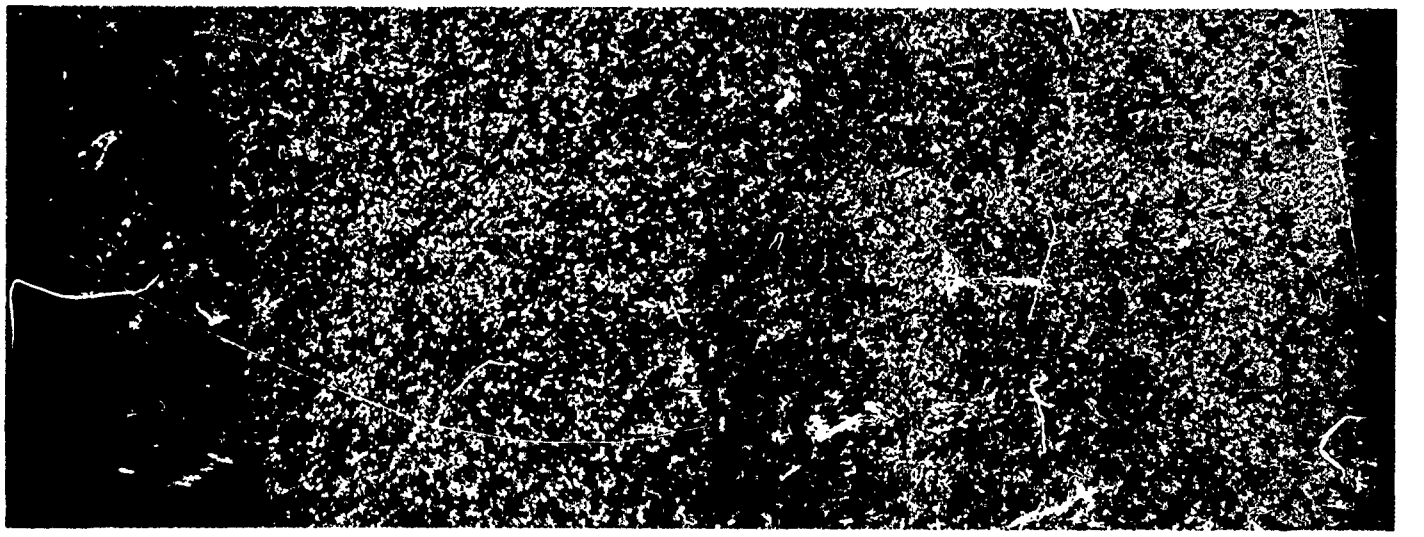
The Y_2O_3·15Ti crucible (number 7) used in Casting Trial "B" and an as-fired crucible (number 5) were metallographically evaluated. Crucible number 5 had been fabricated in an identical fashion to number 7 as well as the two crucibles used during Casting Trial "A" (numbers 3 and 4).

As fabricated microstructures of crucible number 5 indicate a depletion of titanium on the inside surface (Figure 52). This depleted condition promoted microcracking in this area, which during melting operations would be expected to cause accelerated crucible degradation. The reason for this titanium depletion was not established but fogging in the firing furnace, mentioned earlier, may be evidence of this titanium loss. However, the depleted condition at the inside surface may be a possible benefit since it would result in a yttria zone which would possibly be less reactive with molten titanium. However, microstructural examination of the melting crucible (number 7) after use in Trial "B" showed a titanium re-enrichment of the depleted inside surface (Figure 53) indicating the depleted surface was not maintained throughout the melting operation.

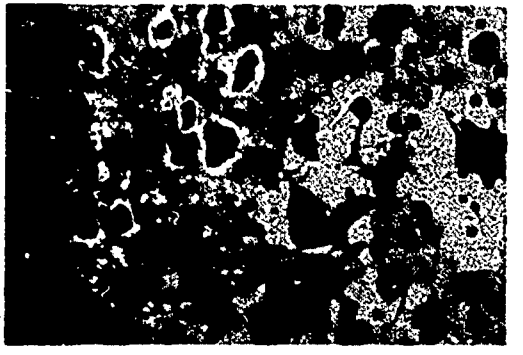
3.6.5 Summary - Casting Trial "B"

Program tensile property goals were achieved with cast Ti-13Cu-1.5Al alloy in the HIP plus heat treated condition. Metallurgical evaluation of the three alloys cast in Trial "B" (Ti-13Cu-1.5Al, Ti-13Cu and Ti-13Cu-4.5Ni) also showed:

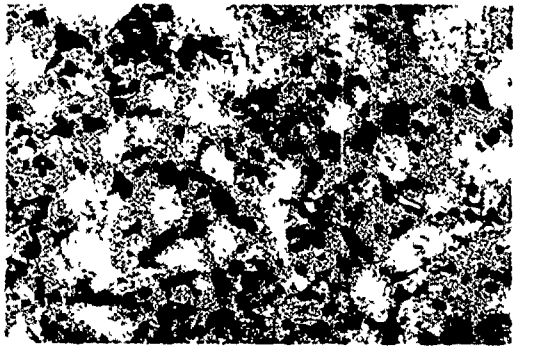
- Of the three alloys cast, Ti-13Cu-1.5Al was found to be the most attractive for achieving the program tensile goals. However, if a lower melting point alloy (<2600°F) is required, higher copper-containing titanium alloys would be a viable extension, with major effort devoted to heat treatment as a means of obtaining maximum ductility.



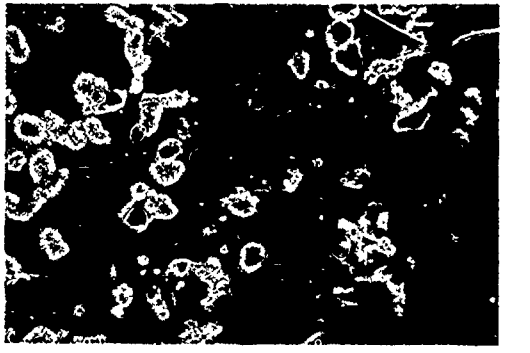
INSIDE SURFACE (a) SIDE WALL NEAR BOTTOM (OPPOSITE SITE PORT) (5-16, 50X) OUTSIDE SURFACE



(b) INSIDE SURFACE (500X)

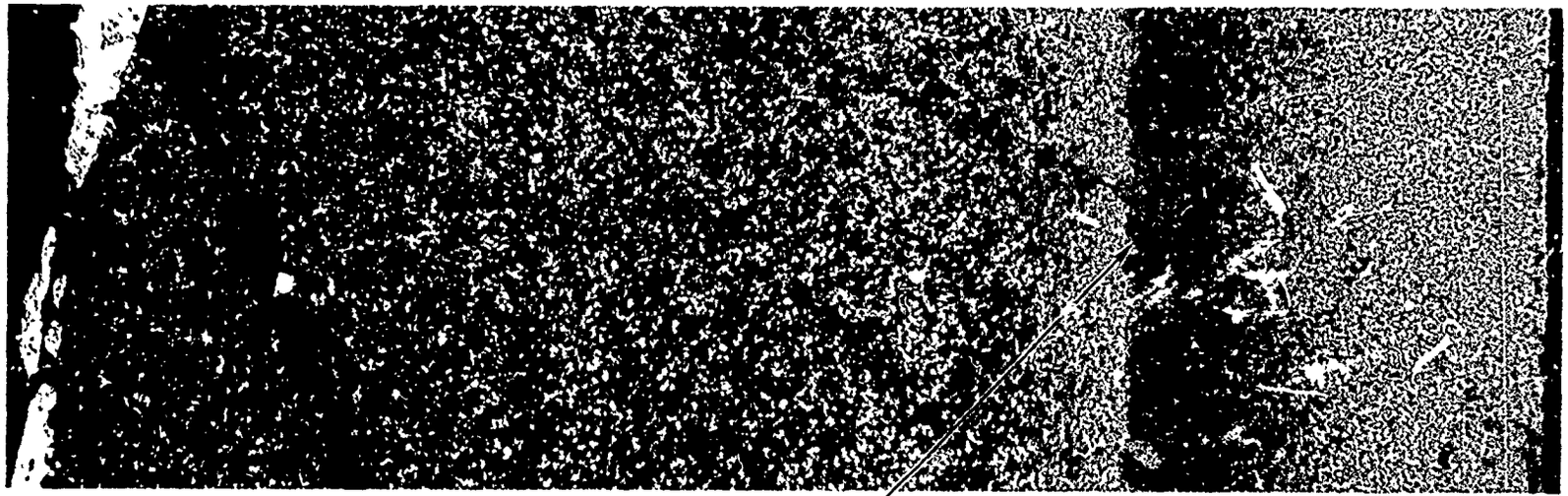


(c) CENTER (500X)

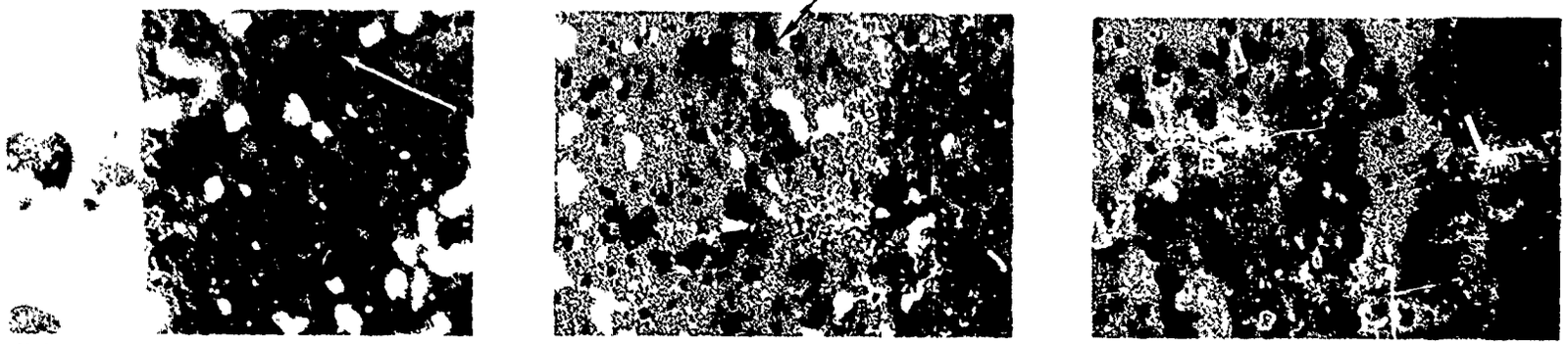


(d) OUTSIDE SURFACE (500X)

Figure 52. Typical Microstructures of As-Fabricated Y_2O_3•15Ti Melting Crucible Fired at 3000°F. Note Titanium Depletion at Inside Wall (b) and Associated Cracking.



INSIDE SURFACE (a) SECTION THROUGH SIDE WALL (50X) OUTSIDE SURFACE



(b) INSIDE SURFACE (500X) (c) CENTER (500X) (d) OUTSIDE SURFACE (500X)

Figure 53. Typical Microstructures of Y_2O_3·15Ti Crucible (Fired at 3000°F) Used in Casting Trial "B". Note Titanium Re-Enrichment of Inside Surface Compared to Figure 52. Also Observe Second Phase Formation in the Yttria in (b) at the White Arrow.

- o Program room temperature tensile goals were nearly met with Ti-13Cu alloy in both as-cast and the cast plus duplex heat treated conditions while the cast (or cast plus HIP) plus duplex heat treated Ti-13Cu-4.5Ni also met the room temperature goals. These results are in marked contrast to Trial "A" tensile results, which did not meet program goals.

- o Both oxygen and yttrium contamination were found to be lower in castings of the lower melting point Ti-13Cu-4.5Ni alloy (2425°F) compared to the higher melting Ti-13Cu (2630°F) and Ti-13Cu-1.5Al (2605°F) castings.

- o Consistent and reproducible tensile properties were obtained between ingot and cast material confirming expected behavior from previously-discussed alloying and heat treatment concepts.

Metal, induction melted in the Y_2O_3•15Ti crucible, again demonstrated acceptably low oxygen levels (0.2 - 0.4 percent), which did not severely degrade cast alloy ductility. Yttria second phase particles continue to be observed in castings made with these crucibles. Castings made with the experimental Y_2O_3/K_2SiO_3 facecoat mold and the Howmet Monograf molds showed acceptably low surface contamination.

3.7 Summary - Phase II

Titanium casting trials were conducted at the AiResearch Casting Company (ACC) using conventional superalloy vacuum investment casting techniques. Two casting trials were conducted using the above conventional foundry procedures to produce castings from three low melting titanium alloys, Ti-13Cu (MP = 2630°F), Ti-13Cu-1.5Al (MP = 2605°F), and Ti-13Cu-4.5Ni (MP = 2425°F). These alloys were selected on the basis of tensile

properties, heat treatment response and melting temperature. Alloys having a range of melting temperatures were selected to permit an assessment of the influence of melting point on the casting process.

During the first trial, Ti-13Cu and Ti-13Cu-4.5Ni alloys were cast into standard zircon molds to produce bars for tensile testing, metallurgical evaluation, and chemical analysis. This more reactive zircon facecoat mold system was used due to slurry stability and firing problems encountered with an experimental mold system. Tensile results for machined bars indicated room temperature and 600°F properties generally equal to ingot properties, but below program strength goals. Bars tested with the cast surface intact showed decreased ductility but the 2-3 percent elongation levels were considered promising considering the reactive mold system which was used (zircon facecoat).

For the second casting trial, a Ti-13Cu-1.5Al alloy was selected in order to obtain the required room temperature and 600°F tensile strength levels. The addition of aluminum had been shown during Phase I to provide significant strengthening improvements without serious degradation in ductility for heat treated material. The Ti-13Cu-1.5Al alloy, as well as the previous two alloys (Ti-13Cu and Ti-13Cu-4.5Ni), were all cast during the second trial using a variety of mold systems including the Howmet Corporation Monograf, experimental Y_2O_3/K_2SiO_3 and Y_2O_3-TiO_2-SiO_2 systems, and the ACC zircon. Varying levels of internal defects were encountered with castings, therefore requiring the use of hot isostatic pressing prior to testing. Poor soundness resulted from the low mold preheat temperature (600°F) used with the Monograf mold system. The Ti-13Cu-1.5Al alloy, cast into a Howmet Monograf mold, matched ingot properties and met program tensile goals at room temperature and 600°F in the HIP plus heat treated condition with the exception of room temperature tensile ductility that was slightly low (4.7 vs 5.0 percent elongation).

The Ti-13Cu-4.5Ni alloy also met the program room temperature tensile goals which was particularly encouraging due to its low melting point (2425°F).

Induction melting of these alloys during the second trial promoted oxygen levels from 0.2 to 0.4 percent and yttrium levels from 0.2 to 0.55 percent in castings. These contamination levels were equivalent to those obtained in the first casting trial and did not severely degrade tensile ductility, indicating the three low melting point titanium alloys had good tolerance to contamination and the presence of the Y_2O_3 inclusions. Castings were made into several mold systems and indicated the Howmet Monograf and the experimental Y_2O_3/K_2SiO_3 types were the best containment materials of those evaluated. Both promoted low contamination of surface metal, thereby producing ductile castings. The Y_2O_3/K_2SiO_3 type formulation for mold facecoats indicated good promise for further development because of its low contamination quality and its capability for high mold preheat temperature.

The above results established feasibility for the casting of titanium alloys (low melting point) using conventional superalloy vacuum investment techniques. Selected castings displayed good surface and internal soundness, tensile properties which met the program goals, and a tolerance for contamination. Areas which require additional investigation are: (1) determination of mold facecoat compositions which will sinter to a hard condition at conventional foundry capabilities (near 2000°F), (2) defining the effect of Y_2O_3 inclusions on mechanical properties (fatigue, notch tensile, etc.) of cast metal, and (3) reduction of the melting crucible reactivity and tendency to crack during casting activities.

4.0 CONCLUSIONS AND RECOMMENDATIONS

4.1 Conclusions

The concept of producing titanium castings using low-melting alloys, vacuum induction melting in a ceramic crucible and low-reactivity investment molds was successfully demonstrated. Development work conducted in achieving this objective established the following:

- Reducing the melting temperature and required process temperature significantly decreases the reactivity of titanium alloys.

- A series of low-melting alloys based on the titanium-copper system exhibited an attractive combination of melting temperature (<2600°F), castability, heat treatment response and mechanical properties.

- Yttria and yttria-base ceramic materials exhibit the least reactivity with molten titanium alloys.

- Titanium modification of the yttria ceramic materials was effective in improving the thermal shock resistance to allow its use as a melting crucible.

- The yttria/potassium-silicate mold facecoat system produced minimal mold/metal reaction with titanium.

- Castings of the Ti-13Cu-1.5Al alloy using the above technologies demonstrated a good tolerance for oxygen contamination and Y_2O_3 inclusions and nearly met all the program tensile property goals.

4.2 Recommendations

Demonstration of the above concept (induction melting and casting of low-melting titanium alloys) provides a firm foundation from which a final manufacturing process can be developed. The following areas are recommended for investigation to fully establish a low-cost process for investment casting of titanium alloys:

- Develop mold facecoat fabrication techniques, for low reactivity ceramic materials. The Y_2O_3/K_2SiO_3 system provides an excellent base for this work. This is of primary importance to the process and to the low cost approach.

- Additional evaluation of moderately reactive mold systems should also be conducted in conjunction with chemical milling of the casting surfaces to establish the most cost-effective process.

- Optimize the melting crucible composition, configuration and structure to improve its performance during melting operations.

- Optimize the current low melting titanium alloy system (Ti-Cu) and heat treatment to provide better alloy castability and improved properties.

- Conduct additional casting evaluations to fully demonstrate size and configuration flexibilities of the process.

- Fatigue and structure sensitive mechanical properties should be evaluated to define the effect of Y_2O_3 type inclusions as well as completely characterizing the cast low-melting alloy.

APPENDIX A

CHEMICAL ANALYSIS RESULTS

Description	Table No.
Chemical Composition of Phase I Ingots	A-1
Chemical Composition of Phase II Ingots Used for Casting Trials	A-2
Compilation of Chemical Analysis Results for Casting Trial "A"	A-3
Compilation of Chemical Analysis Results for Casting Trail "B"	A-4

TABLE A-1

CHEMICAL COMPOSITION OF PHASE I INGOTS

Heat No.	Nominal Composition	Weight, percent				O %	H ppm
		C	N	Fe	Others		
TASK I							
24033	Ti-11Co	0.02	0.014	0.04	10.8Co	0.148	146
34029	Ti-13Cu	0.01	0.011	0.02	13.1Cu, 0.090_2	0.078	38
24034	Ti-11Ni	0.01	0.013	<0.01	10.1Ni	0.160	122
24031	Ti-4Si	0.01	0.014	0.05	3.7Si	0.107	109
24032	Ti-8Cu-6.5Ni	0.02	0.012	0.01	7.8Cu, 6.6Ni	0.069	93
24036	Ti-14Mn-0.03Y	0.01	0.012	0.04	12.5Mn	0.106	79
24037	Ti-20Cr-0.03Y	0.01	0.017	0.14	19.9Cr	0.080	40
24035	Ti-9Fe-0.03Y	0.01	0.013	8.7	0.02Y	0.086	115
24106	Ti-1Be	0.01	0.011	0.04	1.2Be	0.108	64
24105	Ti-1Be-2Si	0.01	0.010	0.05	1.2Be, 2Si	0.102	69
24108	Ti-2.7Be-2.5V-0.3Al	0.02	0.015	0.05	2.6V, 0.38Al, 3.0Be	0.104	73
24107	Ti-2.7Be-5Zr	0.01	0.012	0.03	5.0Zr, 3.0Be	0.090	94
24038	Ti-2.7Be	0.01	0.013	0.01	2.7Be	0.079	105
TASK II							
24217	Ti-16Cu	0.01	0.007	0.01	16.3Cu	0.083	
24218	Ti-13Cu-2.5Fe	0.02	0.008	2.4	13.6Cu	0.081	
24219	Ti-10Cu-2.5Fe	0.01	0.007	2.4	10.3Cu	0.077	
24220	Ti-10Cu	0.01	0.008	0.03	10.3Cu	0.082	79
24221	Ti-13Cu-1Co	0.02	0.012	0.04	13.6Cu, 0.9Co	0.093	87
24222	Ti-7Fe-0.03Y	0.02	0.010	6.5		0.084	81
24223	Ti-7Fe-5Mn-0.03Y	0.01	0.009	6.4	4.7Mn	0.096	91
24224	Ti-13Cu-4.5Ni	0.02	0.008	0.07	13.7Cu, 4.5Ni 13.1Cu	0.094	99
34267	Ti-13Cu-1Be	0.01	0.016	0.01	13.1Cu	0.086	
24268	Ti-7Fe-1Be-0.03Y	0.02	0.020	6.7		0.112	
24269	Ti-2.7Be-5V	0.01	0.016	0.04	5V	0.139	
24264	Ti-13Cu-3Al	0.01	0.014	0.03	12.8Cu, 3.2Al	0.093	
TASK III							
24273	Ti-13Cu-0.20 O_2	0.01	0.014	0.01	13.0Cu	0.185 0.187 0.22	
24275	Ti-13Cu-2Al	0.01	0.010	0.04	13.3Cu, 2.1Al	0.077	
24276	Ti-13Cu-4Sn	0.01	0.010	0.01	13.5Cu, 4.2Sn	0.070	
24277	Ti-10Cu-2.5Fe-2Al	0.01	0.010	2.5	10.4Cu, 2.5Fe	0.074	
24278	Ti-16Cu-1.5Al	0.01	0.011	0.01	16.4Cu, 1.5Al	0.077	
24279	Ti-19Cu	0.02	0.015	0.01	18.7Cu	0.063	
24280	Ti-19Cu-1Al	0.01	0.010	0.01	18.3Cu, 1.0Al	0.074	
24281	Ti-13Cu-0.25Y_2O_3	0.01	0.010	0.01	13Cu, 0.09Y	0.125 0.160	

TABLE A-2

CHEMICAL COMPOSITIONS OF PHASE II INGOTS USED FOR CASTING TRIALS

Heat No.	Nominal Composition	C	N	Fe	Cu	Al	Ni	O
25056	Ti-13Cu	0.01	0.01	0.02	13.3	--	--	0.052
25057	Ti-13Cu-4.5Ni	0.01	0.01	0.01	13.3	--	4.6	0.052
25254	Ti-13Cu-1.5Al	0.02	0.009	0.01	13.7	1.4	--	0.06

TABLE A-3

COMPILIATION OF CHEMICAL ANALYSIS RESULTS FOR CASTING TRIAL "A"

Pour Number	Sample Numbers	Chemical Analysis (Wt-%)								
		O_2	Y	Zr	Al	Si	Na	C	Cu	Ni
Typical Analyses										
1	196, 212	0.26	0.44	0.006		0.005			12.71	
2	194, 204	0.28	0.49	0.006	0.005	0.008	0.001			
3										
4	236, 235, 234	0.20	0.44					0.006		
5	189, 190	0.21	0.28	0.017	0.007	0.010	0.003			3.93
6	192, 193	0.19	0.26			0.008				
7	223, 222	0.14	0.19							
8	207, 213	0.68	0.37	0.045		0.025			12.99	
9	225, 224	0.31	0.55							
10	197, 198	0.29	0.50		0.004	0.008				
11	214, 231 200, 208, 209	0.55 0.36 0.30	0.54	0.023		0.031			12.65	
12										
13	199, 201	0.18	0.27		0.006	0.011				
14	202, 203	0.28	0.37	0.020	0.006	0.013			13.07	4.01
15	227, 226	0.25	0.28							
Special Analyses										
5-4 Skin removed	191			0.005		0.008				
11-1, low X-ray gas	230, 208, 209	0.41 0.30								
14-1, high X-ray gas	210, 211	0.35 0.35								
2-3 surface shavings	215	0.68								
5-4 surface shavings	216	0.52								
10-3 surface shavings	217	0.74								
13-3 surface shavings	221	0.62								
5-4 bulk, w/o above surface	218	0.22								
10-3 bulk, w/o above surface	220	0.24								
13-3 bulk, w/o above surface	219	0.16								
4 surface layer	236							0.029		

*Oxygen by Neutron Activation, others by Spectrochemical

TABLE A-4

COMPILATION OF CHEMICAL ANALYSIS RESULTS FOR CASTING TRIAL "B"

Alloy	Mold	Pour	Sample Location	Chemical Analysis (Weight-Percent)											
				O_2	Y	Zr	Al	Si	Na	C	Cu	Ni	K	N_2	Fe
Ti-13Cu	Zircon	16	Bulk	0.37	0.51	--	--	--	--	0.035	--	--	--	0.024	--
			Surface (0.010")	0.92	--	0.28	--	0.25	--	--	--	--	--	--	--
Ti-13Cu-4.5Ni	Monograf	17	Bulk	0.19	0.29	--	--	--	--	--	--	--	--	--	--
			Surface (0.010")	0.33	--	--	--	--	--	0.035	--	--	--	--	--
Ti-13Cu-4.5Ni	Y_2O_3-Silicate	18	Bulk	0.22	0.33	--	--	--	--	--	--	--	--	--	--
			Surface (0.010")	0.48	0.53	--	--	0.062	--	--	--	--	<.001	--	--
Ti-13Cu-1.5Al	Monograf	19	Bulk	0.32	0.46	--	0.70	--	--	0.018	12.67	0.31	--	0.014	--
			Surface (0.08"-.04")	0.35	--	--	--	--	--	0.040	--	--	--	--	--
Ti-13Cu-1.5Al	Monograf	20	Bulk	0.34	--	--	--	--	--	--	--	--	--	--	--
Ti-13Cu-1.5Al	Y_2O_3-TiO_2-SiO_2	21	Bulk	0.30	0.49	--	--	--	--	--	--	--	--	--	--
			Surface (0.030")	1.13	0.92	--	--	0.015	--	--	--	--	--	--	--
Ti-13Cu-1.5Al	Monograf	22	Bulk	0.39	-	--	--	--	--	--	--	--	--	--	--
Ti-13Cu-4.5Ni	Zircon	23	Bulk	0.22	0.29	--	0.15	--	--	--	--	--	--	--	--
Ti-13Cu	Ingot	--	Bulk	0.052	0.052	--	--	--	--	0.01	13.3	--	--	0.01	0.02
Ti-13Cu-4.5Ni	Ingot	--	Bulk	0.052	--	--	--	--	--	0.01	13.3	4.6	--	0.01	0.01
Ti-13Cu-1.5Al	Ingot	--	Bulk	0.06	--	--	1.4	--	--	0.02	13.7	--	--	0.009	0.01

APPENDIX B

COMPILATION OF TENSILE PROPERTIES

Description	Table No.
Summary of Room Temperature Tensile Properties and Hardness for All Phase I Alloys	B-1
Alloy Ti-13Cu: Compilation of Tensile Properties for Phase II, Task II Test Bar Castings	B-2
Alloy Ti-13Cu-4.5Ni: Compilation of Tensile Properties for Phase II, Task II Test Bar Castings	B-3
Tensile Properties (Room Temperature) for Bars Machined From Test Bar Casting Center Sprues	B-4
Additional Tensile Properties for Phase II, Task II Castings	B-5
Tensile Tests for Casting Trail "B"	B-6

TABLE B-1

SUMMARY OF ROOM TEMPERATURE TENSILE PROPERTIES AND HARDNESS FOR ALL PHASE I ALLOYS

Heat treatments listed in the table are identified by the following:

(a) Heat treatments listed as furnace cool (FC) have been cooled at a rate of 100°F/hr. to 900°F and then air cooled, unless otherwise stated.

(b) AC refers to air cooled

(c) WQ refers to water quenched

INDEX TO ALLOYS

Composition (M.P.)*	Page	Composition (M.P.)	Page
Ti-8Cu-6.5Ni (2515)*	207	Ti-19Cu (2415)*	214
Ti-10Cu (2725)*	207	Ti-19Cu-1Al (2410)	214
Ti-10Cu-2.5Fe (2625)	207 & 208	Ti-7Fe-0.03Y (2740)	214 & 215
Ti-10Cu-2.5Fe-2Al (2595)	208	Ti-7Fe-1Be-0.03Y (2570)	215
Ti-13Cu (2615)*	208 & 209	Ti-7Fe-5Mn-0.03Y (2680)	215
Ti-13Cu-2.5Fe (2570)*	209 & 210	Ti-9Fe-0.03Y (2695)	215
Ti-13Cu-1Co (2595)*	210	Ti-14Mn-0.03Y (2695)*	215 & 216
Ti-13Cu-4.5Ni (2425)*	210	Ti-20Cr-0.03Y (2820)	216
Ti-13Cu-1Be (2505)	211	Ti-1Be (2805)*	216
Ti-13Cu-2Al (2605)	211	Ti-1Be-2Si (2660)*	216
Ti-13Cu-3Al (2595)*	211 & 212	Ti-2.7 Be-2.5V-0.3Al (2570)	217
Ti-13Cu-0.2 O (2635)	212	Ti-2.7Be-5V (2570)	217
Ti-13Cu-0.25 Y_2O_3 (2635)	212	Ti-2.7Be-5Zr (2570)	217
Ti-13Cu-4Sn (2590)	212	Ti-4Si (2695)	218
Ti-16Cu (2515)*	213	Ti-11Co (2500)	218
Ti-16Cu-1.5Al (2500)	213 & 214	Ti-11Ni (2695)	218
		Ti-2.7Be (2570)*	

*Alloy melting points (°F) having * were experimentally determined in the program.

TABLE B-1 - Continued

Heat Number	Composition	Heat Treatment	Rockwell A Hardness	Room Temperature Tensile Properties				
				UTS ksi	YS ksi	EL %	RA %	
24032	Ti-8Cu-6.5Ni	Arc Melted Ingot	62.1	114	91	2.0	2.0	Broke outside Gauge Marks
				114	84	6.0	6.2	
		1360F-1 hr-FC	58.2					
		1450F-1 hr-FC	58.0	95	64	5.5	7.9	
				98	66	5.0	4.0	Broke at G.M.
		1700F-8 hrs-FC	65.2					
		1725-1 hr-FC	59.1	97	71	4.0	4.8	
				97	71	4.0	5.9	
		1725F-1 hr-FC+ 1360F-24 hrs-AC	58.8					
		1760F-1 hr-AC+ 1300F-8 hrs-AC		120	87	4.0	3.0	
				125	86	6.0	5.0	
		1760F-1 hr-AC+ 1400F-8 hrs-AC		120	83	8.0	9.0	
				112	79	6.0	7.0	
24220	Ti-10Cu	Arc Melted Ingot	60.9	136	102	7.0	9.7	
				133	100	5.0	9.4	
		1400F-1 hr-FC	54.0					
		1560F-1 hr-FC	53.7	81	61	22.0	27.3	
				82	61	24.0	27.3	
		1760F-1 hr-FC	61.3	107	75	10.0	10.2	
				107	80	10.0	8.2	
		1760F-1 hr-AC	68.0					
		1760F-1 hr-AC+ 1150F-8 hrs-AC	69.1					
		1760F-1 hr-AC+ 1300F-8 hrs-AC	65.2					
		1760F-1 hr-AC+ 1450F-8 hrs-AC	65.0					
24219	Ti-10Cu-2.5Fe	Arc Melted Ingot	63.1	148	128	2.5	2.8	
				156	132	4.5	4.8	
		1400F-1 hr-FC	57.2					
		1560F-1 hr-FC	60.5	106	77	14.0	11.7	
				105	71	11.5	12.0	
		1760F-1 hr-FC	64.9	112	80	6.5	5.2	
				112	78	7.5	6.6	
		1760F-1 hr-AC	74.8					

TABLE B-1 - Continued (Page 3 of 13)

Heat Number	Composition	Heat Treatment	Rockwell A Hardness	Room Temperature Tensile Properties UTS ksi	YS ksi	EL %	RA %	
24219 (Contd)	Ti-10Cu-2.5Fe	1760F-1 hr-AC+ 1300F-8 hrs-AC	70.1					
		1760-1 hr-AC+ 1400F-8 hrs-AC		132	99	5.0	6.3	
		1760F-1 hr-AC+ 1400F-16 hrs-AC		130	102	5.0	6.0	
		1760F-1 hr-AC+ 1450F-8 hrs-AC	70.0					
		1760F-1 hr-AC+ 1500F-8 hrs-AC		136	106	3.5	2.8	
		1760F-1 hr-AC+ 1560F-8 hrs-AC		151	124	5.0	3.2	
24277	Ti-10Cu-2.5Fe-2Al	Arc Melted Ingot	70.4	175 170	168 160	2.0 2.0	4.0 4.0	
		1400F-1 hr-FC	65.1	136 137	114 114	5.0 5.0	5.5 7.0	
		1560F-1 hr-FC	64.4	132 131	106 106	7.0 7.0	4.1 7.1	
		1650F-1 hr-AC+ 1450F-24 hrs-AC	69.5					
		1760F-1 hr-AC+ 1150F-8 hr-AC	73.3					
		1760F-1 hr-AC+ 1300F-8 hr-AC	70.6					
		1760F-1 hr-AC+ 1450F-8 hrs-AC	63.6					
		1760F-1 hr-AC+ 1450F-24 hrs-AC	68.6					
		1760F-1 hr-AC+ 1450F-96 hrs-AC	71.8					
34029	Ti-13Cu	Arc Melted Ingot	58.3	104 105	82 82	10.5 10.0	9.7 11.6	Broke 1/8" inside G.M.
		1300F-8 hrs-AC	59.1					
		1560F-1 hr-FC	53.0	85 83	62 59	13.0 14.0	16.0 20.0	
		1560F-1 hr-FC@ 600F/hr to 900F-AC		88	68	12.0	17.0	

TABLE B-1 - Continued

Heat Number	Composition	Heat Treatment	Rockwell A Hardness	Room Temperature Tensile Properties			
				UTS ksi	YS ksi	EL %	RA %
34029 (Contd)	Ti-13Cu	1760F-1 hr-FC	59.3	74 74	58 59	5.0 5.0	6.0 5.0
		1760F-1 hr-FC@ 200F/hr to 900F-AC	54.3				
		1760F-1 hr-FC@ 575F/hr to 900F-AC	61.3				
		1760F-1 hr-FC@ 600F/hr to 900F-AC		96	74	10.0	12.0
		1760F-1 hr-AC	69.9				
		1760F-1 hr-AC+ 1150F-8 hrs-AC	62.7				
		1760F-1 hr-AC+ 1200F-8 hrs-AC	63.1				
		1760-1 hr-AC+ 1250F-2 hrs-AC	64.6				
		1760F-1 hr-AC+ 1250F-4 hrs-AC	66.8	126 123	91 90	7.0 6.0	9.4 9.4
		1760F-1 hr-AC+ 1250F-8 hr-AC	65.6	118 114	88 88	6.0 6.0	8.6 9.3
		1760F-1 hr-AC+ 1300F-4 hrs-AC	65.9				
		1760F-1 hr-AC+ 1300F-8 hrs-AC	64.1	118	88	10.0	12.0
		1760F-1 hr-AC+ 1350F-8 hrs-AC	62.7				
		1760F-1 hr-AC+ 1400F-8 hrs-AC	63.3				
		1760F-1 hr-AC+ 1450F-8 hrs-AC	61.3	106	82	10.0	11.0
		1760F-1 hr-FC+ 1560F-4 hrs-AC	66.0				
		1760F-1 hr-FC+ 1560F-24 hrs-AC	63.6				
		1760F-1 hr-AC+ 1560F-8 hrs-AC	60.7				
	Ti-13Cu-2.5Fe	Arc Melted Ingot	63.7	122 126	98 97	4.0 4.0	2.0 3.2
		1400F-1 hr-FC	56.6				
		1560F-1 hr-FC	59.1	100 97	75 73	5.5 5.0	3.6 2.8

TABLE B-1 - Continued

Heat Number	Composition	Heat Treatment	Rockwell A Hardness	Room Temperature Tensile Properties UTS ksi	YS ksi	EL %	RA %
34029 (Contd)	Ti-13Cu-2.5Fe	1760F-1 hr-FC	63.4	77 85	70 72	5.0 1.0	- - } Broke outside G.M.
		1760F-1 hr-AC	72.6				
		1760F-1 hr-AC+ 1300F-8 hrs-AC	70.4	134 127	115 120	4.0 3.0	4.0 3.0
		1760F-1 hr-AC+ 1400F-8hrs-AC		123 130	102 102	3.0 4.0	5.0 6.0
		1760F-1 hr-AC+ 1450F-8hrs-AC	68.6				
24221	Ti-13Cu-1Co	Arc melted ingot	59.8	106 110	86 88	5.0 8.0	10.0 9.0
		1400F-1 hr-FC	55.4				
		1560F-1 hr-FC	56.8	91 89	62 62	10.5 10.0	7.1 8.2
		1760-1 hr-FC	60.5	81 75	63 63	6.5 4.5	3.6 3.2
		1760F-1 hr-AC	70.5				
		1760F-1 hr-AC+ 1300F-8 hrs-AC	68.2	121 117	99 97	6.0 5.0	7.0 6.0
		1760F-1 hr-AC+ 1400F-8 hrs-AC		110 114	92 87	8.0 9.0	6.0 10.0
		1760F-1 hr-AC+ 1450F-8 hrs-AC	65.5				
24224	Ti-13Cu-4.5Ni	Arc melted ingot	57.3	92 103	78 76	- 6.0	- } Broke outside 4.3 G.M.
		1400F-1 hr-FC	55.8				
		1560F-1 hr-FC	56.3	89 87	63 65	5.0 5.0	2.4 } Broke 1/8" 2.8 } inside G.M.
		1760F-1 hr-FC	58.9	75 78	59 62	3.0 3.0	1.2 1.2
		1760F-1 hr-AC	70.5				
		1760F-1 hr-AC+ 1300F-8 hrs-AC	67.9	118	118	-	- Broke outside G.M.
		1760F-1 hr-AC+ 1400F-8 hrs-AC		108	82	5.0	6.0
		1760F-1 hr-AC+ 1450F-8 hrs-AC	63.5				
		1760F-1 hr-AC+ 1475F-8 hr-AC		98	74	4.0	4.0
		1760F-1 hr-AC+ 1560F-8 hrs-AC		102	77	4.0	3.0
		1760F-1 hr-AC+ 1375F-8 hr-AC		119	104	4.0	6.0

TABLE B-1 - Continued

Heat Number	Composition	Heat Treatment	Rockwell A Hardness	Room Temperature Tensile Properties			
				UTS ksi	YS ksi	EL %	RA %
24267	Ti-13Cu-1Be	Arc melted ingot	61.7	72 77	- -	- -	- } Broke outside - } G.M.
		1400F-1 hr-AC	59.0				
		1560F-1 hr-AC	53.2	65 59	46 45	2.0 2.0	- -
		1760F-1 hr-FC	54.5	60 52	53 50	1.0 1.0	- -
		1760F-1 hr-AC	69.5				
24275	Ti-13Cu-2Al	Arc melted ingot	64.8	143 [illegible]	138 140	1.0 1.0	- } Broke outside - } G.M
		1560F-1 hr-FC	58.9	104 106	92 92	12.0 12.0	13.8 13.9
		1760F-1 hr-AC+ 1150F-8 hr-AC	69.4				
		1760F-1 hr-AC+ 1300F-8 hr-AC	64.6				
		1760F-1 hr-AC+ 1450F-8 hrs-AC	62.1	127 126	104 105	6.5 6.5	7.5 7.0
24264	Ti-13Cu-3Al	Arc melted ingot	64.7	147 143	- -	- -	- -
		1400F-1 hr-FC	63.6				
		1450F-8 hrs-AC	64.9				
		1560F-1 hr-FC	62.3	122 118	104 106	10.0 5.5	10.8 6.5 Broke outside G.M.
		1560F-2 hrs-FC	63.9				
		1560F-4 hr-FC	63.4				
		1560F-8 hr-FC	61.6				
		1560F-8 hrs-AC	67.4				
		1560F-24 hr-AC	64.1				
		1650F-8 hrs-AC	71.0				
		1760F-1 hr-FC	66.5	140 137	121 119	2.5 2.5	3.6 2.0
		1760F-1 hr-AC	72.1				
		1760F-1 hr-AC+ 1300F-8 hr-AC		156 156	135 137	2.0 2.0	< 2.0 < 2.0
		1760F-1 hr-AC+ 1400F-8 hrs-AC		145	127	6.0	6.0
		1760F-1 hr-AC+ 1475F-8 hrs-AC		138	122	6.0	7.0
		1760F-1 hr-AC+ 1500F-8 hrs-AC		137	124	6.0	8.0

TABLE B-1 - Continued

Heat Number	Composition	Heat Treatment	Rockwell A Hardness	Room Temperature Tensile Properties				
				UTS ksi	YS ksi	EL %	RA %	
24264 (Contd)	Ti-13Cu-3Al	1760F-1 hr-AC+ 1500F-16 hrs-AC	63.1					
		1760F-1 hr-AC+ 1500F-24 hrs-AC	65.8					
		1760F-1 hr-AC+ 1560F-8 hrs-AC		146	128	7.0	7.0	
		1760F-1 hr-AC+ 1560F-16 hrs-AC	66.7					
24273	Ti-13Cu-0.2 O	Arc melted ingot	63.6	132 120	109 102	3.0 3.0	2.0 2.0	
		1560F-1 hr-FC	59.6	95 95	72 72	5.0 4.0	5.6 3.5	
		1760F-1 hr-AC+ 1300F-8 hrs-AC	65.9	134 136	108 108	3.5 4.0	2.0 4.8	
		1760F-1 hr-AC+ 1450F-4 hrs-AC	64.8					
		1760F-1 hr-AC+ 1450F-8 hrs-AC	64.7	122 125	102 100	5.0 5.0	4.8 5.9	
24281	Ti-13Cu-0.2% Y_2O_3	Arc melted ingot	57.8	104 102	76 76	9.0 7.0	10.8 9.1	
		1560F-1 hr-FC	54.5	87 86	56 54	10.0 12.0	15.7 16.8	
		1760F-1 hr-AC+ 1150F-8 hrs-AC	63.9					
		1760F-1 hr-AC+ 1300F-8 hrs-AC	66.0					
		1760F-1 hr-AC+ 1450F-8 hrs-AC	60.2	106 104	77 75	8.0 8.0	3.0 Broke outside 8.7 G.M.	
24276	Ti-13Cu-4Sn	Arc melted ingot	62.7	118 116	100 99	8.0 8.0	8.6 10.9	
		1560F-1 hr-FC	58.7	95 94	78 77	8.0 9.0	9.8 10.5	
		1760F-1 hr-AC+ 1150F-8 hrs-AC	69.5					
		1760F-1 hr-AC+ 1300F-8 hrs-AC	66.6					
		1760F-1 hr-AC+ 1450F-8 hrs-AC	64.6					
		1760F-1 hr-AC+ 1450F-16 hrs-AC	61.8					

TABLE B-1 - Continued

Heat Number	Composition	Heat Treatment	Rockwell A Hardness	Room Temperature Tensile Properties			
				UTS ksi	YS ksi	EL %	RA %
24217	Ti-16Cu	Arc melted ingot		97 97	75 76	9.0 9.0	10.0 12.0
		1300F-8 hrs-AC	59.0				
		1400F-1 hr-FC	49.3				
		1400F-8 hrs-AC	58.9				
		1400F-16 hrs-AC		100 100	81 78	5.0 5.0	6.7 5.9
		1500F-1 hr-AC+ 1300F-8 hrs-AC	55.1				
		1560F-1 hr-FC		82 84	56 58	9.0 10.0	8.9 9.0
		1560F-1 hr-AC+ 1300F-8 hrs-AC	56.9				
		1760F-1 hr-AC	68.9				
		1760F-1 hr-AC+ 1100F-8 hrs-AC	63.0				
		1760F-1 hr-AC+ 1200F-4 hrs-AC	62.8	119 120	97 99	3.5 4.0	4.0 6.3
		1760F-1 hr-AC+ 1200F-8 hrs-AC	62.5				
		1760F-1 hr-AC+ 1200F-16 hrs-AC	64.2				
		1760F-1 hr-AC+ 1300F-4 hrs-AC	67.6				
		1760F-1 hr-AC+ 1300F-8 hrs-AC	64.4	110 112	91 92	4.0 5.0	6.0 8.0
		1760F-1 hr-AC+ 1300F-16 hrs-AC	60.7				
		1760F-1 hr-AC+ 1400F-4 hrs-AC	62.8				
		1760F-1 hr-AC+ 1400F-8 hrs-AC	62.9	112 108	91 92	6.0 6.0	6.0 8.0
		1760F-1 hr-AC+ 1400F-16 hrs-AC	63.5	106 109	92 94	4.0 5.0	4.5 5.9
		1760F-1 hr-FC	57.4	70 74	56 56	4.0 5.0	2.0 2.0
24278	Ti-16Cu-1.5Al	Arc melted ingot	63.3	113 114	97 97	4.0 4.0	5.3 5.2
		1560F-1 hr-FC	58.8	94 94	79 78	4.5 6.0	5.6 4.1
		1760F-1 hr-AC+ 1150F-8 hrs-AC	70.1				
		1760F-1 hr-AC+ 1300F-8 hrs-AC	67.7				

TABLE B-1 - Continued

Heat Number	Composition	Heat Treatment	Rockwell A Hardness	Room Temperature Tensile Properties			
				UTS ksi	YS ksi	EL %	RA %
24278 (Contd)	Ti-16Cu-1.5Al	1760F-1 hr-AC+ 1450F-8 hrs-AC	65.8				
		1760F-1 hr-AC+ 1450F-16 hrs-AC	63.4	122 120	[illegible] 113	4.5 3.0	5.2 4.8
24279	Ti-19Cu	Arc melted ingot	57.0	87 90	65 65	4.0 4.0	4.0 2.8
		1560F-1 hr-FC	53.0	69 68	53 52	1.0 4.0	- Broke outside G.M. 3.2
		1760F-1 hr-WQ	73.5				
		1760F-1 hr-WQ+ 1050F-8 hrs-WQ	73.5				
		1760F-1 hr-AC+ 1150F-8 hrs-AC	56.3				
		1760F-1 hr-AC+ 1300F-8 hrs-AC	55.4				
		1760F-1 hr-AC+ 1450F-8 hrs-AC	56.6				
		1760F-1 hr-WQ+ 1450F-8 hrs-AC	61.4	92 97	74 80	4.0 4.0	2.4 2.8
24280	Ti-19Cu-1Al	Arc melted ingot	59.8	98 95	80 73	3.0 3.0	2.4 2.4
		1560F-1 hr-FC	56.3	86 90	65 68	5.0 5.0	7.4 5.9
		1760F-1 hr-AC+ 1150F-8 hrs-AC	64.9				
		1760F-1 hr-AC+ 1300F-8 hrs-AC	63.5				
		1760F-1 hr-AC+ 1450F-8 hrs-AC	60.4	97 101	79 78	4.0 4.0	3.2 4.5
24282	Ti-7Fe-0.03Y	Arc melted ingot	65.2	142 137	120 116	3.0 3.0	3.3 3.6
		1425F-1 hr-FC	62.7	116 116	82 84	2.0 3.0	3.0 3.0
		1525F-1 hr-FC	63.7	123 118	102 86	5.0 8.0	5.8 6.3
		1525F-1 hr-WQ	71.9				
		1525F-1 hr-WQ+ 1025F-24 hrs-AC	64.7	125 123	- -	- -	- Broke in shank -
		1525F-1 hr-WQ+ 1025F-96 hrs-AC		121 118	121 -	1.0 1.0	- Broke outside G.M. -

TABLE B-1 - Continued

Heat Number	Composition	Heat Treatment	Rockwell A Hardness	Room Temperature Tensile Properties			
				UTS ksi	YS ksi	EL %	RA %
24268	Ti-7Fe-1Be-0.03Y	Arc melted ingot	64.6	120 103	119 -	1.0 -	- - Broke through yield
		1425F-1 hr-FC	61.5				
		1425F-1 hr-WQ	73.0				
		1525F-1 hr-FC	64.6	77 94	- 89	- 2.5	- Broke outside - G.M.
		1525F-1 hr-WQ+ 1025F-24 hr-AC	66.3	113 -	- -	1.0 -	- - Broke while machining
24223	Ti-7Fe-5Mn-0.03Y	Arc melted ingot	62.5	79 65	- -	- -	- Broke outside - G.M.
		1425F-2 hrs-FC	67.7				
		1525F-1 hr-WQ	67.7				
		1525F-1 hr-FC	69.2	27 43	- -	- -	- -
		1525F-1 hr-WQ+ 1025F-24 hr-AC	71.1	107 71	- -	- -	- Broke into 3 pcs. - Broke outside G.M.
24035	Ti-9Fe-0.03Y	Arc melted ingot	71.4	169 142	- -	- -	- -
		1025F-1 hr-FC	69.2				
		1025F-12 hrs-AC	68.9				
		1025F-24 hrs-AC	67.5				
		1025F-48 hrs-AC	67.3				
		1200F-1 hr-FC	67.8	126 115	118 -	1.0 -	- -
		1500F-1 hr-FC	65.7	134 140	112 112	1.5 2.0	4.0 1.6
		1500F-1 hr-WQ	71.1				
24036	Ti-14M -0.03Y	Arc melted ingot	66.6	142 140	138 134	1.5 2.0	2.0 2.8
		975F-1 hr-FC	68.7				
		975F-12 hrs-AC	70.1				
		975F-24 hrs-AC	69.8				
		975F-48 hrs-AC	69.9				
		975F-96 hrs-AC	69.3				
		1100F-1 hr-FC	68.4				
		1290F-1 hr-WQ	67.0	113 105	- -	- -	- -

TABLE B-1 - Continued

Heat Number	Composition	Heat Treatment	Rockwell A Hardness	Room Temperature Tensile Properties UTS ksi	YS ksi	EL %	RA %	
24036 (Contd)	Ti-14Mn-0.03Y	1290F-1 hr-FC	66.3	136 140	136 135	2.0 2.5	1.8 2.8	
		1670F-1 hr-WQ	70.0					
24037	Ti-20Cr-0.03Y	Arc melted ingot	64.4	125 123	121 118	6.0 4.5	19.0 14.7	
		1190F-1 hr-FC	65.0					
		1190F-12 hr-AC	65.1 64.4					
		1190F-24 hrs-AC	64.9					
		1190F-48 hrs-AC	62.4	72 78	- -	- -	- -	
		1670F-1 hr-WQ	66.2					
		1670F-1 hr-FC	61.6	89 94	- -	- -	- -	
24106	Ti-1Be	Arc melted ingot	57.7	87 84	72 68	3.0 3.0	1.6 2.0	
		1775F-1 hr-FC	51.0	66 64	48 49	8.0 6.0	7.0 4.8	
		1775F-1 hr-AC	61.8					
		1775F-1 hr-FC to 1400F-4 hrs-AC	53.4	62 67	52 53	3.0 6.0	2.0 4.4	
		1775F-1 hr-AC+ 1400F-4 hrs-FC	55.3					
24105	Ti-1Be-2Si	Arc melted ingot	62.9	97 96	92 92	1.0 1.0	- -	
		1775F-1 hr-FC	59.0	72 62	67 -	0 -	- Broke outside G.M. - Broke before yield	
		1775F-1 hr-AC	67.0					
		1775F-1 hr-FC to 1400F-4 hrs-AC	61.7	60 72	- 70	- -	- Broke during yield - Broke outside G.M.	
		1775F-1 hr-AC+ 1440F-4 hrs-AC	62.3					

TABLE B-1 - Continued

Heat Number	Composition	Heat Treatment	Rockwell A Hardness	Room Temperature Tensile Properties UTS ksi	YS ksi	EL %	RA %	
24108	Ti-2.7Be-2.5V-0.3Al	Arc melted ingot	61.2	92	87	1.0	-	Broke at shank
				96	82	1.0	-	
		1775F-1 hr-FC	54.3	85	74	2.5	0.8	
				83	75	2.5	0.4	
		1775F-4 hrs-FC		79	71	2.0	-	
				80	72	2.0	-	
		1775F-8 hrs-FC		67	-	1.0	-	Broke through yield
				73	68	1.0	-	
		1775F-1 hr-AC	63.3					
		1775F-1 hr-FC to 1400F-4 hrs-AC	62.8					
		1775F-1 hr-AC+ 1400F-4 hrs-FC	58.6	80	80	2.0	-	Broke at yield
				93	79	2.0	1.2	
24269	Ti-2.7Be-5V	Arc melted ingot	63.5	111	94	1.0	-	
				112	90	1.0	-	
		1775F-1/2 hr-FC	53.5	61	52	1.0	-	
				62	-	-	-	Broke outside G.M.
		1775F-1/2 hr-FC to 1400F-4 hrs-AC	61.3	74	50	1.0	-	
				75	46	1.0	-	
		1775F-1/2 hr-AC	64.7					
		1775F-1 hr-FC	54.2					
		1775F-1 hr-AC	64.3					
		1775F-1 hr-AC+ 1400F-8 hrs-AC	61.9					
		1775F-1 hr-WQ	78.4					
24107	Ti-2.7Be-52r	Arc melted ingot	60.4	92	80	0.5	-	Broke outside G.M.
				93	81	1.0	-	Broke at shank
		1775F-1 hr-FC	50.7	55	49	5.0	2.8	
				52	48	3.5	1.2	
		1775F-4hr-FC		51	42	4.5	4.8	
				48	41	3.5	3.6	
		1775F-8 hrs-FC		49	42	4.0	4.6	
				52	43	4.0	4.0	
		1775F-1 hr-AC	60.6					
		1775F-1 hr-FC to 1400F-4 hrs-AC	52.6	58	52	3.5	1.6	
				55	50	3.5	1.2	
		1775F-1 hr-AC+ 1400F-4 hrs-FC	55.8					

TABLE B-1 - Continued

Heat Number	Composition	Heat Treatment	Rockwell A Hardness	Room Temperature Tensile Properties			
				UTS ksi	YS ksi	EL %	RA %
24031	Ti-4Si	Arc melted ingot	60.5	95 95	87 87	2.0 2.0	2.0 2.0 Broke outside G.M.
		1500F-1 hr-FC	59.2	89 87	70 70	1.5 1.5	<1.0 1.6
		1825F-1 hr-FC	58.3	77 81	72 70	1.0 1.5	<1.0 <1.0
		2200F-1 hr-FC	71.9				
		2200F-1 hr-FC+ 1500F-24 hrs-AC	71.0				
24033	Ti-11Co	Arc melted ingot	73.0	120 130	- -	- -	- } Broke outside - G.M.
		1225F-1 hr-FC	64.2	121 141	96 89	2.0 1.5	- Broke outside G.M. 1.6
		1700F-1 hr-FC	65.1	119 124	95 64	1.0 1.0	- } Broke outside - } G.M.
		1700F-8 hrs-FC	67.1				
		1700F-1 hr-WQ	69.8				
		1700F-1 hr-FC+ 1225F-24 hrs-AC	64.1				
24034	Ti-11Ni	Arc melted ingot	64.7	69 77	- -	0.5 1.0	- } Broke outside - } G.M.
		1380F-1 hr-FC	59.2				
		1700F-1 hr-FC	55.1	58 54	53 51	1.0 1.0	1.2 <1.0
		1700F-1 hr-WQ	75.0	Broke apart on quenching			
		1700F-1 hr-FC+ 1380F-12 hrs-AC	56.8				
24038	Ti-2.7Be	Hot forged and rolled.	53				
		216[illegible]°F-4m.-FC	56				

TABLE B-2

ALLOY Ti-13Cu: COMPILATION OF TENSILE PROPERTIES FOR PHASE II, TASK II TEST BAR CASTINGS

Condition	Test Temp.	Type of Bar	Sample Number	Tensile Properties UTS (ksi)	YTS (ksi)	Elong (%)	R/A (%)	Fracture Surface Appearance**
As-Cast	RT	CSTB	2-1	90.3	79.5	2.6	3.2	Med. microshrink, med. small cleavage, one gas hole
			8-3	49.3	-	-	-	● Inclusion, high large-clev.
			10-1	83.4	74.1	1.8	5.4	Low microshrink, 1 gas void low sm.-clev.
			AVG. (2)	88.0	77.0	2.2	4.3	
		Machined Bar	10-3	92.1	77.8	4.5	7.8	High sm.-clev. 1 large void
			11-5	104.3	96.7	2.4	4.0	Low microshrink, high large-clev. gas voids
			AVG. (2)	98.0	87.0	3.4	5.9	
	315°C	M.B.	10-4	67.4	44.5	8.7	18.3	Med. porosity, 2 large voids
Heat-Treated*	RT	CSTB	1-1	81.1	74.9	1.3	7.1	1 large void, some small voids, low sm.-clev.
			1-2	78.0	76.2	2.1	4.8	
			2-2	92.0	80.2	6.0	5.6	Fracture origin at surface void, low med.-clev.
			8-2	48	-	-	-	● Gas voids, fractured at radius, low sm.-clev. low microshrink
			10-2	80.0	76.9	7.4	5.3	Med. microshrink, low med.-clev.
			AVG. (4)	82.8	78.0	2.7	5.7	
		M.B.	1-3	58.7	58.7	1.7	4.7	● Inclusion, some voids, low sm.-clev.
			2-3	93.4	72.9	10.0	13.5	Low microshrink, low sm.-clev., some voids
			10-6	90.8	69.8	10.6	19.0	Low microshrink, low med.-clev. some voids
			11-4	104.9	83.8	8.2	7.5	Some porosity on surface, med. varied-clev.
			AVG. (3)	96.4	75.5	9.6	13.3	
	315°C	M.B.	1-5	63.5	43.8	13.1	29.4	Med. microshrink, voids, failed at void area
			1-6	64.9	41.9	9.6	24.7	High microshrink, 1 inclusion, 1 void
			2-5	30.7	29.4	3.1	5.9	● Large void, high microshrink
			10-5	64.3	41.1	12.4	20.5	1 large inclusion, med. microshrink, failed at surface shrink area
			11-3	64.4	46.8	7.6	19.7	Low microshrink, inclusions, void, failed at surface void
			AVG. (4)	64.3	43.4	10.7	23.6	

*Heat-treated in capsule supposedly at 1760°F - 1 hr - AC plus 1450°F - 8 hrs - AC but may have been as high as 1820°F - 1 hr - AC plus 1510°F - 8 hrs - AC.

**Block dots(o) indicate that tensile properties for that specimen were not included in average, because of excessive defects in the fracture surface.

TABLE B-3

ALLOY Ti-13Cu-4.5Ni: COMPILATION OF TENSILE PROPERTIES FOR PHASE II, TASK II TEST BAR CASTINGS

Condition	Test Temp.	Type of Bar	Sample Number	Tensile Properties UTS (ksi)	YTS (ksi)	Elong. (%)	R/A (%)	Fracture Surface Appearance
As-Cast	RT	CSTB	5-1	91.3	70.1	3.3	4.7	Low microshrink, med. sm.-clev.
			6-1	88.9	71.8	2.4	3.2	Low microshrink, med. med.-clev.
			13-1	86.2	70.2	1.8	3.9	Low microshrink med. sm.-clev.
			AVG. (3)	89.0	71.0	2.5	3.9	
		Machined Bar	5-3	102.7	72.5	8.3	7.9	Low microshrink, high sm.-clev., 1 small void
			6-5	102.7	72.8	7.6	8.2	Low microshrink, high sm.-clev.
			13-5	99.6	73.2	6.3	7.5	Low microshrink, high large-clev.
			14-3	102.2	80.2	4.9	6.3	Low microshrink, very large-clev.
			AVG. (4)	102.0	75.0	6.8	7.5	
	315°C	M.B.	5-4	78.8	39.1	27.5	39.2	Low porosity, inclusions
			6-3	72.1	39.6	9.1	17.6	Some cleavage, 1 large gas void
			14-4	79.5	42.2	23.0	27.7	Some porosity
			AVG. (3)	77.0	40.0	19.9	28.2	
Heat Treated*	R.T.	CSTB	5-2	86.3	69.7	2.3	3.9	High large-clev.
			13-2	72.5	70.2	1.5	1.4	Low microshrink high large-clev., some gas
			AVG. (2)	79.4	70.0	1.9	2.7	
		M.B.	5-5	84.5	-	2.2	5.5	1 void, med. large-clev.
			6-6	83.9	65.4	3.6	4.3	High large-clev.
			13-6	83.9	62.5	3.5	7.1	Low microshrink, med. med-clev.
			14-5	83.4	73.0	2.2	1.8	Low microshrink, med. large-clev.
			AVG. (4)	83.9	67.3	2.9	4.7	
	315°C	CSTB	6-2	77.3	40.7	12.2	17.9	Low sm.-clev.
		M.B.	5-6	76.0	38.0	22.7	27.4	1 small void, low large-clev.
			6-4	75.2	34.5	18.4	24.1	Low med.-clev.
			13-4	77.6	39.1	13.8	27.4	2 very small voids (reason for low ductility not apparent
			14-6	77.8	40.7	26.8	33.4	Low microshrink, small inclusion, low large clev.
			AVG. (4)	76.6	38.1	20.4	28.1	

*Heat treated in capsule supposedly at 1760°F - 1 hr - AC plus 1450°F - 8 hr - AC but may have been as high as 1820°F - 1 hr - AC + 1510°F - 8 hr - AC.

TABLE B-4

TENSILE PROPERTIES (ROOM TEMPERATURE) FOR BARS MACHINED FROM TEST BAR CASTING CENTER SPRUES

Alloy/Sample*	R.T. Tensile Properties				Remarks
	UTS (ksi)	YS (ksi)	El (%)	R/A (%)	
Ti-13Cu					
Heat Treated (10-7-2)	88.3	81.9	2.3	5.9	Microshrinkage at failure origin, fracture surface discoloration, med. small-cleavage.
Ti-13Cu-4.5Ni					
As-Cast (6-7-2)	98	71	6.4	7.1	Low microshrinkage, high small-cleavage, no voids.
Heat-Treated (5-7-2)	98.2	74.6	2.6	7.5	Low microshrinkage, med. med-cleavage, no voids.
Heat-Treated (13-7-2)	91.4	81.9	4.2	7.1	Low microshrinkage, low med-cleavage, coarse structure

*Heat treatment in air at 1760°F/1-hr/AC plus 1450°F/8-hrs/AC.

TABLE B-5

ADDITIONAL TENSILE PROPERTIES FOR PHASE II, TASK II CASTINGS

Alloy	Material Description*	Sample Number	R.T. Tensile Properties** UTS (ksi)	YTS (ksi)	Elong. (%)	R/A (%)	Fracture Surface Appearance****
Ti-13Cu	Bars removed from Pour 9 (Slug Poured into ZrO_2):						
	o As-Cast	9-1	76.2	74.0	2.0	6.3	High microshrink, med. sm-clev.
	o Heat Treated (Air)	9-3	39.1	-	-	-	Gross microshrink
	Ingot Control Alloy included with Heat Treatments:**						
	o In Air	6B2-1	95.5	71.7	10.3	12.4	Light microshrinkage
	o In Capsule	6B2-2	81.7	58.5	12.8	18.8	Light microshrinkage plus med. porosity and med.-large cleavage
Ti-13Cu -4.5Ni	Bars removed from slugs solidified in Crucibles***						
	o As-Cast	7-1	84.7	60.5	3.9	6.3	Med. microshrink, med. med-clev.
		15-3	84.1	63.7	3.8	6.3	High large clev.
		15-2	62.5	54.6	2.2	2.4	● Gross microshrink
		AVG. (2)	84.4	62.1	3.8	6.3	
	o Heat Treated (Capsule)	7-3	49.3	-	-	1.6	● Gross microshrink
		15-1	95.7	79.3	3.5	6.3	Med. microshrink, high med. clev.
		15-B	99.6	78.6	4.6	7.1	Low microshrink, high med. clev.
		AVG. (2)	97.6	79.0	4.0	6.7	

* Air treatment was 1760°F - 1 hr - AC plus 1450°F - 8 hrs - AC; capsule heat treat was to be the same but may have been as high as 1820°F - 1 hr - AC plus 1510°F - 8 hrs - AC.

** Machined Bars

*** Samples 7- were from Y_2O_3·15Ti crucible slug and 15- from yttria layer crucible slug.

**** Black dots (●) indicate that tensile properties for that specimen were not included in average because of excessive defects in the fracture surface.

TABLE B-6

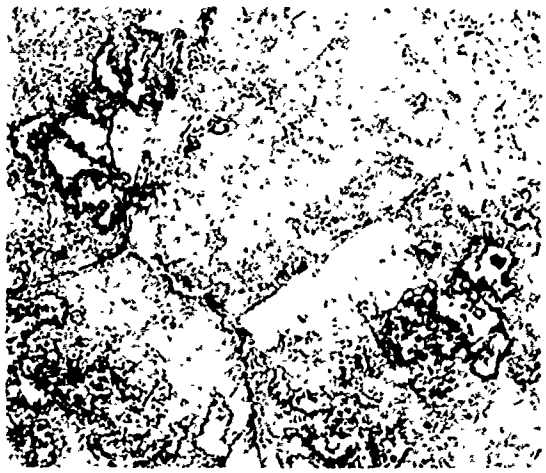
TENSILE TESTS FOR CASTING TRIAL "B"

Sample	Type	Alloy	Mold	Hipped	Heat Treatment	Glass Mill	Machining Afont	Test Temp.	UTS (ksi)	YS (ksi)	%E	%A	Fracture Surface Appearance
16-1	SCTB	-13Cu	Zircon	--	1760/1450(8) - Argon air rate cool	Yes	Threads only	RT	91.3	-	0.7	3.2	Large micros rink at or ; ., surface contam. zo ((0.025")
16-2	1/2" Bar			--	1760/1450(8) - Air	--	Gage	RT	109.5	89.6	7.0	10.1	Microshrink at origin (2)
16-3	1/2" Bar			--	1760/1450(8) - Air	--	Gage	RT	104.5	89.9	4.0	6.3	Small microshrink, large cleavage facet at origin
16-4	SCTB			--	1760/1450(3) - Argon air rate cool	Yes	Threads only	RT	98.0	96.4	0.8	2.8	Small microshrink, low-medium cleavage, surface contam. zone
16-5	1/2" Bar			--	None				No Test	--	--	--	--
16-6	1/2" Bar			--	None	-	Gage	RT	110.0	95.9	7.5	11.6	Medium microshrink, low-medium cleavage
16-7	3/4" Bar			--	-- --	--	--	--	No Test	--	--	--	--
17-1	SCTB	-13Cu-4.5Si	Monograf	--	None	--	Threads	RT	83.0	70.9	(0.3)	2.8	Large void (0.050"), surface contam. zone (0.015")
17-2	1/2" Bar			Yes	None	--	Gage	RT	91.6	67.8	4.5	4.0	Low-medium cleavage
17-3	1/2" Bar			Yes	1760/1450(8) - Air	--	Gage	RT	108.6	94.5	6.5	9.4	Small microshrink, low-medium cleavage
17-4	SCTB			Yes	None	--	Gage	RT	86.9	67.3	(0.1)	2.1	Medium-medium cleavage
17-5	1/2" Bar			Yes	1760/1560(1) - Air	--	Gage	RT	100.8	81.5	3.0	5.5	Small microshrink, medium-medium cleavage, unusual area at origin
17-6	1/2" Bar			Yes	1760/1450(8)-FC - Air	---	Gage	RT	102.0	85.1	4.8	5.1	Small microshrink, low-medium cleavage, both at origin
17-7	3/4" Bar			--	None	--	Gage	RT	96.9	69.9	1.4	2.4	Large microshrink at surface, low-medium cleavage
18-1	SCTB	-13Cu-4.5Si	Y_2O_3-Silicate	--	None	--	Threads	RT	102.3	80.6	(4.1)	2.4	Large voids, medium-medium cleavage
18-2	1/2" Bar			--	--	--	--	--	No Test	--	--	--	--
18-3	1/2" Bar			--	None	--	Gage	RT	92.7	75.6	2.1	1.6	Inclusion at origin, small void, high-medium cleavage
18-4	SCTB			Yes	--	--	--	--	No Test	--	--	--	--
18-5	1/2" Bar								No				
18-6	1/2" Bar			Yes	--	--	--	--	Test	--	--	--	--
18-7	3/4" Bar												
19-1	SCTB	-13Cu-4.5Al	Monograf	Yes	None	--	Gage	RT	111.4	102.1	2.3	5.0	Low-medium cleavage with acicular pattern
19-2	1/2" Bar			Yes		--	--	--	No Test	--	--	--	--
19-3	1/2" Bar			Yes	1760/1450(16) - Air	--	Gage	RT	125.4	108.5	4.9	5.9	No defects, low-small cleavage
19-4	SCTB			Yes	None	-	Gage	RT	110.1	98.4	2.3	5.4	Small inclusion, low-large cleavage
19-5	1/2" Bar			Yes	1760/1450(16) - Air	--	Gage	600°F	94.7	66.6	16.8	25.4	Small inclusions (2)
19-6	1/2" Bar			Yes	1760/1450(16) - Air	--	Gage	600°F	95.3	65.2	22.1	39.4	Small inclusions, small microshrink
19-7	3/4" Bar			Yes	1760/1450(15) - Air	--	Gage	RT	124.4	109.8	4.6	8.6	No defects

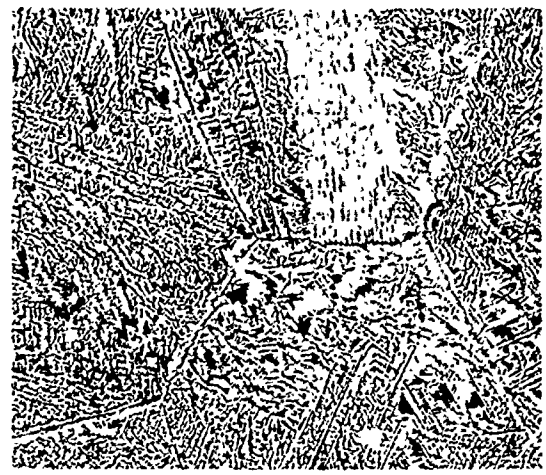
APPENDIX C

COMPILATION OF PHASE I INGOT ALLOY MICROSTRUCTURES

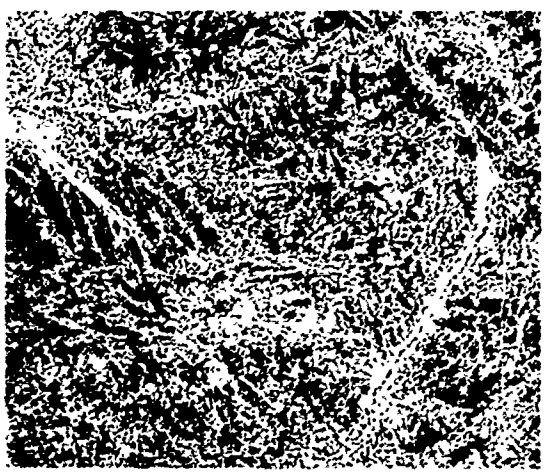
Description	Figure No.
As-Melted Microstructures of Task I Compositions (250X)	C-1
Heat Treated Microstructures of Task I Ingots (250X)	C-2
As-Melted Ingot Microstructures of Task II Compositions Excluding Be-Containing Alloys (250X)	C-3
Heat Treated Task II Ingot Microstructures Excluding Be-Containing Alloys (250X)	C-4
As-Melted Ingot Microstructures of Ti-13Cu-3Al and Task III Compositions (250X)	C-5
Example of Duplex Heat Treatment Applied to the Ingot Ti-13Cu Composition (250X)	C-6
Heat Treated Ingot Microstructures of Ti-13Cu-3Al and Task III Compositions (250X)	C-7
Ingot Microstructures of Beryllium Containing Task II Compositions (250X)	C-8
Heat Treated Ingot Microstructures of Beryllium Containing Task II Compositions (250X)	C-9



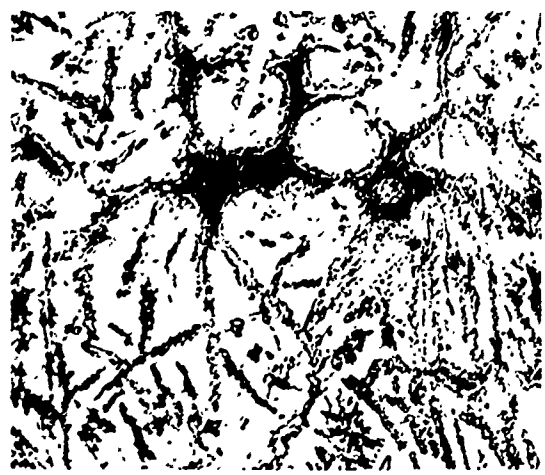
(a) Ti-11Co (8741)
Heat 24033



(b) Ti-13Cu (8726)
Heat 34029

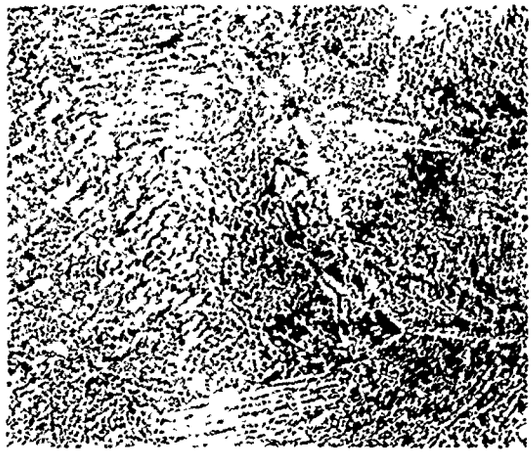


(c) Ti-11Ni (8792)
Heat 24034



(d) Ti-4Si (8725)
Heat 24031

Figure C-1. As-Melted Microstructures of Task I Compositions (250X).



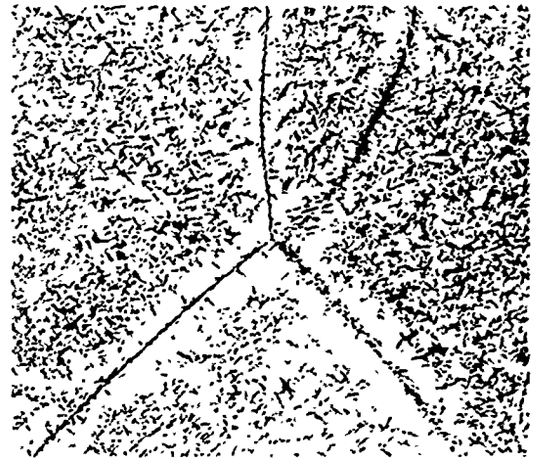
(e) Ti-8Cu-6.5Ni (8735)
Heat 24032



(f) Ti-14Mn-0.03Y (8793)
Heat 24036

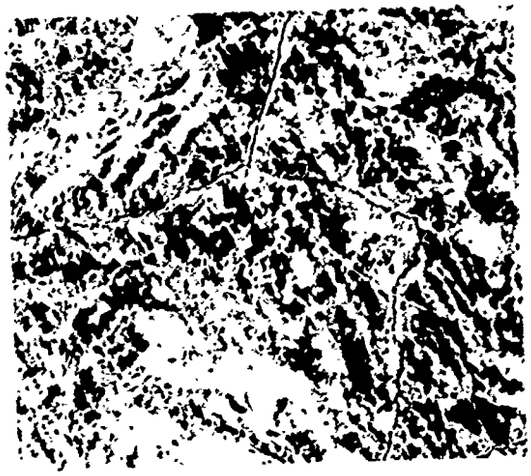


(g) Ti-20Cr-0.03Y (8798)
Heat 24037



(h) Ti-9Fe-0.03Y (8774)
Heat 24035

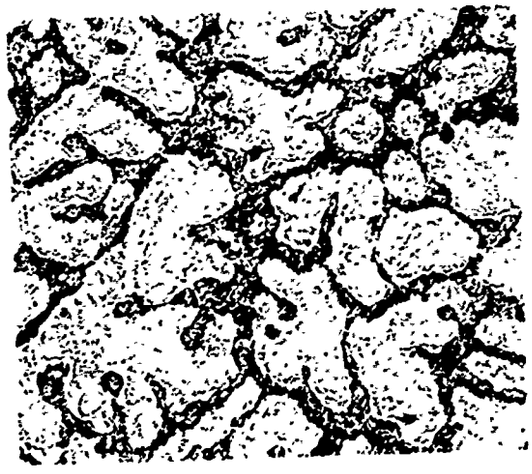
Figure C-1 (Continued) (Page 2 of 3)



(i) Ti-1Be (8991)
Heat 24106



(j) Ti-1Be-2Si (8990)
Heat 24105



(k) Ti-2.7Be-5Zr (8992)
Heat 24107

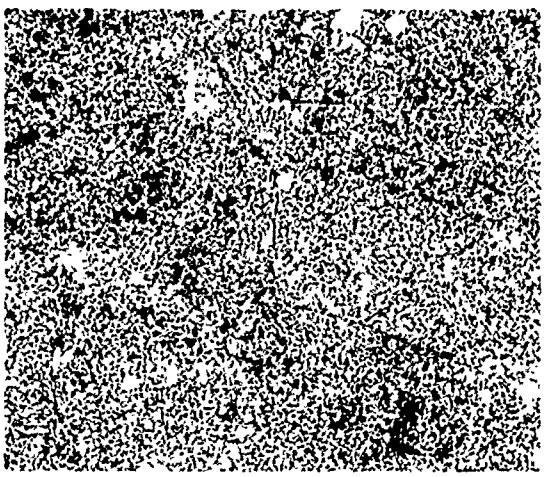


(l) Ti-2.7Be-2.5V-0.3Al (8993)
Heat 24108

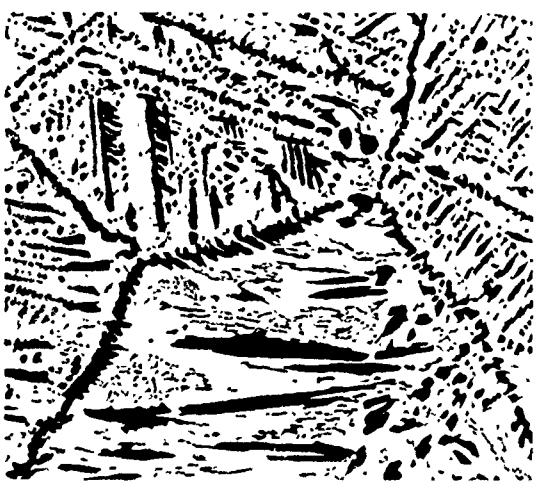
Figure C-1 (Continued) (Page 3 of 3)



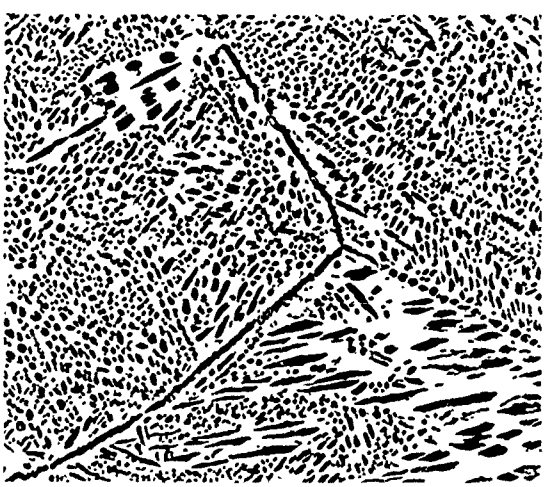
(a) Heat 24033 (8781)
Ti-11Co
1700°F-1Hr-FC



(b) Heat 24033 (8782)
Ti-11Co
1225°F-1Hr-FC



(c) Heat 34029 (8775)
Ti-13Cu
1760°F-1Hr-FC



(d) Heat 34029 (8776)
Ti-13Cu
1560°F-1Hr-FC

Figure C-2. Heat Treated Microstructures of Task I Ingots (250X).



(e) Heat 24034 (9784)
Ti-11Ni
1700°F-1Hr-FC



(f) Heat 24034 (8855)
Ti-11Ni
1700°F-1Hr-FC +
1380°F-12Hr-AC

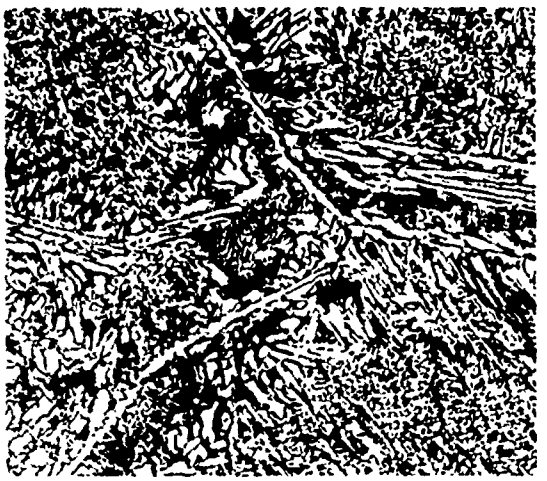


(g) Heat 24031 (8777)
Ti-4Si
2200°F-1Hr-FC

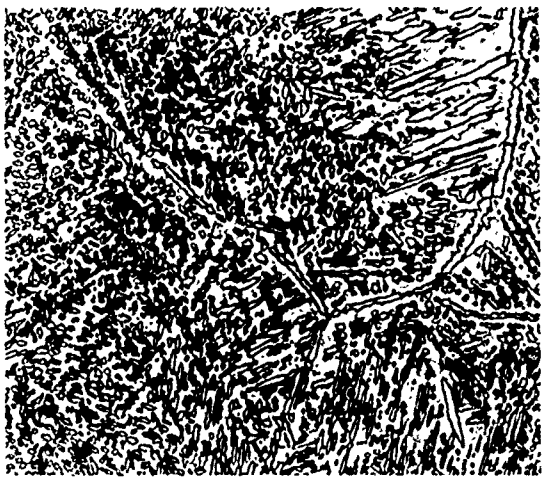


(h) Heat 24031 (8778)
Ti-4Si
1500°F-1Hr-FC

Figure C-2 (Continued) (Page 2 of 6)



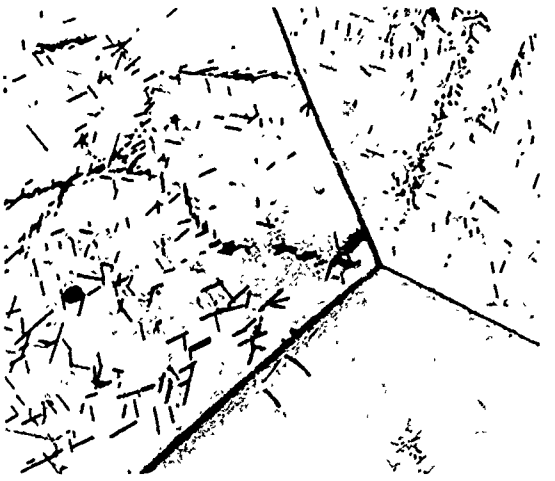
(i) Heat 24032 (8779)
Ti-8Cu-6.5Ni
1725°F-1Hr-FC



(j) Heat 24032 (9258)
Ti-8Cu-6.5Ni
1450°F-1Hr-FC



(k) Heat 24036 (8819)
Ti-14Mn-0.03Y
1290°F-1Hr-FC

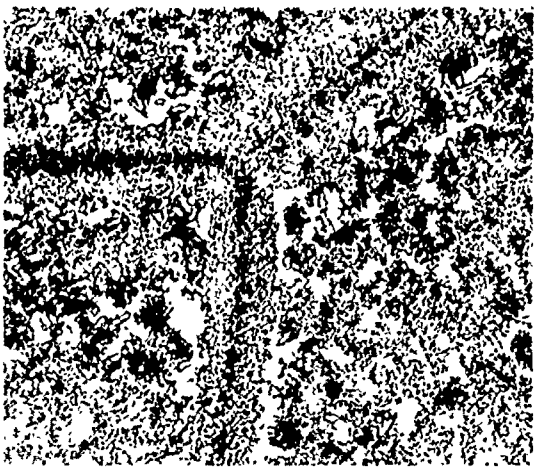


(l) Heat 24036 (8821)
Ti-14Mn-0.03Y
1290°F-1Hr-WQ

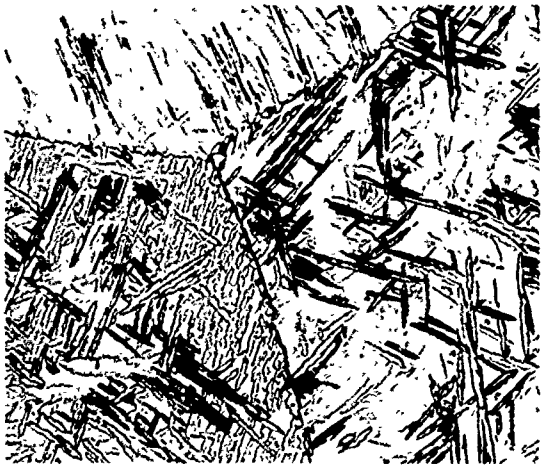
Figure C-2 (Continued) (Page 3 of 6)



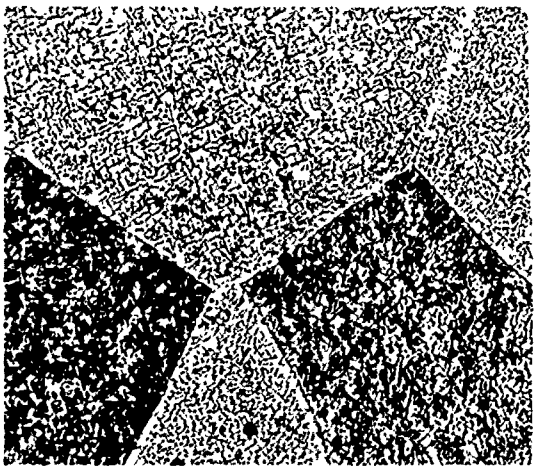
(m) Heat 24037 (8822)
Ti-20Cr-0.03Y
1670°F-1Hr-FC



(n) Heat 24037 (9264)
Ti-20Cr-0.03Y
1190°F-48Hr-AC

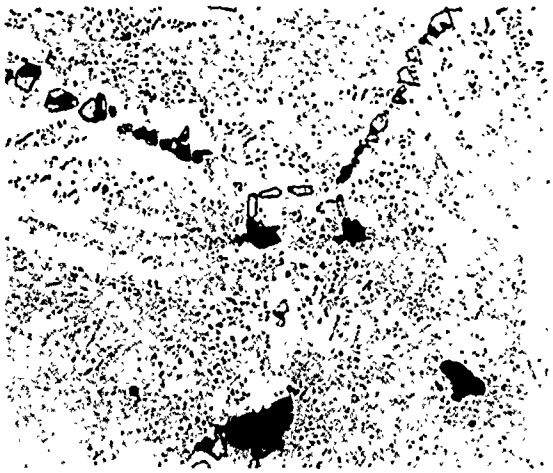


(o) Heat 24034 (8818)
Ti-9Fe-0.03Y
1500°F-1Hr-FC

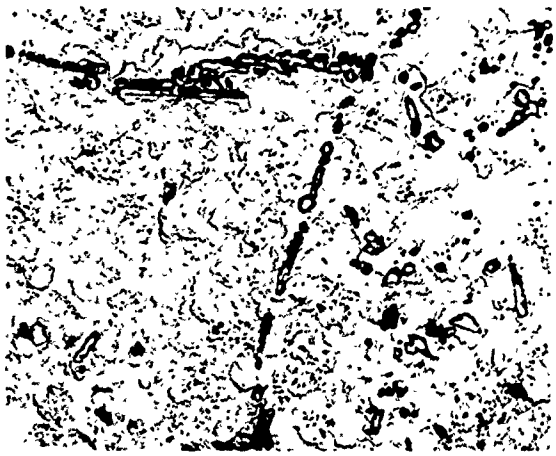


(p) Heat 24034 (9260)
Ti-9Fe-0.03Y
1200°F-1Hr-FC

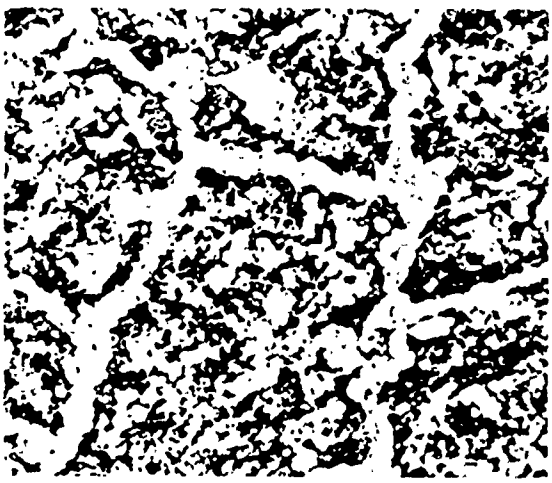
Figure C-2 (Continued) (Page 4 of 6)



(q) Heat 24106 (9270)
Ti-1Be
1775°F-1Hr-FC



(r) Heat 24106 (9272)
Ti-1Be
1775°F-1Hr-FC to
1400°F-4Hr-AC



(s) Heat 24105 (9266)
Ti-1Be-2Si
1775°F-1Hr-FC



(t) Heat 24105 (9268)
Ti-1Be-2Si
1775°F-1Hr-FC to
1400°F-4Hr-AC

Figure C-2 (Continued) (Page 5 of 6)



(u) Heat 24107 (9274)
Ti-2.7Be-5Zr
1775°F-1Hr-FC



(v) Heat 24107 (9276)
Ti-2.7Be-5Zr
1775°F-1Hr-FC to
1400°F-4Hr-AC

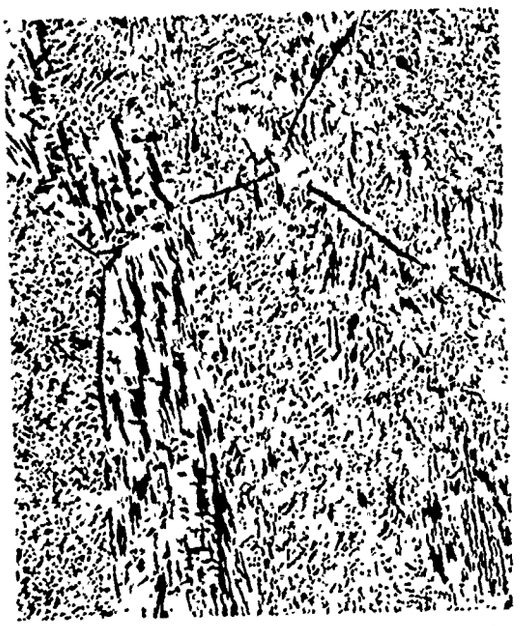


(w) Heat 24108 (9278)
Ti-2.7Be-2.5V-0.3Al
1775°F-1Hr-FC

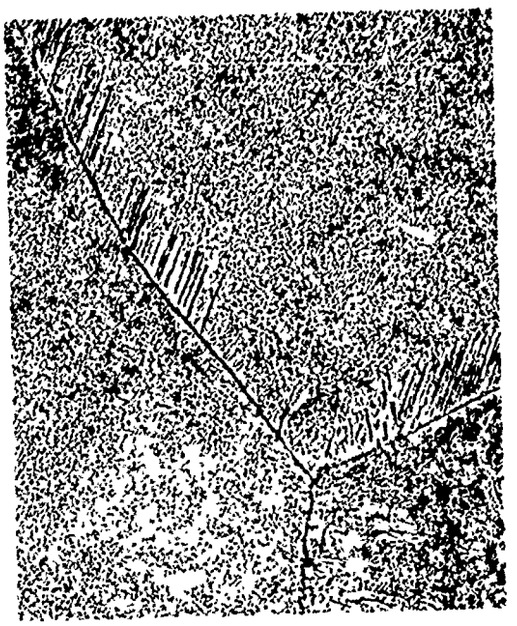


(x) Heat 24108 (9279)
Ti-2.7Be-2.5V-0.3Al
1775°F-1Hr-AC +
1400°F-4Hr-FC

Figure C-2 (Continued) (Page 6 of 6)



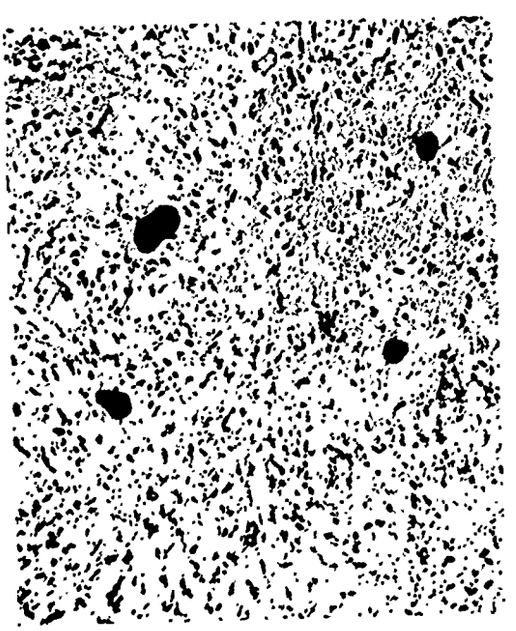
(a) Heat 24217 Ti-16Cu (9432)



(b) Heat 24218 Ti-13Cu-2.5Fe (9436)



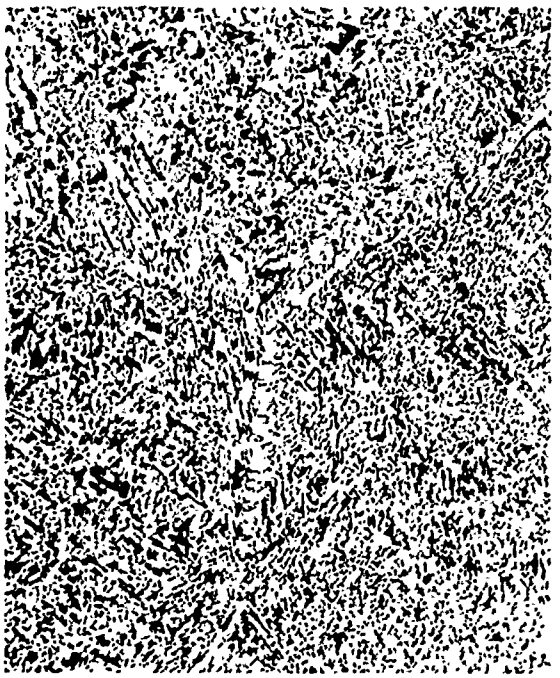
(c) Heat 24219 Ti-10Cu-2.5Fe (9434)



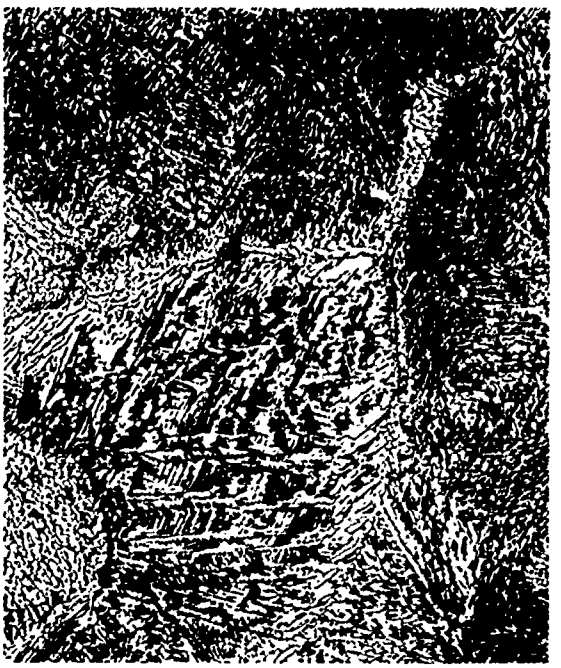
(d) Heat 24220 Ti-10Cu (9435)

Figure C-3. As-Melted Ingot Microstructures of Task II Compositions Excluding Be-Containing Alloys (250X).

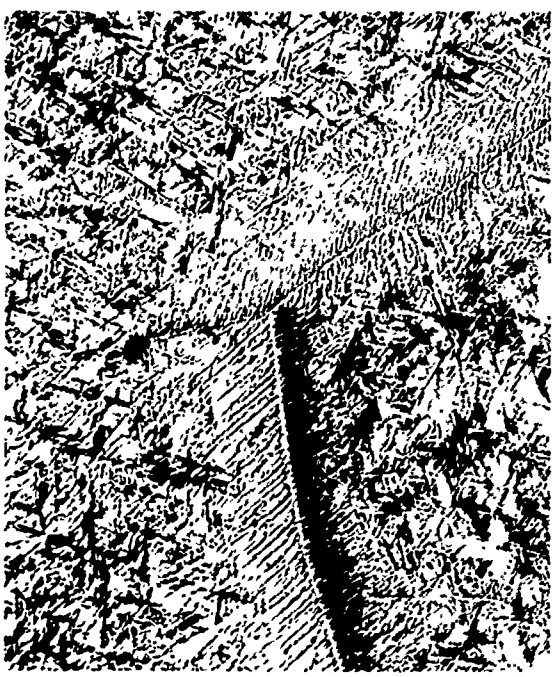
(Page 1 of 2)



(e) Heat 24221 (9433)
Ti-13Cu-1Co



(f) Heat 24224 (9455)
Ti-13Cu-4.5Ni

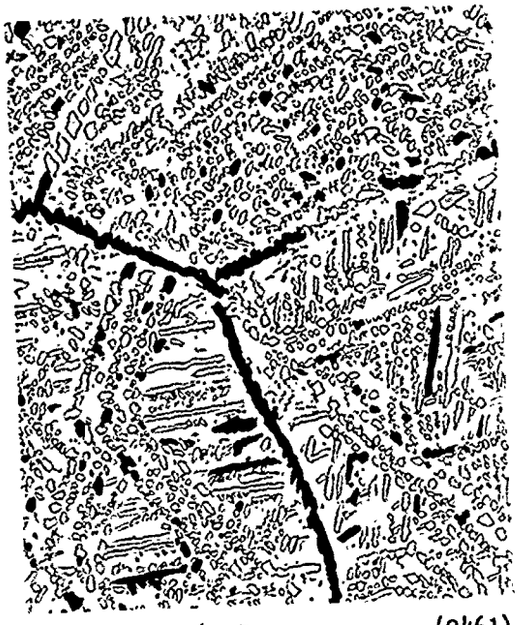


(g) Heat 24222 (9431)
Ti-7Fe-0.03Y

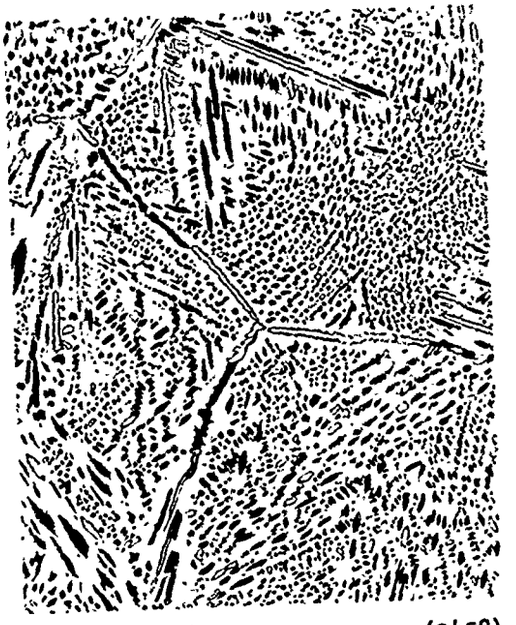


(h) Heat 24223 (9456)
Ti-7Fe-5Mn-0.03Y

Figure C-3 (Continued) (Page 2 of 2)



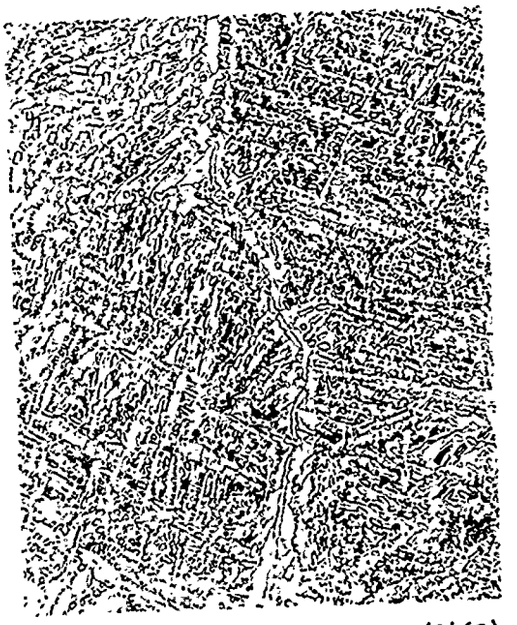
(a) Heat 24217
Ti-16Cu
1760F-1hr-FC (9461)



(b) Heat 24217
Ti-16Cu
1560F-1hr-FC (9458)



(c) Heat 24218
Ti-13Cu-2.5Fe
1760F-1Hr-FC (9465)



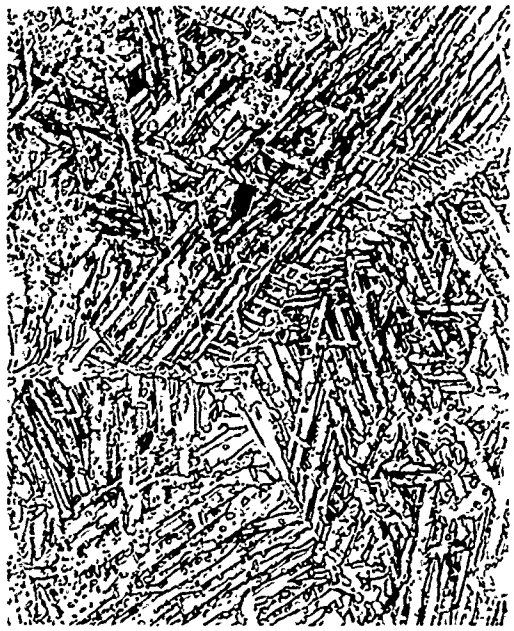
(d) Heat 24218
Ti-13Cu-2.5Fe
1560F-1hr-FC (9463)

Figure C-4. Heat Treated Task II Ingot Microstructures Excluding Be-Containing Alloys (250X).

(Page 1 of 4)



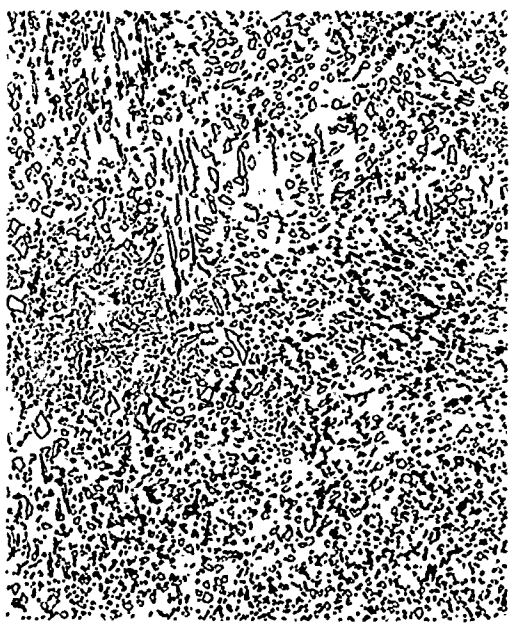
(e) Heat 24219 (9469)
Ti-10Cu-2.5Fe
1760F-1hr-FC



(f) Heat 24219 (9467)
Ti-10Cu-2.5Fe
1560F-1hr-FC



(g) Heat 24219 (9473)
Ti-10Cu
1760F-1hr-FC

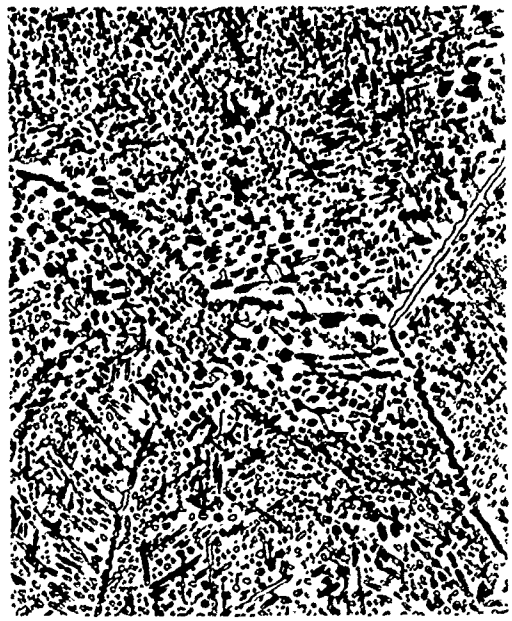


(h) Heat 24219 (9471)
Ti-10Cu
1560F-1hr-FC

Figure C-4 (Continued) (Page 2 of 4)



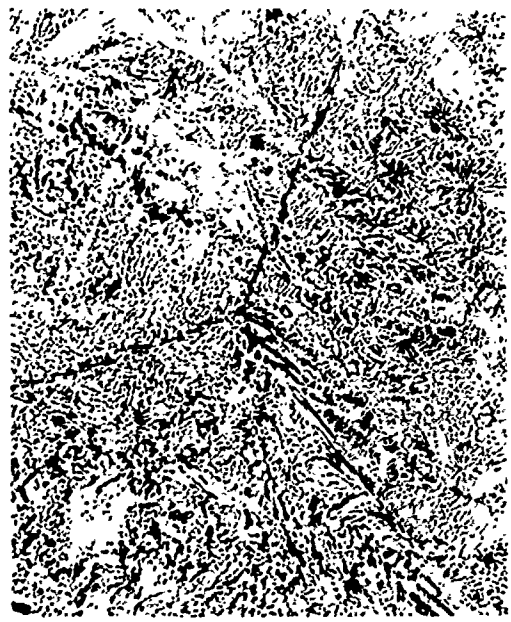
(i) Heat 24221 (9477)
Ti-13Cu-1Co
1760F-1hr-FC



(j) Heat 24221 (9475)
Ti-13Cu-1Co
1560F-1hr-FC



(k) Heat 24224 (9491)
Ti-13Cu-4.5Ni
1760F-1hr-FC

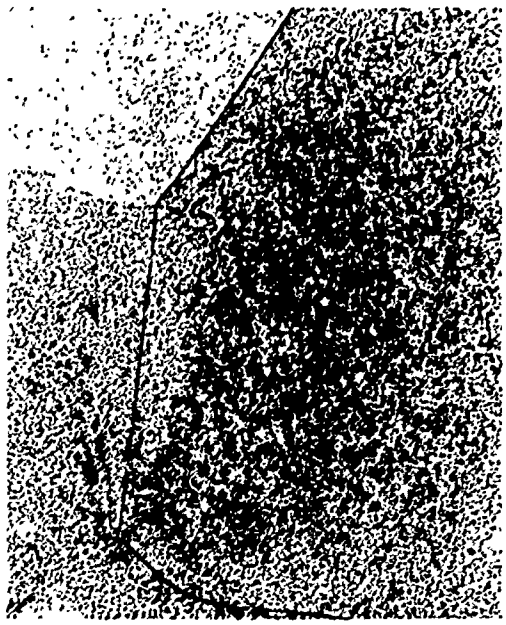


(l) Heat 24224 (9493)
Ti-13Cu-4.5Ni
1560F-1hr-FC

Figure C-4 (Continued) (Page 3 of 4)



(m) Heat 24222 (9480)
Ti-7Fe-0.03Y
1525F-1hr-FC



(n) Heat 24222 (9481)
Ti-7Fe-0.03Y
1525F-1hr-WQ +
1025F-24hr-AC



(o) Heat 24223 (9487)
Ti-7Fe-5Mn-0.03Y
1525F-1hr-FC

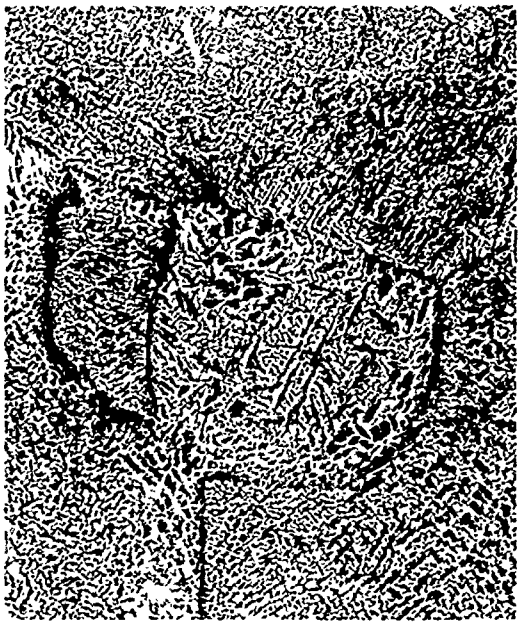


(p) Heat 24223 (9489)
Ti-7Fe-5Mn-0.03Y
1525F-1hr-WQ +
1025F-24hr-AC

Figure C-4 (Continued) (Page 4 of 4)



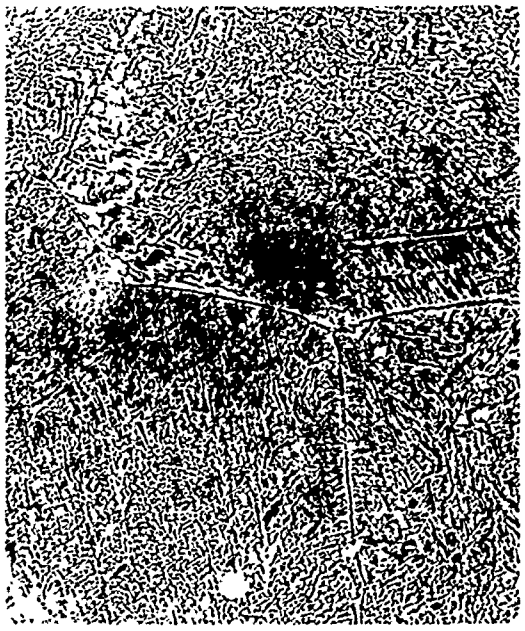
(a) Heat 24264 (9516)
Ti-13Cu-3Al



(b) Heat 24273 (9572)
Ti-13Cu-0.20



(c) Heat 24275 (9573)
Ti-13Cu-2Al

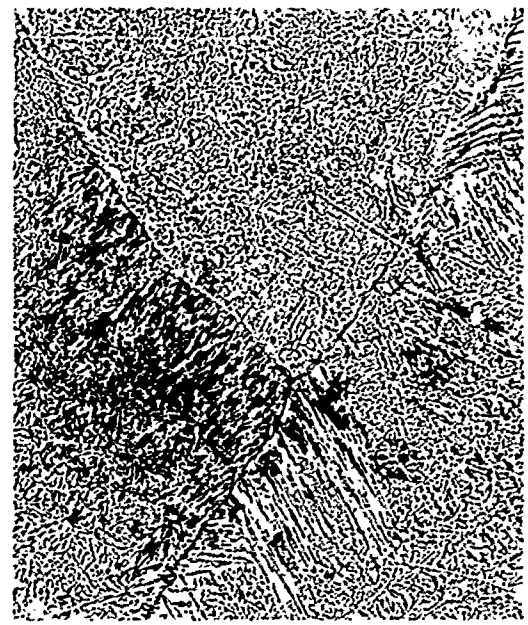


(d) Heat 24276 (9571)
Ti-13Cu-4Sn

Figure C-5. As-Melted Ingot Microstructures of Ti-13Cu-3Al and Task III Compositions (250X).



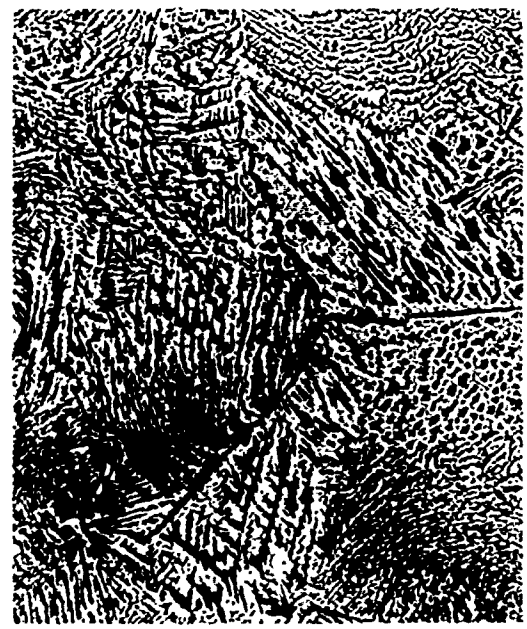
(e) Heat 24277 (9581)
Ti-10Cu-2.5Fe-2Al



(f) Heat 24278 (9582)
Ti-16Cu-1.5Al

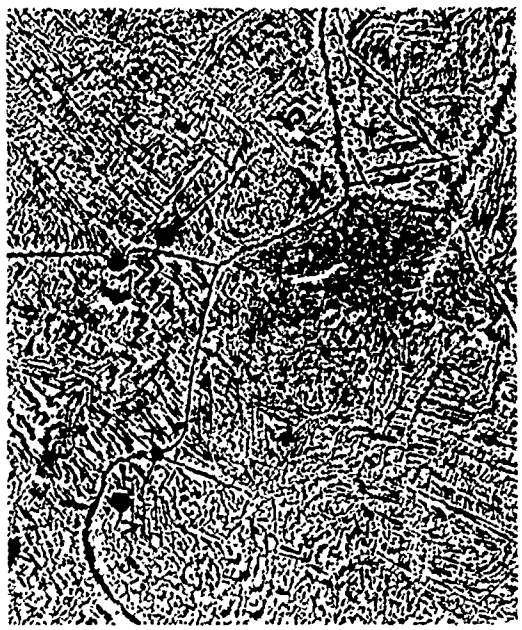


(g) Heat 24279 (9583)
Ti-19Cu



(h) Heat 24280 (9596)
Ti-19Cu-1Al

Figure C-5 (Continued) (Page 2 of 3)



(i) Heat 24281 (9597)
Ti-13Cu-0.25Y_2O_3 (250X)



(j) Heat 24281 (9597)
Ti-13Cu-0.25Y_2O_3 (1000X)

Figure C-5 (Continued) (Page 3 of 3)



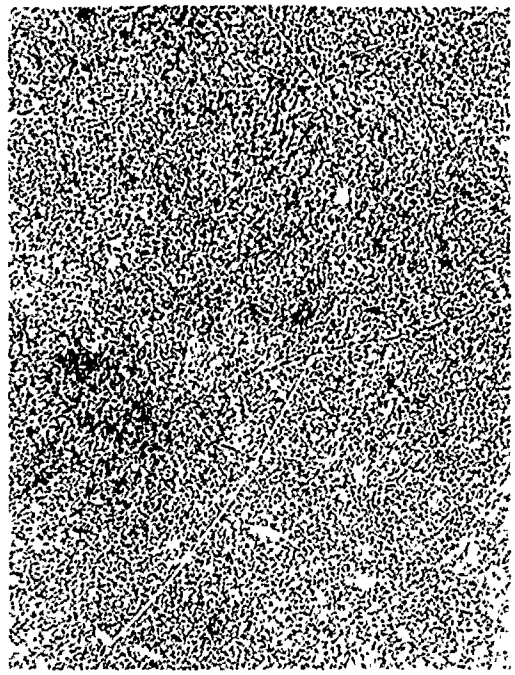
HEAT 34029 (9538)

Ti-13Cu
1760F- 1 hr-AC
+1300F-8 hr-AC

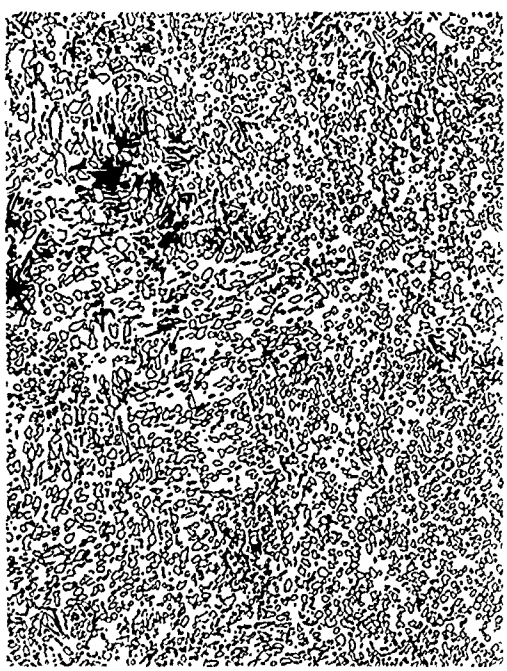
Figure C-6. Example of Duplex Heat Treatment Applied to the Ingot Ti-13Cu Composition (250X).



(a) HEAT 24277 (9606)
Ti-10Cu-2.5 Fe-2Al
1560F-1 hr-FC



(b) HEAT 24277 (9631)
Ti-10Cu-2.5Fe-2Al
1400F-1 hr-FC

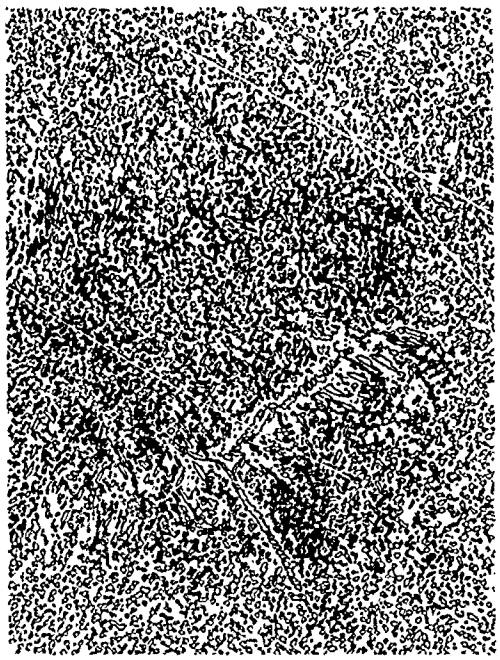


(c) HEAT 24264 (9356)
Ti-13Cu-3Al
1560F-1 hr-FC

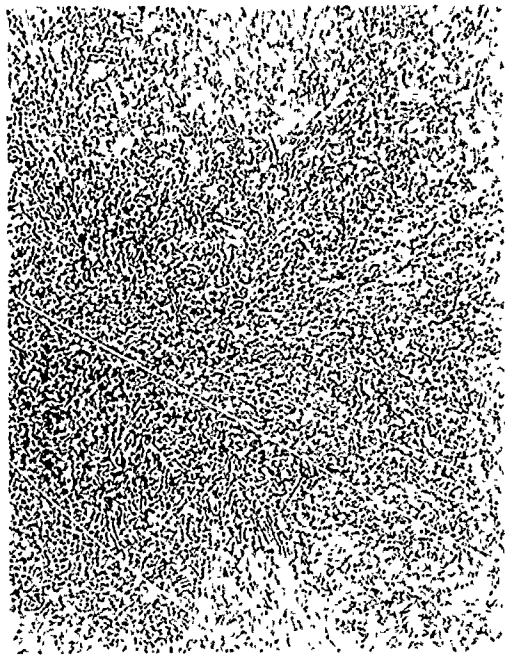


(d) HEAT 24264 (9542)
Ti-13Cu-3Al
1760F-1 hr-AC
+1300F-8 hr-AC

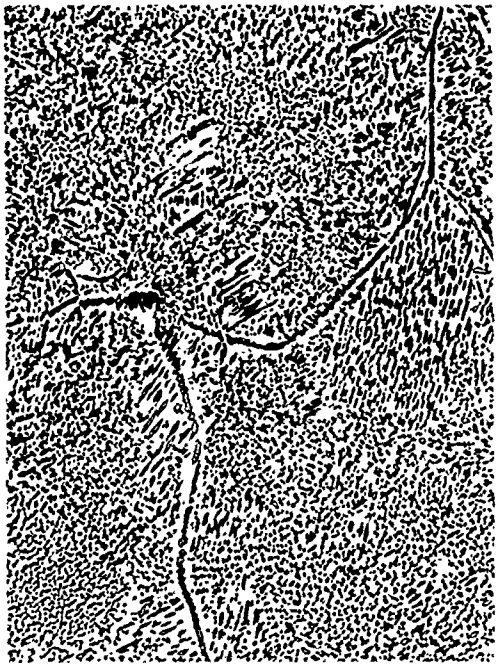
Figure C-7. Heat Treated Ingot Microstructures of Ti-13Cu-3Al and Task III Compositions (250X). (Page 1 of 5)



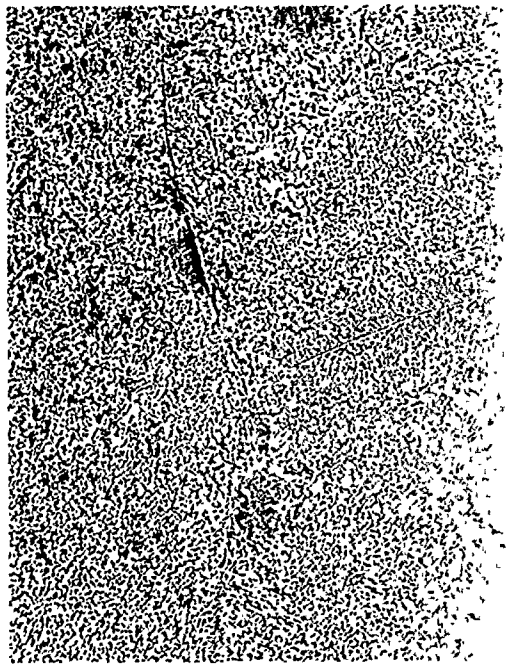
(e) HEAT 24275 (9568)
Ti-13Cu-2Al
1560F-1 hr-FC



(f) HEAT 24275 (9567)
Ti-13Cu-2Al
1760F-1 hr-AC
+1450F-8 hr-AC

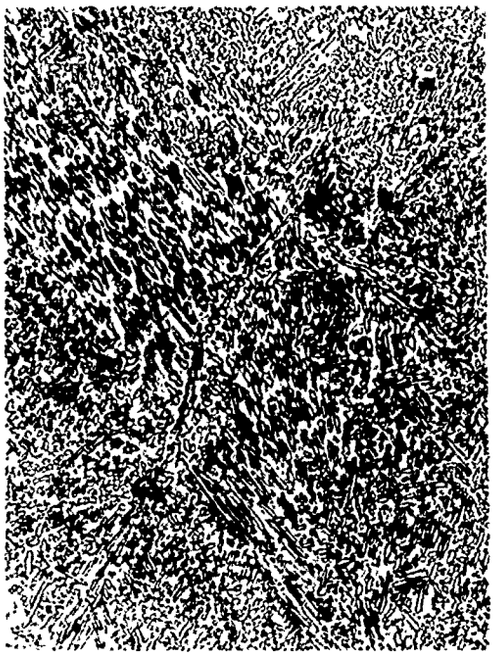


(g) HEAT 24276 (9604)
Ti-13Cu-4Sn
1560F-1 hr-FC

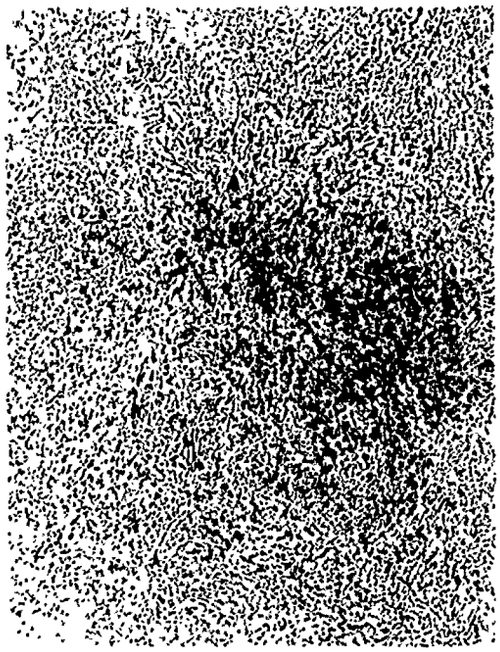


(h) HEAT 24276 (9605)
Ti-13Cu-4Sn
1760F-1 hr-AC
+1450F-8 hr-AC

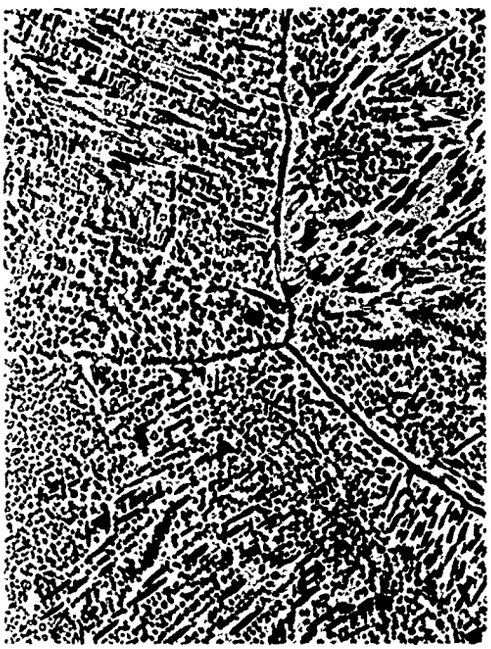
Figure C-7 (Continued) (Page 2 of 5)



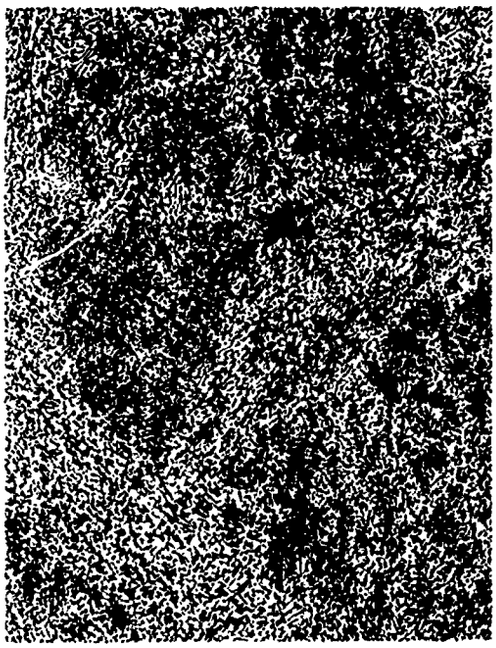
(i) HEAT 24273 (9570)
Ti-13Cu-0.2O
1560F-1 hr-FC



(j) HEAT 24273 (9566)
Ti-13Cu-0.2O
1760F-1 hr-AC
1450F-8 hr-AC



(k) HEAT 24281 (9620)
Ti-13Cu-0.25 Y_2O_3
1560F-1 hr-FC



(l) HEAT 24281 (9632)
Ti-13Cu-0.25 Y_2O_3
1760F-1 hr-AC
+1450F-8 hr-AC

Figure C-7 (Continued) (Page 3 of 5)



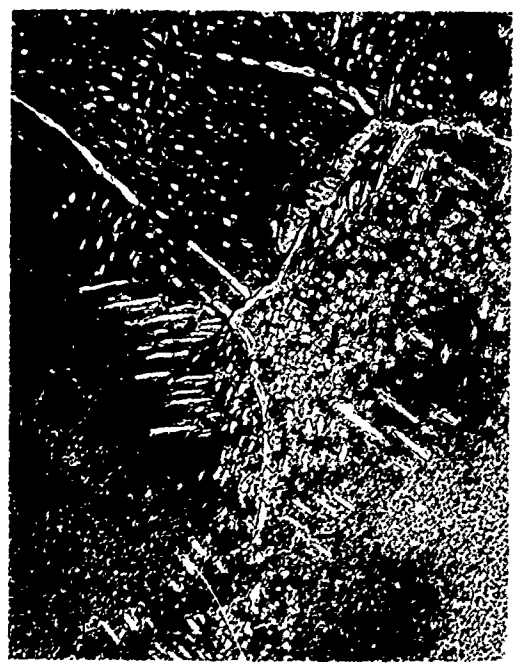
(m) HEAT 24279 (9608)
Ti-16Cu-1.5Al
1560F-1 hr-FC



(n) HEAT 24278 (9607)
Ti-16Cu-1.5Al
1760F-1 hr-AC
1450F-16 hr-AC



(o) HEAT 24279 (9609)
Ti-19Cu
1560F-1 hr-FC

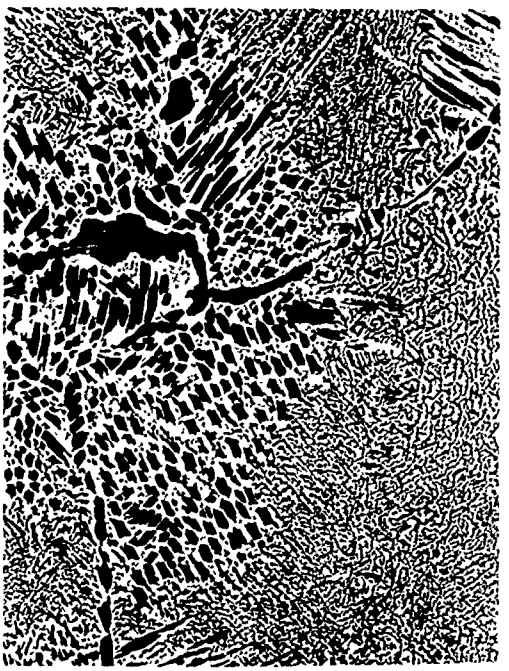


(p) HEAT 24279 (9629)
Ti-19Cu
1760F-1 hr-WQ
+1450F-8 hr-AC

Figure C-7 (Continued) (Page 4 of 5)

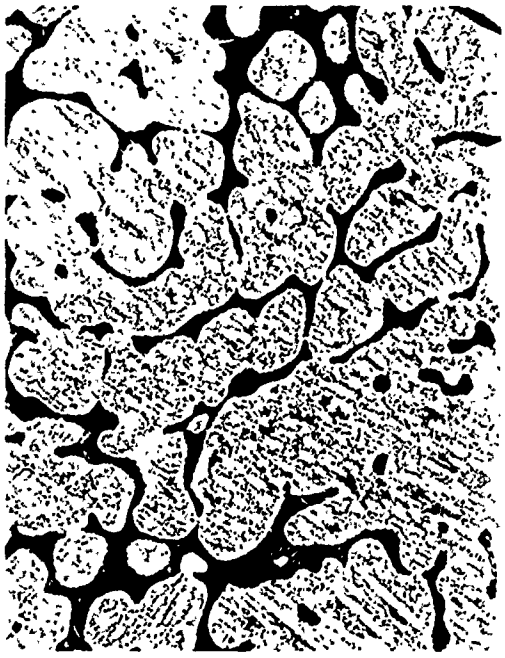


(q) HEAT 24280 (9619)
Ti-19Cu-1Al
1560F-1 hr-FC



(r) HEAT 24280 (9630)
Ti-19Cu-1Al
1760F-1 hr-AC
+1450F-8 hr-AC

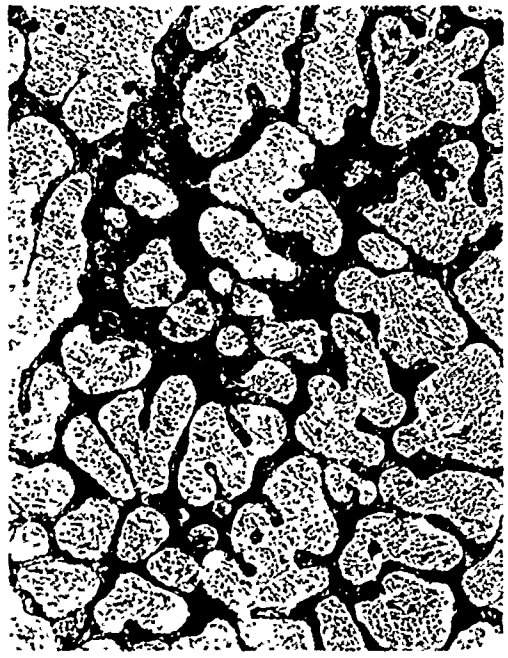
Figure C-7 (Continued) (Page 5 of 5)



(a) HEAT 34267 (9534)
Ti-13Cu-1Be

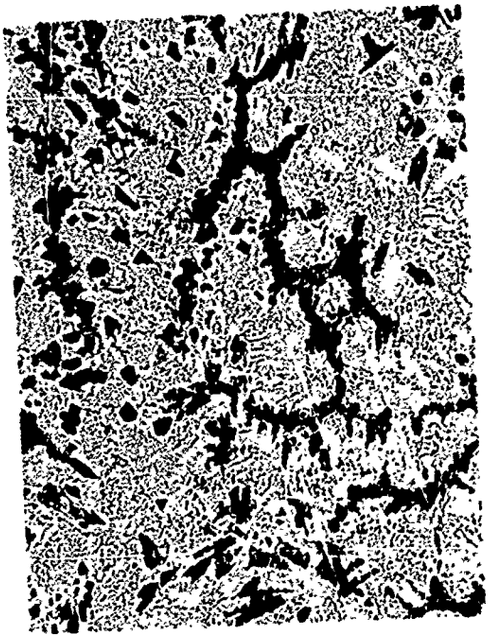


(b) HEAT 24268 (9662)
Ti-7Fe-1Be-0.03Y



(c) HEAT 24269 (9535)
Ti-2.7Be-5V

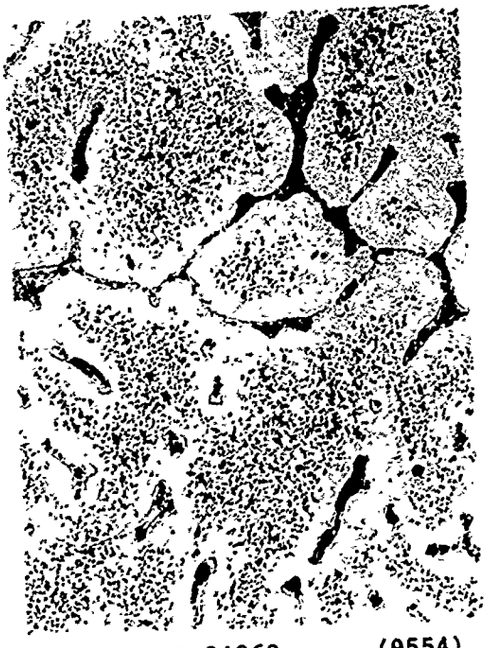
Figure C-8. Ingot Microstructures of Beryllium Containing Task II Compositions (250X).



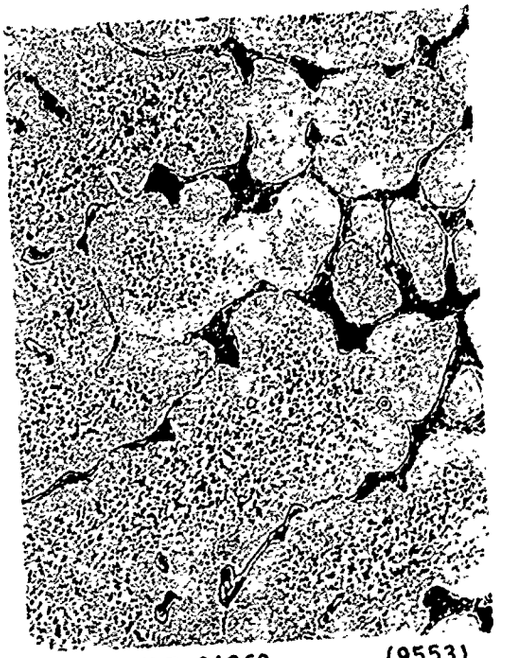
(a) HEAT 34267 (9551)
Ti-13Cu-1Be
1560F-1 nr-FC



(b) HEAT 34267 (9552)
Ti-13Cu-1Be
1760F-1 hr-FC



(c) HEAT 24268 (9554)
Ti-7Fe-1Be-0.03Y
1525F-1 hr-FC



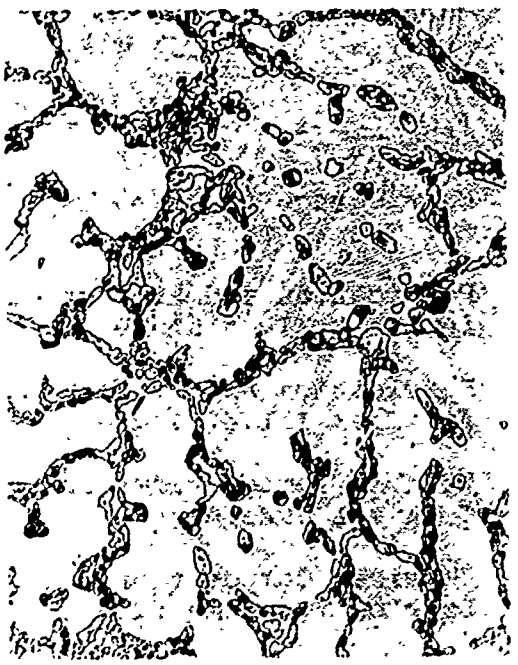
(d) HEAT 24268 (9553)
1525-1 hr-WQ
+1025F-24 hr-AC

Figure C-9. Heat Treated Ingot Microstructures of Beryllium Containing Task II Compositions (250X).

(Page 1 of 2)



(e) HEAT 24269 (9555)
Ti-2.7Be-5V
1775F-1/2 hr-FC



(f) HEAT 24269 (9556)
Ti-2.7Be-5V
1775F-1/2 hr-FC
to 1400F-4 hr-AC

Figure C-9 (Continued) (Page 2 of 2)

APPENDIX D

FABRICATION AND MATERIALS FOR CRUCIBLE/MOLD INVESTIGATIONS

Description	Table No.
Fabrication and Properties of Crucibles Procured for Task I of Phase I	D-1
Fabrication and Properties of Crucibles Procured for Task II of Phase I	D-2
Fabrication and Properties of Crucibles Procured for Task III of Phase I	D-3
Firing Temperatures and Properties for Phase I Task III Crucibles	D-4
Chemical Composition and Properties for Several Lots of Yttrium-Oxide Used For The Program	D-5
Analytical Results for Several Lots of Titanium Powder Used for Crucible Fabrication	D-6
Fabrication History of Phase II, Casting Trial "A" Melting Crucibles	D-7
Fabrication History of Phase II, Casting Trial "B" Melting Crucibles	D-8
Properties of Heavy Rare Earth Concentrates Used for Laboratory Mold Investigations	D-9

TABLE D-1

FABRICATION AND PROPERTIES OF CRUCIBLES PROCURED FOR TASK I OF PHASE I

MATERIALS	Material Source and Lot	Pressing Conditions (psi)	Pressed Density (g/cc)	Sintering		Sintered Density		Color		As-Received Crucible Appearance
				Temp (°F)	Shrinkage (%)	(g/cc)	% of Theor.	As Received	Sintered	
Cold Pressed and Sintered(Coors)										
Y_2O_3	Moly. Corp. - 572	20,000/10,000	2.28	3000	27	4.68	92.4	White	Cream	Bottom OD Circumferential Cracks
Y_2O_3	Moly. Corp. - 724	20,000/20,000**	2.22	3200	24	4.55	90.1	White	Cream	
Y_2O_3-15Ti(wt-%)		20,000/10,000	2.18	3000	14	3.3			Br & Wh	Sound, Ti on Inner Surface
Dy_2O_3	R.C.*-Dy-0-3-051	20,000/10,000	3.60	3780	28	7.25	89.0	White	Lt Yel	Light OD Bottom Cracking
La_2O_3	R.C.*-La-0-4-023	20,000/10,000	2.51	3000	-	-	-	White	White	Unsuccessful, Cracking
Light Rare Earth Mixed Oxides (LREMO)	Moly. Corp.-HO-221	20,000/ 8,500	2.51	3000	31	5.3	-	Lt Gr-Wh	Red.-Br	Sound
Heavy Rare Earth Mixed Oxides (HREMO)	R.C.*	20,000/ 8,500	1.63	3180	46	5.25	-	Lt Or-Br	Red.-Br	Sound
CaO	MERCK	- /10,000	1.72	3200	34	2.65	79.8	White	White	Sound
CaO-15Ti(wt-%)		20,000/10,000	1.24	3000	20	2.0			WhGr & Br	No Cracks, Distorted Body
MgO	Eng'd Mat'l	20,000/10,000	1.06	3200	46	3.3	92.4	White	White	Some with OD Circumferential Cracks
Hot Pressed (Cerac)										
Y_2O_3						4.68	93.0		White	Sound
ThO_2						8.64	96.4		White	Sound
CaS						5.43	91.6		Red	Sound
SiC						2.15	67.0		Black	Sound
Other										
SiC, Reaction Bonded(Norton)						2.69	84.0		Black	Sound
Pyrolytic Graphite(Super Temp Co)						2.13	96.8		Black	Sound

* Research Chemicals
** Isostatically Pressed

TABLE D-2

FABRICATION AND PROPERTIES OF CRUCIBLES PROCURED FOR TASK II OF PHASE I

Materials	Material Source and Lot	Pressing Conditions (psi)	Pressed Density (g/cc)	Sintering		Sintered Density		Color		As-Received Crucible Appearance
				Temp (°F)	Shrinkage (%)	(g/cc)	% of Theor.	As Received	Sintered	
Iso* pressed and sintered										
Y_2O_3	Moly. Corp. - 724	ISO-20,000 psi	2.22	3200	24	4.55	90.1	White	Cream	Sound
Y_2O_3.6Ti	Moly. Corp. - 724	ISO-10,000 psi	2.37	3090	8.3	4.15			Lt. Grey	Sound
Y_2O_3.8Ti	Moly. Corp. - 724	ISO-10,000 psi	1.71	3000	8.7	2.65			Lt. Grey	Sound
Y_2O_3.15Ti	Moly. Corp. - 724	ISO-10,000 psi	2.40	3090	8.6	3.89			Dk. Grey	Sound
Y_2O_3.15Ti	Moly. Corp. - 724	ISO-10,000 psi	1.72	3000	9.0	2.43			Lt. Grey	Sound, Light Bottom OD Cracking
Heavy Rare Earth Mixed Oxide (HREMO)	RC**	20,000/8,500	1.85	3180	45.5	5.24		Lt.Or.-Brn.	Red-Br.	Sound
HREMO - 15Ti	RC	ISO-10,000 psi	2.35	3090	8.3	4.67			Dk. Grey	Crumbling
HREMO - 15Ti	RC	ISO-10,000 psi	1.65	3000	9.1	3.16			Grey	Sound
CaO (1")	Merck E-67562	20,000/10,000	1.18	3180	31	2.63	79.6	White	White	Sound
CaO (2")	Merck E-67562	ISO-20,000 psi	--	3180	35	2.1	63.5	White	White	Sound
Y_2O_3 Slip Cast into SiC Crucible	DCI***									
ThO_2 Slip Cast	DCI			4300		8.93	89		White	Sound

*ISO indicates iso static cold pressures
**Research Chemicals, Inc.
***Deposits and Composites, Inc.

TABLE D-3

FABRICATION AND PROPERTIES OF CRUCIBLES PROCURED FOR TASK III OF PHASE I

Materials	Material Source and Lot	Pressing Conditions (psi)	Pressed Density (g/cc)	Sintering		Sintered Density		Color		As-Received Crucible Appearance
				Temp. (°F)	Shrinkage (%)	(g/cc)	% of Theor. ***	As Received Powder	Sintered Crucible	
Cold pressed and sintered										
Y_2O_3·15Ti (Group 1)	Moly Corp.-#8529	ISO-10,000*	2.60	3000	13.2	4.08	89	White	Black	Nearly Sound Interior· Spalling, Cracking of Exterior
HREMO.8Ti (Group 1)	Research Chem.	ISO-10,000	2.35	3000	24.5	4.68	99	Lt.Or-Brn.	Black	Interior Cracks· Exterior Cracks and Blisters
Y_2O_3·15Ti (Group 2)	Moly Corp.-#8529	ISO-10,000	2.28	3000	10.0	3.37	73	White	Grey-Grn	Bottom ID Crack, Crucibles A and B
Y_2O_3·15Ti (Group 2)	Moly Corp.-#8529	ISO-10,000	2.33	3060	12.2	3.69	80	White	Grey-Grn	Bottom ID Crack, Crucibles C, D and E
HREMO.8Ti (Group 2)	Research Chem.	ISO-10,000	2.20	3000	19.0	4.41	93	Lt.Or-Brn.	Grey-Black	Bottom ID Crack, Crucibles F and G
HREMO.8Ti (Group 2)	Research Chem.	ISO-10,000	2.21	3060	20.3	4.64	98	Lt.Or-Brn.	Grey-Black	Bottom ID Crack, Crucibles H, I, J and K
Slip cast and sintered										
Y_2O_3 into a SiC Crucible	DCI**	2,000 psi Argon during sintering	-	-	-	-	-	White	Black	Y_2O_3 Converted to Foreign Compound

*ISO indicates isostatic cold pressing

**Deposits and Composites, Inc., Reston, Virginia

***Theoretical Density of Y_2O_3·15Ti taken as 4.60 from highest measured density for high fired crucible. Theoretical density for HREMO·8Ti taken as 4.73.

TABLE D-4

FIRING TEMPERATURES AND PROPERTIES
FOR PHASE I TASK III CRUCIBLES

Crucible	As-Received		Additional Thermal Treatment		
	Fired (°F)	Density* (g/cc)	Fired (°F)	Time (Hrs)	Density** (g/cc)
Y_2O_3·15Ti-A	3000	3.40	None	-	3.01
Y_2O_3·15Ti-B	3000	3.35	3685	1	4.38
Y_2O_3·15Ti-E	3055	3.77	3355	1	4.12
HREMO·8Ti-F	3000	1.39	3175	1	5.19
HREMO·8Ti-G	3000	4.43	None	-	4.80
HREMO·8Ti-H	3055	4 55	3355	1	5.19

*Calculated density based upon calculated volume

**Measured density by water immersion

TABLE D-5

CHEMICAL COMPOSITION AND PROPERTIES
FOR SEVERAL LOTS OF YTTRIUM-OXIDE
USED FOR THE PROGRAM

Properties	FIRST		SECOND		THIRD	FOURTH	FIFTH	SIXTH
	Moly Corp Lot 572		Moly Corp Lot 724		Moly Corp Lot 8529	Moly Corp Lot 787	Moly Corp Lot 792	Moly Corp Lot 790
	Phase I, Task I Crucibles		Phase I, Tasks I & II Crucibles		Phase I, Task III Crucibles	Phase II, Task I Crucibles	Phase II Plasma Spray Mold Fab	Phase II Task III Crucibles
	Coors Analysis	Moly Corp Analysis	Coors Analysis	Moly Corp Analysis	Moly Corp Analysis	Moly Corp Analysis	Moly Corp Analysis	Moly Corp Analysis
Screen Analysis	--		--	--	--	99.9%-325	8. 62%-325	--
MSA (microns)	3.4		2.6	--	--	1.1	8.1 (Fisher)	
BET (m^2/g)	4.8		8.1	--	--	--	--	--
Density (g/cc)	4.8		5.04	--	--	5.04	--	--
Purity (%)		99.99		99.99	99.99	99.99	99.99	99.99
Impurities as oxides (ppm)								
La	<300	--	<100	--	--	<0.2	<0.2	<0.2
Pr	--	3	--	0.7	4	0.5	<1.2	0.3
Nd	--	4	--	0.5	5.9	1.2	1.0	0.4
Sm	<300	0.2	<500	0.3	1.2	1.3	2.9	0.2
Eu	<500	0.1	<500	0.2	0.06	0.1	0.2	0.1
Gd	<500	4	<500	16	5	6	10	8 8
Tb	<500	0.1	<1000	0.6	0.26	0.2	2.5	<0.05
Dy	<500	<0.1	<500	0.09	0.20	1.2	2.4	0.07
Er	<500	<11	<500	<15	<7	<8	<11	<9
Tm	<500	3	<1000	< 5	<2	<2	< 3	<2
Yb	<100	8	<100	0.4	2	1.2	1.6	0.4
Ce	<1000	<10	<1000	<10	<11	<10	<10	<10
Ho	<1000	<30	<1000	<30	<30	<30	<30	<30
Lu	<500	--	<500	--	--	--	--	--
Sc	<100	--	<100	--	--	--	--	--
B	50	--	20	--	--	--	--	--
Si	600	--	20	--	--	--	--	--
Fe	20	--	<10	--	--	--	--	--
Ca	200	--	<100	--	--	--	--	--
Other non-RE are each:	<500	--	<500	--	--	--	--	--
Al	<100	--	<100	--	--	--	--	--
Accuracy	±50%	--	±50%	--	--	--	--	--

TABLE D-6

ANALYTICAL RESULTS FOR SEVERAL LOTS OF
TITANIUM POWDER USED FOR CRUCIBLE FABRICATION

PROPERTIES AND ANALYSIS	FIRST **	SECOND **	THIRD	
	VENTRON LOT MC-7404	RMI SPONGE FINES LOT 29	VENTRON LOT M3-270	
			VENDOR	AIRESEARCH**
Catalog No.			00383	
Used During:	Phase I, Task I	Phase I, Tasks II & III	Phase II	
Average Particle Size (Microns)			7.7	--
TiO (By XRD)	N.D.*	N.D.*		N.D
$Ti(OH)_4$ (By XRD)	N.D.	N.D.		N.D.
TiO_2 (By XRD)	N.D.	N.D.		N.D
SiO_2 (By XRD)	N.D.	N.D.		N.D
Fe_2O_3 (By XRD)	N.D.	N.D.		N.D.
Unidentified (By XRD)	Yes	Yes		Yes
ANALYSES (WT-%)				
Aluminum	0.01 - 0.1	0.1 - 1.0	0.45	0.1 - 1.0
Calcium	0.01 - 0.1	0.03 - 0.3	0.50	0.1 - 1.0
Iron	0.1 - 1.0 (0.05-Coors)	0.1 - 1.0	0.07	0.1 - 1.0
Magnesium	0.0003 - 0.003	0.03 - 0.3	0.01	0.01 - 0.1
Silicon	0.01 - 0.1	0.1 - 1.0	0.06	0.1 - 1.0
Carbon	(0.06-Oremet)		N.D	
Nickel	N.D.	N.D.		0.03 - 0.3
Zinc	0.03 - 0.3	--		N.D. (<0.0)
Copper	0.0001 - 0.001	0.0001 - 0.001		0.001 - 0.01
Manganese	N.D.	N.D.		0.03 - 0.3
Tin	0.03 - 0.3	0.001 - 0.01		
OTHERS (WT-%)	All N.D.	All N.D.		All N.D.
Ag, Sc, Na, In, Y, V, Be, B, Nb, Ge, W, Bi, Cr, Te				
Hydrogen			N.D.	
Chlorine	0.07 (0.005-Coors)	0.09	--	--
Oxygen	(0.65-Oremet)			
Nitrogen	(0.61-Oremet)			

* N.D. means analyzed for and not detected

** AiResearch spectrographic results listed as relative values.

TABLE D-7

FABRICATION HISTORY OF PHASE II, CASTING TRIAL "A" MELTING CRUCIBLES

Crucible Composition	Material Source and Lot	Pressing Conditions (psi)	Calculated Pressed Density (g/cc)	Sintering		Sintered Density		Color		As-Received Crucible Appearance
				Temp. (°F) / Time (hrs)	Shrinkage (%)	(g/cc)	% of Theor. **	Mixed Powder	Sintered Crucible	
Y_2O_3.15Ti (No. 1)	Y_2O_3 Moly corp Lot 787 Ti Powder Ventron Lot MD-270	20,000 Isostatic Cold Pressed	1.7	3145 ±144/3	13.8	4.74	100.0	Grey	Brown + reddish	Sound, outside surface scale at bottom
Y_2O_3.15Ti (No. 4)			--	3000 ±16/4	14.8	4.30	91.0		Dark grey	Sound, reddish area at sight port position
Y_2O_3.15Ti + Y_2O_3 Layer (No. 2)			--	3000 ±18/4	14.5	4.38	92.5		Dark grey	Sound, reddish area at sight port position
Y_2O_3.15Ti + Y_2O_3 Layer (No. 3)			--	3010 ±22/4	14.6	4.34	91.6		Dark grey	Sound, reddish area at sight port position
Y_2O_3.15Ti (Control Crucible)			--	3000/4	21.2	4.48	94.5		Dark grey w/slight red cast	Interior crack, doesn't open to outside surface
Y_2O_3.15Ti + Y_2O_3 Layer (Control Crucible)			--	3000/4	19.3	4.44	93.7		Dark grey w/slight red cast	Sound

*Crucible 1 through 4 are 4 in. d x 8 in h and the control crucibles are 1 in d x 1 in h

**Theoretical density of Y_2O_3.15Ti previously taken as 4.60 from highest measured density of a high fired crucible. Density now is placed at 4.74 as a result of the density of large crucible No. 1 above.

TABLE D-8

FABRICATION HISTORY OF PHASE II, CASTING TRIAL "B" MELTING CRUCIBLES

Crucible Composition (4" ϕ X 8" h)	Material Source and Lot	Pressing Conditions (psi)	Calc. Pressed Density (g/cc)*	Sintering		Sintered Density		Color		As-Received Crucible Appearance
				Temp. (°C) Time (hrs)	Height Shrinkage (%)	(g/cc)*	% of Theor. **	Mixed Powder	Sintered Crucible	
Y_2O_3·15Ti										
No. 5	Y_2O_3 - Moly Corp Lot 790 ****	20,000 Isostatic Cold Pressed ****	(2.86)	1646 ±20/4	14.6	4.53	95.5	grey	dark grey	Axial crack in one wall extending from top to 2 inches above the bottom.
No. 6	Titanium Powder Ventron Lot Mc-270 ****		(3.15)	1650 ±10/4.1	14.3	4.68	94.5	grey	dark grey	Sound
No. 7***			(2.70)	1651 ±11/4.5	13.1	4.44	93.7	grey	dark grey	Sound
No. 8***			--	1651 ±1/4.5	13.9	4.69	84.4	grey	dark grey	Sound

*Numbers in parenthesis were calculated rather than measured.

**Theoretical density of Y_2O_3·15Ti previously taken as 4.60 from highest measured density of a high fired crucible. Density now is placed at 4.74 as a result of the density of large crucible No. 1 reported previously.

***Crucible 7 and 8 fired in one furnace load.

****Applicable to all four crucibles.

TABLE D-9

Properties of Heavy Rare Earth Concentrates used for Laboratory Mold Investigations

Heavy Rare Earth Concentrate	Estimated Formula	Formula Molecular Weight*	Estimated Y_2O_3 Content of Material Converted to Oxide %	Estimated Non-Rare Earth Impurities** (%)	pH in H_2O	Density (g/cc)*** Loose	Tap	Bulk	Remarks
Low Purity Single Precipitation									
HRE-OXALATE	$RE_2(C_2O_4)_3 \cdot 9H_2O$	604	57	6.0 max.	4.6	--	0.93	2.39	White fine uniform powder, estimate typical particle size near 2-microns
HRE-CARBONATE	$RE_2(CO_3)_3 \cdot 3H_2O$	412	36 min.	40.0 max	4.4	0.5	0.68	3.05	Light grey partial chunky powder, estimate typical particle size less than 1-micron
HRE-HYDROXIDE	$RE(OH)_3$	140	36 min	40.0 max.	10.4	0.7	0.64	2.70	Dark tan partial chunky powder, estimate typical particle size less than 1-micron
HRE-FLUORIDE	REF_3	146	57 YF_3	6.0 max.	4.2	1.0	0.91	3.83	White powder with hard chunks, small particle size which will agglomerate.
High Purity Double Precipitation									
HRE-OXALATE	$RE_2(C_2O_4) \cdot 9H_2O$	604	59	0.2 max.	6.4	--	0.87	2.51	White fine uniform powder
HRE-CARBONATE	$RE_2(CO_3)_3 \cdot 3H_2O$	412	57	6.0 max.	9.4	0.6	0.48	2.20	White partial chunky powder, XRD confirms conversion to oxide at 1075°C, weight measurements suggest possible conversion to oxide as low as 485°C
HRE-HYDROXIDE	$RE(OH)_3$	140	57	6.0 max.	8.8	0.8	0.86	1.80	Light yellow fine powder, XRD confirms conversion to oxide at 1075°C, weight measurements suggest possible conversion to oxide as low as 315°C or 815°C, XRD pattern weak and diffuse but suggests composition may be $RE(OH)(CO_3)$
HRE-FLORIDE	REF_3	146	59 YF_3	0.2 max.	4.4	1.2	1.46	1.25	White powder with hard chunks

* Based upon rare earths as 100% yttrium
** Primary impurities are CaO, TiO_2 and Al_2O_3
*** Tap density to ±0.07 g /cc and Bulk density (water immersion) to ±0.05 g/cc.

APPENDIX E

EXPERIMENTAL MOLD FACECOAT SLURRY COMPOSITIONS AND PROPERTIES

Description	Table No.
Group 2 Ceramic Mold Material Compositions and Properties	E-1
Influence of Firing Temperature on Properties of Group 3 Mold Facecoat Slurry Compositions	E-2
Compositions and Results for Group 4 Mold Facecoat Slurries Slip Cast into Crucibles	E-3
Group Five Mold Facecoat Preparation and Properties	E-4
Sintering Response of Group 5 Mold Compositions After Firing Bulk Samples at 1970°F for 1 Hour	E-5
Sintering Response of Group 5 Mold Compositions After Firing Bulk Samples at 2200°F	E-6
General Mold Fabrication Procedures	E-7
Experimental Mold Fabrication at AiResearch Casting Company	E-8

TABLE E-1

GROUP 2 CERAMIC MOLD MATERIAL COMPOSITIONS AND PROPERTIES

Sample Number	Sample Composition	Slurry Consistency	Green Strength	Sintering Temp/Time	Degree of Sintering
1	99.8% HREMO 0.2% Methocel	Excess water required. Possible stability problem. pH > 8.5	Too fragile to handle.	2000°F/15 hrs.	None
2	94.8% HREMO 5.0% CaF_2 0.2% Methocel	--	Slight improvement required.	2000°F/15 hrs.	Adequate.
3	89.8% HREMO 10.0% CaF_2 0.2% Methocel	--	Improvement required	2000°F/15 hrs.	Adequate. Excess CaF_2
4	74.8% HREMO 25.0% CaF_2 0.2% Methocel	--	Improvement required	2000°F/15 hrs.	Adequate. Excess CaF_2
5	94.8% HREMO 5.0% LiF 0.2% Methocel	--	Improvement required	2000°F/15 hrs.	Very little
6	89.8% HREMO 10.0% LiF 0.2% Methocel	--	Improvement required	2000°F/15 hrs.	Very little
7	83.2% HREMO 16.6% Colloidal Silica Solution 0.2% Methocel	Excess water required, Possible stability problem. pH > 8.5	Adequate	2000°F/15 hrs.	Slight improvement required
8	83.4% Al_2O_3 16.6% Colloidal Silica Solution	Requires optimization of solid liquid content.	Adequate	1900°F/15 hrs.	Hard surface, softer interior
9	90.8% Al_2O_3 9.1% Colloidal Silica Solution 0.1% Methocel	--	Adequate	1900°F/15 hrs.	Hard surface, softer interior
10	95.1% Al_2O_3 4.8% Colloidal Silica Solution 0.1% Methocel	--	Adequate	1900°F/15 hrs.	Hard surface, softer interior
11	79.8% Al_2O_3 20.0% CaF_2 0.2% Methocel	--	Poor	1950°F/15 hrs.	Adequate. Slight discoloration
12	89.8% Al_2O_3 10.0% CaF_2 0.2% Methocel	--	Poor	1950°F/15 hrs.	Adequate. Slight discoloration
13	89.8% Al_2O_3 10.0% LiF 0.2 Methocel	--	Poor	1950°F/15 hrs.	Hard surface, softer interior
14	79.8% Al_2O_3 20.0% LiF 0.2% Methocel	Requires optimization of solid liquid content.	Poor	1950°F/15 hrs.	Hard surface, softer interior

TABLE E-2

INFLUENCE OF FIRING TEMPERATURE ON PROPERTIES OF GROUP 3
MOLD FACECOAT SLURRY COMPOSITIONS

Composition and Sintering Conditions*	Density, g/cc		Green-to-Fired Changes		
	Green	Fired	Density Change, %	Weight Loss, %	Volume Shrinkage, %
CC-1					
1970°F/3H/Air	1.346	1.536	+14.1	4.7	16.4
2075°F/3H/Air	1.318	1.643	+24.6	4.8	23.6
2195°F/3H/Air	1.338	1.94	+45.0	5.0	34.6
CC-2					
1970°F/3H/Air	1.405	1.473	+ 4.8	5.9	10.3
2075°F/3H/Air	1.397	1.871	+33.9	8.9	32.0
2195°F/3H/Air	1.351	1.86	+37.7	6.0	31.9
CC-3					
1970°F/3H/Air	1.646	1.681	+ 2.1	11.6	13.4
2075°F/3H/Air	1.758	1.664	- 5.3	16.3	11.6
2195°F/3H/Air	1.651	1.651	0.0	12.8	12.8

*Compositions are as follows:

CC-1 55% solids (95% HREMO + 5% CaF_2) in water, 1% Methocel 4000 plus antifoam and wetting agents.
CC-2 Same as CC-1 except liquid was 50% water and 50% colloidal silica solution.
CC-3 Same as CC-1 except liquid was 25% water and 75% colloidal silica solution.

TABLE E-3

COMPOSITIONS AND RESULTS FOR GROUP 4 MOLD FACECOAT SLURRIES SLIP CAST INTO CRUCIBLES

Code	Solids, %	Solids Composition, wt-%	Other Binders	Sintering Results			
				1900°F/1 Hour		2190°F/2 Hours	
				Sintering	Remarks	Sintering	Remarks
CC-4	58	90 HREMO/ 10 CaF_2 (slip)	0.37% Methocel	None	Shrink cracks		
CC-5	57	85 HREMO/ 15 CaF_2 (slip)	0.39% Methocel	None	Shrink cracks		
CC-6	56	100 HREMO (slip)	4% Col. SiO_2	None	Shrink cracks		
CC-7	58	100 HREMO (slip)	8.3% Col. SiO_2	Minor	Shrink cracks		
CC-8	57	100 HREMO (slip)	12.2% Col. SiO_2	Minor	Shrink cracks	Minor	-
CC-9	46	100 HREMO (slip)	17% Col. SiO_2	Minor	Shrink cracks		
CC-10*	∿50	100 HREMO (painted)	- Col. SiO_2	Moderate	Shrink cracks		
CC-11	∿50	92 HREMO/ 8 CaF_2 (painted)	- Methocel	None	No cracks		
CC-12	∿50	83 HREMO/ 17 CaF_2 (painted)	- Methocel	None	Minor cracks	Minor	Minor cracks
CC-13*	∿50	57 HREMO/ 29 Al_2O_3 (painted)	14% CaF_2	None	No cracks	None	Phase reaction
CC-14*		Same as CC-13	- Methocel	None	No cracks		
CC-15*		Same as CC-14**	-	None	No cracks		

*Methyl alcohol primary fluid, all others are water base
**Dried, reground and methyl alcohol again added.

TABLE E-4

GROUP FIVE MOLD FACE COAT PREPARATION AND PROPERTIES

Preparing compositions for mold face coats followed a general procedure that evolved after a series of trials. The procedure established for group five compositions, including the identification of pertinent deviations, is given below.

(a) Weigh and blend dry powders in a ball mill (Al_2O_3 balls) for ten minutes. Some compositions were blended wet in a ball mill ("C" compositions) and some were mixed wet by hand in a beaker ("H" compositions).

(b) A water solution with wetting and anti-foam agents was mixed with either colloidal silica or methocel (organic binder) as follows:

Silica Mixture	Methocel Mixture
o 20 mls H_2O	o 20 mls H_2O
o 1 dr Nalco 6020 (wetting agent)	o 1 dr Nalco 6020
o 1 dr Dow Corning 4-10 (anti-foam agent)	o 1 dr Dow Corning 4-10
o 10 mls Colloidal Silica (Nalco 1130, 30% SiO_2 by weight)	o 10 mls Methocel (1%) MC 4000

(c) Blended dry powders were hand mixed, in increments, into the water solution. Powder was added until the mixed slurry would just drip from a glass stirring rod (maximum solids content yet allowing the slurry to be poured).

(Page 1 of 2)

TABLE E-4 (Concluded)

(d) The slurry was poured into a plastic form and dried at room temperature for 40 to 48 hours.

(e) Rectangular bulk samples were removed from the dried mass (about 0.1 X 0.2 X 0.4-in.), weighed and dimensioned.

(f) Samples were placed in alumina dishes and inserted into a furnace at room temperature. The furnace was heated to 1075°C (1965°F) in approximately 3 hours, held for 1 hour and then furnace cooled. Samples were withdrawn at a temperature less than 425°C (800°F). No samples fractured as a result of these slow heating and cooling rates.

Samples were weighed and dimensioned, after firing, and changes in density, volume and weight calculated and an assessment of sintering response indicated in Tables E5 and E6.

TABLE E-5

SINTERING RESPONSE OF GROUP 5 MOLD COMPOSITIONS* AFTER FIRING BULK SAMPLES AT 1970°F FOR 1 HOUR

PRIMARY MOLD FACECOAT MATERIAL	A 100% HREC NO BINDER	B 100% HREC + METHOCEL	C 90% HREMO 10% HREC COLLOIDAL TiO_2	D 30% HREMO 30% HREC COLLOIDAL SiO_2	E 90 HREMO 9 HREC 1 LiF METHOCEL	F 90% HREC 10% CaF_2 METHOCEL	G 80% HREC 20% $CaO \cdot SiO_2$ METHOCEL	H 75% HREMO/ HREC 25% TiO_2 COLLOIDAL SiO_2	I 75% HREMO HREC 25% CaO COLLOIDAL SiO_2	J 90% HREC 10% TiO_2 COLL SiO_2	K LO% HREMO HREC 20% (Na_2... Al SiO_2 METHOCEL	L 3[illegible] HRE [illegible]% [illegible].SiO_2 [illegible] THOCEL	M 60% HREMO 30% HREC 10% TiO_2 METHOCEL	N 75% HRE 25% TiO_2 METHOCEL	P 60% HRE 40% TiO_2 METHOCEL	Q 85% HREMO 10% HREC 5% LiF COLL.SiO_2	R 65% HREMO 10% HREC 5% LiF METHOCEL
0 HREMO	-					--	MS	AS	--		MS	--			AS		
1 HREC-OXALATE (LOW PUR.)	--	--	MS														
2 HREC-CARBONATE (LOW PUR.)	AS	AS	MS	--			AS										
3 HREC-HYDROXIDE (LOW PUR.)	MS	MS	MS	MS			AS										
4 HREC-FLUORIDE (LOW PUR.)	MS	MS	MS	--	--	MS	--										
5 HREC-OXALATE (HIGHER PUR.)	--	--	MS														
6 HREC-CARBONATE (HIGHER PUR.)	--	--	MS			AS	MS	AS	--	--	--	--	--	--			
7 HREC-HYDROXIDE (HIGHER PUR.)	--	--	MS			--	--	MS	--		MS	--					
8 HREC-FLUORIDE (HIGHER PUR.)	MS	MS	MS	MS	--	MS	--									--	--

AS = Adequate Sinter
MS = Moderate Sinter
- - = Inadequate Sinter
= Compositions not prepared.

*Mold facecoat compositions may be determined in any composition group (A through R) by observing the percentage of HREMO combined with the percentage of [illegible] particular Heavy Rare Earth Concentrate (HREC). This may be illustrated by composition 2C which would have 90% HREMO and 10% Low Purity Heavy Rare Earth carbon[illegible] or by composition 7C which would be 90% HREMO plus 10% high purity Heavy Rare Earth Hydroxide. Also note several compositions do not contain HREMO (1B, 2G, etc.) or do not contain one of the concentrates (OF, OG, OH, etc.)

TABLE E-6

SINTERING RESPONSE OF GROUP 5 MOLD COMPOSITIONS AFTER FIRING BULK SAMPLES AT 2200°F*

PRIMARY MOLD FACECOAT MATERIAL	A 100% HREC NO BINDER	B 100% HREC + METHOCEL	C 90% HREMO 10% HREC COLLOIDAL SiO_2	D 50% HREMO 50% HREC COLLOIDAL SiO_2	E 90 HREMO 9 HREC 1 LiF METHOCEL	F 90% HREC 10% CaF_2 METHOCEL	G 80% HREC 20% $CaO \cdot SiO_2$ METHOCEL	H 75% HREMO/ HREC 25% TiO_2 COLLOIDAL SiO_2	I 75% HREMO/ HREC 25% CaO COLLOIDAL SiO_2	J 90% HREC 10% TiO_2 COLL. SiO_2	K 80% HREMO /HREC 20% $(Na,K)Al\ SiO_4$ METHOCEL	M 60% HREMO 30% HREC 10% TiO_2 METHOCEL	N 75% HRE 25% TiO_2 METHOCEL	P 60% HRE 40% TiO_2 METHOCEL
HREMO						--	--	AS			--			AS
1 HREC-OXALATE (LOW PUR.)														
2 HREC-CARBONATE (LOW PUR.)	AS	AS	--											
3 HREC-HYDROXIDE (LOW PUR.)	AS			AS										
4 HREC-FLUORIDE (LOW PUR.)						AS								
5 HREC-OXALATE (HIGHER PUR.)														
6 HREC-CARBONATE (HIGHER PUR.)			--			AS	AS	AS		--		--	--	
7 HREC-HYDROXIDE (HIGHER PUR.)							--	AS			AS			
8 HREC-FLUORIDE (HIGHER PUR.)				AS		AS								

AS = Adequate Sinter
MS = Moderate Sinter
- = Inadequate Sinter
= Compositions not prepared.

*Samples fired for 17 or 64 hours in air.

TABLE E-7

GENERAL MOLD FABRICATION PROCEDURES

Operatior	Conventional Mold	Experimental Mold
Wax pattern configuration	Two cast-to-size bars four 1/2" round bars per mold	Same as conventional
Pattern etching	15-second immersion in chloroethane.	Same
Facecoat slurry composition	$ZrSiO_4$ colloidal silica wetting and antifoam agents. Solids content about 75%	Composition CC2 85% HREMO 11% colloidal silica 4% CaF_2 wetting agent (Nalco 6020) 1.1 ml/# of solids Antifoam (Dow 4-10) 1.1 ml/# of solids Solids content about 43%
Facecoat Slurry preparation	Add fluids to paddle mix tub and then solids gradually. Add antifoam and wetting agents last. Mix for a minimum of 24 hours prior to use.	Add fluids to ball mill and then 75% of the required solids and mill for 1 hour minimum. Add wetting and antifoam agent and mill a minimum of 20 minutes. Add balance of solids and mill a minimum of 15 hours.

TABLE E-7 - Continued

Operation	Conventional Mold	Experimental Mold
Facecoat Dip operation	Dip wax pattern in slurry and then dust with $ZrSiO_4$ sand (stucco). Perform this operation two times.	Dip wax pattern in CC2 slurry and then dust with $ZrSiO_4$ stucco. Perform this operation two times.
Drying operation	Dry in room with minimum of 55% humidity and at a temperature of 68-72°F for 1-3 hours.	Same
Backup coating composition	Calamo ($Al_2O_3 \cdot AlSiO_4$), $ZrSiO_4$, Colloidal Silica wetting and antifoam agents.	Same
Backup slurry preparation	Add fluids to paddle mix tub and then solids gradually. Add wetting and antifoam agents last. Mix for a minimum of 24 hours prior to use.	Same

TABLE E-7 - Continued

Operation	Conventional Mold	Experimental Mold
Backup Dip Operation	Dip pattern with dry facecoat into backup slurry and then dust with calamo stucco. Perform this operation four times with a drying operation between each coat as follows:	Same
Backup Drying Operation	Dry in a room with a minimum of 55% humidity and a temperature of 68 - 72°F.	Same
Final Backup Operation	Dip mold shell in backup slurry and do not dust it with stucco.	Same
Final Drying	Dry in low humidity room for 24 hours minimum.	Same
Dewax Operation	Molds with wax cup and the balance of above mold: steam autoclave at 300°F to remove wax.	Same
Flash Firing	Flash fire by inserting directly into furnace at 1038°C (1800°F) to sinter shell and remove final traces of wax.	Not Done
Mold Preheat	Insert into a preheat furnace at 1038°C (1900°F) and hold until necessary to perform casting. A minimum time of 3 hours is required.	Same Used for sintering of shell and wax removal.

TABLE F-8

EXPERIMENTAL MOLD FABRICATION AT THE AIRESEARCH CASTING COMPANY

Several experimental facecoat compositions were prepared for mold construction at the AiResearch Casting Company (ACC). These molds were fabricated for use in casting Trial "B", also performed at ACC. Facecoat compositions are given below, and discussed in detail in the following sections.

(a) Experimental composition "C"; Colal "P" plus alumina

(b) Experimental composition "Y"; Yttria-potassium silicate plus coarse yttria

(c) Experimental composition "T"; Yttria plus titania plus colloidal silica

Colal "P" Plus Alumina

Colal "P" is a refractory binder produced by DuPont. It is a mildly acid aqueous dispersion of colloidal alumina-silica (30 weight-percent SiO_2 + Al_2O_3). It was selected for evaluation because the SiO_2 is coated with an Al_2O_3 layer, which would result in a significant decrease in exposure of molten metal to SiO_2 during casting. Ability to use an all alumina mold system would have a favorable economic impact in the overall low-melting casting process.

Slurries were prepared as follows:

TABLE E-8 (Continued)

Primary Slurry	Secondary and Tertiary Slurry
o Composition:	o Composition:
114 oz colal "P"	105 oz Colal "P"
1.1 oz wetting agent	1.1 oz wetting agent
0.5 oz antifoam agent	0.5 oz antifoam agent
390 oz 325 mesh tabular alumina (77 weight-percent)	320 oz 325 mesh tabular alumina (75 weight-percent)
o Viscosity: Zahn 4 ~ 25 sec	o Viscosity: Zahn 4 ~ 17 sec
o Solids Content: 84 weight-percent	o Solids Content: 82 weight-percent

Both slurries were milled at least 20 hours in alumina ball mills with 1/2-inch alumina grinding cylinders. Both slurries were uniform, and had stability and coating properties comparable to production foundry slurries.

Etched wax patterns were dipped in the primary slurry, allowed to drain, and stuccoed with 90 grit Al_2O_3. Coating and stucco were uniform, and were allowed to dry at 21°C (70°F) for 2 hours. The secondary coating was applied by dipping, followed again with a 90 grit Al_2O_3 stucco. The secondary slurry was slightly high in viscosity (Zahn 4, 10-13 seconds would have been preferred) and required more careful draining than normal. After the secondary coating was allowed to dry 2 hours, an identical tertiary coating was applied. Following adequate drying, the remaining backup coatings were applied using standard foundry backup materials and procedures.

A total of four test bar cluster molds and two single bar molds were prepared. The molds are shown after firing (see following pages). The facecoat was smooth, uniform, and crack free on all six molds.

(Page 2 of 7)

TABLE E-8 (Continued)

Yttria-Potassium Silicate Plus Coarse Y_2O_3

Acheson EC-3327 consists of fine particle Y_2O_3 dispersed in colloidal potassium silicate solution. Solids content was approximately 56 weight-percent, with 1 fluid ounce weighing approximately 2 ounces. This material sintered well and could be used as a facecoating, but it was too thin and permited stucco to protrude. Therefore, an attempt was made to optimize the slurry by adding coarse particle size Y_2O_3 (Molycorp Lot 792).

Primary Slurry	Secondary and Tertiary Slurry
o Composition:	o Composition:
68 fl oz EC-3327 (79 oz solids; 62 oz liquid)	1 fl oz colloidal silica added to primary slurry
53 oz coarse Y_2O_3 (Molycorp Lot 792)	o Solids Content: 64 weight-percent
10 fl oz colloidal SiO_2 solution	
0.4 oz antifoam agent	
0.4 oz wetting agent	
o Solids Content: 66 weight-percent	

Both slurries were ball milled in excess of 20 hours in an alumina ball mill with 1/2-inch alumina cylinders. Both were slightly thixotropic, resulting in draining difficulties prior to stucco. Three coatings were applied following the same procedures previously outlined for Colal "P", using 90 grit Al_2O_2 as the stucco. Standard foundry backup was used to complete the molds.

Three test bar cluster molds and two single bar molds were prepared. The molds, after firing (see following page) were relatively



Figure E8-1. Appearance of Colal P-Alumina Facecoat Mold After Firing at 1900°F (1040°C). Note Very Smooth Appearance of Surface. (Page 4 of 7)

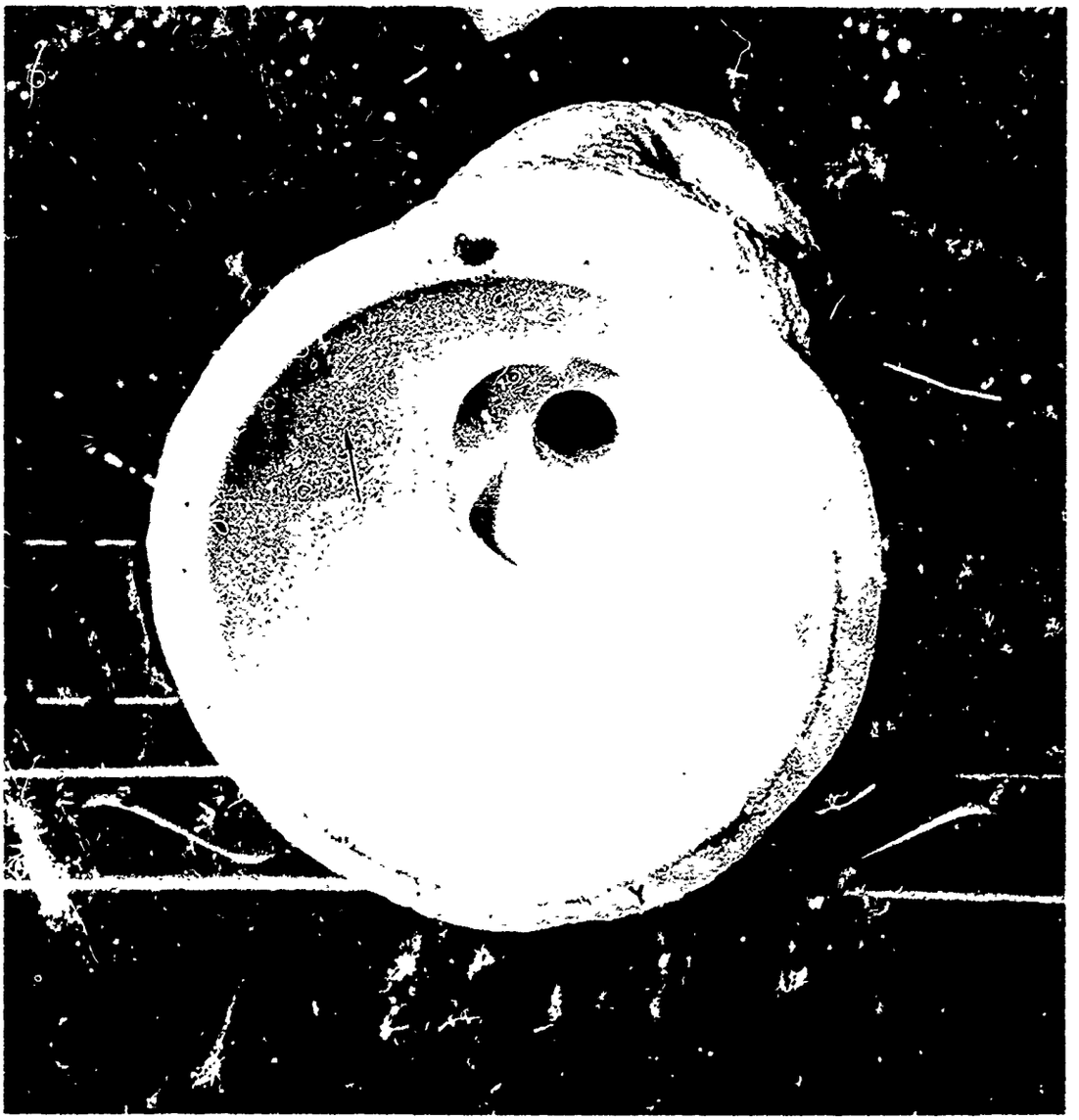


Figure E8-2. Appearance of Y_2O_3-Silicate Facecoat Mold Fired at 1900°F (1040°C). Note the Dark Specks (Arrow) Which are Voids and Alumina Stucco Showing Through the Facecoat.

(Page 5 of 7)

TABLE E-8 (Continued)

uniform and free of cracks. However, the facecoat was not as smooth as normal for the standard foundry system. Pores and pits were present, and the stucco showed through in many places.

$\underline{Y_2O_3 \text{ Plus } TiO_2 \text{ Plus Colloidal Silica}}$

Laboratory studies indicated that TiO_2 additions to yttria-containing slurries resulted in imporved sintering. As a result the following slurry was prepared for primary, secondary, and tertiary coatings.

- Composition: 35 oz Y_2O_3 (80 weight-percent of solids)
  3.5 oz TiO_2 (8 weight-percent of solids)
  17 fl oz colloidal silica (12 weight-percent of solids)
- Viscosity: Zahn 4 < 10 sec
- Solids Content: 75 percent

The slurry was ball milled for at least 20 hours, resulting in a uniform, but rather low viscosity slurry. The slurry adhered well, but produced too thin a coating such that the stucco penetrated through to the wax. Three facecoat layers were applied, as with the two previous systems, using 90 grit Al_2O_3 stucco, followed by standard foundry backup. Four single bar molds were produced (see following page). The facecoat surface was more highly pitted than the yttria-silicate molds described above, and requires further process optimization.

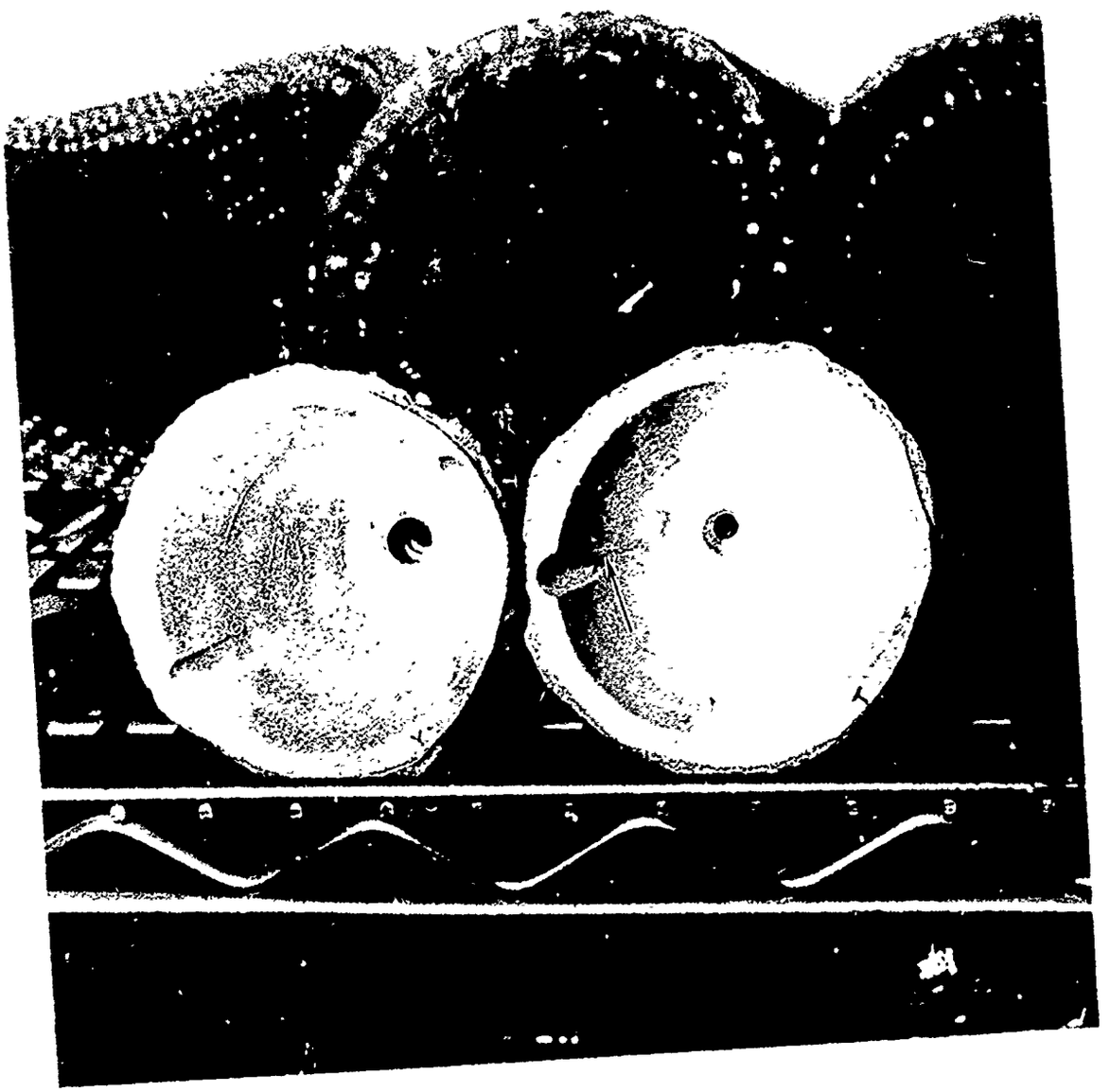


Figure E8-3. Appearance of Y_2O_3-Silicate (Left) and Y_2O_3-TiO_2-SiO_2 (Right) Facecoat Single Test Bar Molds. Cracks in Y_2O_3-TiO_2-SiO_2 Mold (Arrow) are Related to Backup Ceramic Rather Than Facecoat. (Page 7 of 7)

APPENDIX F

INITIAL SELECTION OF CERAMIC MATERIALS

INITIAL SELECTION OF CERAMIC MATERIALS

Selection of materials for crucible/mold applications was based upon information available from literature, previous AiResearch evaluations and AFML research. The basis for selection of each material is discussed below.

- Y_2O_3 (Two Forms: Hot Pressed; Pressed/Sintered) - AiResearch work as well as other several investigations[32,34,40] indicated Y_2O_3 displayed the least reaction with commercial or low-melting point titanium alloys. Cost of the material, however, is high and it has poor thermal shock resistance. The two forms should provide different thermal shock behavior as well as reaction with molten titanium as a result of fabrication and density differences.

- Y_2O_3·15(w/o)Ti (Pressed/Sintered) - The titanium metal addition to Y_2O_3 will be evaluated primarily to improve thermal shock resistance. An improvement in reaction resistance may occur as a result of the titanium metal tendency to reduce the oxygen stoichiometry of Y_2O_3.

- ThO_2 (Slip Cast) - Several evaluations[41] have shown reasonably low reactivity with commercial and low melting alloys. ThO_2 has poor thermal shock resistance, but is lower in cost than Y_2O_3.

---

[40] Helferich, R.L. and C.A. Zanis, "An Investigation of Yttrium Oxide as a Crucible Material for Melting Titanium," NSRDC Report 3911, January 1973.

[41] Chapin, E.J. and W.H. Friske, "A Metallurgical Evaluation of Refractory Compounds for Containing Molten Titanium",

Part I - Oxides. NRL, Report 4447, November 18, 1954.
Part II - Carbon, Graphite, and Carbides. NRL, Report 4467, December 15, 1954.
Part III - Borides and Sulfides. NRL, Report 4478, January 17, 1955.

- o Dy_2O_3 (Pressed/Sintered) - Lyon, et al [32] have shown this material to have promising low reactivity with commercial titanium alloys, however this material has a high cost.

- o La_2O_3 (Pressed/Sintered) - Per Lyon, et al[32], La_2O_3 has promising low reactivity with commercial titanium alloys. This material is also the cheapest of the above materials. La_2O_3 is somewhat hygroscopic and will require appropriate handling.

- o CaO (Pressed/Sintered) - AiResearch work as well as others[42] indicated that CaO has a promising low reactivity with commercial and low-melting titanium alloys. This material is also hygroscopic, but has the lowest cost of all ceramics considered.

- o MgO (Pressed/Sintered) - AiResearch investigations had indicated that MgO displays adequate low reactivity with commercial titanium alloys. This material is hygroscopic, but has a relatively low cost.

- o CeS (Pressed/Sintered) - Per Garfinkle and Davis[43] this material was the most resistant to titanium reactivity among several carbides, borides, silicides, and sulfides evaluated. Thermodynamic stability, however, rates the oxysulfide (Ce_2O_2S) as a better material and it may be evaluated later. However, Ce_2O_2S is still slightly inferior thermodynamically to Y_2O_3 or Ce_2O_3.

---

(42) Piwonka, T.S. and C.C. Clark, "Resistance of Selected Coors Ceramic Crucibles to Molten Titanium", TRW Technical Report R&D No. 18, September 1, 1969.

(43) Garfinkel, M. and H.M. Davis, "Reaction of Liquid Titanium With Some Refractory Compounds", ASM Trans., Volume 48, No. 4 (1965) 520-530.

- Graphite, Pyrolytic - Commercial processes use graphite successfully as a mold material in the casting of titanium alloys. Pyrolytic graphite should display the optimum reactivity resistance of a variety of graphites and carbons.

- CaO·15(w/o)Ti (Pressed/Sintered) - Titanium metal addition primarily improves the resistance of CaO to hydration and thermal shock cracking. An improvement in reaction resistance may also occur as a result of reduced oxygen stoichiometry in CaO.

- Light Rare Earth, Oxide Concentrate, (Pressed/Sintered) - No previous work has been performed but this material (50-percent CeO_2, 33-percent La_2O_3, 12-percent Nd_2O_3, 4-percent Pr_6O_{11}) is low cost and may display adequate reaction resistance, especially for mold applications.

- Heavy Rare Earth Oxide Concentrate (Pressed/Sintered) - No previous work has been attempted but this material (60-percent Y_2O_3, 9-percent Sm_2O_3, 8-percent Er_2O_3, 7-percent Yb_2O_3) has a substantially lower cost than Y_2O_3 and may display good reaction resistance for both crucible and mold applications.

- SiC (Two Forms: Hot Pressed; Reaction Bonded) - Thermodynamics predict this material to be very poor in reaction resistance to molten titanium. However, this material is highly thermal shock resistant and may find application as a substrate for low reactivity coatings. The basic reaction with low melting titanium alloys will therefore be established.

APPENDIX G

DETAILED DESCRIPTION OF INVESTMENT CASTING PROCEDURES

DETAILED DESCRIPTION OF INVESTMENT CASTING PROCEDURES

Chronological details of the process used to pour castings for Trial "A" are given below. Specific information regarding each casting is given in the text and the descriptions below provide generalized parameters.

(a) Crucible Preparation and Bake-Out - The melting crucible (3.5-in. dia. X 8-in. h.) was packed into an appropriate induction coil using dry mixed MgO plus Al_2SiO_5 powders. This dry mix was then capped with a wet mix to hold the entire assembly in place.

The crucible/induction-coil assembly was then air dried for 2 hours for the Y_2O_3·15Ti crucible (No. 4) and 40 hours for the Y_2O_3·15Ti plus Y_2O_3 layer crucible (No. 3).

The Y_2O_3·15Ti crucible induction-coil assembly was loaded with a 17-lb charge of a nickel superalloy (GMR-235) and was placed in the vacuum furnace, pumped down to <100-microns and then the charge heated to about 1615°F, held 2 hours (vacuum reached 5-microns) and then cooled overnight prior to the first days casting effort. The crucible showed about 7-10 cracks in the bottom and bottom-sides after bakeout.

The Y_2O_3·15Ti plus Y_2O_3 layer crucible assembly was loaded with a carbon block resting on a kaowool pad. The assembly was then loaded into the furnace and pumped down to 110-microns whereupon induction heating was started. The temperature was brought to near 1615°F and held for nearly 1 hour and the pressure reached 6-microns. Power was

turned off and the crucible was cooled under vacuum to a point where red heat disappeared (7 minutes) and the furnace was then opened in preparation for the first charge of metal. This crucible displayed only one crack in the crucible bottom.

As a result of the high pressure levels encountered during the subsequent melt following the bakeout, it is recommended that longer bakeout procedures be used as were followed for crucible No. 4. The long air drying time used for crucible No. 3 did not appear to assist the drying operation significantly.

(b) Metal charges consisted normally of at least two pieces of alloy sectioned from 8-in. diameter double melted ingot (vacuum and then under argon) provided by RMI. Each section contained varying amounts of ingot surface which was not trimmed.

Charges (3-8 pounds) were loaded into the crucible by hand, which involved opening the furnace to ambient condition after each pour. This has several disadvantages including losing the gettering activity of the previous melt, limiting the vacuum attainable for each melt and increasing the time between pours.

(c) After loading metal, the furnace was pumped down to 5-microns vacuum before power was applied (ranged from 15-35 minutes).

(d) Melting of the charge was performed slowly (10-20 minutes) using power settings of 20 kw (10 kw was required to hold charge at about 1430°C). Excessive spitting would occur if power inputs were much higher.

The metal melting would occur from the bottom and vacuum could be maintained near 5-microns during melting. A viscous top surface was present as the last portion of the ingot was melted but would then become very fluid and highly agitated by the induction stirring action.

A light copper vapor deposit would build-up on the sight port during melting, precluding the use of optical pyrometer temperature measurements. The vapor deposit did not appear to be excessive and it is not believed that significant copper losses were occurring from the melt.

(e) Superheated metal, at power settings of 15-20 kw, was used to wash down the metal skull from the previous melt. This precluded crucible opening blockage, thus preventing ingot loading problems.

The power setting was then reduced to an appropriate level to hold the metal near the pour temperature. This setting was maintained for a short time (2-4 minutes) and then a thermocouple was immersed in the melt. The thermocouple was best protected from the melt using the yttria coated alumina protection tube. The power was then adjusted to the correct level to maintain the pour temperature at 200°F above the liquidus.

(f) The thermocouple was left in the melt for as short a time as possible during temperature stabilization whereupon it is removed and the metal poured into the mold. All molds were preheated to near 1066°C (1950°F), were uninsulated, required 1.5-2 minutes between removal from preheat to poured metal, and had an estimated temperature at the time of pour of 900°C (1650°F) (based upon cooling rates measured by ACC for similar mold configurations).

(g) Castings were held under vacuum for 25-35 minutes before removal into air.

(h) The casting was then cooled completely in air before removal of the mold material. A section of the bottom gate was removed with the mold intact to provide material for metallography and chemical analysis.

(i) The mold was then broken away from the casting and a light grit blast used to remove final traces of mold as well as a dark thin skin on the cast surface.

(j) The time between pours was generally 1.5 hours, but for several of the last pours, approached 1 hour by reducing the mold cooling time in vacuum and the melting time of the subsequent alloy charge.

REFERENCES

1. Glasunov, S. G., "Precision Casting of Titanium, the Science, Technology, and Application of Titanium." Pergamon Press, New York, pp. 143-148, 1970.

2. Hansen, M., "Constitution of Binary Alloys," McGraw-Hill, New York, 1958.

3. Elliott, R. P., "Constitution of Binary Alloys, First Supplement," McGraw-Hill, New York, 1965.

4. Shunk, F. A., "Constitution of Binary Alloys, Second Supplement," McGraw-Hill, New York, 1969.

5. Molchanova, E. K., "Phase Diagrams of Titanium Alloys," Daniel Davey & Co., Inc., New York, N.Y., 1965.

6. Yakymyshyn, F. W., et al, "The Relationship Between the Constitutional and Mechanical Properties of Titanium-Rich Alloys of Titanium and Cobalt." Preprint of Forty-Second Annual Convention of the ASM, October 1960, No. 198.

7. Fedotov, S. G., et al, "The Physical Properties of Binary Alloys of Titanium in the Quench-Hardened State." Translation, NASA Scientific and Technical Information Facility, 1966 (N66-32990).

8. Kolachev, B. A., and Livano, V. A., "Relationship of Structures Formed on Quenching Titanium Alloys to Equilibrium Phase Diagrams, Physical Metallurgy of Titanium." I. I. Kornilov, Editor, Science Publishing House, Moscow, 1964, NASA Technical Translation, NASA TT F-338, November 1965.

9. Orrell, F. L., Jr., and Fontana, M. G., "The Titanium-Cobalt System," ASM Transactions, Vol 47, 1955, pp 554-563.

10. Mack, David J., "Nonferrous Eutectoid Structures, Metallography Structures and Phase Diagrams," American Society for Metals, Metals Park, Ohio, 1973, Metals Handbook, Vol. 8, pp 193.

11. Holden, F. C., et al, "Heat Treatment and Mechanical Properties of Ti-Cu Alloys." AIME Transactions, Vol. 203, 1955, pp 117-125.

12. Margolin, Herold, et al, "Titanium-Nickel Phase Diagram," AIME Transactions, Vol. 197, 1953, pp 243-247.

REFERENCES (Continued)

13. Kalabukhova, S. V., and Mikheev, V. S., "Investigation of Mechanical Properties of Ti-Mo-Ni Alloys." Translation National Lending Library for Science and Technology, November 1970 (N71-36904).

14. Hansen, M., et al, "The Titanium-Silicon System," Transactions of the ASM, Vol. 44, 1952, pp 518-538.

15. Epremian, E., "The Phase Diagram and Properties of Titanium-Silicon Alloys." Office of Naval Research, London, Technical Report ONRL-61-53, May 1961.

16. Maykuth, D. J., et al, "The Titanium-Manganese, Titanium-Tungsten, and Titanium-Tantalum Phase Diagrams," Battelle Memorial Institute. Prepared for Wright Air Development Center, AF Technical Report 6516, Part 2, July 1959.

17. Holden, F. C., "Heat Treatment, Structure, and Mechanical Properties of Ti-Mn Alloys," AIME Transactions, Vol. 200, 1954 pp 169-184.

18. Fontana, M. G., "Titanium-Chromium Binary Alloys," Ohio State University Research Foundation. Prepared for United States Air Force, Air Material Command, AF Technical Report No. 5496, May 1950.

19. Douglass, R. W., et al, "Metallurgical and Mechanical Characteristics of High-Purity Titanium Base Alloys," Battelle Memorial Institute, for Wright Air Development Divisions, WADC Technical Report 59-595, March 1960.

20. Meyer, Herbert M., and Rostoker, William, "Study of Effects of Alloying Elements on the Weldability of Titanium Sheet," Armour Research Foundation, for Wright Air Development Center Technical Report 53-230, May 1953.

21. Petrova, L. A., "Metastable Phases in the Alloys of Titanium with β-Alloying Metals, Titanium Alloys for Modern Technology," N. P. Sazhin, et al, NASA Technical Translation NASA TT F-596, March 1970, pp 138-152.

22. Hehner, N., et al, "Mechanical Properties of Cast Titanium-Iron and Titanium-Aluminum-Iron Alloys," Frankford Arsenal, Philadelphia, Pa., Report No. R-1416, November 1957.

23. Kaufman, L. and Nesor, H., "Computer Analysis of Alloy Systems," Technical Report AFML-TR-73-56, Manlabs, Inc., March 1973.

24. Hunter, D. B., "The Titanium-Beryllium Phase Diagram Up to 10 Wt-Pct Be," AIME Trans. V. 236, p.900, June 1966.

25. Magnitskiy, O. N., "Casting Properties of Titanium Alloys," 1968. Translation by Foreign Technology Division, Wright-Patterson Air Force Base, Ohio. FTD-HT-23-386-69, April 1970.

26. Buchanan, K. M., et al, "Titanium-Based Casting Alloys," British Non-Ferrous Metals Research Assn., for Procurement Executive, Ministry of Defense, Final Report, S295/11, July 1973.

27. Williams, J. C., "An Electron Microscopy Study of the Phase Transformations in Ti:Cu Alloys," PhD dissertation, University of Washington, 1968. Available University Microfilms, Inc., Ann Arbor, Michigan, 69-13, 640.

28. Bunshah, R. F., and Margolin, H., "Microstructure and Mechanical Properties of Ti-Cu-Al and Ti-Cu-Al-Sn Alloys," Transactions of the American Society for Metals, Vol. 51, 1959, pp 961-980.

29. Seagle, Stan R., "Principles of Alloying Titanium, Lesson 3, Titanium and Its Alloys, Course 27." Edited by Harold D. Kessler, Metals Engineering Institute, American Society for Metals, 1968.

30. Smeltzer, C. E., and Compton, W. A., "Titanium Braze System for High Temperature Applications," First Interim Technical Report, Solar Division of International Harvester Co., AF Contract F33615-74-C-5118, August 1974.

31. S. R. Lyon, Personal Communication, August 21, 1973.

32. Lyon, S. R., S. Inouye, Alexander. C. A., and Niesz, D. E., "The Interaction of Titanium with Refractory Oxides," Titanium Science and Technology, Volume 1, Edited by R. I. Jaffee and H. M. Burte (1973) 271-284.

33. McCoy, L. G., N. M. Griesenauer, C. A. Alexander, T. R. Wright and D. E. Niesz, "Interaction Between Titanium and Y_2O_3," Research on Metallurgical Synthesis, AFML-TR-72-238 Part II, January 1974.

34. Alexander, C. A., N. M. Griesenauer, D. P. Moak, L. P. McCoy, and D. E. Niesz, "Evaluation of Refractory Oxide Crucible Material for Induction Melting of Titanium," AFML-TR-72-238 (1972), pp 76-93.

35. Clites, P. G. and R. A. Beall, "Inductoslag Melting of Titanium Scrap and Sponge," Metallurgical Society of AIME, Paper Selection A72-36, 1972.

36. Brown, Robert A., "Precision Casting of Titanium." Lecture 11-A; paper presented at New York University Titanium Course, September 8-11, 1969.

37. McClaren, S. W., et al, "Processing, Evaluation, and Standardization of Titanium Alloy Castings." LTV Aerospace Corporation for Air Force Materials Laboratory, Wright-Patterson Air Force Base, Ohio. Technical Report TR-68-264, April 1, 1969.

38. Brown, R. A., et al, "Production, Properties and Applications of Precision Titanium Castings." Paper presented at Fall Meeting of AIME, Detroit, Michigan, October 18-21, 1971.

39. Dieter, George E., Jr., "Mechanical Metallurgy," McGraw-Hill Book Company, New York, 1961, pp 324-325.

40. Helferich, R. L. and C. A. Zanis, "An Investigation of Yttrium Oxide as a Crucible Material for Melting Titanium," NSRDC Report 3911, January 1973.

41. Chapin, E. J. and W. H. Friske, "A Metallurgical Evaluation of Refractory Compounds for Containing Molten Titanium,"
Part I - Oxides. NRL, Report 4447, November 18, 1974.
Part II - Carbon, Graphite, and Carbides. NRL, Report 4467, December 15, 1954.
Part III - Borides and Sulfides. NRL, Report 4478, January 17, 1955.

42. Piwonka, T. S. and C. C. Clark, "Resistance of Selected Coors Ceramic Crucibles to Molten Titanium," TRW Technical Report R&D No. 18, September 1, 1969.

43. Garfinkel, M. and H. M. Davis, "Reaction of Liquid Titanium with Some Refractory Compounds," ASM Trans., Volume 48, No. 4 (1965) pp.520-530.